UNIVERSITY OF LONDON THESIS

Degree PhD Year 2005 Name of Author GROOT, K.R.

Functional analysis of the cornified envelope precursors, periplakin and envoplakin.

Karen Renée Groot

Thesis presented in partial fulfilment of the degree of Doctor of Philosophy at University College London

October 2004

ProQuest LLC
789 East Eisenhower Parkway
P.O. Box 1346
Ann Arbor, MI 48106-1346

Abstract

Periplakin and envoplakin are components of the epithelial cornified cell envelope (CE). The CE is a crosslinked protein structure that forms beneath the plasma membrane of differentiating keratinocytes and is essential for epidermal barrier function.

Periplakin and envoplakin belong to the plakin family of cytolinker proteins. Their N termini are thought to mediate their interaction with the plasma membrane. I found that the N terminus of envoplakin does not efficiently localise to desmosomes or microvilli, suggesting a dependence on periplakin for membrane localisation. I found that the first 133 amino acids of periplakin targets the protein to the apical plasma membrane. In a yeast two-hybrid screen, using this region as 'bait', a novel protein was identified and named kazrin. There are four alternatively spliced transcripts, encoding three proteins with different N termini. The interaction between periplakin and all three kazrin isoforms was confirmed by pull-down reactions.

Kazrin was expressed in all layers of stratified squamous epithelia and was incorporated into the CEs of cultured keratinocytes. Kazrin localised to the cell periphery of differentiated cells, however it was more diffusely localised in cells of the basal layer. In stratified keratinocyte cultures kazrin partially colocalised with desmoplakin and periplakin at the desmosomes and periplakin at the interdesmosomal plasma membrane. In transient transfections, kazrin proteins localised predominantly to the apical plasma membrane of primary keratinocytes. The exogenous expression of kazrin proteins caused changes in keratinocyte cell shape and the actin cytoskeleton.

I carried out *in vivo* analysis of the function of periplakin and envoplakin using mice lacking periplakin, envoplakin and involucrin expression. Triple knockout mice produced slightly larger CEs and had a slight delay in epidermal barrier formation relative to control mice. In future it would be interesting to establish the consequence of deleting the kazrin gene in mice.

To Mum and Dad

Table of Contents

List of Figures

skin.

List of Tables

Acknowledgements

Well firstly I would like to thank Fiona, my supervisor, for taking me into her lab and for all the help, guidance and inspiration she has provided on the plakin project through out the years.

It has been a great experience to work in the Keratinocyte Lab with so many enthusiastic and talented people. Thank you to all the members (past and present) of the Keratinocyte Lab for your help and advice, for being shoulders to cry when it all got too much and for being great company (and drinking partners) every step of the way; sorry cant mention you all personally there are just too many now!! In particular I would like to say thank you to Simon and Liz without whom the lab would not function so smoothly and efficiently. I would like to thank Kaz for isolating the kazrin and setting the ball rolling on the kazrin field. Thanks to my 'plakin buddies', Lisa and Arto, for the collaborations and so many helpful discussions trying to figure out what it all means.

The support staff at LIF have been of immense help, especially Rose and Steve from the Electron Microscopy department for persevering with the high-pressure freezing technique and carrying out the immuno-EM staining.

Thanks to the 'Edinburgh posse' especially Kate, Nic and Morag for listening to my endless bletherings about proteins you'd never heard of. Thanks to Bry, Becks and Clare for making Claverley Grove a great place to live and reminding me that there is life outside science, 'ugly corner' still rules though. I would especially like to thank Neil for enduring so much in endlessly long phone calls.

And finally I would also like to thank Mum and Dad for your never-ending support throughout the years!

Chapter 1. Introduction

The topic of my thesis is periplakin and envoplakin, members of the plakin family of cytolinkers and components of the epithelial cornified cell envelope (CE). I examine the domains of periplakin and envoplakin that are necessary for their plasma membrane localisation. I also describe kazrin, a novel protein that associates with periplakin.

In this introductory chapter, I will present an overview of the epidermis and the structure of the CE. In particular I will focus on what is known about periplakin and envoplakin as members of the plakin family and components of the CE.

1.1 Organisation of the epidermis

The skin serves as a mechanical, chemical, microbial and water barrier between the organism and the environment (reviewed in Holbrook, 1994; Odland, 1991). The skin comprises an outer stratified epithelium, the epidermis, and an inner dermis. The epidermis is separated from the dermis by the basement membrane, composed of a variety of proteins, such as type IV collagen and laminin 1. Underlying the skin is fatty and areolar connective tissue.

The epidermis consists of a stratified squamous epithelium, the interfollicular epidermis with associated hair follicles, sebaceous glands and sweat glands. In this thesis I will focus on the interfollicular epidermis. The interfollicular epidermis contains several specialised cell types such as sensory Merkel cells, antigen-presenting Langerhans cells and pigment-producing melanocytes. By far the major cell type of the interfollicular epidermis is the keratinocyte.

Epidermal keratinocytes form distinct cell layers known as the basal, spinous, granular and cornified layers. The cells of each layer have distinct morphologies, differentiation statuses and express different proteins (Fig 1.1). Cells furthest away from the dermis are the most differentiated and have become anucleate, tough, water-resistant squames. These cells carry out much of the protective function of the skin.

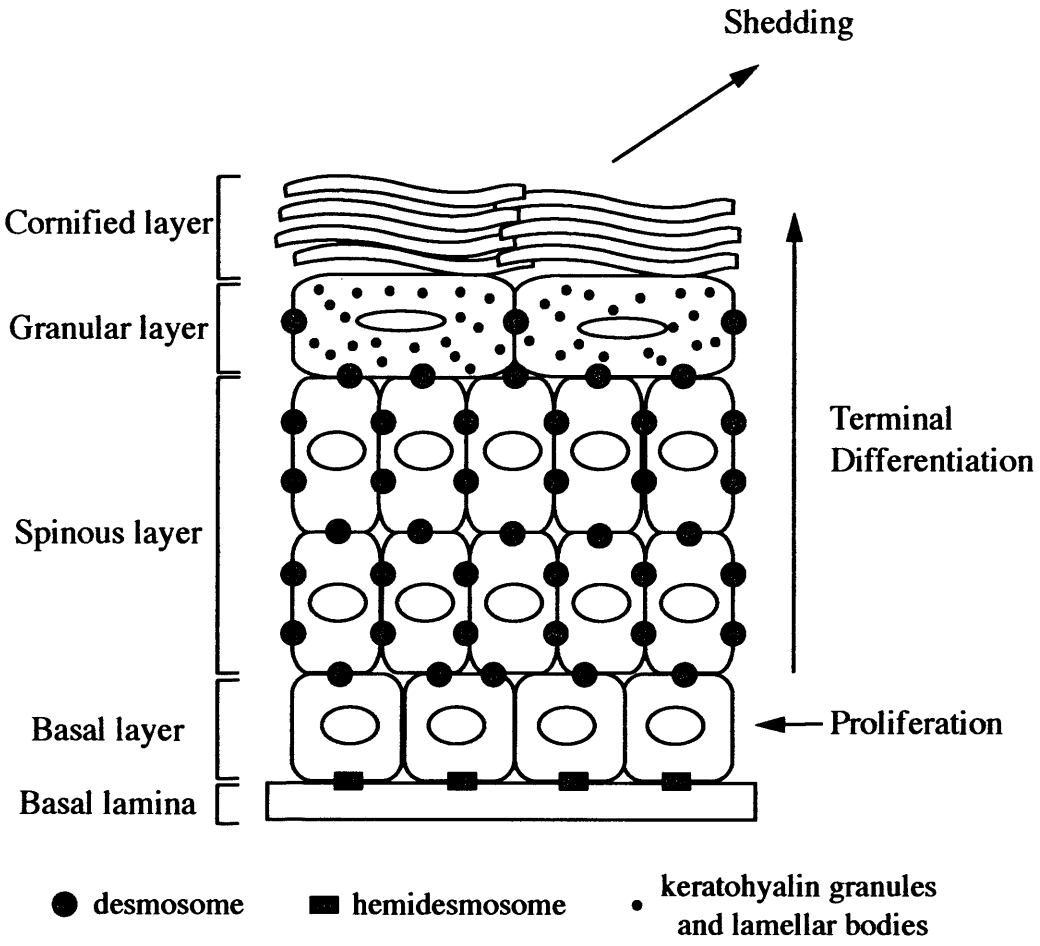

Fig 1.1 Organisation of the interfollicular epidermis. The epidermis is composed of several cell layers. The basal layer is attached to the basal membrane through hemidesmosomes. The desmosomes tether keratinocytes to each other. The keratin intermediate filament cytoskeleton which links into the desmosomes is not shown. Keratohyalin granules and lamellar bodies accumulate in the granular layer. Cornified cells are anucleate and highly flattened. Cornified cells are continually shed from the surface of the skin to be replaced by differentiating cells from below.

In the basal layer, closest to the dermis, cells are small, low columnar and proliferative. Cells of the basal layer are anchored to the basement membrane by hemidesmosomes. As basal keratinocytes detach from the basement membrane and move into the spinous layer, they begin to terminally differentiate (Fig. 1.1).

The spinous layer is composed of non-proliferative, early-differentiated keratinocytes. Human epidermis typically has three or four layer of spinous cells. The cells of the spinous layer are polygonal with those closest to the granular layer more flattened than those below.

The granular layer comprises two or three cell layers, and are the last viable cell layer of the epidermis. Granular layer cells are flat and contain numerous cytoplasmic keratohyalin granules and lipid-containing lamellar bodies.

As cells enter the cornified layer the nuclei and organelles are destroyed. Cornified cells are composed of a tough structure of crosslinked proteins known as the CE. The CE has an extracellular lipid layer, known as the corneocyte lipid envelope (CLE), covalently attached. The interstices of the cornified cells are filled with lamellar lipids, which are crucial components of the water barrier of the skin. The structure and formation of the CE and CLE are discussed further below. The cornified cell layer comprises 15-20 layers of dead, anucleate squames, which are continually sloughed off from the surface of the epidermis to be replaced by newly differentiated cells from below. The transition of a cell from the basal layer to the outer cornified layer takes between 26-42 days, depending on the region of the body.

The cells of the epidermis are held together by intercellular adhesive structures known as desmosomes. Desmosomes are linked, on their intracellular sides, to the distinctive cytoskeleton of keratinocytes, the keratin intermediate filament cytoskeleton.

1.2 Keratin intermediate filaments

There are over 45 different keratin genes, which can be divided into two groups, group I (acidic) keratins and group II (basic) keratins. Keratins form filaments through the multimerisation of coiled coil heterodimers. Heterodimers contain one group I keratin

protein and one group II keratin protein. Keratin expression is controlled in a tissue and differentiation specific manner. Keratins 5 and 14 are expressed in keratinocytes of the basal layer. Cells of the spinous layer express keratins 1 and 10. In specialised epidermal areas other keratins may be expressed e.g. keratin 9 in the palms of the hands and soles of the feet (Porter and Lane, 2003).

In the basal layer, keratin accounts for ~30% of the cell proteins; this increases up to 85% in the cornified layer. Keratin filaments aggregate and align as cells become cornified. Keratohyalin F-granules, visible in the granular layer of the epidermis, contain profilaggrin. Profilaggrin is proteolytically processed as cells differentiate to form filaggrin. Filaggrin, a matrix protein, is important for the formation of the thick keratin bundles, tonofibrils, of differentiated keratinocytes (Holbrook, 1994).

1.3 Desmosomes

Desmosomes are cell-cell adhesive complexes, particularly prominent in tissues that are subjected to mechanical stress such as the skin. The association of the desmosomes with the intermediate filament cytoskeleton allows them to integrate the cytoskeletal networks of cells, thereby helping to distribute tensile and shearing forces and maintain tissue integrity. As cells of the epidermis differentiate the number of desmosomes and the size of the desmosomes increases (Skerrow et al., 1989).

Desmosomes have a central core, lying between the plasma membranes of adjacent cells, and an intracellular plaque. The extracellular domains of the desmosomal cadherins, desmoglein 1 to 4 and desmocollin 1 to 3, form the desmosomal core. The intracellular domains of the desmosomal cadherins, desmoplakin and the armadillo-family members plakoglobin, plakophilin (PKP 1 to 3) and p0071 are components of the desmosomal plaque (Fig. 1.2) (reviewed in Getsios et al., 2004; Kowalczyk et al., 1999a).

The importance of desmosomal adhesion is highlighted by a variety of autoimmune and genetic diseases. Patients with the autoimmune diseases pemphigus foliaceus and pemphigus vulgaris produce antibodies to desmoglein 1 (Dsg 1) and desmoglein 3 (Dsg 3), respectively. The autoantibodies cause a loss of intercellular adhesion and skin

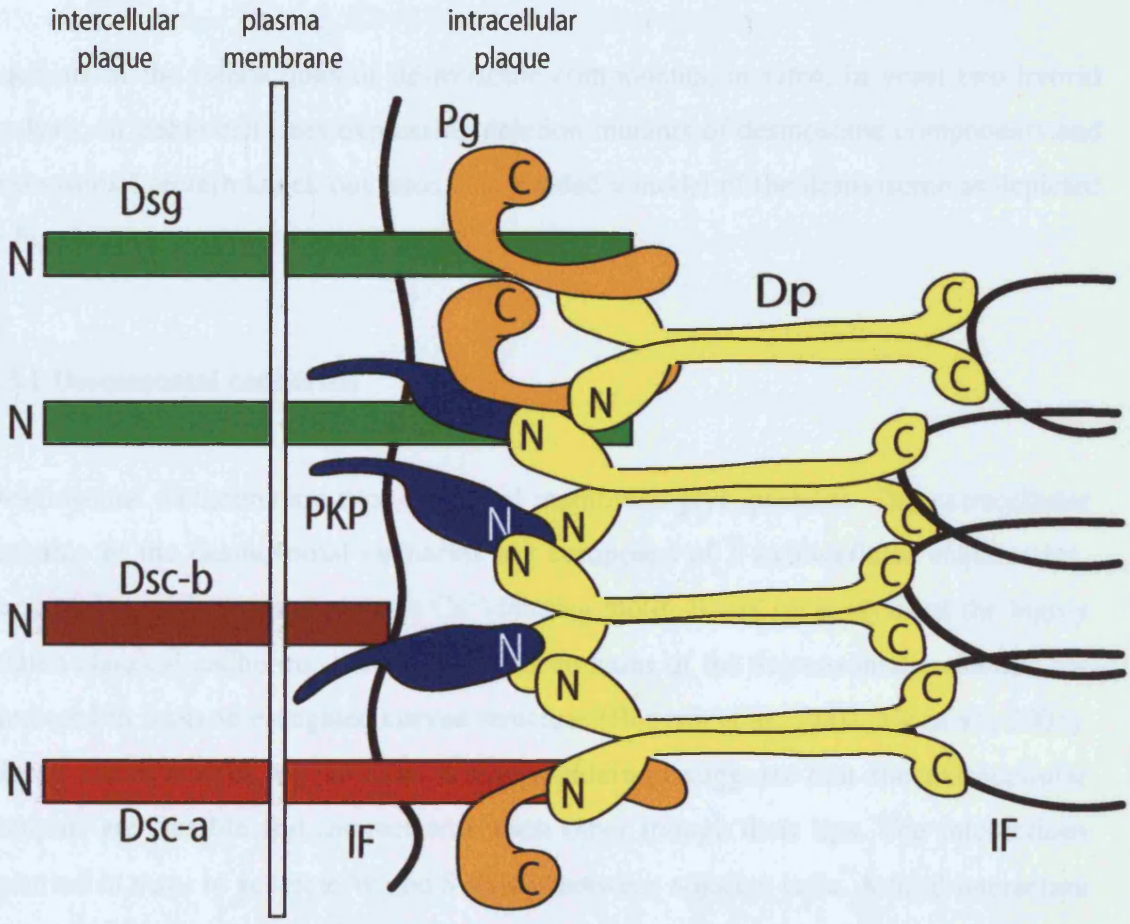

Fig 1.2 Model of desmosome structure. Desmoplakin (Dp) forms parrallel homodimers. The C terminus of Dp links the desmosomes to the intermediate filament (IF) cytoskeleton. The N terminus of Dp associates predominantly with itself, plakoglobin (Pg) and plakophilin (PKP) which in turn interact with the desmosomal cadherins, desmogleins (Dsg) and desmocollins (Dsc). Figure based on model described in Hatsell and Cowin, 2001. See text for further details of the protein-protein interactions of the desmosome. Model is not to scale.

blistering (Amagai et al., 1995; Amagai et al., 1994). The level of desmoplakin expression is crucial for normal cell-cell adhesion. Loss of one copy of the desmoplakin gene causes a form of palmoplantar keratoderma in which affected skin shows a reduction in the linkage of the desmosomes to the keratin intermediate filament cytoskeleton and reduced cell-cell adhesion (Armstrong et al., 1999).

Analysis of the interactions of desmosome components, *in vitro*, in yeast two hybrid analysis, in stable cell lines expressing deletion mutants of desmosome components and desmosomal protein knock out mice, has yielded a model of the desmosome as depicted in Fig. 1.2.

1.3.1 Desmosomal cadherins

Desmosomal cadherins are type I integral membrane glycoproteins. The extracellular domains of the desmosomal cadherins are composed of 5 extracellular subdomains. Each of the subdomains contains a Ca^{2+}-binding motif. Based on analysis of the highly related classical cadherins, the extracellular domains of the desmosomal cadherins are predicted to form an elongated curved structure (Boggon et al., 2002; He et al., 2003). Electron tomography of neonatal mouse epidermis suggests that the extracellular domains are flexible and interact with each other though their tips. The interactions occurred in *trans* to generate W and S shapes between adjacent cells. A third interaction formation is seen, the λ shape, between three desmosomal cadherin extracellular domains. The λ formation is generated from the interaction of two cadherins in *cis* with another in *trans* (He et al., 2003). Only a small proportion (<9%) of cadherin molecules were not involved in W, S or λ type interactions (He et al., 2003).

The electron tomography analysis did not differentiate between desmoglein and desmocollin proteins. Expression of desmosomal cadherins in cells that lack endogenous desmosomal components or express them at low levels and analysis of the interactions of recombinant desmosomal cadherins extracellular domains have been used to elucidate the interactions between desmoglein and desmocollin proteins. Analysis suggests that the extracellular domains of the desmogleins and desmocollins can form homo and hetero-dimers (Chitaev and Troyanovsky, 1997; Marcozzi et al., 1998; Syed et al., 2002). The heterophilic interactions of desmoglein and desmocollin

proteins are Ca^{2+}-dependent (Chitaev and Troyanovsky, 1997; Marcozzi et al., 1998; Syed et al., 2002). The Ca^{2+}-dependence of desmoglein and desmocollin homophilic interactions are less clear (Marcozzi et al., 1998; Syed et al., 2002).

The intracellular domains of the desmosomal cadherins are components of the desmosomal plaque and specifically interact with many components of the plaque. The intracellular domains of desmoglein proteins are composed of several subdomains: a membrane proximal intracellular anchor domain, intracellular catenin-binding site segment, a proline-rich linker, a repeating unit domain and a C-terminal desmoglein terminal domain. The desmocollin intracellular domains are much smaller. Desmocollin 'a' splice variants have an intracellular anchor domain and a C-terminal catenin-binding site segment. Desmocollin 'b' variants have an intracellular anchor domain and a short C-terminal region the function of which is not well understood (Getsios et al., 2004).

1.3.2 Plakoglobin and plakophilins

Plakoglobin and plakophilin 1-3 are members of the Armadillo family of proteins. The family also includes α and β catenin, components of the actin-associated adherens junctions.

Plakoglobin is a component of both the desmosomes and adherens junctions. In the desmosomes plakoglobin interacts with the intracellular domains of desmogleins and desmocollin 'a' splice forms through a central Armadillo repeat-containing domain (Fig. 1.2) (Bornslaeger et al., 2001; Witcher et al., 1996). In adherens junctions plakoglobin interacts with classical cadherins and, via α-catenin, to the actin cytoskeleton (reviewed in Perez-Moreno et al., 2003). The binding sites for α-catenin and the desmosomal cadherins are mutually exclusive, helping to segregate desmosome components from adherens junction components (Witcher et al., 1996; Troyanovsky et al., 1994). In the absence of plakoglobin the components of the junctions become mixed up, as seen in plakoglobin null embryos. In plakoglobin null mice β-catenin localises to desmosomes and associates with desmogleins 1 and 3 (Bierkamp et al., 1999; Ruiz et al., 1996).

Strong cell-cell adhesion through desmosomal cadherins is dependent upon both types of desmosomal cadherin and plakoglobin (Marcozzi et al., 1998). The association of plakoglobin with the desmoglein tails may be stronger than its interaction with the desmocollin cytoplasmic tails (Smith and Fuchs, 1998). Overexpression of plakoglobin lacking a C-terminal domain causes the formation of extended desmosomal junctions between cells. Based on these results, plakoglobin is important for limiting the size of the desmosome possibly by limiting lateral protein:protein interactions between desmosome components (Palka and Green, 1997). However, the desmosomes of plakoglobin$^{-/-}$ mouse epidermis, although ultrastructurally altered, lacking an inner dense plaque and having a reduced linkage to the IF cytoskeleton, have not been reported to be larger (Bierkamp et al., 1996; Bierkamp et al., 1999; Ruiz et al., 1996).

Plakophilin proteins are related to p120^{CTN}, an adherens junction component that is also found in the nucleus. Plakophilin proteins localise to desmosomes and the nucleus (Bonné et al., 1999; Mertens et al., 1996; Schmidt et al., 1997). There are three plakophilin genes, plakophilin 1, 2 and 3. Plakophilins 1 and 2 are expressed as 'a' and 'b' splice variants (Mertens et al., 1996; Schmidt et al., 1997). Based on data from p120^{CTN}, plakophilin may regulate the stability and clustering of desmosomal cadherins and in the nucleus may associate with transcription factors (Getsios et al., 2004).

Loss of plakophilin 1 expression in humans results in skin fragility, with a reduction in the size and number of desmosomes formed and reduced insertion of keratin filaments into the desmosomes, especially in lower suprabasal layers (McGrath et al., 1997). Plakophilin 1 has been shown to interact with desmocollin 1a and to a lesser extent to desmoglein 1 (Smith and Fuchs, 1998). Plakophilin 2 interacts with desmoglein 1 and 2 and desmocollin 1a and 2a (Chen et al., 2002). Plakophilin 3 interacts with all three desmogleins and with desmocollins 1a, 2a, 3a and 3b (Fig. 1.2) (Bonné et al., 2003).

There are reports that plakophilins are able to interact with keratin intermediate filaments *in vitro* (Bonné et al., 2003; Hofmann et al., 2000; Smith and Fuchs, 1998). Immuno-electron microscopy of plakophilin 1 suggests that it is located close to the plasma membrane and therefore far from the region at which the keratin fibres insert into the desmosome (North et al., 1999). Plakophilin may interact with forms of keratin filaments that penetrate further into the desmosomal plaque; alternatively it may interact

with cortical bands of keratin filaments (Fig. 1.2) (North et al., 1999; Vasioukhin et al., 2001). Thus plakophilin may increase the interaction of the desmosomes with the keratin intermediate filament cytoskeleton directly.

1.3.3 Desmoplakin

Desmoplakin is a ubiquitous component of the desmosomal plaque and member of the plakin family of cytolinker proteins, to which envoplakin and periplakin also belong (Leung et al., 2001). The N-terminal globular region targets desmoplakin to the desmosomes. Desmoplakin forms a parallel coiled coil homodimer through its central rod domain. The C-terminal domain is crucial for mediating the connection of the desmosomes with the intermediate filament cytoskeleton (Fig. 1.2) (Stappenbeck et al., 1993). Desmoplakin has two splice variants, which differ only in the length of their central rod domains. Desmoplakin 1 is the longer form; desmoplakin 2 is the shorter form. Both isoforms are widely expressed, although desmoplakin 2 is expressed at slightly lower levels in simple epithelia and is absent in the heart (Angst et al., 1990; Green et al., 1990).

The desmoplakin N-terminus interacts with many components of the desmosomal plaque (Fig. 1.2). There are weak interactions between desmoplakin and the desmosomal cadherins; but by far the more crucial interactions are via the Armadillo-family members, plakoglobin and plakophilin (Bornslaeger et al., 2001; Chen et al., 2002; Hatzfeld et al., 2000; Kowalczyk et al., 1997; Smith and Fuchs, 1998; Troyanovsky et al., 1994). The head domain of desmoplakin binds itself and the central armadillo repeats of plakoglobin. Expression of desmoplakin is necessary to cluster the desmosomal cadherins and plakoglobin at the plasma membrane (Kowalczyk et al., 1997; Smith and Fuchs, 1998). The interaction between desmoplakin and plakoglobin is disrupted upon epidermal growth factor receptor-dependent tyrosine phosphorylation of plakoglobin. The C-terminal phosphorylation of plakoglobin does not affect the interaction of plakoglobin with the Dsg 2 tail domain (Gaudry et al., 2001).

The head domain of desmoplakin interacts with plakophilin 1, 2 and 3 (Bonné et al., 2003; Chen et al., 2002; Kowalczyk et al., 1999b). Two desmoplakin binding sites have been identified on plakophilin 3 (Bonné et al., 2003). The potential of plakophilins to interact with more than one desmoplakin molecule may allow them to increase lateral interactions between desmosome components and thereby increase desmosome size, as seen in the differentiated layers of the epidermis (Bonné et al., 2003; Kowalczyk et al., 1999b). Plakophilin 2 and 3 have also been shown to interact with plakoglobin; an interaction between plakophilin 1 and plakoglobin has thus far not been identified (Bonné et al., 2003; Chen et al., 2002).

Desmoplakin preferentially binds plakophilin 1 to plakoglobin in transfected cells, but both proteins are important components of the desmosomal plaque. The formation of punctate desmosomal plaque structures in cells that have few desmosomes requires the coexpression of desmoglein 1 and desmoplakin in the presence of plakoglobin and plakophilin 1 (Bornslaeger et al., 2001). Quadruply transfected cells form punctate structures resembling desmosomal plaques and have numerous associated IFs while cells lacking plakophilin form extended desmosomal plaque structures (Bornslaeger et al., 2001).

The C-terminus of desmoplakin is crucial to link the desmosomes to the IF cytoskeleton. Overexpression of the head domain of desmoplakin disrupts the linkage between the desmosomal plaque and the intermediate filament cytoskeleton. The disruption results in reduced intercellular adhesion (Bornslaeger et al., 1996; Huen et al., 2002).

In mice, the loss of expression of desmoplakin has drastic effects early in development. Embryos die at embryonic day 6.5 (E6.5) due to a failure to form sufficient and effective desmosome structures in embryonic and extra-embryonic tissues (Gallicano et al., 1998). Desmoplakin$^{-/-}$ desmosomes are considerably smaller in number and size than wild type desmosomes and are not linked to the IF cytoskeleton, indicating that desmoplakin is important for assembly or stability of the desmosomal plaque. Desmoplakin$^{-/-}$ embryos generated by tetraploid aggregation, to bypass the defects in the extra-embryonic tissues, die at E10.5. At this stage the embryos die due to defects in the microvasculature due to problems in the formation of complexus adherens junctions. There are also defects in many desmosome-containing tissues such as the skin and heart

(Gallicano et al., 2001). An epidermis-specific knock-out of desmoplakin was generated by crossing mice in which exon 2 of the desmoplakin gene was bordered by loxP sites with mice expressing Cre recombinase under the control of the K14 promoter. The K14 promoter becomes active in the developing skin epithelium, and specifically deletes the desmoplakin gene there, around E13.5 (Vasioukhin et al., 2001). Deletion of desmoplakin specifically in the epidermis indicates that desmoplakin is crucial for maintenance of an interaction of the desmosome with the IF cytoskeleton. The keratinocytes are able to adhere but intercellular adhesion is weaker, particularly in lower epidermal layers. Coincident with a defect in desmosome structure and function, the adherens junctions fail to mature (Vasioukhin et al., 2001).

1.3.4 Changes in the protein composition of desmosomes during epidermal terminal differentiation

The composition of desmosomes varies in a tissue- and differentiation-specific manner. Plakophilin 1 is expressed in all layers of the epidermis but is upregulated as cells differentiate (Moll et al., 1997). Plakophilin 2 is expressed predominantly in the basal layer of the epidermis (Mertens et al., 1996). Plakophilin 3 is expressed in all living layers of the epidermis (Bonné et al., 2003).

Periplakin and envoplakin localise to the desmosomes of differentiated keratinocytes. Periplakin and envoplakin are expressed in the spinous layer of the epidermis (Ma and Sun, 1986; Ruhrberg et al., 1997; Ruhrberg et al., 1996).

Desmoglein 2 and desmocollin 2 are expressed predominantly in the basal layer (Schafer et al., 1994; Theis et al., 1993). Desmoglein 1 and desmocollin 1 are upregulated in the spinous layer (Amagai et al., 1996; Arnemann et al., 1993). Desmocollin 3 and desmoglein 3 are expressed in the basal and immediately suprabasal layers of the epidermis (Amagai et al., 1996; Arnemann et al., 1993). Desmoglein 4 is expressed in suprabasal layers of the epidermis (Kljuic et al., 2003).

The complex expression patterns of desmosomal components suggests that there are functional differences between the desmosomes of different tissues or between the desmosomes of cells at different stages of differentiation.

Transgenic mice expressing Dsg 3 from the involucrin promoter and from its endogenous promoter thereby express Dsg 3 throughout the epidermis (Elias et al., 2001). The mice exhibit loss of cell-cell adhesion at the transition of the granular layer and the cornified layer in contrast to wild type mice where the loss of cell-cell adhesion occurs within the cornified layer. The epidermis of these mice does not function efficiently as a permeability barrier; thus the desmoglein isoform type is important for proper cornified layer structure (Elias et al., 2001).

Desmoglein 3 knock-out mice have cyclical baldness due loss of cell-cell adhesion between the outer root sheath of the hair follicle and the telogen hair club (Hanakawa et al., 2002). Expression of Dsg 1 in these mice from the K14 promoter, thereby replacing Dsg 3 with Dsg 1 in the basal layer, rescues the hair phenotype suggesting that the desmoglein isoforms can compensate for each other in some cases (Hanakawa et al., 2002).

Thus some differences in the epidermis can be seen as a result of altering the relative levels of expression of different desmogleins within the epidermis (Elias et al., 2001). The desmosomes of the K14-Dsg 1 mice crossed with Dsg $3^{-/-}$ mice function under normal conditions, however it cannot be ruled out that there are subtle differences in the structure or strength of the desmosomes of the transgenic mice versus wild type mice (Hanakawa et al., 2002).

In order to fully understand the differences between the desmosomes of different tissues we need to know more about the biophysical properties of desmosomes and the interactions of proteins within the desmosome.

1.4 The cornified cell envelope and corneocyte lipid envelope

The stratum corneum, the outer layer of the epidermis, is composed of cornified anucleate, squamous cells (Holbrook, 1994; Odland, 1991). Cornified cells have lost many of the organelles and structures found in other cells such as mitochondria and nuclei. The cornified cells contain a cornified cell envelope (CE), which encases a cytoplasm filled with thick keratin bundles (Holbrook, 1994; Odland, 1991). The CE is an insoluble 10nm thick layer of crosslinked protein with a 5nm thick extracellular layer of covalently attached ceramide lipids. The CE forms beneath the plasma membrane of terminally differentiating keratinocytes. The ceramide lipids, which are covalently linked to CE proteins form the corneocyte lipid envelope (CLE). In this introduction I will talk separately about the formation of the crosslinked protein component of the CE and the crosslinking of ceramide lipids to CE component proteins i.e. formation of the CLE. Lipid lamellae lie between the cornified cells (Kalinin et al., 2001; Kalinin et al., 2002).

The CE with the covalently attached CLE and the lamellar lipids are important components of the physical and water barrier of the skin (Holbrook, 1994). The CE is formed in many stratified squamous epithelia, however formation of the CLE and the deposition of lamellar lipids are unique to dry epithelia such as foreskin epidermis, as well as the rodent forestomach (Jarnik et al., 1996; Kalinin et al., 2001).

The proteins of the CE are predominantly crosslinked by the action of tranglutaminase 1 and 3 (TGase 1 and 3). TGase 1 and 3 catalyse the formation of N-ε-(γ-glutamyl)lysine bonds, between glutamine and lysine side chains of substrate proteins, in a Ca^{2+} dependent manner. In addition to protein crosslinking TGase 1 is thought to catalyse the attachment of ceramide lipids to CE components (Marekov and Steinert, 1998; Nemes et al., 1999a). TGase 1 has an acyl lipid adduct which targets the protein to the plasma membrane (Chakravarty and Rice, 1989). TGase 3 is cytosolic (Kim et al., 1990).

In mice lacking TGase 1 there is a large reduction in the number of CE and CLE produced and the lamellar lipids are disorganised (Kuramoto et al., 2002). The skin of TGase $1^{-/-}$ mice no longer functions as a water barrier and the mice die within hours of birth due to dehydration (Matsuki et al., 1998). In patients with lamellar ichthyosis (LI)

there is often a loss of TGase 1 expression or crosslinking activity. LI patients fail to form normal CEs and the lamellar lipids are disorganised (Elias et al., 2002; Huber et al., 1995; Russell et al., 1995). In the absence of TGase 1, mice and LI patients form thick scaly skin to prevent dehydration from the skin surface (Kuramoto et al., 2002). No diseases in which there is loss of TGase 3 have thus far been reported (Lorand and Graham, 2003).

CE proteins, such as involucrin and periplakin, were initially identified as protein that became insoluble upon induction of CE formation by the activation of TGase enzymes (Rice and Green, 1979; Simon and Green, 1984). More detailed analysis of the protein composition and mechanism of formation of the CE has been done by sequential proteolysis of CEs and identification of the peptides released, by immunoelectron microscopy of CEs and by comparison of the amino acid composition of CEs relative to the amino acid compositions of known CE components (Steinert and Marekov, 1999).

The CE is thought to form in three main stages. In the first stage early CE proteins, periplakin, envoplakin and involucrin, are crosslinked by TGase 1 to themselves and each other to form an insoluble protein scaffold beneath the plasma membrane. The CE scaffold encompasses the desmosomes and interdesmosomal plasma membrane (Kalinin et al., 2001; Steinert and Marekov, 1999). During or after CE scaffold formation lamellar bodies, containing the lipids necessary for the formation of the CLE and lipid lamellae, fuse with the plasma membrane to release their contents into the intercellular spaces. At this stage a proportion of the ceramide lipids is crosslinked to protein components of the CE including periplakin and envoplakin. Finally late CE proteins, such as loricrin, which make up the bulk of the CE, are crosslinked to the CE scaffold to form the mature CE structure (Fig. 1.3) (Kalinin et al., 2001).

Mature CE can be isolated from the outer layers of the epidermis and other tissues such as the rodent forestomach (Jarnik et al., 1996; Michel et al., 1988). Immature or early forms of the CE can be isolated from lower layers of the epidermis or from cultured cells (Michel et al., 1988; Steinert and Marekov, 1999).

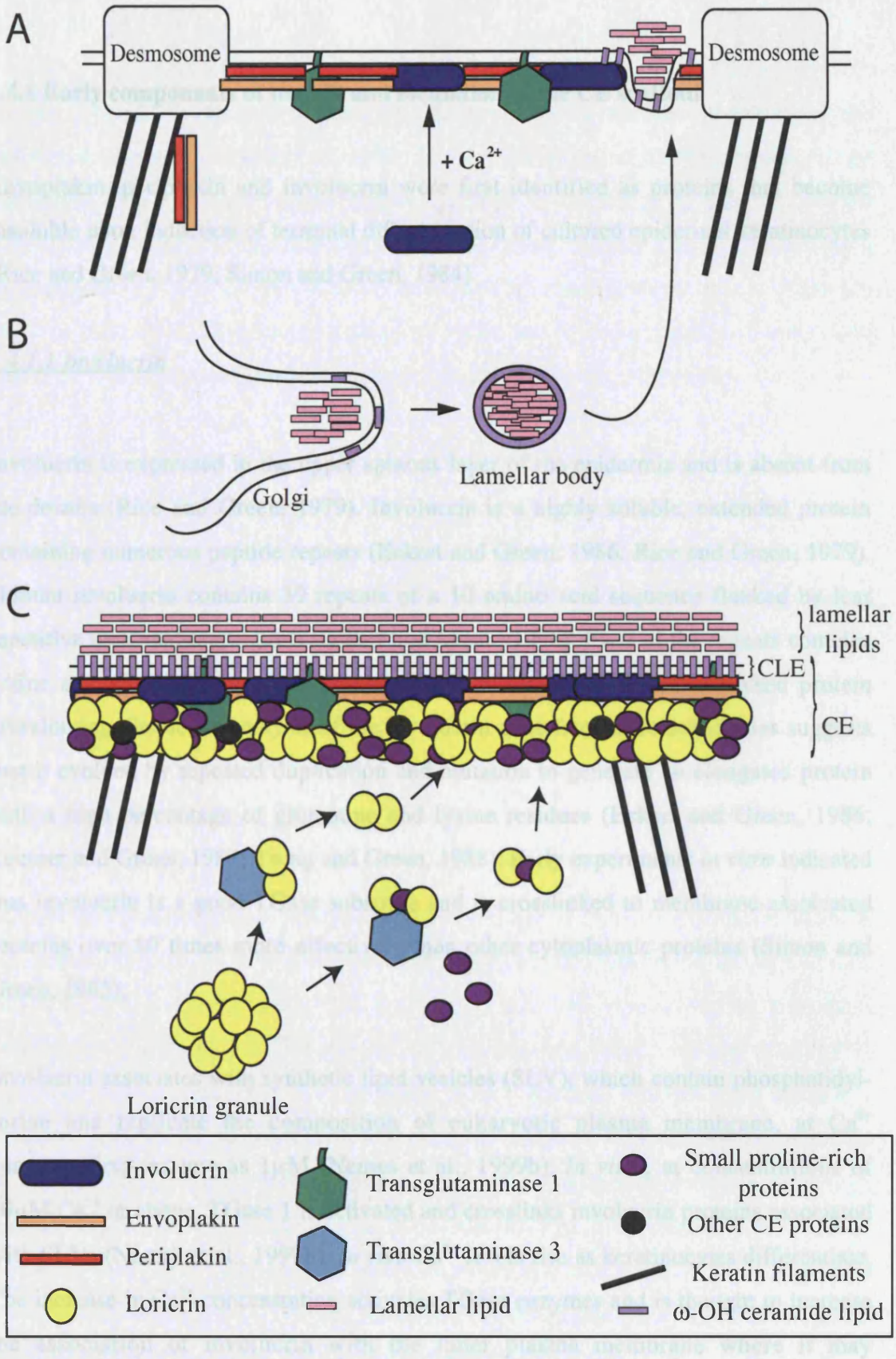

Fig 1.3 Model of cornified envelope (CE) formation. (A) Envoplakin, periplakin and involucrin are expressed early in differentiation and form the scaffold between and around the desmosomes on the inner side of the plasma membrane. (B) Lipid-containing lamellar bodies are pinched off from the Golgi complex. The lamellar bodies fuse with the plasma membrane to release the lipids into the intercellular space. The long ceramide lipids span the plasma membrane and are crosslinked to CE components. (C) In the final stages loricrin, small proline-rich proteins and other CE poteins are crosslinked onto the CE scaffold to form the mature CE structure. See text for further details. Model based on Kalinin *et al.*, 2001.

1.4.1 Early components of the CE and formation of the CE scaffold

Envoplakin, periplakin and involucrin were first identified as proteins that become insoluble upon induction of terminal differentiation of cultured epidermal keratinocytes (Rice and Green, 1979; Simon and Green, 1984).

1.4.1.1 Involucrin

Involucrin is expressed in the upper spinous layer of the epidermis and is absent from the dermis (Rice and Green, 1979). Involucrin is a highly soluble, extended protein containing numerous peptide repeats (Eckert and Green, 1986; Rice and Green, 1979). Human involucrin contains 39 repeats of a 10 amino acid sequence flanked by less repetitive head and tail regions (Eckert and Green, 1986). Each of the repeats contains lysine and glutamine residues which act as substrates for TGase-catalysed protein crosslinking. Sequence analysis of the involucrin gene from different species suggests that it evolved by repeated duplication and mutation to generate an elongated protein with a high percentage of glutamine and lysine residues (Eckert and Green, 1986; Teumer and Green, 1989; Tseng and Green, 1988). Early experiments *in vitro* indicated that involucrin is a good TGase substrate and is crosslinked to membrane-associated proteins over 80 times more effectively than other cytoplasmic proteins (Simon and Green, 1985).

Involucrin associates with synthetic lipid vesicles (SLV), which contain phosphatidyl-serine and replicate the composition of eukaryotic plasma membrane, at Ca^{2+} concentrations as low as 1μM (Nemes et al., 1999b). *In vitro,* at concentrations of 10μM Ca^{2+} or above, TGase 1 is activated and crosslinks involucrin proteins associated with SLVs (Nemes et al., 1999b). *In vivo* Ca^{2+} levels rise as keratinocytes differentiate. The increase in Ca^{2+} concentration activates TGase enzymes and is thought to increase the association of involucrin with the inner plasma membrane where it may subsequently be crosslinked to form part of the CE scaffold (Nemes et al., 1999b). Members of the annexin and S100 Ca^{2+}-dependent family of proteins, which localise to the plasma membrane in a Ca^{2+}-dependent manner, may help anchor involucrin at the plasma membrane (Robinson et al., 1997).

Involucrin is readily detected in immature CEs generated in culture or isolated from the epidermis (Steinert and Marekov, 1997; Steinert and Marekov, 1999). Proteolysis of epidermal CEs indicates that extensive digestion is necessary in order to release involucrin-derived peptides (Steinert, 1995). In contrast, if the CEs are treated with methanol and potassium hydroxide to remove the CLE lipids from the outside of the CE prior to proteolysis, involucrin-derived peptides are released quickly (Steinert and Marekov, 1997). This suggested that involucrin is an early CE component.

Involucrin expression is not restricted to the interfollicular epidermis; it is also expressed in the inner root sheath and the companion layer of the hair follicle (Li et al., 2000). Involucrin is expressed in the suprabasal layers of the epithelia of the oral cavity, oesophagus, anus, vagina and exocervix. Involucrin is also detected in the transitional epithelia of the renal pelvis, ureter and urinary bladder (Li et al., 2000; Rice et al., 1984). Involucrin is expressed in the Hassell's corpuscles of the thymus (Rice et al., 1984).

1.4.1.2 Envoplakin and periplakin

In the epidermis envoplakin and periplakin expression is highest in the upper spinous and granular layers. Neither envoplakin nor periplakin is expressed in the dermis (Ma and Sun, 1986; Ruhrberg et al., 1997; Ruhrberg et al., 1996). Periplakin and envoplakin are proteins of 195 and 210 kDa respectively (Ma and Sun, 1986; Ruhrberg et al., 1997; Ruhrberg et al., 1996). They are composed of an N-terminal globular head domain, a central α-helical rod domain and a C-terminal globular domain. Envoplakin and periplakin form envoplakin/periplakin heterodimers and periplakin homodimers through their central rod domain (Kalinin et al., 2004; Ma and Sun, 1986; Ruhrberg et al., 1997; Ruhrberg et al., 1996). Envoplakin homodimers are also thought to form (DiColandrea et al., 2000; Ruhrberg et al., 1997). The domain structure and functions of the domains of envoplakin and periplakin are discussed in more detail below.

Periplakin and envoplakin localise to the plasma membrane of keratinocytes, where they partially colocalise with desmoplakin at desmosomes. Periplakin and envoplakin can also be detected at the interdesmosomal plasma membrane. Confocal microscopy

reveals that desmosomes labelled with antibodies to desmoplakin and desmocollins are surrounded more diffuse periplakin and envoplakin staining (DiColandrea et al., 2000; Ma and Sun, 1986; Ruhrberg et al., 1997; Ruhrberg et al., 1996). At the apical interdesmosomal membrane periplakin localises to plasma membrane projections known as microvilli (Bretscher et al., 2002; Ma and Sun, 1986).

Full length recombinant periplakin and envoplakin, like involucrin, are able to bind SLV in a Ca^{2+}-dependent manner (Kalinin et al., 2004). The desmosomal and interdesmosomal plasma membrane localisation of periplakin and envoplakin is important for their crosslinking by TGase 1, which is localised at the plasma membrane.

Envoplakin and periplakin are thought to be early CE components as they localise to the site of formation of the CE early in differentiation. In the case of envoplakin it is frequently found crosslinked to involucrin and desmoplakin, which are early CE components (Steinert et al., 1998; Steinert and Marekov, 1999).

The expression of periplakin and envoplakin is not restricted to the interfollicular epidermis. Periplakin is expressed in the inner root sheath of the hair follicle (Ma and Sun, 1986). Envoplakin and periplakin expression can be detected at the cell periphery of cells in keratinized and non-keratinized oral mucosa, cervical mucosa, corneal epithelium, the transitional epithelium of the urinary bladder, the pseudostratified epithelium of the mammary glands and the simple gastric mucosa (Ma and Sun, 1986; Ruhrberg et al., 1997; Ruhrberg et al., 1996). In the oesophageal mucosa periplakin is found in all suprabasal layers of the epithelium, in contrast to envoplakin, which is detected only in the outermost layers (Ruhrberg et al., 1997; Ruhrberg et al., 1996). Periplakin is also expressed in the Hassell's corpuscles of the thymus (Ruhrberg et al., 1997). Periplakin is found at the cell periphery in association with the cortex adhaerens of lens fiber cells. The cortex adhaerens junctions are adhesive junctions, which also contain ezrin, desmoyokin and periaxin (Straub et al., 2003). Periplakin is not confined to epithelial cells as periplakin mRNA transcripts are detected in several regions of the brain. The cellular localisation and the function of periplakin in the brain are not known. However, recent data suggests that periplakin may interact with mu opioid G protein-coupled receptors thereby modulating their signalling output (Feng et al., 2003; Ma and Sun, 1986).

1.4.1.3 Early crosslinking partners

Steinert and Marekov analysed the protein composition, localisation and crosslinking pattern of CEs generated in culture. Confluent human epidermal keratinocytes were cultured for 2 to 7 days in high calcium medium to induce CE formation. The CE yield and the extent of protein crosslinking increases as the cells are grown at confluence for longer periods. The culture system allows the analysis of the earliest stages of CE formation as at all time points the CEs are immature relative to those direct from epidermis (Steinert and Marekov, 1999). At the early stages desmosomal remnants are clearly visible on the surface of the CEs (Steinert and Marekov, 1999). Desmoplakin remains unequally localised along the length of the CE, suggesting that desmoplakin and possibly other desmosomal proteins are components of mature CEs (Robinson et al., 1997; Steinert and Marekov, 1999). Indeed, Robinson et al. (1997) have in addition to desmoplakin isolated desmoglein, desmocollin, plakoglobin and plakophilin derived peptides from proteolytically digested CEs from cultured keratinocytes.

In the early stages of CE formation envoplakin and periplakin, like involucrin, are found predominantly at interdesmosomal areas of early CEs. As the CEs develop further, the epitopes for envoplakin and involucrin can be found equally distributed along the CE (Steinert and Marekov, 1999). The epitope for periplakin is not detected in later CE preparations possibly due to loss or masking of the epitope (Steinert and Marekov, 1999). Immuno-EM data from other labs and from epidermal CEs and peptide sequencing data of epidermal CEs, suggest that periplakin is a component of mature CEs, is located at the outer edge of the CE and is covalently linked to ceramide lipids of the CLE (Marekov and Steinert, 1998; Simon and Green, 1984).

In the initial stages, involucrin and envoplakin are predominantly crosslinked to themselves and each other in the CEs. At this stage involucrin makes up about 50% of the protein mass of the CEs. Involucrin proteins are crosslinked to each other in a head to head and head to tail fashion. At later stages involucrin and envoplakin both become crosslinked to desmoplakin (Steinert and Marekov, 1999). The crosslinking of desmoplakin with envoplakin and involucrin is concomitant with the presence of envoplakin and involucrin epitopes in both interdesmosomal and desmosomal areas of

the CE. The change in the pattern of crosslinking of the CE components and their localisation suggests that the formation of the CE scaffold initiates at the interdesmosomal plasma membrane and subsequently incorporates desmosomal areas of the plasma membrane (Steinert and Marekov, 1999). The localisation of envoplakin and periplakin to the sites of initiation of CE scaffold formation and their crosslinking to involucrin at the plasma membrane suggests that they are important components of the CE scaffold (Fig. 1.3 A) (Steinert and Marekov, 1999).

Periplakin, envoplakin and involucrin single knock-out mice have been generated in our lab and others (Aho et al., 2004; Djian et al., 2000; Määttä et al., 2001). Periplakin, envoplakin and involucrin single knock-out mice develop normally and are fertile. All three types of knock-out mice are able to produce CEs and to generate a functional epidermal water permeability barrier. However, in the case of envoplakin the formation of the barrier is slightly delayed (Aho et al., 2004; Djian et al., 2000; Määttä et al., 2001). Periplakin, envoplakin and involucrin single knock-out mice are described in more detail in Chapter 6.

1.4.2 Formation of the CLE

The CLE is a monomolecular layer of ω-OH-ceramide lipids covalently attached to the outside of the CE. As keratinocytes differentiate they produce a variety of differentiation-specific lipids. The lipids accumulate in the *trans* Golgi network. Lipid-containing vesicles bud off from the *trans* Golgi to form cytoplasmic lamellar bodies (LBs) (Fig. 1.3 B). The LBs contain long chain (C_{28}-C_{36}) ω-OH-ceramide lipids, which span the limiting membrane. Within the LBs are ceramide lipids, free fatty acids, cholesterol and cholesterol derivatives (Kalinin et al., 2002).

In the upper granular layer of the epidermis the LBs fuse with the plasma membrane and release their contents into the intercellular space. The ω-OH ceramide lipids span the keratinocyte plasma membrane and become covalently linked to CE proteins. The phospholipids of the plasma membrane are gradually reabsorbed and replaced by the ω-OH ceramides as differentiation proceeds (Kalinin et al., 2002). The remaining LB lipids form lipid lamellae, which separate the cornified cells (Kalinin et al., 2002). It is thought

that the CLE is important for the organisation of the lipid lamellae. In the absence of ω-OH ceramide lipid synthesis there is a disruption in the formation of organised lipid lamellae and the CLE (Behne et al., 2000).

ω-OH ceramide lipids are attached to glutamine residues of CE proteins via an ester linkage. Greater than 50% of the ceramide-linked peptides isolated from proteolytically digested foreskin CEs are derived from involucrin, periplakin and envoplakin (Marekov and Steinert, 1998). The lipopeptides isolated do not contain crosslinks to other proteins, suggesting that the sites of protein crosslinking and ceramide attachment are different (Marekov and Steinert, 1998).

The ceramides are attached to various glutamine residues in the head domain of involucrin. One ceramide attachment site is located in the central rod domain of involucrin. The central rod domains of envoplakin and periplakin are used predominantly for ceramide lipid attachment (Marekov and Steinert, 1998). The remaining lipid-associated peptides are related to sequences found in many different CE proteins (Marekov and Steinert, 1998). The attachment of many of the ceramide lipids to periplakin, envoplakin and involucrin is consistent with the idea that they are early CE components and are important for the formation of the CLE (Fig. 1.3 B).

In vitro, TGase 1 can catalyse the addition of an analog of a natural ceramide lipid to several specific glutamine residues in the head domain of involucrin. The sites of attachment of the ceramides *in vitro* have been shown to also occur *in vivo* (Nemes et al., 1999a). The dual function of TGase 1 in protein crosslinking and ceramide lipid attachment may explain why TGase $1^{-/-}$ mice fail to form CEs, have sparse CLEs and disorganised lipid lamellae (Kuramoto et al., 2002). Some patients with LI are able to form CLEs, as evidenced by EM, but have defective CEs and lipid lamellae (Elias et al., 2002). Thus, at present it is not known if TGase 1 is responsible for catalysing the attachment of all ceramide lipids to CE proteins.

1.4.3 CE scaffold reinforcement

Analysis of CEs suggests that the CE scaffold is reinforced by the addition of other CE proteins, such as loricrin and members of the small proline-rich (SPR) protein family (Fig. 1.3 C).

1.4.3.1 Loricrin and the small proline-rich proteins

Loricrin is a major component of many mature CEs (Hohl et al., 1991; Mehrel et al., 1990; Steinert et al., 1998). Loricrin is first detected in the granular layer of the epidermis, where it accumulates in small insoluble aggregates known as keratohyalin L-granules (Hohl et al., 1991; Mehrel et al., 1990; Steven et al., 1990). Keratohyalin L-granules are smaller and more regularly shaped than the keratohyalin F-granules, which contain profilaggrin (Steven et al., 1990). As cells become cornified loricrin is detected at the cell periphery, on the inner side of the CE (Mehrel et al., 1990).

Loricrin has an unusual amino acid composition with a high percentage of glycine and serine residues (77%) separated by cysteine and aliphatic residues (tyrosine, phenylalinine, isoleucine). There are four clusters of glutamine/lysine-rich sequences, two internally, one at the C-terminus and one at the N-terminus. Loricrin is predicted to form a series of flexible glycine loops, which come together at the aliphatic residues (Candi et al., 1995; Hohl et al., 1991). The clusters of glutamine/lysine residues are within areas that are predicted to be inflexible and accessible for crosslinking reactions (Hohl et al., 1991). Loricrin is predicted to form a compact yet flexible protein structure. The amino acid composition and the formation of intra- or inter-peptide disulphide bonds are thought to contribute to the insolubility of loricrin in the granular layer (Hohl et al., 1991).

Members of the SPR family of proteins are important components of the CE. The *SPR* genes are located in a cluster in the epidermal differentiation complex (Cabral et al., 2001; Song et al., 1999). The epidermal differentiation complex is a region on human chromosome 1q21 where many other genes for proteins important in keratinocyte differentiation, such as involucrin and loricrin, are located (Mischke et al., 1996).

The SPR proteins have a common structure, with glutamine/lysine-rich head and tail domains. The head and tail domains are crosslinked to other CE proteins by transglutaminase enzymes. The central domain of the SPR proteins consists of a variable number of short proline-rich repeats (Cabral et al., 2001). The sequences of the repeats are predicted to confer different levels of flexibility to the proteins. SPR2 proteins (A to I) are thought to be less flexible than SPR1A, B and SPR3 (Kartasova et al., 1995).

The majority of the SPR proteins are upregulated as keratinocytes differentiate (Cabral et al., 2001). The level of expression of the different SPR proteins varies between tissues. SPR proteins expressed at higher levels in dry epithelia are generally expressed at lower levels in wet internal epithelia, and vice versa (Cabral et al., 2001).

Loricrin, in insoluble keratohyalin L-granules, is crosslinked to itself or to the soluble SPR proteins, by TGase 3 to form small homo-and heteromultimers. The multimers are thought to be more soluble and more easily incorporated into the CE scaffold (Candi et al., 1999). *In vitro* experiments indicate that TGase 3 activity is necessary prior to TGase 1 activity in order to produce large crosslinked protein complexes of SPR1 and loricrin. TGase 3 and TGase 1 use different lysine and glutamine residues on SPR1 for crosslinking. Data suggest that TGase 1 and 3 have nonoverlapping crosslinking functions, which is consistent with the finding that TGase 3 cannot compensate for the absence of TGase 1 in TGase $1^{-/-}$ mice (Candi et al., 1999). In TGase $1^{-/-}$ mice abnormal loricrin aggregates were detected at the cell periphery, but these were not sufficiently crosslinked to function as a CE (Matsuki et al., 1998).

1.4.3.2 Modulation of the biomechanical properties of the CE

The sum of the level of loricrin and SPR proteins in the CEs of different tissues is between 83 and 85% (Steinert et al., 1998). The actual levels of SPR proteins in the CE vary greatly and depend on the physical requirements of the tissue (Jarnik et al., 1996; Steinert et al., 1998). Higher levels of SPR proteins are found in the mouse forestomach (22%), which undergoes large amounts of mechanical stress, relative to human foreskin epidermis (4%) or human/mouse trunk epidermis (<1%) (Steinert et al., 1998). The incorporation of loricrin into the CE is thought to increase the pliability of

the CE due the proposed flexible nature of the loricrin molecule (Hohl et al., 1991; Steinert et al., 1998). The addition of SPR proteins, which act as crossbridgers, is thought to increase the rigidity and strength of the CE, while maintaining its flexibility (Jarnik et al., 1996; Steinert et al., 1998). The level of specific SPR proteins is also influenced by external insults, such as UV radiation, or by ageing and disease. Thus the composition of the CE and the type of barrier formed is adapted in response to various physiological and environmental states (Cabral et al., 2001).

Analysis of the CEs from cultured cells suggests that SPRs are not only involved in late stages of CE formation but also in the early stages. SPR1 is predominantly interdesmosomal in early CE structures. Isolated CE peptides suggest SPR1 and 2 proteins can be crosslinked to envoplakin, involucrin and desmoplakin (Steinert and Marekov, 1999). Thus SPR proteins may be important for increasing the mechanical strength of early CE structures as well as modulating the physical properties of mature CEs.

Late envelope proteins (LEPs) constitute a family of 18 related proteins expressed late in terminal differentiation (Marshall et al., 2001). LEPs are small proteins (89-118aa), which contain numerous proline/lysine/cysteine repeats at their N-termini. Proline/lysine/cysteine repeats are also found in members of the SPR family of proteins. At the C-terminus LEPs are rich in serine/glycine/cysteine residues, which is also a feature of loricrin (Marshall et al., 2001). The LEPs accumulate in intracellular aggregates. The numerous lysine and glutamine residues of the LEPs make them suitable TGase substrates. LEPs are crosslinked to the CE after the incorporation of loricrin into the CE. The LEP proteins have tissue-specific expression patterns. Through their tissue specific expression patterns and/or subtle differences in protein sequence the LEPs, like SPRs, are predicted to affect the biomechanical properties of the CE (Marshall et al., 2001).

1.4.3.3 Keratins and other CE components

Keratins 1, 2e, 5, 6 and 10 are crosslinked directly to components of the CE (Candi et al., 1998; Steinert and Marekov, 1995; Steinert and Marekov, 1999). A conserved lysine in the head domain of group II keratins is frequently used as the crosslinking site.

Mutation of the conserved lysine in keratin 1 to an isoleucine results in a dominant form of diffuse nonepidermolytic palmar-plantar keratoderma (Candi et al., 1998). The mutant keratin monomers are able to form filaments. However, in cells of the granular and cornified layers there is retraction of the keratin tonofibrils from the desmosomes and cell periphery and distortion of cell shape (Candi et al., 1998). The association of keratin tonofibrils to the CE is necessary for proper structural integrity of the cornified cell and is most prominent in cells that are subjected to large amounts of mechanical stress, such as the human palmar-plantar skin and rodent forestomach (Candi et al., 1998; Steinert et al., 1998).

Keratin filaments are crosslinked to both early (involucrin, envoplakin) and late (loricrin, SPRs) CE components (Candi et al., 1998). This suggests that keratin filaments may be associated with CE components at desmosomal remnants in addition to associating with CE components at the cytoplasmic side of the CE (Candi et al., 1998; Steinert and Marekov, 1995; Steinert and Marekov, 1999). Filaggrin, which is associated with the keratin filaments of terminally differentiated cells, can be crosslinked to loricrin (Steinert and Marekov, 1995).

There are many other components and putative components of the CE such as elafin, cystatin α , S100A10 and A11 and annexin 1 (Nakane et al., 2002; Robinson et al., 1997; Steinert et al., 1998; Steinert and Marekov, 1995; Steinert and Marekov, 1997). The function of these proteins within the CE is not well understood.

Elafin is a serine proteinase inhibitor found in lamellar bodies and the CE. In the CE, elafin is crosslinked to keratins, loricrin and SPR proteins as well as envoplakin and involucrin (Nakane et al., 2002; Steinert and Marekov, 1995; Steinert and Marekov, 1997; Steinert and Marekov, 1999). Cystatin α is a cysteine proteinase inhibitor protein found in keratohyalin granules and the CE. In the CE, cystatin α is crosslinked to loricrin, SPR proteins, keratin, envoplakin, desmoplakin and involucrin (Steinert and Marekov, 1997; Steinert and Marekov, 1999; Takahashi et al., 1992). Annexin 1, S100A10 and S100A11 belong to the Ca^{2+}-binding S100 protein family. Annexin 1, S100A10-and S100A11-derived peptides have been identified in proteolytically digested CEs. However, immunoEM of annexin 1 suggests that it is not major component as annexin 1 antibody staining of CEs from human keratinocyte cultures is not above

background levels (Robinson et al., 1997; Steinert and Marekov, 1999). In response to the increased Ca^{2+} levels of differentiating keratinocytes, S100A11 translocates from the cytoplasm along microtubules to the cell periphery, thereby placing it in proximity to TGase 1 at the plasma membrane (Broome and Eckert, 2004).

1.5 Plakin family proteins

Envoplakin and periplakin belong to the plakin family of cytolinker proteins, whose other members include desmoplakin, plectin, bullous pemphigoid antigen 1 (BPAG1), microtubule-actin crosslinking factor (MACF1) and epiplakin. Plakin family members are large multi-domain proteins that impart mechanical stability to cells and tissues by linking cytoskeletal networks to each other and to membrane-associated adhesive sites such as desmosomes and hemidesmosomes (Fig. 1.4).

Conventional plakin proteins have an N-terminal plakin domain, a central rod domain, a series of C-terminal plakin repeats and a conserved linker subdomain. Some conventional plakin proteins such as plectin have an actin-binding domain and MT-binding domain. The spectraplakins have actin-binding domains, a plakin domain, a central spectrin repeat domain and C-terminal putative Ca^{2+}-binding EF hands, a GAR domain and a GSR domain. In general, the domains required for association with desmosomes and hemidesmosomes or the actin cytoskeleton are located in the N-terminus of plakins, while those involved in binding to intermediate filaments (IFs) or microtubules are found in the C-terminus.

The central coiled-coil rod domain of plakins is responsible for their dimerisation. Spectraplakins do not have a coiled-coil rod domain but have a central domain composed of multiple spectrin repeats (Jefferson et al., 2004; Leung et al., 2002). Spectrin repeats are composed of 110-120 amino acids, which fold into a three-helix bundle. Spectrin repeats are though to impart flexibility to spectraplakin proteins and may mediate their dimerisation (Jefferson et al., 2004; Leung et al., 2002).

Many plakin proteins are alternatively spliced, bringing together different functional domains. Many of the splice variants are expressed in a tissue-specific manner, such that

the type of cytolinker protein and its exact crosslinking capabilities are variable. However, thus far no splice variants of periplakin and envoplakin have been identified.

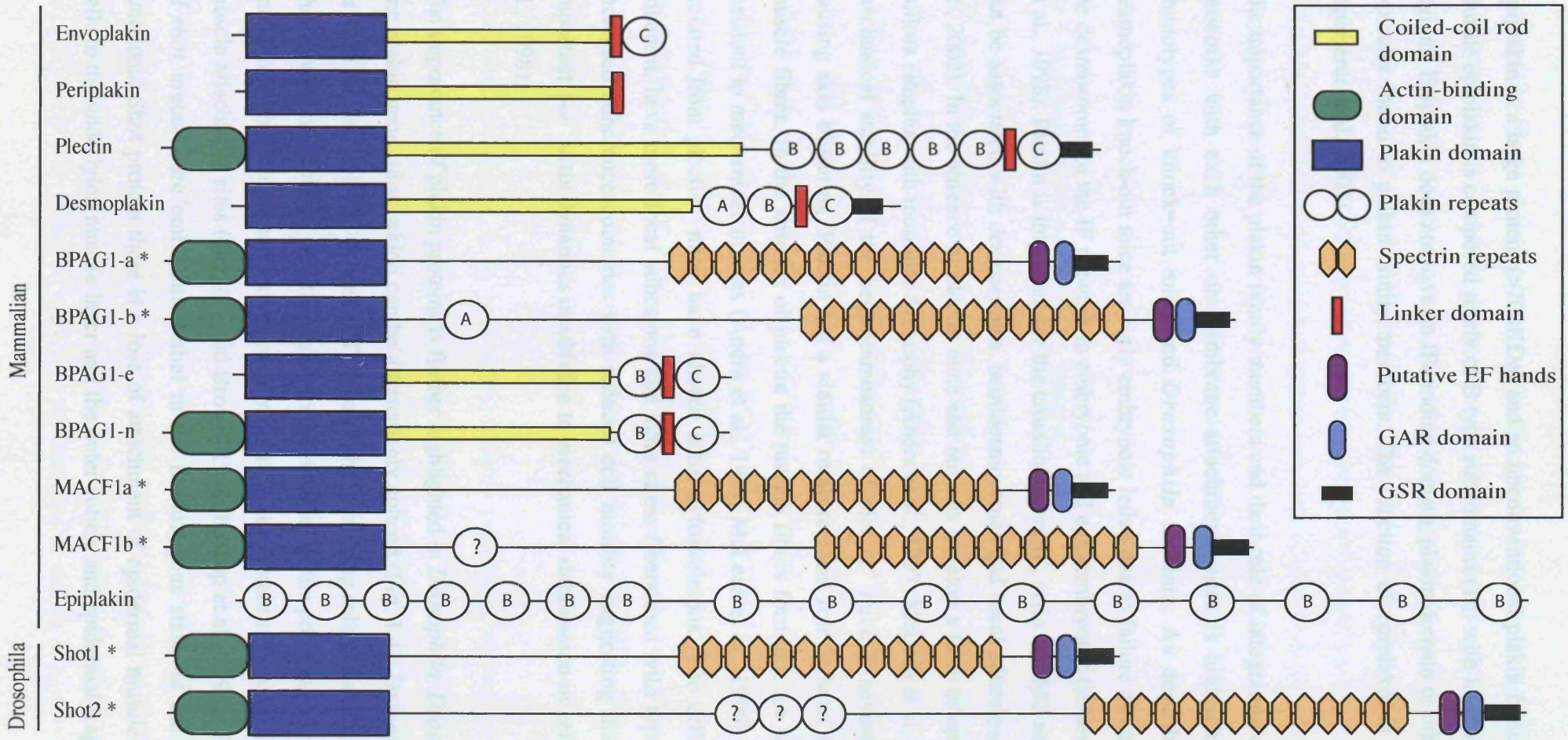

Fig 1.4 The plakin family of cytolinker proteins. See text for description of the domains and their function. Proteins and protein domains are not drawn to scale.The plakin domain is composed of NN, Z, Y, X, W and V subdomains. In the case of the spectraplakins (marked by *) the central coiled-coil rod domain is replaced by a series of spectrin repeats. The spectrin repeats may mediate antiparallel dimerisation. Several of the plakin splice variants are shown. However, plectin, MACF1 and BPAG1 have many alternative 5' start sites generating proteins which differ in the length of the actin-binding domain and N-terminal extensions; these are not shown. In addition, desmoplakin 2 is identical to desmoplakin 1 except it has a shorter rod domain. The plakin repeats which cannot be described as being of the A, B or C variety are marked with a ?.

Epiplakin is a large protein (>700KDa) and an unconventional plakin family member. Murine epiplakin is composed solely of B type subdomains (16) with intervening linker regions. Epiplakin does not have an IF-binding domain, plakin domain or other domains typically found in plakin family members. The function of epiplakin is not known (Spazierer et al., 2003).

The importance of the plakin family members and their role of integrating cytoskeletal networks with each other or membrane attachments sites is highlighted by the phenotypes of knock-out mice and *Drosophila* mutants. As described earlier, desmoplakin knock-out mice are early embryonic lethal due to failure of attachment of the desmosomes to the IF network in embryonic and extraembryonic tissues (Gallicano et al., 1998). Plectin is important for the crosslinking of IF, actin and MT networks and can be associated with desmosomes, hemidesmosomes and focal adhesions (Leung et al., 2002). In the absence of plectin mice and humans develop a form of epidermolysis bullosa simplex with muscular dystrophy (Ändra et al., 1997; McLean et al., 1996). The mechanical stability of the hemidesmosomes of plectin$^{-/-}$ mice is severely reduced causing skin blistering. Plectin has a similar reinforcement role in heart and skeletal muscle fibres. In the absence of plectin the muscle fibres form but are no longer as resistant to mechanical stresses (Ändra et al., 1997; McLean et al., 1996). Fibroblasts isolated from plectin$^{-/-}$ mice have altered actin cytoskeletons. The cells are more adherent, have more focal adhesions and more stress fibers than wild type cells. The increased adherence coincides with reduced cell motility suggesting that plectin is important for actin dynamics in addition to mechanical stabilisation of cells (Ändra et al., 1998).

The importance of plakin proteins is further highlighted in *Drosophila*. *Drosophila* have one plakin gene, *shot,* which can be alternatively spliced (Fig. 1.4). *Drosophila* do not have an IF cytoskeleton; instead, MTs assume the stabilising role in tissues. Mutants of *shot* have a multitude of defects related to the inability of the proteins to crosslink MT and actin cytoskeletons and link them to membrane attachment sites, such as epidermal muscle attachment sites (Gregory and Brown, 1998; Prokop et al., 1998). The majority of *shot* mutants are embryonic lethal in the homozygous state. In the absence of functional Shot protein there is a loss of attachment of epidermal muscle attachment cells to the underlying muscle layer and the outer cuticle and epidermal fragility due to

loss of adhesion through the actin-associated adherens junctions (Gregory and Brown, 1998; Prokop et al., 1998; Roper and Brown, 2003). In neurons, lack of Shot protein results in defects in axon outgrowth and dendritic branching (Lee and Kolodziej, 2002; Prokop et al., 1998). The expression of a Shot protein containing only the actin- and MT-binding domains is sufficient to rescue the axon outgrowth defect, provided that the MT and actin domains are joined. This emphasises the importance of plakin proteins in integrating different cytoskeletal networks (Lee and Kolodziej, 2002). Shot is highly related to mammalian forms of MACF1, which are discussed further below.

1.5.1 Intermediate filament binding domain

The IF binding domains are generally located at the C-terminus of plakin proteins. The C-terminus encodes a number of plakin repeat domains (PRDs) separated by loops of variable length. Each of the PRDs forms a globular subdomain. The PRDs are thought to fold up to form a globular end domain (Choi et al., 2002; Foisner and Wiche, 1987; O'Keefe et al., 1989). Each PRD is composed of 4 and a half repeats of a 38 amino acid sequence, which forms a β-hairpin followed by two anti-parallel α-helices (Choi et al., 2002). There are three types of PRDs, A, B and C, based on the sequences of the PRDs of desmoplakin (Green et al., 1992). Envoplakin contains one C type PRD and periplakin, the smallest plakin family member, contains no PRDs (Ruhrberg et al., 1997; Ruhrberg et al., 1996).

The linker subdomain is the region most highly conserved between plakin family members and between mouse and human envoplakin (Määttä et al., 2000). The linker region generally precedes the last PRD. The linker region contains a partial 38 amino acid repeat and is thought to form an α-helix (Leung et al., 2002). Envoplakin and periplakin both have a conserved linker subdomain (Fig. 1.4).

The IF-binding domain of plakin proteins has been analysed by yeast-two and-three-hybrid assays, *in vitro* binding assays, transient transfections of deletion proteins and analysis of their alignment with IF cytoskeletal networks and X-ray crystallographic studies. The studies suggest that the linker domain is important for IF binding but that the PRDs also play a part in stabilising the interactions and/or in proper folding and

alignment of the protein domains (Choi et al., 2002; Fontao et al., 2003; Karashima and Watt, 2002; Kazerounian et al., 2002; Nikolic et al., 1996; Steinbock et al., 2000).

The periplakin linker subdomain coaligns with the IF cytoskeletons of cultured keratinocytes and Cos7 cells (DiColandrea et al., 2000). Two regions, known as homologous boxes 1 and 2, within the linker subdomain are highly conserved between plakin family members. Homologous boxes 1 and 2 of periplakin are both necessary for strong interactions with IFs, such that the interaction is maintained even if the Cos7 cells are extracted in an imidazole buffer containing 1% Triton X-100 or 0.6% saponin prior to staining (Karashima and Watt, 2002). Overlay assays suggest that periplakin has different affinities for different IF proteins (Karashima and Watt, 2002). The envoplakin C terminus does not efficiently coalign with the IF cytoskeletons of keratinocytes or Cos7 cells. In contrast when it is cotransfected with a C-terminal periplakin construct the binding of both proteins with IFs is strong, as assessed by non-extractability of the envoplakin and periplakin mutant proteins in the extraction buffer described above. Thus, periplakin is important for the association of periplakin and envoplakin with IFs (Karashima and Watt, 2002).

The desmoplakin C-terminal domain colocalises with simple keratin and vimentin IF networks in transient transfected cells (Stappenbeck et al., 1993). Removal of more than 48 amino acids from the very C-terminus of desmoplakin disrupts the ability of desmoplakin to coalign with simple keratin filaments but does not affect vimentin binding (Stappenbeck et al., 1993).

X-ray crystallographic analysis of the B- and C-type PRDs indicated that they are globular and contain a groove on their surface lined with basic residues. It was hypothesised that this groove was important for binding the vimentin rod domain. This idea is somewhat disputed as the *in vitro* binding of vimentin by the B and C PRDs alone is very weak in contrast to the *in vitro* binding affinity of B- and C-PRDs together with the linker subdomain. Further transient transfection analysis and yeast three hybrid assays suggest that the linker subdomain and the C-terminal region of desmoplakin are important sites for IF binding, while the B- and C-type PRDs are though to play a minor role in IF binding (Fontao et al., 2003). The B- and C-type PRDs are thought to be important for the proper folding and alignment of the major IF-binding domains (Fontao

et al., 2003). Desmoplakin interacts with epidermal and simple keratins in addition to vimentin and desmin of cardiac myocytes (Fontao et al., 2003; Meng et al., 1997). The relative importance of the major IF binding sites is different for different IF types (Fontao et al., 2003). The interaction of desmoplakin with epidermal keratins is most dependent upon the C-terminal tail and is stabilised by the presence of the C-type PRD. Interactions with vimentin and the simple keratins (K8 and K18) are dependent upon the linker subdomain. The interaction of desmoplakin and vimentin or the simple keratins is stabilised by the presence of the upstream B-type PRD. Simple keratins can also bind desmoplakin through the linker subdomain and B-type PRD (Fontao et al., 2003).

Phosphorylation of a serine residue within the desmoplakin C-terminal tail inhibits its interaction with keratins K8/K18 (Stappenbeck et al., 1994). Mutation of this serine to a glycine, thereby preventing phosphorylation at this site, increases the interaction of desmoplakin with keratins K8/K18. Interestingly, though the C-terminal tail of desmoplakin is not essential for vimentin binding phosphorylation at this site influences the strength of the interaction between desmoplakin and vimentin. Mutation of the phosphorylatable serine of the desmoplakin C-terminal tail to a glycine increases the strength of binding between vimentin and desmoplakin (Meng et al., 1997).

BPAG1 is a component of hemidesmosomes of basal keratinocytes. BPAG1 specifically interacts with K5/K14 heterodimers but not with simple keratins or vimentin. The interaction requires the linker subdomain and surrounding B-and C-type PRDs and the short C-terminal tail of BPAG1 (Fontao et al., 2003).

The plectin C-terminus is composed of 5 B-type PRDs, a linker subdomain and a C-type PRD. The IF-binding domain of plectin has been mapped to part of the terminal B-type PRD and half of the linker subdomain. Within the region of the linker subdomain used, four basic residues are essential for the binding activity (Nikolic et al., 1996). The intermediate filament-binding region of plectin also mediates oligomerisation and binding to the hemidesmosomal protein β4-integrin (Geerts et al., 1999; Rezniczek et al., 1998; Steinbock et al., 2000). An additional intermediate filament binding site may be located within the actin-binding domain of plectin proteins (Sevcik et al., 2004).

The binding affinity of plectin to vimentin increases upon *in vitro* phosphorylation of plectin by protein kinase A and decreases upon cell cycle specific phosphorylation by cdk1 and phosphorylation by PKC (Foisner et al., 1996; Foisner et al., 1991). The cdk1 phosphorylation site of plectin is located within the C-type PRD. Thus, regions outside of the mapped IF-binding domains can affect the extent of binding thereby allowing fine-tuning of the interaction of plectin with IFs in a cell type-and cell state-specific manner (Foisner et al., 1996; Nikolic et al., 1996).

1.5.2 Periplakin linker subdomain interacting proteins

Periplakin has been found to associate with a variety of other proteins via regions involving the latter part of the rod domain and linker subdomain.

A region of protein kinase B (PKB) interacts with the latter part of the rod and linker subdomain of periplakin. The binding of PKB with periplakin does not affect the activation of PKB directly as insulin-mediated PKB activation is unaffected by overexpression of periplakin (van den Heuvel et al., 2002). In MCF7 cells, which express relatively high levels of periplakin and low levels of vimentin, periplakin is associated with IFs and mitochondria and can be seen in the nucleus. Coexpression of PKB in these cells suggests that in the presence of periplakin, PKB is retained in the cytoplasm thereby preventing nuclear PKB signalling. Thus periplakin does not affect PKB signalling directly but can modulate the extent of nuclear PKB signalling by acting as a scaffold protein to PKB (van den Heuvel et al., 2002).

Periplakin also interacts with periphilin, a novel protein, through a small portion of the rod domain and the entire linker subdomain (Kazerounian and Aho, 2003). Periphilin, contains a functional nuclear localisation signal in the N-terminal region and homodimerises through a domain in the C-terminus. Periphilin partially colocalises with periplakin at the cell-cell junctions of differentiated keratinocytes and is crosslinked by TGases *in vitro* suggesting it may be a CE component (Kazerounian and Aho, 2003).

A portion of the periplakin rod domain and the periplakin linker subdomain links periplakin to the C-terminal tail of the mu opiod G-protein-coupled receptors (MOP-1

and MOP-1A) (Feng et al., 2003). The mu opiod receptors mediate the effects of morphine and heroin in the brain. The interaction between periplakin and MOP-1/MOP-1A does not disrupt agonist-induced internalisation of the receptors. However, the interaction specifically disrupts the activation of the downstream G protein thereby affecting the MOP-1/MOP-1A signalling pathway (Feng et al., 2003).

Immunoglobulin receptors (FcRs) are important for immunological responses. The cytoplasmic domain of FcγR1 (CD64), which is a receptor for immunoglobulin of the γ type, interacts with a portion of the rod domain and the linker subdomain of periplakin. FcγRI is expressed specifically in myeloid cells and is upregulated during inflammation. The interaction decreases ligand binding by the receptor and exogenous expression of the FcγRI-interaction domain of periplakin increases ligand-bound FcγRI endocytosis (Beekman et al., 2004).

1.5.3 Actin-and microtubule-binding domains

Many members of the plakin family, including the spectraplakin sub-family, contain actin-binding domains (ABDs) at their N-termini (Leung et al., 2002). The ABDs are composed of two adjacent calponin-homology domains (CH1 and CH2). The CH1 domain is capable of efficiently binding actin, in contrast to CH2, which only has a weak actin-binding activity (Fontao et al., 2001). The ABDs, and upstream regions, of plectin and BPAG1 isoforms can homodimerise and heterodimerise with each other, thereby crosslinking actin filaments (Fontao et al., 2001; Young et al., 2003).

Many plakin proteins are alternatively spliced, with some of the splicing events affecting the ABDs and upstream sequences (Fuchs et al., 1999; Karakesisoglou et al., 2000; Yang et al., 1996; Young et al., 2003). Some plectin 5' splice variants have a higher affinity for actin filaments than others, allowing modulation of the strength of actin binding in a tissue-specific manner (Fuchs et al., 1999). BPAG1n3 and MACF1a3 are splice variants that do not have a CH1 domain (Karakesisoglou et al., 2000; Yang et al., 1999).

Some isoforms of plectin localise to the hemidesmosomes where they interact directly with β4-integrin. The hemidesmosomal targeting domain of plectin coincides with the ABD and the binding of actin and β4-integrin are mutually exclusive such that hemidesmosomes are linked exclusively to IFs (Geerts et al., 1999; Rezniczek et al., 1998).

Microtubule (MT)-binding domains of plakin proteins are generally located at the C-terminal end. The spectraplakins contain both a GAR domain and a glycine-serine-arginine (GSR) repeat domain (Fig. 1.4). The GAR domain of plakins was so named due to its sequence similarity to domains in growth arrest specific-2 (GAS2) and GAS2-related protein on chromosome 22 (GAR22). The GAR domains of GAS2 and GAR22 coalign with MTs of transfected cells (Jefferson et al., 2004). The GAR and GSR domains of MACF1 and BPAG1 can independently associate with MTs in transfected cells (Sun et al., 2001). The GAR and GSR domains together, in one molecule, bind MT very strongly causing the MTs of transfected cells to bundle and rendering them resistant to MT-depolymerising drugs (Sun et al., 2001).

Some of the conventional plakins, plectin and desmoplakin, have a C-terminal GSR domain but lack the GAR domain (Fig. 1.4). The GSR domain of plectin coaligns with the MT cytoskeleton in contrast to the GSR domain of desmoplakin (Sun et al., 2001).

Loss of the CH1 domain in the N-terminus of BPAG1n3 prevents its association with the actin cytoskeleton and is thought to reveal an otherwise cryptic microtubule - binding domain within its head domain (Yang et al., 1999). A weak MT binding site is also present in this region of MACF1 (Karakesisoglou et al., 2000).

1.5.4 Rod domains

The rod domains of conventional plakins, such as desmoplakin and BPAG1, are composed of heptad repeats, which allow the proteins to form α-helical coiled-coil homodimers. Purified desmoplakin and BPAG1 proteins form long, flexible, parallel, in-register homodimers (O'Keefe et al., 1989; Tang et al., 1996). Plectin proteins also form parallel in-register homodimers; these in turn form antiparallel homodimers, i.e.

plectin tetramers, which associate through their folded end domains (Foisner and Wiche, 1987; Wiche et al., 1991).

Periplakin and envoplakin both have a central heptad repeat containing-region predicted to form a coiled-coil rod (Ruhrberg et al., 1997; Ruhrberg et al., 1996). The rod domains of envoplakin and periplakin are more related to each other than to those of other plakin family members (Ruhrberg et al., 1997). Sequence analysis of the heptad repeat regions of envoplakin and periplakin suggests that parallel in-register periplakin and envoplakin homodimers can form in addition to parallel in-register envoplakin/periplakin heterodimers (Ruhrberg et al., 1997; Ruhrberg et al., 1996). The formation of heterodimers between envoplakin and periplakin is unusual and thus far has not been seen for other members of the plakin family.

Periplakin/envoplakin hetero-oligomers were first identified in immunoprecipitation (IP) experiments, which showed that immunoprecipitation with an antibody to envoplakin pulled down periplakin and *vice versa* (Ruhrberg et al., 1997).

In transient transfections of keratinocytes, full length human envoplakin forms nuclear and cytoplasmic aggregates (DiColandrea et al., 2000). The envoplakin rod domain is necessary for the formation of these aggregates. Coexpression of full length periplakin in a 1:1 ratio with full length envoplakin prevents the formation of envoplakin aggregates. The periplakin rod domain is necessary and sufficient to prevent the formation of envoplakin aggregates (DiColandrea et al., 2000).

In vitro experiments with recombinant envoplakin and periplakin proteins, as well as their individual head, rod and tail domains, suggests that full length and rod-containing envoplakin protein fragments are insoluble *in vitro* (Kalinin et al., 2004). In contrast, full length periplakin and periplakin rod domain–containing fragments are soluble *in vitro*. Periplakin forms parallel in-register homodimers, as seen by electron microscopy and as previously predicted by Ruhrberg et al. (1997) (Kalinin et al., 2004). Envoplakin proteins become soluble when refolded, by gradual dialysis out of an 8M urea-containing buffer, in the presence of periplakin. Protein gel electrophoresis indicates that envoplakin and periplakin form heterodimers and their rod domains are sufficient for heterodimer formation.

Though periplakin can form homodimers *in vitro* it preferentially forms envoplakin/periplakin heterodimers (Kalinin et al., 2004). Periplakin/envoplakin heterodimers form higher order oligomers, *in vitro*, in the presence of their tail domains. These hetero-oligomers are further stabilised by the presence of their head domains (Kalinin et al., 2004). These *in vitro* experiments and the finding that periplakin and envoplakin can interact in transiently transfected cells where either one lacks a rod domain, suggest that envoplakin and periplakin can interact through regions outside their rod domains (Karashima and Watt, 2002). The mode of association of the heterodimers within the multimers is not known (Kalinin et al., 2004).

Some plectin and BPAG1 isoforms lack both a coiled-coil rod domain and spectrin repeats (Elliott et al., 1997; Okumura et al., 2002). The functions of these proteins and their ability to dimerise is not known, although the ABDs of plectin and BPAG1 and the intermediate filament binding domain of plectin have been shown to mediate dimerisation (Fontao et al., 2001; Steinbock et al., 2000; Young et al., 2003).

1.5.5 The amino terminal plakin domains

The N-termini of plakin proteins, including the spectraplakins, are composed of 6 plakin subdomains known as NN, Z, Y, X, W, and V, which together constitute the plakin domain. The NN, Z, Y, X, W, and V subdomains are composed of short heptad repeats (<4) thought to form α-helices, which in turn form antiparallel bundles. Nonhelical regions separate the antiparallel bundles and thus the subdomains (Green et al., 1992; Ruhrberg et al., 1996). The plakin subdomains are thought to fold such that they form an elongated globular domain (Green et al., 1992; O'Keefe et al., 1989; Tang et al., 1996).

The plakin domain of the conventional plakins acts as a protein-protein interaction domain and is thought to be important for targeting plakin proteins to membrane attachment sites (Jefferson et al., 2004). BPAG1e localises to the hemidesmosome, via interactions of the N-terminus with the transmembrane proteins BP180 and β4-integrin (Koster et al., 2003). The interaction with BP180 requires the Y subdomain of the

plakin domain. The N-terminal extension of BPAG1e, unique to this isoform, is essential for the interaction of the protein with the β4-integrin tail and is stabilised by the NN subdomain (Koster et al., 2003). The desmoplakin plakin domain is important for orchestrating many of the interactions of desmoplakin at the desmosomal plaque. The region involved in interactions with plakoglobin and plakophilin proteins includes the NN, Z, Y and most of the X subdomain of desmoplakin (Bornslaeger et al., 2001; Kowalczyk et al., 1997).

In the case of plectin and the spectraplakins, such as MACF1 and BPAG1a and b, little is known about the interaction partners of the plakin domain (Jefferson et al., 2004).

The plakin domains of envoplakin and periplakin have the same predicted structure as that of other plakin family members. Preceding the plakin domain, envoplakin has an N-terminal extension containing two tandem pairs of KGSP repeats, which are not found in other plakin family members and may constitute a PKC phosphorylation site (Ruhrberg et al., 1997; Ruhrberg et al., 1996).

Since the plakin domains of BPAG1e and desmoplakin mediate the interaction of the protein with plasma membrane attachment sites and the envoplakin and periplakin plakin domains have a similar predicted structure it was thought that the envoplakin and periplakin plakin domains may mediate their localisation to desmosomal and interdesmosomal plasma membrane sites. In the case of desmoplakin an N-terminal fragment encoding the NN, Z, Y and most of the X subdomains was sufficient to localise the protein to plasma membrane attachment sites (Bornslaeger et al., 1996). A similar construct of envoplakin (E1/2N, encoding the first 500 amino acids) does not efficiently localise to the desmosomes or the interdesmosomal plasma membrane (DiColandrea et al., 2000).

In contrast to envoplakin, expression of full length periplakin by transient transfection of primary keratinocytes does not cause the formation of protein aggregates. Full length periplakin localises to the apical plasma membrane and partially colocalises with desmoplakin at the desmosomes (DiColandrea et al., 2000). The first 495 amino acids of periplakin (P1/2N), encoding all of the NN, Z, Y and X subdomains, localise efficiently to the apical plasma membrane but have limited colocalisation with

desmoplakin (DiColandrea et al., 2000). At the apical plasma membrane, periplakin P1/2N localises to microvilli colocalising there with CD44 and actin (DiColandrea et al., 2000). Transfected periplakin P1/2N and endogenous periplakin of stratified keratinocyte cultures redistributes to actin-rich patches upon depolymerisation of the actin cytoskeleton by latrunculin B or cytochalasin D (DiColandrea et al., 2000).

1.6 Aims of thesis

Periplakin and envoplakin localise to the desmosome and interdesmosomal plasma membrane. The localisation of periplakin and envoplakin proteins at the plasma membrane, particularly the interdesmosomal plasma membrane, is thought to be important for the formation of the CE scaffold onto which the final CE structure is assembled (Ma and Sun, 1986; Ruhrberg et al., 1997; Ruhrberg et al., 1996; Steinert and Marekov, 1999).

The aim of my thesis was to understand how periplakin and envoplakin localise to the plasma membrane. Analysis of envoplakin E1/2N suggests that when transfected this domain does not efficiently localise to the desmosomes or microvilli (DiColandrea et al., 2000). Thus it was of interest to understand which domains of envoplakin are important for its localisation to the desmosomal and interdesmosomal plasma membrane and to understand the function of the KGSP repeats at the N-terminus of envoplakin, which are not found in other plakin family members.

Results suggest that periplakin can localise to the desmosomes and interdesmosomal plasma membrane independently of envoplakin (DiColandrea et al., 2000; Kalinin et al., 2004). Thus it was of interest to understand how periplakin associates with the actin cytoskeleton at the interdesmosomal plasma membrane as this may help us to understand more about the initiation of formation of the CE.

Yeast two-hybrid analysis, using the periplakin N-terminus as bait, identified a novel protein, which we have named kazrin. I shall describe my analysis of the kazrin gene, kazrin mRNA expression and the localisation of endogenous and transfected kazrin proteins in primary human keratinocytes.

In my thesis I describe analysis of triple envoplakin, periplakin and involucrin knock-out mice generated from the single knock-out mice (Aho et al., 2004; Djian et al., 2000; Määttä et al., 2001). Triple knock-out mice were analysed in order to understand further the role of envoplakin, periplakin and involucrin in the formation of the CE and the water permeability barrier of the skin.

My thesis provides further insight into the role of periplakin and envoplakin in the formation of the cornified envelope.

Some of the data described in this thesis have been published:

Määttä, A., DiColandrea, T., Groot, K. and Watt, F.M. (2001) Gene targeting of envoplakin, a cytoskeletal linker protein and precursor of the epidermal cornified envelope. *Mol Cell Biol*, **21**, 7047-7053.

Groot, K.R., Sevilla, L.M., Nishi, K., DiColandrea, T. and Watt, F.M. (2004) Kazrin, a novel periplakin-interacting protein associated with desmosomes and the keratinocyte plasma membrane. *J Cell Biol*, **166**, 653-659.

Chapter 2. Materials and Methods

2.1 Molecular Biology

2.1.1 General solutions

General solutions were supplied by Cancer Research UK (CR-UK) Central Services.

L-broth (LB) (CR-UK)

L-broth (LB) for bacterial culture comprised 1% Bacto-Tryptone (Difco), 0.5% yeast extract (Difco) and 170mM NaCl and was sterilised by autoclaving.

L-agar (CR-UK)

L-agar comprised 1.5% bacto-agar (Difco, w/v) in LB. The agar was dissolved by heating in a microwave oven and allowed to cool to 50°C before adding the selection antibiotic. The solution was then poured into 100mm bacteriological petri dishes and left to set on a level platform. Agar dishes were stored at 4°C, agar side up.

Antibiotic stock solutions

Ampicillin (Sigma, stock 100 mg/ml in dH_2O) was used as a selection antibiotic and was added to LB or L-agar to a final concentration of 100 μg/ml. Kanamycin (Sigma, 10mg/ml stock in dH_2O) was used to select at a final concentration of 50μg/ml

Tris/EDTA buffer (TE)

TE was used as a general storage buffer for DNA and comprised 10mM Tris-HCl and 1mM EDTA, pH8.0.

Tris-acetate-EDTA buffer (TAE)

A 50x stock solution was prepared by dissolving 242g Trizma base and 57.1ml glacial acetic acid (BDH) in dH_2O. 100ml 0.5M EDTA, pH8.0 were added and the final volume was made up to 1l.

Agarose/TAE gel

This was used in the electrophoresis of DNA. 0.8-2% (w/v) ultra pure agarose (Gibco BRL) was melted in a microwave oven in 1x TAE buffer. Ethidium bromide was added at 0.05 μg/ml to agarose solution before casting in gel mould. Typically, DNA was electrophoresed at constant voltage of 80-100V in 1x TAE buffer.

DNA loading buffer

6x DNA gel loading buffer comprised 0.25% bromophenol blue (Sigma), 0.25% xylene cyanol (Sigma) and 30% (v/v) glycerol in dH_2O. The loading buffer was stored at RT.

2.1.2 DNA techniques

Polymerase Chain Reaction (PCR) for cloning

PCRs were carried out using PWO (Roche), a high fidelity polymerase, lacking nuclease activity but retaining proofreading activity, which generates blunt ended PCR products.

PCR reaction mix; 25ng template DNA (plasmid containing sequence of interest)
0.5 units PWO (Roche)
0.2μM dNTP (Roche)
0.5 μmol of each primer
1x buffer with $MgCl_2$ as provided with kit
in total volume of 50 μl

In the case of PCRs of kazrin A and B fragments DMSO was added to 5% in order to improve PCR efficiency.

PCR reactions conditions; PCRs were typically carried out using the program below:
1:Initial denaturing step, 94°C for 2 mins
2:Denature at 94°C for 30 secs
3: Annealing carried out at 55 to 65°C for 30 secs
4: Extension at 72°C for 1 min per kilobase of sequence being amplified
5: steps 2 to 4 were repeated 30 times
6: Extension was completed with 2 mins at 72°C.

Enzymatic manipulation of DNA fragments

Restriction enzymes and T4 DNA ligase were purchased from NEB and used for restriction digestions and DNA ligations, respectively. Calf intestinal alkaline phosphatase (Boehringer Mannheim) was used to remove 5' phosphate groups from vector DNA fragments to prevent vector religation, without the incorporation of insert DNA (containing 5' phosphate groups) in ligation reactions.

Bacterial transformation

One Shot TOP10 competent E. coli (Invitrogen) were used for cloning of DNA. 0.1μg DNA from ligations or 1ng of plasmid DNA was added to a 25 μl aliquot of competent cells. The transformation was performed by heat shock according to the Manufacturer's instructions. BL21 cells (Amersham Pharmacia Biotech), used for production of bacterially expressed GST fusion proteins, were transformed by heat shock as per Manufacturer's instructions.

Preparation of plasmid DNA

To screen colonies after ligation and transformation, single colonies were picked and inoculated in 5 ml LB media containing the appropriate antibiotic, then grown overnight in a 37°C agitator. 2 ml of the overnight culture was used for small scale preparation of plasmid DNA whilst the remainder was stored at 4°C. Qiagen mini-prep kits (Qiagen Ltd.) were used for this initial plasmid purification.

For maxi preparations, 0.5 ml of the overnight culture was added to 200 ml LB plus antibiotic and incubated overnight at 37°C in an agitator. Bacteria were pelleted by centrifugation at 6000 g for 15 min in a Beckman J2-21 centrifuge. The plasmid DNA was then purified using a Qiagen maxi kit according to the Manufacturer's instructions.

Quantitation of nucleic acids

Nucleic acids were diluted in 10 mM Tris-HCl pH 8.5 and placed in disposable plastic UVettes (Eppendorf). Absorbance at 260nm and 280nm was read in an Eppendorf BioPhotometer with the correct DNA or RNA program set-up.

Purification of PCR or restriction enzyme digestion products

Reactions were run out on agarose gels. DNA fragments were visualised by ethidium bromide under low power UV light. Bands were excised using clean scalpels. Agarose gel fragments were melted and the DNA isolated using the QIAGEN gel extraction kit according to the Manufacturer's instructions.

2.1.3 Vectors and primers

IMAGE clones

IMAGE clones containing the cDNAs encoding mouse kazrin a (No. 3667377), human kazrin a (No.6180253), human kazrin b (No.4556194), human kazrin c (No.4651187), or human kazrin d (No. 4472821) were obtained from the MRC UK HGMP Resource Centre (Cambridge) and confirmed by sequencing the 5' UTRs and coding regions. Sequencing reactions were set up as described below.

Vectors

pCINeo (Promega) for transient transfection of mammalian cells

pEFlink–HA in pUC12 for transfection of N-terminal HA- tagged proteins in mammalian cells

pCINeo-F9 as described DiColandrea et al. (2000) for transfection of N-or C-terminally FLAG-tagged proteins in mammalian cells

pGEX6P-1 (Amersham Pharmacia Biotech) for expression of GST fusion proteins in E. coli

pCR-Blunt (Invitrogen) for subcloning PCR fragments

pGBKT7 (Clontech) for yeast two-hybrid screening. pGBKT7 encodes the GAL4 DNA-binding domain which can be fused upstream of a bait protein. pGBKT7 can be selected for in yeast by growth in media lacking tryptophan

pGAD10 (Clontech) was used for yeast two-hybrid screening. pGADT7 encodes the GAL4 AD which can be fused upstream of a prey protein. pGADT7 can be selected for in yeast by growth in media lacking leucine

Vectors were digested as described below. The resulting fragments were purified and treated with CIP to remove 5' phosphate groups and thus prevent re-ligation of the vector in the absence of insert DNA. Ligations were set up with a molar ratio of vector to insert of 1:1 and 1:3 or 1:5. Ligations were set up with 1xT4 ligase buffer and 1 unit T4 ligase (NEB).

Primers and cloning strategies.

Envoplakin primers were used to amplify DNA, which was inserted into the pCI-neo-F9 vector (pre-digested with SmaI) such that the envoplakin protein encoded was tagged at its C-terminus with a FLAG tag (Table 2.1).

Table 2.1 Envoplakin cloning primers

Primer Name	Sequence
hEnvN500R.dir	AAGGCCAGTGCTGTGGAGTCTCTTCGGCCCAGC
hEnvN500R.rev	AGGGCTCTCGGAGCCCTGCTTTGCATCATGGGT
EnvN1.dir	GCCACCATGTTCAAGGGGCTGAGCAAAGGCTCCCAG
EnvX.rev	CCGAAGAGACTCCACAGCACTGGCCTTCAG
EnvN41.dir	CTTCTCATCTCCCGCATGCAAGCCAACGCC
Env27.dir	TCCCCCAGCAGGCACAGCCGGGCTGCCACC
hEnvN41.rev	AAGGGCCAGCTCCTGGGTGGCAGCCCGGCTGTG
hEnvN32.rev	GCTGTGCCTGCTGGGGGAGCCTTTGGG
hEnvN117.rev	CTTCTCAATCTCCTCAGCCTGCGGGTGC
hEnvN100.rev	GTCCAGGAAGAGGTCCTTGAGCAGCAC
hEnvN139.rev	CTTCTCGTACAGGGCACGGTACTCCGCAC

Periplakin cloning primers were used to generate DNA fragments which were ligated into pCI-neo vectors pre-digested with EcoRI and SalI thus producing vectors encoding periplakin tagged with a HA tag at the C-terminus (Table 2.2).

Table 2.2 Periplakin cloning primers

Primer Name	Sequence
P63+HA+STOP.rev	CTAAGCGTAGTCTGGCACGTCGTATGGGTACCGACCCTCCTGCAGCCGAGCC AGGTCACTCTG
P133+HA+STOP.rev	CTAAGCGTAGTCTGGCACGTCGTATGGGTAATCCACTTCCTTCACCGCCAGC CTGTAG
P80+HA+STOP.rev	CTAAGCGTAGTCTGGCACGTCGTATGGGTACTTCTCAGAGTCCAACACCTTC TGCAGGGTCAC
P16+koz/atg+EcoR1.dir	GCGAATTCCGAGCGCCACCATGACTGTGCAGACCCGGAGCATCTC
P1+koz+ATG+EcoR1.dir	GCGAATTCCGAGCGCCACCATGAACTCGCTCTTCAGG

Periplakin PCR products, generated from the primers listed below, were used to generate yeast two-hybrid GAL4 DNA binding domain fusion proteins as used in the yeast two-hybrid screen which is described in more detail below. The yeast two-hybrid vector pGBKT7 was pre-digested with EcoRI and SalI (Table 2.3).

Table 2.3 Yeast Two-Hybrid Periplakin cloning primers

Primer Name	Sequence
P133PP-R1Sal	CGTCGACATCCACTTCCTTCACCGCCAGCCTGTA
P16 fwd-EcoR1	CGAATTCACTGTGCAGACCCGGAGCATCTCTAACAAG
P80 rev-Sal1	CGTCGACCTTCTCAGAGTCCAACACCTTCTGCAGGGTCAC
P63 rev-Sal1	CGTCGACCCGACCCTCCTGCAGCCGAGCCAGGTCACTCTG
P500F1-EcoR1	CGAATTCATGAACTCGCTCTTCAGGAAGAGAAAC

Kazrin yeast two-hybrid constructs were made by PCR amplification using the primers shown in Table 2.4. PCR fragments were digested with EcoRI/XhoI and inserted into a similarly digested pGAD10 vector.

Table 2.4 Kazrin yeast-two-hybrid cloning primers

Primer Name	Sequence
KC1 fwd	CTATTCGATGATGAAGATACCCCACCAAACC
KC89 fwd	GGAATTCCACCGCAAGGAGAGCGAGGATGCGGTCAAA
KC164 fwd	GGAATTCCATTCCCTCGCCATGCCGGGCGAGACGGTG
KC240 fwd	GGAATTCCCGAGCGACATCAACTCCCCTCGACACCGGACA
KC327 rev	GTGAACTTG CGGGGTTTTTCAGTATCTACGAT
KC239 rev	GCTCGAGTCATGTGGACGACCGGTCGCCTTCGGCGGCAGA
KC163 rev	GCTCGAGTCACCGCTTGGGGACGTCCTTGGTCAGCGTAGC
KC88 rev	GCTCGAGTCACTGCTCATAGTTGCGGATGAAGTCTCGGAG

The primers listed below were used for RT-PCR reactions to identify the kazrin mRNA isoforms expressed in different cell types (Table 2.5).

Table 2.5 Kazrin alternative splicing primers

Primer Name	Sequence
KIAA-5'- R1	CTCTCCTTGCGGTGCTGCTCATAGTTG
KIAA-5'control - F1	GGCAGATGAAGGAGATGTTGGCGAAGG
KIAA-1a-5' - F1	GTGACCAACCTGCGAGCCGAACTC
KIAA-1b-5' - F1	GCAGCCTGCGAGCAGTGCGTGGACG
KIAA-1c-5' - F1	TTGGAGGAAATTCGGAACCAGAAGAGTG
KIAA-1d-5' - F1	CCAGTTCCAGAACCACTGCTCTTCACTG

Kazrin HA primers were used to generate DNA fragments which were inserted into EFplink –HA in pUC12 predigested with BamHI and EcoRI in the case of kazrin A and B, or pre-digested with EcoRI alone in the case of kazrin C (Table 2.6).

Table 2.6 Kazrin HA transfection vector construction

Primer Name	Sequence
1A	GCGGGATCCATGATGGAAGACAATAAG
1B	CGGGGATCCATGCGGGCGGCCGACTCG
1C	GGAATTCGCCACCATGAAGGAGATGTTGGCGAAGGACCTGGAG
3'	GCGGAATTCTCACCAGTCCGCGTCCTC

Kazrin GST fusion constructs were made using the pGEX-6P-1 vector. A construct encoding GST protein fused to amino acids 49-327 of human kazrin C was made by excising the original clone obtained from the yeast two-hybrid screen with *EcoRI* and *XhoI*, followed by ligation into similarly digested pGEX-6P-1. A vector encoding GST protein fused to kazrin C was amplified using the primers listed in Table 2.7. The PCR fragment was digested with EcoRI and SalI and inserted into a similarly digested pGEX-6P-1 vector. The 3' primer was used in conjuction with 5' primers 1A and 1B listed in Table 2.6 to generate PCR fragments which were digested with BamHI and EcoRI. PCR fragments were inserted into similarly digested pGEX-6P-1 vectors.

Table 2.7 Kazrin GST fusion protein vector construction

Primer Name	Sequence
1C	GGAATTCGCCACCATGAAGGAGATGTTGGCGAAGGACCTGGAG
3'	GGTCGACTCACCAGTCCGCGTCCTCCTCTATGTAATA

DNA sequencing

In cases where the insert of a construct was generated by PCR the whole insert sequence was analysed. In cases where a fragment was subcloned from one vector to another the borders of the cloning sites were sequenced. Sequencing reactions were set up using BigDyeTerminator mix as made by the Equipment Park (CR-UK). Sequencing reactions were set up according to the Manufacturer's instructions and purified using DyeEx spin columns (QIAGEN). Samples were run on capillary sequencing gels (Prism 3730) by the Equipment park (CR-UK).

IMAGE clones were sequenced to confirm that the sequence data available on the public database were correct. Kazrin a, kazrin b, kazrin c and kazrin d coding sequences and 5'UTRs were submitted to GenBank/EMBL/DDBJ under accession numbers AY505119, AY505120, AY505121, and AY505122 respectively.

Primers used for sequencing were either conventional sequencing primers, such as T7, T3, Sp6, M13rev, M13 forward, were primers previously used for cloning purposes, or were specifically designed for sequencing. Primers used specifically for sequencing are listed in Table 2.8.

2.8 Sequencing primers

Primer name	Primer sequence
T7	AATACGACTCACTATAG
T3	ATTAACCCTCACTAAAC
Sp6	CATACGATTTAGGTGACACTATAG
M13 reverse	CAGGAAACAGCTATGAC
M13 forward	GTAAAACGACGGCCAGT
Envoplakin 1	TGAAGGCCTCGGAGCACGCATGCGCT
Envoplakin 2	CCTACCGCTGCTCTTTGGAGCCCAC
Envoplakin 3	CCCACACCCTTGGAGGACTT
Envoplakin 4	CCGTGCCCTGTACGAGAAGAT
Envoplakin 5	GGAGTACGAGCACTTCAAGC
Envoplakin 6	CCCACACCCTTGGAGGACTTG
Envoplakin 7	CCGTGCCCTGTACGAGAAGATG
Kazrin 1	TTGAGACCGCTGCTGTTC
Kazrin 2	ACCACGGGGTCAATGTTCTGC
Kazrin 3	GGCATGCGGGCGGCCGACTC
Kazrin 4	GGACATCAAAAACAGACCAC
Kazrin 5	ATTCGGAACCAGAAGAGTG
Kazrin 6	ATCTGTCCTCAGGCATTGGC
Kazrin 7	CGAGGGACATTTACAAGCAC
Kazrin 8	CAAAAACAGACCACATCCTC
Kazrin 9	GTTTTCACTTGTTAGAGGCG
Kazrin 10	AACCTGCGAGCCGAACTC
Kazrin 11	TCCGAGACTTCATCCGCAAC
Kazrin 12	AACAGACTCTCTACCACTCACAC
Kazrin 13	GGCAGATGAAGGAGATGTT
Kazrin 14	TCACCAGGTCTGTCTTCTCG
Kazrin 15	ACACCGAGCGACATCAACTC
Kazrin 16	ACATCTCCTTCATCTGCCG
Kazrin 17	AAGGCTTCTTTGGCTCTG
Kazrin 18	AGAGCCAAAGAAGCCTTG

2.1.4 RNA techniques

Radiolabelling of probes for Northern blotting

50ng gel-purified DNA fragments were denatured at 95°C for 5 minutes and radiolabelled by random priming using the Rediprime DNA labelling system (Amersham) and 50μCi [32P]-α-dCTP (ICN). The kit was essentially based on the method of Feinberg and Vogelstein (Feinberg and Vogelstein, 1983) with the exception that the heat-denatured DNA fragments were labelled for only 30 minutes at 37°C, using nonamers as primers instead of hexamers. Un-incorporated [^{32}P]-α-dCTP was removed using a Nick column (Pharmacia).

Northern blotting

A MessageMap Northern blot of multiple tissues from BALB-c mice (Stratagene) was used according to the Manufacturer's instructions. The kazrin probe was made by digestion of the IMAGE clone 3667377, encoding mouse kazrin a, with AfeI/XhoI. The probe was 585bp long, corresponding to nucleotides 755 to 1340 of the mouse kazrin A mRNA. This probe was able to recognise both kazrin a and b mRNAs. A β-actin control probe was supplied by Stratagene. Northern blots were exposed to Kodak X-Omat film at -80°C with an intensifying screen.

2.2 Yeast techniques

2.2.1 Yeast two-hybrid screening

Yeast two-hybrid protein interaction experiments and library screenings were performed using the MATCHMAKER GAL4 two-hybrid system 3 (BD Biosciences) according to the Manufacturer's's instructions. The host yeast strain was AH109 (MATa, trp-901, leu2-3, 112, ura3-52, his3-200, gal4D, gal80D, LYS2::GAL1UAS-GAL1TATA-HIS3, MEL1, GAL2UAS-GAL2TATA-ADE2, URA3::MEL1UAS-MEL1TATA-lacZ). The plasmids pGBKT7 and pGAD10 were used as the DNA-BD cloning vector and the AD cloning vector, respectively. Yeast were transformed by the modified lithium acetate method, using YEASTMAKER™ Yeast Transformation System 2 according to the Manufacturer's protocol (BD Biosciences).

The AH109 yeast host strain was transformed with the bait plasmid and a human keratinocyte MATCHMAKER™ cDNA library in the cloning vector pGAD10. Interactions were screened by the ability of cells to grow on selective medium (lacking leucine, tryptophan, histidine, and adenine) for 7 days at 28°C. Colonies that appeared were restreaked onto SD agar, lacking leucine and tryptophan (L^-T^-), but containing X-α-Gal (BD Biosciences), a chromogenic substrate used to detect α-galactosidase activity derived from the MEL1 gene. The pGAD10 plasmids from positive blue yeast colonies were identified by PCR sequencing. A single clone was obtained during screening that was successfully reconfirmed by co-transformation. The sequence was rescued by yeast plasmid rescue using YEASTMAKER™ plasmid isolation kit (BD Biosciences) according to the Manufacturer's instructions. The rescued plasmids were sequenced and found to encode part of the predicted protein KIAA1026 (kazrin). Library screening, reconfirmation and the identification of KIAA1026 was kindly performed by Kazunori Nishi (Keratinocyte laboratory, CR-UK).

2.2.2 Yeast transformation

To map the interaction between periplakin and kazrin further yeast transformations were carried out. Constructs used in the analysis are listed above. Solutions necessary for yeast transformations are listed in Table 2.9

Transformation-competent yeast were made by growing the yeast overnight on YPD agar at 30°C. Cells were scraped off the following day using a sterile bacterial loop, and swirled into 1ml dH_20. Yeast were spun down at 700g for 5mins and resuspended in 1ml solution 1. Yeast were again spun down and resuspended in a volume equivalent to 50μl per transformation reaction to be carried out.

Each transformation was carried out using 1μg bait plasmid (pGBKT7) and 1μg prey (pGAD) and 5μl herring testes carrier DNA (heated to 100°C for 5 mins to linearise the DNA and cooled on ice for 5 mins prior to use).

The DNAs were mixed and 50μl competent yeast added. Solution 2 (500μl per transformation) was added and the cells mixed thoroughly. Cells were incubated at 30°C for 30 mins and mixed every 10 mins. DMSO (20μl) was added and the cells incubated

Table 2.9 Yeast transformation solutions and agars

Solution 1	1.1xTE + 1.1xLiAc in dH_20
Solution 2	1xTE + 1x LiAc + 40% polyethylene glycol (PEG)
Solution 3	0.9% sterile NaCl
YPD agar	10% yeast extract, 20% Bacto-Petone, 20% D-glucose, 20% agar
L^-T^- agar	6.7% yeast nitrogen base, 20% D-glucose, 20% agar plus MATCHMAKER™ yeast transformation kit supplements lacking leucine and thymine. L^-T^- agar selects for presence of prey and bait vectors in the transformed yeast.
$A^-T^-H^-L^-$agar	6.7% yeast nitrogen base, 20% D-glucose, 20% agar plus MATCHMAKER™ yeast transformation kit supplements lacking adenine, leucine, histidine and thymine. $A^-T^-H^-L^-$agar selects for presence of prey and bait vectors and interaction of the proteins of interest they encode, in the transformed yeast.

10x TE, 10x LiAc and 50% PEG stocks were provided with the MATCHMAKER™ yeast two-hybrid kit.

at 42°C for 15mins, with mixing every 5mins. Cells were spun down and resuspended in 120µl solution 3. 60µl was spread on an L^-T^- control plate and 60µl on a selective $A^-L^-T^-H^-$ plate. Yeast were grown at 30°C for 4-6 days prior to analysis of growth. Individual roughly equal-sized yeast colonies grown on the L^-T^- plates were diluted in 100µl dH_20, a 5µl drop of this was put onto L^-T^- and $A^-L^-T^-H^-$ plates and grown for 2-4 days at 30°C, in order to accurately score growth or lack of growth on selective medium.

2.3 Computer analysis

2.3.1 Computer analysis of the predicted nucleotide sequences

The BLAST 2.0 (NCBI, Bethesda, MD) and BLAT (Golden Path Genome Browser, Santa Cruz, CA) programs were used to search mouse and human EST databases and genome sequences in order to identify the kazrin mRNA isoforms and genomic layout.

2.3.2 Computational analysis of the predicted amino acid sequences

BLAST 2.0 (NCBI, Bethesda, MD) searches were carried of human, mouse and non-mouse/non-human EST databases to search for homologies between kazrin and other known proteins and to analyse the sequence conservation between species. MacVector 6.5.3 (International Biotechnologies Inc., Cambridge, UK) was used for sequence alignments, analysis of hydrophilicity, and for predictions of secondary structure and the presence of transmembrane domains, molecular weight predictions and analysis of the relative amino acid compositions. Coiled-coil analyses were performed using COILS version 2.2 (Lupas et al., 1991). Nuclear localisation signals were analysed by NLS on Prosite (Cokol et al., 2000). Protein domain searches were performed through Pfam 10.0 at the Sanger Centre (Cambridge, UK) and CD-search at the NCBI (Bethesda, MD).

2.4 Cell Culture

2.4.1 General solutions

The Central Cell Services of CR-UK provided sterile distilled deionised water (dH_2O) and solutions that are indicated by "CR-UK". All reagents used were of tissue culture grade and kept sterile.

Phosphate buffered saline (PBS, CR-UK)

8g NaCl, 0.25g KCl, 1.43g Na_2HPO_4 and 0.25g KH_2PO_4 were dissolved in 1l dH_2O, the pH was adjusted to 7.2 and the solution was autoclaved. PBS was supplemented with 1mM $CaCl_2$ (B) and 1mM $MgCl_2$ (C) to make PBS-ABC.

EDTA solution (versene, CR-UK)

8g NaCl, 0.2g KCl, 1.15g Na_2HPO_4, 0.2g KH_2PO_4 and 0.2g ethyldiaminotetraacetic acid (EDTA) and 1.5ml 1% (w/v) phenol red solution were dissolved in 1l dH_2O, the pH was adjusted to 7.2 and the solution was autoclaved.

Trypsin solution (CR-UK)

8g NaCl, 0.1g Na2HPO4, 1g D-glucose, 3g Trizma Base, 2ml 19% (w/v) KCl solution and 1.5ml of 1% phenol red solution were dissolved in 200ml dH_2O, the pH was

adjusted to 7.7 and 0.06g penicillin and 0.1g streptomycin (Gibco BRL) were added. 2.5g pig trypsin (Difco, 1:250) was dissolved in 200ml dH_2O; air was bubbled through the solution until the trypsin dissolved. The trypsin solution was added to Tris-buffered saline, made up to 1l with dH_2O, sterilised by filtration through a 0.22μm filter (Millipore) and stored at -20°C.

Mitomycin C stock solution

Mitomycin C is an inhibitor of DNA synthesis and nuclear division (Tomasz et al., 1987). It is used to metabolically inactivate J2-3T3 cells for the keratinocyte cultures. 4mg mitomycin C powder (Sigma) was dissolved in 10ml PBS. The stock solution (0.4 mg/ml) was sterilised by filtration through a 0.22μm filter, aliquoted and stored at -20°C. In the treatment of J2-3T3 cells, mitomycin C solution was added to the cell culture medium at a final concentration of 0.4 μg/ml.

2.4.2 Cultured cell types

Human epidermal keratinocytes were isolated from neonatal foreskins, grown and serially passaged as described below. J2-3T3 cells were used as feeder cells to support human keratinocyte growth. Primary mouse keratinocytes were isolated from 3-4 day old mice as described below, and cultured to generate cell lines.

HeLa, NIH-3T3, EJ-28, COS and A431 cells were obtained from ATCC. Cells were all grown in E4 with 10% FBS and passaged every few days at a density of 1:6-12. Cells lines were transfected for isolation of protein lysates or the analysis of cells by immunofluorescence. Cells lines were transfected with Polyfect-TM (QIAGEN), GeneJuice (Novagen), or in the case of COS cells Lipofectamine-2000 (Invitrogen), according to the Manufacturer's instructions.

All cells, except for primary mouse keratinocytes, were cultured on plastic dishes or flasks of tissue culture grade (Falcon) in a humidified incubator at 37°C with 5% CO_2. Primary mouse keratinocytes were cultured on Biocoat Collagen I – coated dishes (BD Biosciences) at 32°C, 5% CO_2 , as above.

Media or any solutions added to cells were first warmed to 37°C. All cells were confirmed by the CR-UK Cell Production Unit as being negative for mycoplasma infection. Any cells with mycoplasma contamination were discarded.

2.4.3 J2-3T3 feeder cells

J2-3T3 cell cultures

Clone J2 of 3T3 Swiss mouse embryo fibroblasts is a clone selected for its ability to support keratinocyte growth (Rheinwald and Green, 1975; Watt, 1998). J2-3T3 cells were cultured in Dulbecco's modification of Eagle's medium (DMEM) (E4, CR-UK) supplemented with 10% (v/v) donor calf serum (DCS, Gibco BRL). When J2 cells approached confluence they were harvested by rinsing with versene and incubating at 37°C in trypsin diluted 1:5 in versene for 5 min. The trypsin was subsequently inactivated by dilution in serum-containing culture medium and the cells replated at a dilution of 1:10 or 1:20. J2-3T3 cells were replaced every 6-9 weeks with a new batch of low-passage cells to avoid overgrowth of transformed J2-3T3s.

Freezing and thawing of J2-3T3 cells

Cells were harvested as described above and pelleted. Cells obtained were resuspended in DCS containing 10% (v/v) sterile dimethyl sulphoxide (Gibco BRL). Cell suspensions from a confluent 75cm^2 flask were aliquoted into 4-6 cryovials (Nunc). Cryovials were stored in an insulated box at -70°C overnight and subsequently transferred to liquid nitrogen for long term storage. Cells were thawed by transferring the cryotube of cells from liquid nitrogen directly to a water bath at 37°C. As soon as the cell suspension was thawed, it was added to 10ml medium and centrifuged at 200g for 3 min. The recovered cells were resuspended into 15 ml medium and plated onto a 75cm^2 flask.

2.4.4 Primary human keratinocytes

Keratinocyte culture medium (FAD + FCS + HICE)

FAD powder (F12 + adenine + DMEM: Imperial Labs) was supplemented with 3.07 g/l NaHCO3, 100 IU/l penicillin and 100 μg/l streptomycin. FAD medium (CR-UK) was bubbled with CO_2 until the pH dropped below 7.0, then sterilised by filtration through a 0.22μm filter. Medium was stored at 4°C until use.

Stock solutions of additives were kindly prepared by Simon Broad (Keratinocyte Lab, CR-UK). 10^{-5} M cholera enterotoxin (ICN) was stored at 4°C. Hydrocortisone (Calbiochem) was dissolved in 95% ethanol at 5 mg/ml and stored at -20°C. 100 mg/ml recombinant human epidermal growth factor (Peprotech) was prepared by first dissolving in 1/100 volume 0.1M acetic acid (BDH) before adding to FAD medium containing 10% (v/v) batch-tested foetal calf serum (FCS, Imperial Labs.) and stored at -20°C. The additives were combined into a 1000x stock solution (HCE): 1ml hydrocortisone, 100µl cholera enterotoxin and 1ml epidermal growth factor stock solutions were added to 7.9ml FAD medium with 10% FCS and stored at -20°C. The final concentrations in the medium were 10^{-10} M cholera enterotoxin, 0.5 µg/ml hydrocortisone and 10 ng/ml epidermal growth factor. 1000x insulin stock solution (5 mg/ml in 5mM HCl, Sigma) was stored at -20°C. The final concentration in the medium was 5µg/ml insulin. Complete keratinocyte medium (FAD + FCS + HICE) was prepared by adding 10% (v/v) FCS, 1000x HCE stock solution and insulin solutions to the FAD medium prior to use (Watt, 1998).

Preparation of J2-3T3 cells as feeder cells

The culture of human keratinocytes is supported by co-cultivation with mitotically inactivated J2-3T3 cells, which are referred to as feeder cells (Rheinwald and Green, 1975). Feeder cells were incubated with 0.4 µg/ml mitomycin C for 2-3h at 37°C in order to inhibit mitosis. Cells were harvested and plated such that a 75cm^2 flask of treated J2-3T3s was divided equally between 9x 25cm^2 flasks. Keratinocytes were added within 24 hours of preparing the feeder layer.

Isolation of primary human keratinocytes

Primary human keratinocytes were kindly prepared by Simon Broad (Keratinocyte Laboratory, CR-UK). Neonatal foreskins were provided with the informed consent of the parents. Isolation of primary keratinocytes was carried out as soon as possible after circumcision (Watt, 1998). Under sterile conditions, using a pair of forceps and curved scissors, a piece of foreskin was trimmed of dermal and fatty tissues. The foreskin was cut into pieces of about 5mm^2 and transferred into a Wheaton Cellstir (Jencons) containing 5ml trypsin and 5ml versene and stirred over a magnetic stirrer at 37°C. Dissociated cells were collected every 30 min and added to 5ml keratinocyte culture

medium. The number of cells obtained was counted using a haemocytometer. Dissociation of cells from the tissue was continued with addition of fresh versene and trypsin solution. This procedure was repeated 2 to 3 times before the number of cells obtained started to decrease. The yield from a neonatal foreskin was usually between 1-5x 10^7 cells. Feeder cells had been plated onto 25cm^2 flasks in readiness. Isolated cells were pooled, pelleted and plated at a density of 10^5 cells per 25cm^2 flask. Cells were cultured until just confluent. One flask of cells was tested for mycoplasma infection by the CR-UK Cell Production Unit, while the remaining cells were harvested and frozen at 10^6 cells per ml as for J2-3T3 cells.

Serial culture of human keratinocytes

Frozen keratinocytes (passage 2-5) were thawed as described for J2-3T3 cells. The strains used were named km, kq, and kt. Each strain corresponds to keratinocytes isolated from a single individual. Cells were typically seeded at a density of 1-2x 10^5 per 25cm^2 flask; keratinocytes which were freshly thawed were plated at a density of 4-8x 10^5 cells per 25cm^2 flask to allow for loss of viability resulting from freezing and thawing.

Fresh medium was given to keratinocytes every 2 days. A day prior to any experimental manipulation, keratinocytes were fed with fresh medium. Keratinocytes were passaged just before they reached confluence. The cultures were rinsed once with versene and then incubated with versene for 5-10 min at 37°C. This treatment caused any remaining feeder cells to detach. Keratinocytes would round up but would not detach from the flask. The versene solution was discarded and the remaining keratinocytes were incubated in 5ml trypsin/versene solution (1 part trypsin and 4 parts versene) at 37°C for about 10 min, until all keratinocytes had detached from the flask. 5ml medium was added to the suspension and the number of cells was counted using a haemocytometer. The cells were pelleted and resuspended in medium as described and plated onto flasks with feeder cells. Keratinocytes could be cultured for up to 6-8 passages before they had to be discarded due to poor growth and excessive accumulation of terminally differentiated cells. Keratinocytes used for transfections were typically of early passage, passage 2-5.

Depolymerisation of actin cytoskeleton

In some cases cells were treated with latrunculin B (Calbiochem) or cytochalasin D (Calbiochem) for depolymerisation of the actin cytoskeleton prior to fixation. Latrunculin B (stock solution 400μg/ml in DMSO, stored at –20°C for no longer than 3 weeks) was used at a concentration of 200ng/ml for 3 hours. Cytochalasin D (stock solution 1.25mM in DMSO, stored at 4°C) was used at a concentration of 1.25μM for 2 hours as per (Xia et al., 1996).

Transfection of primary keratinocytes.

Primary keratinocytes were transfected on glass coverslips for immunofluorescence analysis. Glass coverslips were prepared as described below. Primary keratinocytes were harvested and plated at a density of 5-6.5x 10^5 per well of a 6-well plate in FAD+FCS+HICE. Cells were allowed to adhere for 1-2 hrs before being rinsed twice in PBS to remove any cells not adhered. Cells were subsequently cultured overnight in keratinocyte serum-free medium (KSFM, Gibko BRL) supplemented with bovine pituitary extract and insulin (Invitrogen) as per the Manufacturer's instructions. Keratinocytes were transfected with Fugene-6 (Roche). Fugene-6, 6μl, was added to 94μl of DMEM (Invitrogen) and left for 5 mins at RT. Subsequently the DMEM-Fugene mixture was added to 2μg of DNA to be transfected and mixed well by pippetting. The DMEM-DNA-Fugene mix was left at RT for 15-20 mins before addition of 700μl of KSFM with additives. The mixture was pippetted gently up and down twice before being added to the keratinocytes, which had been pre-washed in PBS. The transfection mixture , was left on the cells at 37°C for 2hrs. Following transfection,cells were rinsed twice with KSFM with additives, to remove any remaining transfection mixture and cultured overnight. Prior to fixation cells were grown in FAD+FCS+HICE for 1.5-5 hours. In the case of double transfections the total amount of DNA used was 2μg, using 1μg of each plasmid. In some cases the expression of one construct was more efficient than the other in this case the ratio of the two constructs was 1:2, i.e. more of the construct that was harder to transfect.

In some cases transfected keratinocytes or keratinocyte cultures were treated with inhibitors of signalling molecules. The factors used are listed in Table 2.10

Table 2.10 Inhibitors

Compound	Target molecule/s	Stock solution	Working concentration	Source/references
Bisindolylmaleimide (BimI).	PKC	5 mM	5 μM	Sigma (Martiny-Baron et al., 1993)
U0126	MEK1/2	10 mM	10 μM	Promega (Favata et al., 1998)

All stock solutions were made up in DMSO, aliquoted and stored at –20°C.

Keratinocytes treated with UO126 were treated from the time of transfection. Following overnight culture in KSFM with UO126, the keratinocytes were grown a further three hours in FAD+FCS+HICE in the presence of the inhibitor before fixation and analysis. In the case of BimI cells were treated with the inhibitor post-transfection for 20 mins in KSFM and a further 30 mins or 3 hours in FAD+FCS+HICE before fixation and analysis. Untransfected keratinocyte cultures were grown in FAD+FCS+HICE and treated as per post-transfected cells in the case of BimI, alternatively cells were treated with UO126 overnight in KSFM and a further three hours in FAD+FCS+HICE in the presence of UO126 prior to processing for immunofluorescence.

Quantitation of cell shape and actin changes

Human primary keratinocytes were transfected in parallel with HA-tagged kazrin isoforms or GFP vectors and analysed 16-18 hours post-transfection. Cells were stained for the HA tag and with phalloidin to stain the actin cytoskeleton and analysed 'blindly'. Cells with loss of the cortical actin band and altered shape were scored as altered. Cells that could not be assigned to either the normal or altered group were excluded from the statistical analysis. Number of excluded cells/total number cells analysed were as follows; Kazrin A 134/437; Kazrin B, 93/380; Kazrin C, 80/421; GFP, 92/464. Data were pooled from three independent experiments and statistical analysis performed using GraphPad QuickCalcs software.

2.4.5 Mouse keratinocyte culture

Primary mouse keratinocyte culture medium

A low calcium FAD medium was used which was prepared in the same way as normal FAD except calcium salts were not included in the DMEM and F12 formulations. The

calcium present in the FCS used as a supplement was removed by treatment of the serum with Chelex deionising resin (Watt, 1984). Chelex treatment was carried out as follows: 300g of Chelex 100 resin (Biorad; 100-200 mesh, sodium form) were added to 4L of dH_2O and stirred slowly at room temperature for at least an hour to generate a swollen resin form. The pH was adjusted to 7.0-7.5 with HCl and the swollen resin was then recovered by filtering through a stericup (Millipore). The recovered Chelex was added to 1L of FCS and stirred at room temperature for 1 h before being allowed to sit undisturbed for 30-60 min. The Chelex was removed and the FCS sterilised by filtering through a 0.22μm stericup (Millipore). The sterile chelated FCS was then aliquoted and stored at –20°C. Complete low calcium FAD was prepared by adding 10 % chelated FCS to low calcium FAD supplemented with the HICE cocktail at the concentration used for standard complete FAD. Additionally, 1 % standard FAD was added to produce a final free calcium ion concentration of approximately 0.1 mM.

Isolation of primary mouse keratinocytes

Keratinocyte isolation from mouse neonates was performed according to (Roper et al., 2001). Newborn mice (2-4 days old) were killed and placed on ice for at least 1 hour. The mice were then washed sequentially with 10 % Pevidine and twice with 80 % ethanol. Under sterile conditions the tails, limbs and heads of the mice were amputated. A longitudinal cut was then made along the backs of the mice and the skin removed with forceps. Harvested skins were spread out, epidermis side up, in petri dishes and covered with trypsin solution overnight at 4°C. The epidermis was then peeled off from the underlying dermis and minced into complete low calcium FAD using a pair of forceps. The released epidermal cells were pelleted by centrifugation at 200g for 3 min. The pellet was resuspended in complete low calcium FAD and filtered through a 70μm cell strainer (to remove debris) onto Biocoat Collagen I-coated dishes (BD Biosciences). Typically, the cells isolated from 1 mouse were plated onto 1 well of a 6-well plate. Periplakin null mice, a kind gift of S Aho (Thomas Jefferson University, Pennsylvania)(Aho et al., 2004), were used to generate a mouse keratinocyte line lacking periplakin expression (MKP-/-). Envoplakin null mice (Määttä et al., 2001) were used to generate a mouse keratinocyte line lacking envoplakin expression (MKE-/-).

MKWT cell line was generated from a wild type mouse. MKP-/-, MKE-/- and MKWT cell lines were grown in low calcium medium without a J2 feeder layer. MKneg2 cells were previously generated in the lab and are described in Romero et al.

(1999). Mkneg2 cells were grown in high calcium FAD. Mkneg2 cells differentiate as they become confluent.

Passaging of mouse keratinocytes and generation of cell lines

Primary mouse keratinocytes were cultured at 32°C with 5 % CO_2 in a humidified incubator and fed with complete low calcium FAD every 2 days. Cells were passaged when completely confluent and were split at no higher dilution than 1:2 as at low densities they tended to differentiate. To remove cells from the dish, they were rinsed twice with versene then incubated at 37°C with trypsin solution (not diluted in versene) until the keratinocytes detached. Complete low calcium FAD was then added, cells pelleted, resuspended in media and plated. Primary mouse keratinocytes could also be frozen down in a manner similar to other cell types except that chelated FCS with 10 % DMSO was used. Cells were cultured in this way for 10 or more passages at which point foci of transformed cells appeared in the cultures. Once the cells were transformed cells could be split at higher dilutions, typically 1:5.

MKWT, MKP-/- and MKE-/- cell lines were cultured in low calcium medium. To induce the cells to differentiate the cells were grown in high calcium for 4 days.

2.5 Immunological methods

2.5.1 General solutions

Paraformaldehyde solution

A 6% solution was prepared by adding paraformaldehyde powder (BDH) to PBS and heating at 60°C until mostly dissolved. A few drops of 1M NaOH were added to completely clear the solution which was then allowed to cool to room temperature before adjusting the pH to 7.6 with HCl. The stock was aliquoted and stored at –20°C. A 3 % paraformaldehyde solution, diluted in PBS-ABC, was used to fix cells and tissue.

Gelvatol/Mowiol mounting solution

The Gelvatol or Mowiol mounting solution was prepared as described by Harlow and Lane (Harlow and Lane, 1998). 2.4g Gelvatol (Monsanto Chemicals) or 2.4g Mowiol (Sigma) was mixed with 6g glycerol (Sigma) and vortexed. 6ml dH_2O was added, mixed and left to stand for 90 minutes at room temperature. 12.5ml of 200mM Tris-

HCl, pH8.5 was added and the solution was vortexed, heated to 50°C and vortexed again. Heating and vortexing were repeated three times and the solution placed on an end-over-end mixer overnight at room temperature. DABCO (Sigma) was added as an antifade agent to 2.5 % and mixed to dissolve. The solution was then centrifuged at 5500g for 10 minutes at room temperature and stored in aliquots at –20°C until use.

Blocking solutions for immunofluorescence.

PBS-GS/FSG PBS-ABC with 5% goat serum and 0.5% fish skin gelatin

PBS-FBS PBS-ABC with 10% fetal bovine serum

2.5.2 Antibodies

Generation of antibody to kazrin

A peptide corresponding to the last 20 amino acids of the kazrin protein (DPGLFD GTAPDYYIEEDADW) that are conserved between human and mouse kazrin proteins was synthesised by Protein and Peptide Chemistry, CR-UK, and conjugated to keyhole limpet haemocyanin (Perbio) to increase antigenicity. The conjugated peptide was injected into two rabbits (Harlan Sera-Lab limited). The bleed outs from both rabbits were used (LS3, LS4). Improved specificity and intensity of signal was produced by affinity purification of LS4 bleed outs using an aminolink column (BioRad). LS4 was eluted using acidic solutions to generate antibody most efficient for immunostaining, and eluted in acidic and basic solutions to generate antibody most efficient for immunoblotting. Typical dilutions of the affinity purified antibody used were 1:200 for immunostaining and immunoblotting.

A peptide corresponding to a region near the C-terminus of human kazrin (RQSQQTLYHSHPPHPADRQA) was synthesised by Protein and Peptide Chemistry, CR-UK. The peptide was conjugated to keyhole limpet haemocyanin (Perbio). The conjugated peptide was injected into two rabbits (Harlan Sera-Lab limited). The bleed outs from both rabbits used (KN1 and KN2). KN1 and KN2 antibodies were tested by immunoblotting, immunoprecipitation and immunofluorescence and found not to be effective as anti-kazrin antibodies.

Primary and secondary antibodies

All the antibodies used are listed in Tables 2.11 to 2.12. (Key to antibody uses: WB, Western blot; IF, Immunofluorescence).

Table 2.11 Primary antibodies

Antibody Name	Antigen specificity	Species	Dilution	References/ Source
Dp115-F	Desmoplakin	mouse monoclonal	IF 1:30-100	Generous gift of Prof. A. Magee (Parrish et al., 1987) + Prof. D. Garrod.
CR3	Periplakin	rabbit polyclonal	IF 1:500	(Ruhrberg et al., 1997)
TD2	Periplakin	rabbit polyclonal	IF 1:500 WB 1:500	(Määttä et al., 2001)
AE11	Periplakin	mouse monoclonal	IF 1:100 WB 1:500	Generous gift of Dr H. Sun (Ma and Sun, 1986)
CR5	Envoplakin	rabbit polyclonal	IF 1:500 WB 1:500	(Ruhrberg et al., 1997)
SY5	Human involucrin	mouse monoclonal	IF 1:100	(Ruhrberg et al., 1997)
VB3	Plakoglobin	Rabbit polyclonal	WB 1:1000	(Braga et al., 1995)
TUB-1A2	Tyrosinated tubulin	Mouse monoclonal	IF 1:100	Sigma Biosciences(Hudson et al., 1992)
LP34	pan keratin (K6, K18, K5)	mouse monoclonal	IF 1:100.	Generous gift of Dr A. Jetten (Lane et al., 1985)
AC40	Actin	Mouse monoclonal	WB 1:500	Sigma Biosciences (Herman, 1993)
IM7	CD44	rat monoclonal	IF 1:2-10	Generous gift of Dr. C. Isacke (Trowbridge et al., 1982)
ERK2	ERK2	Rabbit	WB	Santa Cruz

Sc-1647		polyclonal	1:1000	
GST	Glutathione S-transferase (GST)	Goat polyclonal	WB 1:1000	Amersham Pharmacia Biotech
HA-Y11 Sc-805	Haemagluti n-in tag	rabbit polyclonal	IF 1:400	Santa Cruz
M2	FLAG tag	mouse monoclonal	IF 1:1200	Sigma Biosciences

Table 2.12 Secondary antibodies

Antigen specificity	Conjugate	Species	Dilution	Source
mouse IgG, whole molecule	Alexa 488	Goat	1:500	Molecular Probes
rat IgG, whole molecule	Alexa 488	Goat	1:500	Molecular Probes
rabbit IgG, whole molecule	Alexa 488	Goat	1:500	Molecular Probes
mouse IgG, whole molecule	Alexa 594	Goat	1:500	Molecular Probes
rat IgG, whole molecule	Alexa 594	Goat	1:500	Molecular Probes
rabbit IgG, whole molecule	Alexa 594	Goat	1:500	Molecular Probes
rabbit IgG, whole molecule	Alexa 633	Goat	1:500	Molecular Probes
mouse IgG, whole molecule	HRP	Sheep	1:5000	BD Biosciences
rabbit IgG, whole molecule	HRP	Donkey	1:5000	BD Biosciences
goat IgG, whole molecule	Biotin	Rabbit	1:5000	DAKO
Streptavidine	HRP	-	1:10000	DAKO

2.5.3 Preparation of Cells for Immunofluorescence Staining

Cells were cultured on glass coverslips (Chance Propper Ltd.). Coverslips were first boiled in 7x detergent (ICN) for 30 minutes to remove silicone coating. They were rinsed thoroughly first in tap water and then in dH_2O. Washed coverslips were rinsed briefly in absolute ethanol and spread out on filter paper to dry completely before autoclaving.

Fixation of cells

Culture medium was discarded from cells and they were rinsed in PBS before fixing in 3% paraformaldehyde solution for 20 minutes at room temperature. The specimens were rinsed three times in PBS and stored in PBS-ABC at 4°C. In some cases cells were treated with CSK buffer for 5 mins at room temperature prior to fixation with paraformaldehyde.

Prior to use, specimens were rinsed in PBS and then incubated in blocking solution, to reduce binding to non-specific proteins, for at least 40 minutes at room temperature. In general, samples were blocked in PBS-GS/FSG, but in the case of the M2 antiFLAG antibody samples were blocked in PBS-FBS. In some cases cells were fixed using ice-cold methanol at –20°C for 2mins, or using a mixture of ice-cold 1:1 Methanol:Acetone for 2 mins at –20°C. Cells were rinsed thoroughly with PBS after fixation with methanol and stored in PBS-ABC at 4°C until ready for use.

Permeabilisation of cells

In order for the primary antibody to enter the cells and access the antigens cells were permeabilised using 0.2% Triton X-100 in PBS for 4 minutes at room temperature before rinsing three times in PBS and then incubated in blocking solution. Cells fixed with a methanol-containing mixture did not require additional permeabilisation with Triton X-100.

2.5.4. Preparation of Cryosections of human foreskin

Human tissues were obtained with appropriate consent. Cryosections were prepared by the Histopathology department (CR-UK). Using a cryomicrotome (Reichart-Jung), 6μm sections were cut from the tissue block in an orientation perpendicular to the surface of the tissue. The sections were mounted onto slides (Superfrost Plus, BDH) and stored at -70°C. All sectioning was performed by the CR-UK Histopathology Unit. To examine the morphology of the tissues frozen sections were stained with haematoxylin and eosin (H&E). For immunofluorescence staining, frozen sections were thawed at room temperature for 15-20 minutes. Sections were either stained after extraction in 0.1% Triton X-100 for 5 mins at room temperature or after fixation in ice-cold methanol at –20°C for 2 mins.

2.5.5. Immunofluorescence staining protocol

Tissue sections or cultured cells were incubated in blocking solution for 40 minutes at room temperature. Primary antibodies were diluted in the blocking solution (dilutions shown in Table 2.1) and applied to cells for 1hr at room temperature. The cells were rinsed three times in blocking solution and then incubated with the secondary antibody diluted in blocking solution (dilutions shown in Table 2.2) for 1hr at room temperature. The cells were then rinsed once in PBS, and three times in dH_2O, before mounting in Gelvatol/Mowiol solution. In some cases coverslips were mounted atop a small pedestal created by nail varnish to avoid squashing the sample as the Gelvatol/Mowiol dried and set.

In co-localisation experiments using a double immunofluorescence method, cells were stained with two primary antibodies. Both primary antibodies were of distinct species and these were subsequently probed with species-specific secondary antibodies conjugated to different fluorophores. The antibodies were applied in the following sequence: first primary; second primary; first and second secondary in combination, with thorough washes in blocking solution between each antibody application.

Stained samples were viewed with a Zeiss Axiophot microscope (Carl Zeiss) or with a laser scanning confocal microscope (LSM 510 equipped with an Argon laser to detect 458nm, 488nm wavelengths, and a helium-neon laser to detect 633nm wavelengths; Carl Zeiss, Inc.) A multitrack set-up was used so that bleed-through between channels was avoided. Pinhole sizes were equal in each laser track such that the thickness of the confocal slice analysed in each channel was equal and thus colocalisation was accurately detected. Lenses used were 63x and 40x pan-APOCHROMAT oil immersion lenses (numerical aperture 1.4) or C-APOCHROMAT water immersion lens (numerical aperture 1.2). Digital images were prepared using AdobePhotoshop 6.0 and Imaris 3.1.

Counterstaining.

TRITC-conjugated phalloidin (Sigma) was used to detect F-actin. A stock solution was made up in ethanol (0.25mg/ml) and diluted 1:500 in blocking solution. Phalloidin was applied to the cells for 15 mins after the secondary antibodies. DAPI (Molecular Probes) was used to detect the nuclei; a stock solution (1mg/ml) was made up in dH_20

and used at a dilution of 1:10,000 in dH_20. DAPI was applied to the cells for 30 mins after the secondary antibodies.

2.5.6 Immunogold electron microscopy

Adult breast epidermis was subjected to cryofixation using the HPM 010 high pressure freezing equipment (Leica) as described by (Studer et al., 1989).The frozen sample was freeze substituted in a Leica CS auto freeze substitution apparatus (Leica, Milton Keynes, UK), first in anhydrous acetone at –70°C for 72 hours, and then by warming to –50°C for 48 hours. The samples were washed with anhydrous acetone and embedded in Lowicryl HM20 resin at -50°C, followed by UV polymerisation at -50°C for 48 hours. Thin sections were prepared with a diamond knife on a Reichert Ultracut E microtome (Leica) and mounted on carbon-coated grids.

To label epidermal sections, grids were incubated on a drop of PBS for 10 min, blocked with 0.05% fish skin gelatin in PBS (FSG/PBS) for 30 min and then incubated with a 1:5 dilution of the primary antibody for two hours at room temperature. Primary antibodies used were LS4 affinity purified polyclonal antibody to kazrin and Dp115F monoclonal to desmoplakin. Dp115F antibody was concentrated five-fold for use in immunogold electron microscopy, using Microcon-30000 concentrators as per the Manufacturer's instructions (Millipore). Sections were washed three times with FSG/PBS and then incubated with the appropriate secondary antibody for 30 min. Protein A conjugated to 10nm gold (Cell Biology Department, Utrecht, The Netherlands) was diluted 1:65 for detection of kazrin polyclonal antibody; goat anti-mouse IgG conjugated to 10nm gold (BBInternational, Cardiff, UK) was used for detection of desmoplakin monoclonal antibody. After three washes each in PBS and distilled water, the sections were air-dried, contrasted with saturated aqueous uranyl acetate (10 min) and lead citrate (4 min), and examined with a Jeol TEM 1010 electron microscope (JEOL UK Ltd. Hertfordshire, UK). Negative control grids were stained using the method as described above but with omission of the primary antibody. Images were captured using a digital Gatan 2K camera (Gatan UK, Oxford, UK). Immunogold electron microscopy and immuno-EM staining was kindly performed by R. Watson and S. Gschmeissner (Electron Microscopy Laboratory, CR-UK).

2.6 Biochemistry

2.6.1 Extraction of proteins

General lysis buffers

Western lysis buffer 10mM Tris pH 7.4, 150mM NaCl, 0.5% NP40, 0.2% CHAPS, 0.1% NaN_3 and 5mM EDTA pH 8.0.

Cytoskeletal extraction buffer (CSK) 50mM NaCl, 300mM sucrose, 10mM PIPES, pH 6.8, 3mM $MgCl_2$ and 0.5% (v/v) Triton X-100 (Fey et al., 1984).

Laemmli sample buffer (LSB) 125mM Tris, pH 6.8, 2% (w/v) SDS, 20% (w/v) glycerol, 10% β-mercaptoethanol and 10mM EDTA, pH 8.0.

Extraction of proteins for Western blot analysis

Keratinocytes that were to be harvested for Western blot analysis were washed twice in PBS, then lysed on ice. The buffer was supplemented with protease inhibitor tablets without EDTA (Roche), 1 per 10ml.

Cells were scraped in the relevant lysis buffer on ice. Cell debris was pelleted by centrifugation at 16000 *g* for 10 min at 4°C in a bench top centrifuge. The supernatant was transferred to a new tube and the lysate stored at –70°C. Immediately prior to use samples were thawed and assayed for protein content.

BCA protein assay

The concentration of protein in samples was determined using a BCA protein assay kit (Pierce). The kit is based upon the Biuret reaction involving the reduction of Cu^{2+} ions to the Cu^{1+} (cuprous) ion by protein in alkaline medium. Chelation of the cuprous ion to bicinchoninic acid (BCA) molecules provides a sensitive colorimetric detection method with the reaction product exhibiting a strong absorbance at 562nm. The absorbance is linear over a 20-2000 μg/ml protein concentration range. A protein standard curve was produced from 0 to 2000 μg/ ml protein by making dilutions of a 2 mg/ml BSA solution (Pierce) into PBS according to the Manufacturer's instructions. Protein samples to be assayed were diluted 1:5 to 1:20 in PBS to minimise interference of lysis buffer detergent and supplements with the reaction, and also to place the protein concentration within the standard curve. The assay was set up on a 96-well plate (DYNEX Technologies) according to the Manufacturer's instructions and all standards and samples were assayed in triplicate wells. The plate was incubated at 37°C for 30 min

and the absorbance at 595nm was then read on a Molecular Devices microplate reader. The protein concentration of each sample was determined against the standard curve.

2.6.2 SDS-PAGE and Western blotting

Laemmli sample buffer

2x Laemmli sample buffer (reducing) comprised 125mM Tris-HCl, pH6.8, 2% SDS, 20% glycerol, 0.02% bromophenol blue and 10% (v/v) β-mercaptoethanol. The sample buffer was aliquoted and stored at RT. β-mercaptoethanol was added just prior to use.

SDS-PAGE

Vertical mini-gel electrophoresis apparatus (Atto) was used. Gels were prepared between glass plates using the method of Laemmli (Laemmli, 1970). Table 2.13 describes the gel compositions. Immediately after pouring the resolving gel solution, 0.5 ml of dH_2O was carefully applied to ensure a level interface, as well as to eliminate an air-acrylamide interface. Gels were allowed to polymerise at room temperature for approximately 60 min. The dH_2O layer was discarded from the top of the resolving gel and the stacking gel solution was then poured. An 8-or 12-well comb was inserted to create wells and the gel was left to polymerise. After the gel had set, the comb was removed and the wells were flushed with SDS-PAGE running buffer comprising 50mM Trizma base, 384mM glycine and 0.1% SDS.

Equal amounts of protein from each sample (typically 10-20μg total protein) were diluted into Laemmli sample buffer and placed in a 100°C hot block for 5 min before being briefly spun down in a bench-top centrifuge and applied to the wells using capillary pipette tips. When running samples to detect the presence of transfected proteins equal volumes from parallel transfected 6-well plate wells was loaded, typically 10μl from 100μl total. 10μl pre-stained rainbow molecular weight markers (Amersham) were added to 10μl Laemmli sample buffer, boiled for 5 min and loaded into one of the wells. Samples were electrophoresed at 120V until the dye front had run off the bottom of the gel and the gel was then removed and prepared for Western blot.

Table 2.13 Preparation of SDS-PAGE gels

Solution	Contents
Solution A	40 % Acrylamide mix (37.5:1 acrylamide to bis-acrylamide ratio) (Amresco)
Solution B	1.5M Tris-HCl, pH 8.8 (BDH)
Solution C	10 % SDS in dH_2O
Solution D	0.5M Tris-HCl, pH 6.8 (BDH)
AP	10 % ammonium persulphate (Bio-Rad) in dH_2O.
TEMED	N,N,N',N'-tetramethylethylenediamine (Bio-Rad)

Resolving gels (16 ml)

	A	B	C	dH_2O	AP	TEMED
8 %	3.2 ml	4 ml	0.15 ml	8.6 ml	50 ml	10 ml
10 %	4 ml	4 ml	0.15 ml	7.8 ml	50 ml	10 ml

Stacking gel (10 ml)

	A	C	D	dH_2O	AP	TEMED
	1.25 ml	0.1 ml	2.5 ml	6.09 ml	50 ml	10 ml

In some cases 4%-12% gradient pre-cast gels (Invitrogen) were used according to the Manufacturer's instructions. These gels were treated the same as self-cast gels.

Transfer buffer

The transfer buffer for Western blotting was made up freshly each time: 9.085g Trizma base and 42.75g glycine were dissolved in 500 ml dH_2O to which was added 15 ml of a 10 % SDS solution. The buffer was made up to 1.2l before the addition of 300 ml of methanol and was then thoroughly mixed.

Western blotting

After electrophoresis, proteins were transferred onto reinforced nitrocellulose (Amersham Biosciences). Mini-Trans Blot Cells (Bio-Rad) were used to transfer the proteins and were set up according to the Manufacturer's instructions. Transfer took place on the bench for 1 hour 15 min at 350mA current using the supplied cooling units. The blot was then rinsed briefly in PBS containing 0.1 % Tween-20 (PBST) before

blocking with 5 % milk powder (99 % fat free, Premier Brands UK Ltd.) dissolved in PBST, for at least 1 hour at room temperature.

Probing blots with antibodies and ECL detection

Blocked membranes were incubated with primary antibody typically diluted in 5 % milk powder solution in PBST. Some antibodies (according to the Manufacturer's instructions) were diluted in 5 % BSA in PBST. Incubation with primary antibody was at 4°C overnight or 2-3 hours at RT, with gentle agitation. After 4 x 15-20 min washes with PBST, the blots were incubated for 1 hour at room temperature with HRP-coupled secondary antibody diluted 1:5000 in 5 % milk, PBST. Membranes were then washed 4 times with PBST again. To detect bound HRP, a chemiluminescence kit was used according to the Manufacturer's instructions (ECL western blot analysis, Amersham Biosciences). X-ray films were exposed in autoradiography cassettes lined with reflective screens.

Prior to the reprobing, blots were stripped in a 200 mM glycine pH 2.5 solution containing 0.4 % SDS for 30 min at room temperature with agitation. Blots were then rinsed in 1M Tris-HCl pH 7.5 and washed 3 times for 5 min each with PBST before re-blocking and subsequent incubation with another primary antibody.

Coomassie staining of SDS-PAGE gels.

In some cases proteins were not transferred to nitrocellulose, but were stained with Coomassie (0.1% Coomassie blue-acid blue 15 in 40% methanol, 10% acetic acid). Gels were stained for 20-60 mins with gentle agitation at room temperature. Gels were subsequently placed in destain (40% methanol, 10% acetic acid) with several changes for 2-6 hrs at room temperature, until distinct protein bands on the gel could be seen.

Coomassie stained gels were placed onto 3mm filter paper and dried in a gel drier at 80°C for 2 hours. Dried gels were kept for further analysis or storage.

2.6.3 Calf intestinal alkaline phosphatase treatments of protein lysates.

COS cells were transfected with Lipofectamine-2000 according to the Manufacturer's instructions in 6-well plates. Cells were transfected with 2μg DNA using 6μl of Lipofectamine reagent, according to the Manufacturer's instructions. 20hrs post-

transfection cells were lysed in WLB as described above. 100μg of protein was used per calf intestinal alkaline phosphatase (CIP) reaction. In control reactions the CIP was replaced by an equal volume of dH_20.

The reaction mix consisted of: 100μg protein, 1mM Mg^{2+}, and 25 units CIP (or dH_20) in a total volume of 100μl. The reactions were carried out for 10 mins at 30°C and quenched by the addition of an equal volume of LSB with β-mercaptoethanol.

2.6.4 Induction of cross-linking by transglutaminases

Confluent keratinocyte cultures were washed twice in serum-free growth medium (FAD alone) and subsequently treated in 4 different ways. Untreated samples were incubated in serum-free medium for 5 hours. Cells were also treated with 0.04% Triton X-100 in serum-free medium for five hours to activate transglutaminases and induce the formation of cornified envelopes (Rice and Green, 1979). To inhibit the activation of transglutaminases by Triton X-100 cells were pretreated with 20mM cystamine, pH7.5 for 30 mins and subsequently with 20mM cystamine in the presence of 0.04% Triton X-100 for 5 hours. As a control for the cystamine treatment, cells were pre-treated with 20mM cystamine for 30 mins followed by treatment with 20mM cystamine alone for 5 hours. At the end of the treatments cells were lysed in equal volumes of Laemmli sample buffer. Equal volumes of lysate were loaded on gels for analysis.

2.6.5 *In vitro* transcription and translation

An *in vitro* transcription and translation (TNT) kit (Promega) was used according to the Manufacturer's instructions. 0.5μg DNA of each construct was used. Prior to use the DNA was cleaned through a PCR purification kit (QIAGEN), used according to the Manufacturer's instructions, in order to remove ions and EDTA which may interfere in the TNT reaction. The DNA was added to 8μl of the TNT reticulocyte lysate and 0.75μl ^{35}S labelled methionine (4μCi) (Amersham Pharmacia); the volume was made up to 10μl with dH_2O. Reaction mixtures were mixed by pipetting and the reaction was carried out at 30°C for 90 mins. 1μl of the reaction was run on a 10% gel for analysis. Gels were stained with Coomassie and then dried as described above. The dried gels were exposed to Kodak X-Omat photographic film to detect the ^{35}S methionine-labelled proteins.

2.6.6 GST pull-down assay

GST fusion protein production

pGEX6P-1 vectors encoding kazrin proteins downstream of glutathione S-transferase (GST) protein or GST alone, were transformed into BL21 *E. coli*. BL21 cells are a protease-deficient strain for more efficient production and purification of the GST fusion proteins. BL21 cells also express lysozyme under the control of isopropyl-β-D-galactosidase (IPTG) such that as GST protein production is induced by the addition of IPTG to the culture medium, so is the lysozyme. Thus, once cells are pelleted and sonicated lysis occurs rapidly, minimising protein degradation.

Single transformed BL21 colonies were grown overnight in Ampicillin (100μg/ml) and Chloramphenicol (25μg/ml) in LB (see below). The overnight culture was diluted 1:10-20 in Ampicillin/Chloramphenicol in 200ml LB. The culture was grown with shaking at 37°C. At frequent intervals the optical density at 600nm wavelength (OD_{600}) was measured. When the OD_{600} of the cultures was between 0.65 and 0.75 and the cells were in mid-log phase, IPTG was added to a concentration of 1mM. Cultures were subsequently grown at 37°C or 32°C for a further 3 or 4 hours. Samples were taken before the addition of IPTG and after 3 or 4 hours of growth in its presence; these samples were used for analysis as explained below. IPTG induced the production of the GST fusion protein encoded by the pGEX6P-1 vector.

Three to four hours post-induction of protein production by addition of IPTG, cells were pelleted at 4°C for 30 mins at 5000rpm. The supernatant was removed and the pellet stored on ice. The cell pellet was resuspended in 10ml PBS containing 1% Triton X-100 and briefly sonicated (3x5 seconds) on ice in order to lyse the cells and release the proteins. Triton X-100 was added to facilitate solubilisation of proteins. The crude extract was centrifuged at 10,000g for 5 mins at 4°C to separate the insoluble from the soluble proteins. A fraction of the cell pellet and supernatant was analysed on a Coomassie-stained gel, in order to determine the efficiency of protein production and the proportion of the protein that was in the soluble fraction following cell lysis. The level of protein production was roughly equivalent after 3 or 4 hours of induction.

GST fusion protein purification and quantification

Glutathione-Sepharose 4B beads (Amersham) were prepared by washing in cold PBS and pelleting gently at 550g for 3-5 mins at 4°C. The beads were resuspended in cold PBS with 1% Triton X-100 and pelleted as before. The supernatants from GST fusion protein production were added to the beads and the samples left on a rotor at 4°C for 1 hour in the presence of a protease inhibitor tablet (Roche). Beads were pelleted once more and the unbound proteins removed by two washes in cold PBS with 500mM KCl and subsequently with three washes in cold PBS. The GST proteins were eluted off the GST beads by the repeated addition of 1ml of Tris pH 8.0 with 5mM glutathione and protease inhibitors. The beads were pipetted up and down gently and spun down. The supernatant was removed as fraction 1. This process was repeated 5 times to obtain 5 GST fusion protein fractions. 5% glycerol was added to each fraction to improve protein stability in storage at –70°C. Small amounts of each fraction of each kazrin fusion protein type and GST alone were run on a gel, Coomassie-stained and dried in order to determine the quality and quantity of the GST proteins isolated and the fractions to use for the pull-down experiment.

GST pull-down experiment

Glutathione-Sepharose 4B beads were prepared as described above. Roughly 40µl of GST bead slurry were used to bind to 10µg of GST fusion protein or GST protein alone; the volume was made up to 500µl with CSK lysis buffer containing protease inhibitors. The beads and GST proteins were placed on a rotor for 90 mins at 4°C to allow them to rebind. Beads were subsequently pelleted and the supernatant removed.

Primary keratinocyte cultures were lysed in CSK buffer, as described above, and the lysates added to the GST protein/beads. Lysates were made from 1-2 day post-confluent keratinocytes. Lysates generated from 20-25cm^2 of culture were used per pull-down reaction. The lysates and GST protein/beads were rotated at 4°C for either 4 hours or overnight. Beads were pelleted and washed four times with cold PBS. In the final spin as much supernatant as possible was removed and 30µl LSB containing 10mM β-mercaptoethanol was added. Samples were run on SDS-PAGE gels together with a lysate alone control corresponding to 4% of the lysate used in the pull-down reaction. Proteins were subsequently transferred to nitrocellulose and analysed by immunoblotting.

2.7 Mouse techniques

Mice lacking the envoplakin gene, generated in the lab (Määttä et al., 2001), were bred with mice lacking periplakin (Aho et al., 2004) and mice lacking involucrin (Djian et al., 2000) to generate triple knockout mice (lacking expression of envoplakin, periplakin and involucrin). Mouse matings were set up by A. Määttä and L. Sevilla (Keratinocyte Laboratory, CR-UK) in collaboration with the mouse facilities at Clare Hall (CR-UK).

2.7.1 Toluidine Blue barrier function assay

Toluidine blue barrier function assays were done in collaboration with L. Sevilla (Keratinocyte Laboratory, CR-UK). The staining protocol was carried out essentially as described (Hardman et al., 1998; Koch et al., 2000). Timed matings of wild type (BL6) mice and triple knockout mice were set to generate wild type, triple heterozygous and triple knockout litters. The matings were set up in a 12 hour time bracket in order to minimise differences between litters due to differences in the timing of the mating. The middle of the 12 hour time period was considered embryonic day zero. At embryonic days 15.5, 16.5 and 17.5 post plugging the mice were sacrificed and the uteri of the mothers removed and placed in a dish of ice-cold PBS. The amniotic membrane surrounding each embryo was removed. Embryos were weighed and subsequently submerged into a methanol series made in PBS. Embryos were dehydrated by moving them sequentially from 25% methanol, to 50%, to 75% to 100%. Embryos were left in each methanol solution for 60 seconds. Following dehydration the embryos were rehydrated by dipping into 75% methanol solution, followed by dipping in a 50% and a 25% methanol solution prior to a PBS alone solution, again leaving the embryos in each solution for 60 seconds. After the preparations in methanol the embryos were stained in 0.0125% toluidine blue (Sigma), dissolved in H_2O, for 60 secs. The embryos were destained in several changes of PBS and stored in PBS at 4°C overnight. Images were taken using a dissecting microscope and conventional photography.

2.7.2 Isolation of cornified envelopes

Cornified envelope (CE) isolation was carried out as described Määttä et al., (2000). A 5mm by 5mm square of adult mouse ear tip was taken from each mouse and boiled in 500µl CE isolation buffer containing 20mM Tris-HCl (pH7.5), 5mM EDTA, 10mM

dithiothreitol (DTT) and 2% SDS for 20 mins. After boiling, the dermis could be removed from the sample and the CEs pelleted by centrifuging at 5000g. The CEs were washed twice in CE wash buffer (as isolation buffer, but with 0.2% SDS) and stored at 4°C in 200 µl wash buffer. Samples were gently resuspended and 20µl placed on a slide and covered by a coverslip. Nail varnish pedestals were made on the slide such that the sample could be placed underneath. Finally, the coverslip edges were sealed in nail varnish to prevent drying out of the sample. CEs from three triple knockout and two triple heterozygous mice were examined. All the mature envelopes were scored in ten randomly selected photographic fields, corresponding to 215 CEs from heterozygous mice and 433 CEs from triple knock-out mice. Pictures were taken by phase contrast microscopy. The samples were analysed blindly. The surface areas of the CEs were measured in pixels using NIH Image software. Statistical analysis was performed using GraphPad QuickCalcs software.

2.7.3 Scanning electron microscopy

Samples were taken from adult mouse feet either directly or after fixation, dehydration and critical point drying of the feet. Samples were rotary shadowed with platinum and observed using a 6700 field emission gun scanning electron microscope (FEG-SEM, JEOL, UK).

Preparation of unfixed samples

Feet were removed from adult mice. SEM metal sample stubs with attached sticky pads were used directly on mouse paw skin to 'tape strip' away epidermal layers for analysis.

Critical point drying

Samples were obtained and fixed immediately in 2.5% glutaraldehyde/4% PFA in Sorensons PBS (made up by EM department, CR-UK). Samples were transferred to 2% PFA after fixation. Samples were placed in a critical point drying machine and dried according to the Manufacturer's instructions. After drying the samples were prepared for SEM as described for unfixed samples. SEM was done in collaboration with Steve Gschmeissner (Electron Microscopy Department, CR-UK).

2.8 List of suppliers and distributors

Aldrich Chemical Company Ltd. Dorset, UK.

American Tissue Culture Collection (ATCC), Rockville, Maryland, USA.

Amresco, Solon, Ohio, USA.

Amersham Biosciences, Amersham, Buckinghamshire, UK.

Atto – supplied by Bio-Rad.

BBInternational, Cardiff, UK.

BDH Laboratory Supplies Inc., Hemel Hempstead, Hertfordshire, UK.

Beckman Instruments, Palo Alto, California, USA.

Becton-Dickinson, Lincoln Park, New Jersey, USA.

Bio-Rad Laboratories Inc. Hemel Hempstead, Hertfordshire, UK.

Boehringer Mannheim UK Ltd. Lewes, East Sussex, UK.

Calbiochem -Novabiochem (UK) Ltd. Nottingham, UK.

Carl Zeiss Ltd. Welwyn Garden City, Hertfordshire, UK.

Cell Signalling Technology Inc, Beverly, MA, USA.

Clontech, Palo Alto, UK.

Costar Europe Ltd, Badhoevedorp, Holland.

Coulter Electronics Ltd. Harpenden, Herts, UK.

Covance Research Products Inc., Berkeley, CA 94710, USA

DAKO A/S, Denmark.

Developmental Studies Hybridoma Bank (DSHB), University of Iowa, Iowa, USA.

Difco Laboratories, Manston, Wisconsin, USA.

DYNEX Technologies Inc, Chantilly, VA, USA.

Eastman Kodak Co. is distributed by Sigma Chemical Co.

EOS Electronic, South Glamorgan, Wales, UK.

European Collection of Animal Cell Cultures (ECACC), Salisbury, UK.

Gatan UK, Oxford, UK.

Genetics Research Instrumentation Ltd. Dunmow, Essex, UK.

Gibco BRL/Life Technologies Ltd. Paisley, Renfrewshire, UK

Harlan Sera-Lab limited, Hillcrest, UK

Hoefer Scientific Instruments is distributed by Biotech Instruments Ltd., Beds, UK.

Hydro Medical Sciences Division, Brunswick, New Jersey, USA.

ICN Pharmaceuticals Ltd. Thame, Oxon, UK.

Imperial Laboratories (Europe) Ltd. Andover, Hampshire, UK.

Jackson Immunoresearch Laboratories, Luton, Bedfordshire, UK

Jencons, Leighton Buzzard, Beds, UK.

Monsanto Chemicals. Springfield, Massachusetts, USA.

Millipore, Harrow, Middlesex, UK

Molecular Probes, Leiden, Netherlands.

New England Biolabs (NEB). New York, USA.

Nunc A/S, Roskilde, Denmark.

Peprotech, Rocky Hill, New Jersey, USA.

Perkin-Elmer Co. Foster City, California, USA.

Pharmacia Biotech. Uppsala, Sweden.

Pharmingen, San Diego, California, USA.

Pierce, Rockford, Illinois, USA.

Premier Brands UK Ltd. Knighton, Stafford, UK.

Promega UK Ltd. Southampton, UK.

Qiagen Ltd. Crawley, UK.

R&D Systems, Abingdon, Oxford, UK.

Santa Cruz Biotech. Inc. Santa Cruz, California, USA.

Savant supplied by Life Sciences International, Basingstoke, Hampshire, UK.

Serotec Ltd. Kidlington, Oxford, UK.

Scotlab Ltd. Coatbridge, Strathclyde, Scotland, UK.

Sigma Chemical Co. Poole, Dorset, UK.

Transduction Laboratories, Lexington, Kentucky, USA.

Vector Laboratories, Burlingame, California, USA.

Whatman International Ltd. Maidstone, Kent, UK

Zeneca Pharmaceuticals, Macclesfield, UK

Chapter 3.

Plakin proteins localise to plasma membrane attachment sites, such as desmosomes and hemidesmosomes, via their N-termini (Leung et al., 2002). Endogenous envoplakin and periplakin are found at desmosomes and the interdesmosomal membrane (Ma and Sun, 1986; Ruhrberg et al., 1997; Ruhrberg et al., 1996). The localisation of envoplakin and periplakin to desmosomes and the interdesmosomal plasma membrane is important for their integral role in forming the cornified envelope scaffold on the inside of the plasma membrane of keratinocytes (Kalinin et al., 2001; Ma and Sun, 1986; Ruhrberg et al., 1997; Ruhrberg et al., 1996; Simon and Green, 1984).

The first 584 amino acids of desmoplakin were found to be sufficient to target desmoplakin to the desmosomes (Bornslaeger et al., 1996; Kowalczyk et al., 1997). Analysis by DiColandrea et al. (2000) found that the equivalent regions of envoplakin and periplakin had distinct localisation patterns. The periplakin N-terminus localised to actin-rich plasma membrane projections on the apical surface of cultured keratinocytes that are known as microvilli and partially colocalised with desmoplakin at the desmosomes. In contrast, the envoplakin N-terminus localised to the nucleus and cytoplasm. To further understand the role of the envoplakin and periplakin N-termini in determining the localisation of the endogenous proteins, envoplakin and periplakin N-terminal deletion constructs were analysed by transient transfection of primary keratinocytes.

3.1 Analysis of the envoplakin amino terminus

3.1.1 Localisation of envoplakin deletion constructs

I analysed the envoplakin N-terminus in order to understand why E1/2N does not localise to the desmosomes or microvilli. Two possible reasons are the length of the envoplakin N-terminus used for analysis or are related to the KGSP repeats which are potential protein kinase C (PKC) or mitogen activated protein kinase (MAPK)

phosphorylation sites (Fig. 3.1 A) (Davis, 1993; Pearson and Kemp, 1991; Ruhrberg et al., 1996).

The P1/2N construct encoded the NN, Z, Y and X subdomains while the E1/2N construct does not encode a complete X subdomain (DiColandrea et al., 2000). However, expression of a construct containing a complete X subdomain (E508) did not result in efficient localisation of the protein to the desmosomes or microvilli (Fig. 3.1 B).

Periplakin (P1/2N), which lacks KGSP repeats, localises efficiently to the microvilli and desmosomes (DiColandrea et al., 2000). The KGSP repeats of envoplakin may interfere with the localisation of E1/2N to plasma membrane structures through phosphorylation or lack of phosphorylation of these repeats affecting the behaviour of the protein. Removal of the KGSP repeats at the very N-terminus of envoplakin did not result in efficient localisation of the protein to microvilli or the desmosomes of primary human keratinocytes (E27-508, Fig. 3.1 C). A construct encoding the KGSP repeats and the start of the NN helical domain (E41) was not efficiently expressed or unstable and thus undetectable by immunofluorescence.

Although the extreme N-termini of desmoplakin and periplakin have been found to target the proteins to their plasma membrane attachment sites, envoplakin may rely on another part of its plakin head domain for correct targeting to the desmosomes and microvilli. However, a construct incorporating amino acids 500 to 907 of envoplakin, up to the start of the envoplakin rod domain, localised to the nucleus and cytoplasm (Fig 3.1 D).

3.1.2 Effect of kinase inhibitors on the localisation of envoplakin.

The two pairs of tandem KGSP repeats preceding the NN subdomain of envoplakin each contain a minimal PKC or MAPK phosphorylation site, suggesting that envoplakin may be phosphorylated (Davis, 1993; Pearson and Kemp, 1991; Ruhrberg et al., 1996). The ability of desmoplakin to localise to the intermediate filament cytoskeleton is regulated by a phosphorylation site at its C-terminus. Phoshorylation of desmoplakin by protein kinase A negatively affects its ability to interact with intermediate filaments

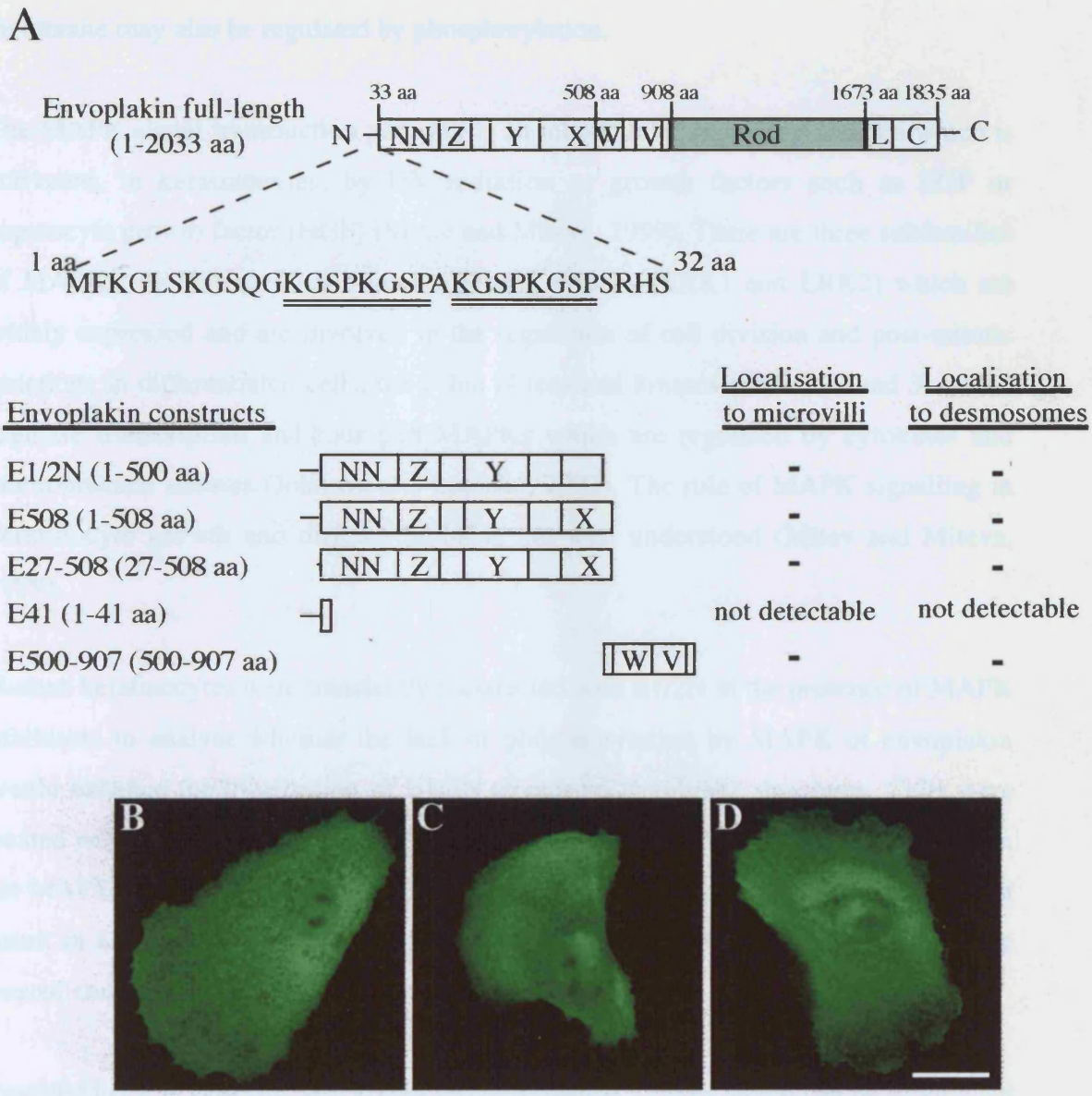

Fig 3.1 Envoplakin N-terminal constructs do not efficiently localise to the desmosomes or microvilli of primary human keratinocytes. (A) Schematic of full length human envoplakin protein and related N-terminal deletion constructs made for use in transient transfection experiments. All constructs were tagged at their C-termini with a FLAG tag. Domain nomenclature as used in DiColandrea et al. (2000). Double underlining highlights the potential phosphorylation sites (KGSP repeats): aa, amino acid. (B-D) Single confocal slices of primary human keratinocytes transfected with envoplakin N-terminal constructs. (B) E1-508, (C) E27-508, (D) E500-907. Green fluorescence: FLAG tag (M2 antibody). Scale bar: 20μm

(Stappenbeck et al., 1994). The localisation of envoplakin to sites at the plasma membrane may also be regulated by phosphorylation.

The MAPK signal transduction pathway is an intracellular signalling cascade which is activated, in keratinocytes, by UV radiation or growth factors such as EGF or hepatocyte growth factor (HGF) (Mitev and Miteva, 1999). There are three subfamilies of MAPKs; the extracellular signal-regulated kinases (ERK1 and ERK2) which are widely expressed and are involved in the regulation of cell division and post-mitotic functions in differentiated cells, the c-Jun N-terminal kinases (JNK 1, 2 and 3) which regulate transcription and four p38 MAPKs which are regulated by cytokines and environmental stresses (Johnson and Lapadat, 2002). The role of MAPK signalling in keratinocyte growth and differentiation is not well understood (Mitev and Miteva, 1999).

Human keratinocytes were transiently transfected with E1/2N in the presence of MAPK inhibitors to analyse whether the lack of phosphorylation by MAPK of envoplakin would enhance the localisation of E1/2N to plasma membrane structures. Cells were treated with UO126, an inhibitor of MEK, the kinase upstream of ERK1 and ERK2 in the MAPK cascade. Treatment of E1/2N-transfected keratinocytes with UO126 did not result in a change in its localisation relative to the localisation seen in DMSO alone treated control cells (Fig. 3.2 A-B).

Protein kinase C isoforms are protein serine/threonine kinases which can be subdivided into three subfamilies, conventional PKCs, novel PKCs and atypical PKCs according to their lipid-and calcium-binding properties (Mitev and Miteva, 1999). PKC isoforms have been implicated in the regulation of keratinocyte growth and differentiation (Denning et al., 1995; Papp et al., 2003). In order to analyse whether phosphorylation of E1/2N by a PKC prevented it localising efficiently to microvilli and desmosomes, primary human keratinocytes were transfected with E1/2N in the presence of the PKC inhibitor Bisindolylmaleimide I (BimI). BimI is an inhibitor of conventional PKCs ($\alpha,\beta1,\beta2,\gamma$) and novel PKCs ($\delta,\varepsilon$). E1/2N did not localise to the microvilli or desmosomes in keratinocytes treated with BimI for 30mins or 3hrs (Fig. 3.2 C, E); the E1/2N localisation was similar to that seen in control cells treated with DMSO alone (Fig. 3.2 D, F).

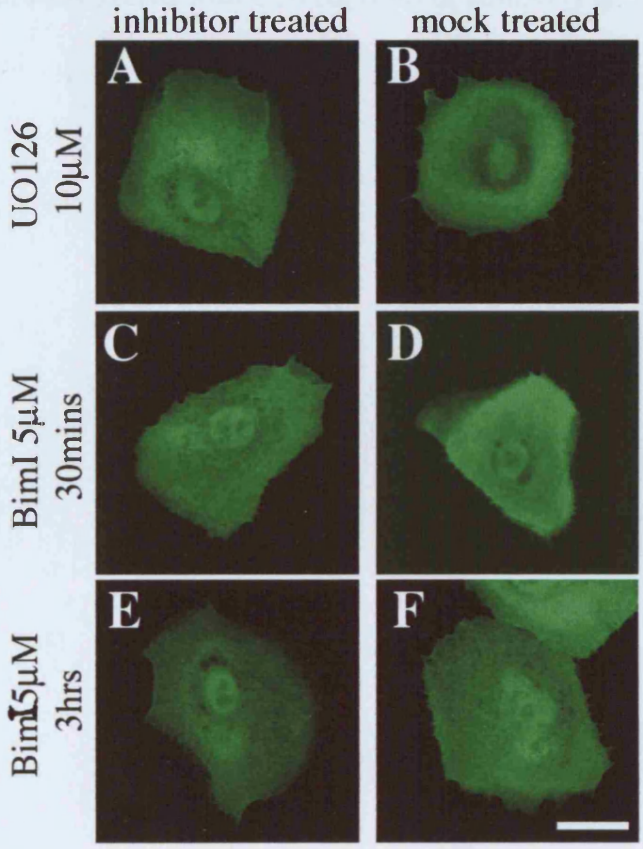

Fig 3.2 Env1/2N localisation is not altered by treatment with kinase inhibitors. Single confocal slices of immunofluorescence staining of transfected primary human keratinocytes. Cells were transfected with E1/2N (FLAG-tagged at C-terminus) in the usual way. Prior to fixation cells were treated with kinase inhibitors, as described in Materials and Methods. (A,C,E) treated with inhibitors; (B,D,F) mock treated with DMSO alone in the same manner. (A-B) UO126 MEK1 inhibitor; (C-D) BimI 5μM, 30 mins; (E-F) BimI 5μM, 3hrs. Green fluorescence, anti-FLAG (M2 antibody). Scale bar: 20μm

In order to confirm that the inhibitor treatments did not affect the localisation of endogenous envoplakin to desmosomes, small colonies of keratinocytes were stained for envoplakin and desmoplakin. Envoplakin colocalised with desmoplakin at the desmosomes of cells treated with UO126, BimI or DMSO (Fig. 3.3).

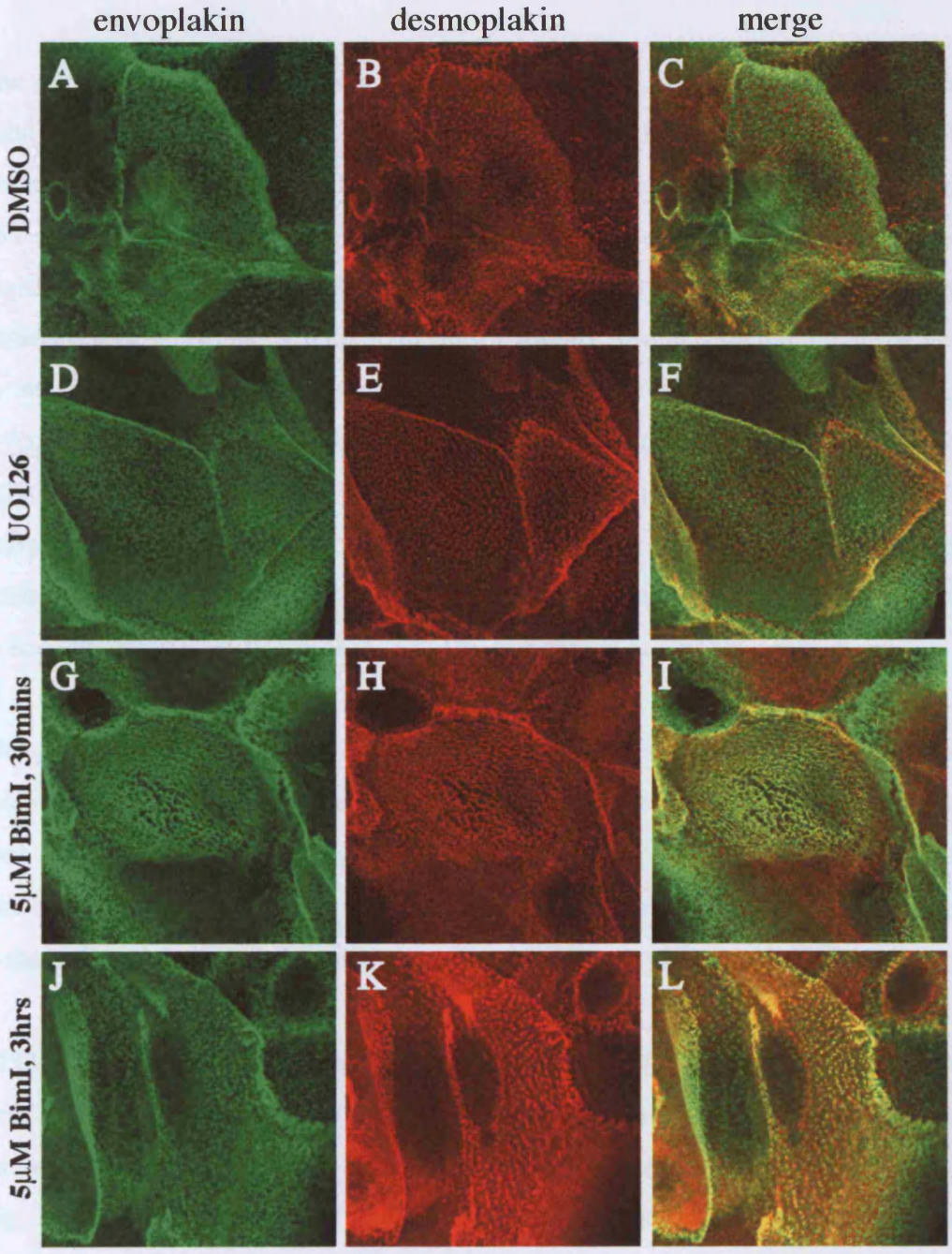

Fig 3.3 Endogenous envoplakin is unaffected by treatments with kinase inhibitors. Small keratinocyte colonies were grown on coverslips and subsequently treated with inhibitors, as explained in text. Green fluorescence, envoplakin (CR5 antibody); red fluorescence, desmoplakin (Dp115F antibody). Scale bar; 20μm.

3.2 Analysis of the periplakin amino terminus

The 495 N-terminal amino acids of periplakin (P1/2N), encoding the NN, Z, Y and X subdomains, are sufficient to mediate the interactions of periplakin with the desmosomes and microvilli (Fig. 3.4 A-C) (DiColandrea et al., 2000). The N-terminal 133 amino acids of periplakin, which encode the NN subdomain and the non-helical region preceding it, were found to localise efficiently to the plasma membrane in keratinocytes, colocalising with actin (Fig. 3.4 D-F). The plasma membrane projections to which P133 localises stained with an antibody to CD44, a transmembrane glycoprotein component of microvilli (Fig. 3.4 G-I) (Yonemura and Tsukita, 1999). In cells treated with Latrunculin B, to depolymerize F-actin, much of the P133 is redistributed into actin-rich clumps (Fig. 3.4 J-L). In conclusion, P133 localises to actin/CD44-positive microvilli and redistributes with actin upon latrunculin B treatment, as seen previously for P1/2N (Fig. 3.4; DiColandrea et al., 2000).

The predicted structure of P133 was analysed further in order to precisely define the microvillar localisation region of periplakin. The NN subdomain is predicted to form four short α-helixes, which may fold into an antiparallel bundle (Green et al., 1992). The region preceding the NN domain is predicted to have a short region of β-turn and β-sheet (Fig. 3.5 A). Deletion constructs were generated as shown in Fig. 3.5 B.

P133 localises to microvilli and the plasma membrane (Fig. 3.6 A-D). Removal of the first 15 amino acids of periplakin prevented efficient localisation of the protein to microvilli as seen when cells were stained to detect actin or CD44 (Fig. 3.6 M-P and Fig. 3.7 G-L). A proportion of P16-133 protein is able to localise to microvilli in some cells (arrows Fig. 3.7 J-K). Despite the inability of P16-133 to localise efficiently to microvilli, it does localise to the plasma membrane to some extent (Fig. 3.6 P). Some P16-133 protein could be detected in the nucleus of primary keratinocytes (Fig. 3.6 M-O and Fig. 3.7 G-L).

The first 63 amino acids of periplakin, encoding the first α-helical domain of the periplakin N-terminus, were incapable of efficiently localising to the microvilli (Fig. 3.6 I-L and Fig. 3.7 D-F). Microvilli structures, stained with actin or CD44, were not co-

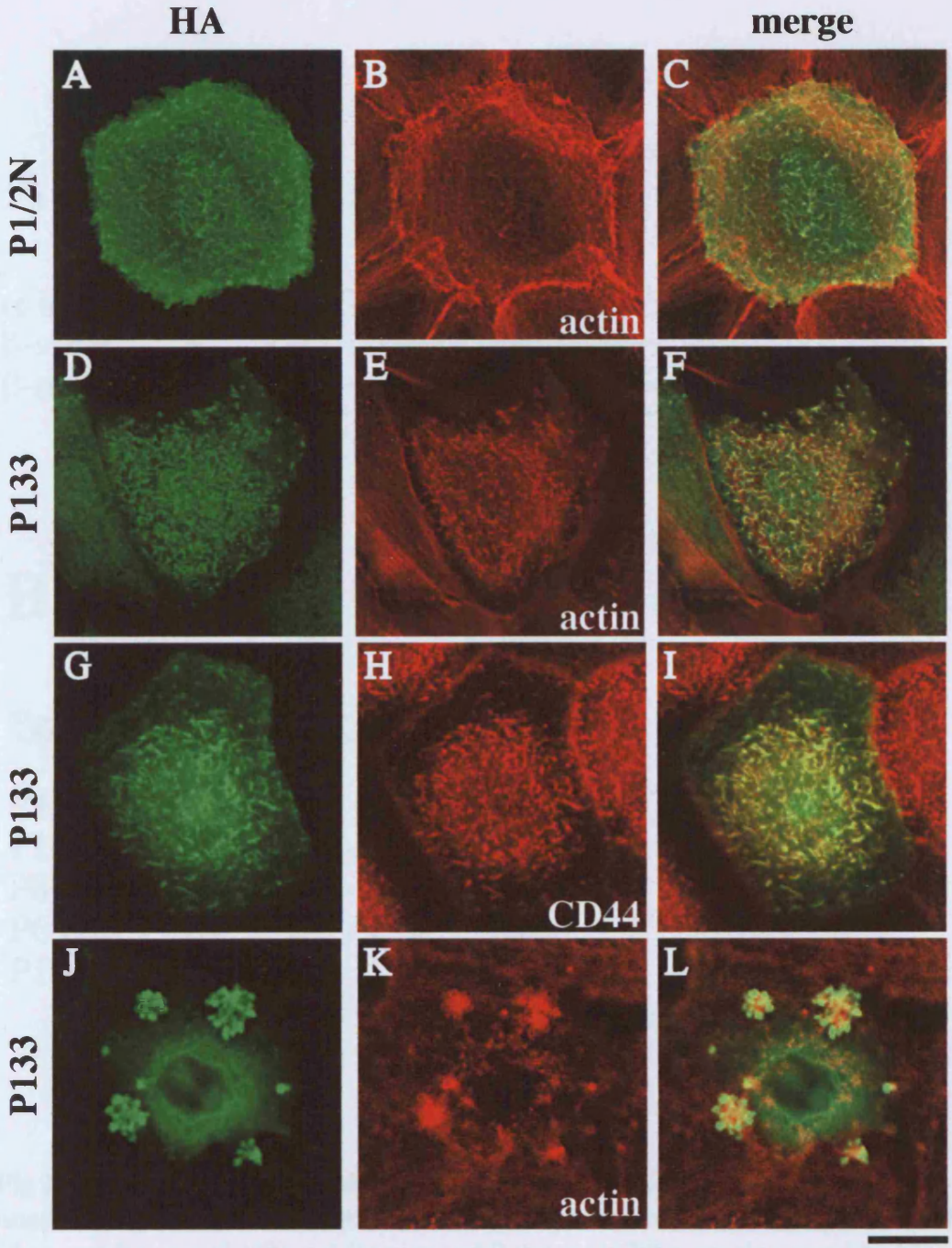

Fig 3.4 The amino terminal 133 amino acids of periplakin (P133) localisesto the microvilli as effeciently as P1/2N and redistributes with actin upon latrunculin B treatment. Primary human keratinocytes transfected with HA tagged P133 (D-L) and P1/2N (A-C) constructs. (J-L) cells were treated with latrunculin B (200ng/ml, 3hrs) before fixation. Green fluorescence: HA tag ; red fluorescence: F-actin in (A-F, J-L), CD44 in (G-I). C, F, I, L show merged images; yellow indicates colocalisation. Scale bar: 20μm in (A-F), 10μm (G-L).

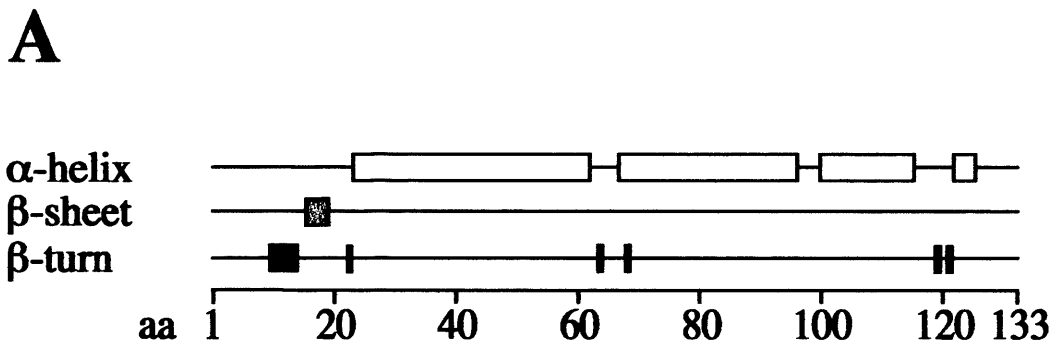

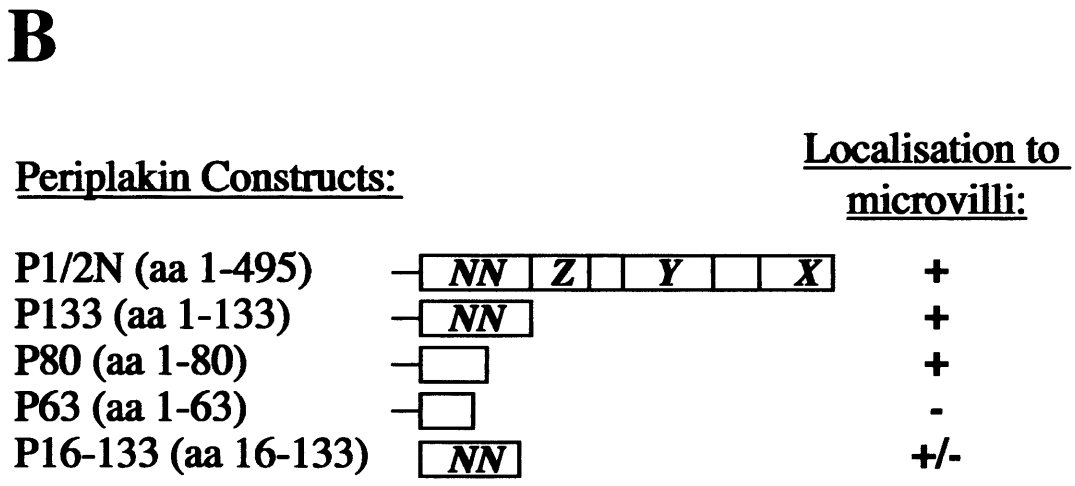

Fig 3.5 Summary of periplakin deletion analysis. (A) Secondary structure predictions of the N-terminal 133 amino acids of periplakin, based on the algorithms of Chou and Fasman (1978) and Garnier and Robson (1978) as implemented by MacVector 6.5.3. (B) Schematic diagram of the periplakin constructs used for transient transfections. Domain nomenclature as described by Ruhrberg et al. (1997). All constructs had C-terminal HA tags.

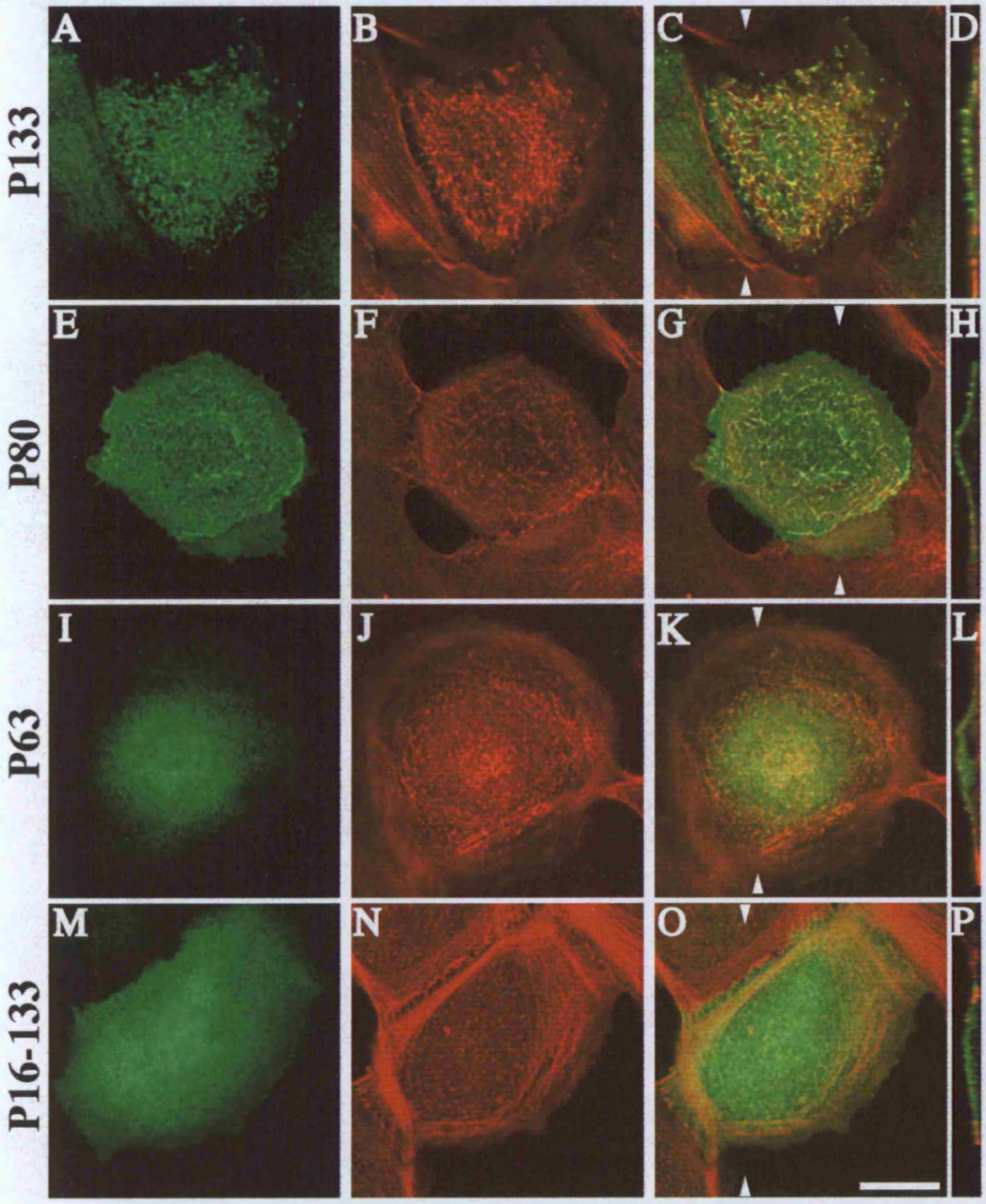

Fig 3.6 P133 is the minimal unit of periplakin which efficiently localises to the keratinocyte plasma membrane and microvilli. Transfection of primary human keratinocytes. Green fluoresence, HA; red fluorescence, F-actin. Confocal projections of z-stacks, (A-C, E-G, I-K, M-O) are shown as ortho gonal views in (D,H,L,P) respectively. Arrow heads indicate position of orthogonal views. Z-stack size: (D) 3.6 µm, (H) 7.2 µm, (L) 6.1 µm, (P) 5.6 µm. Scale bar: 20µm.

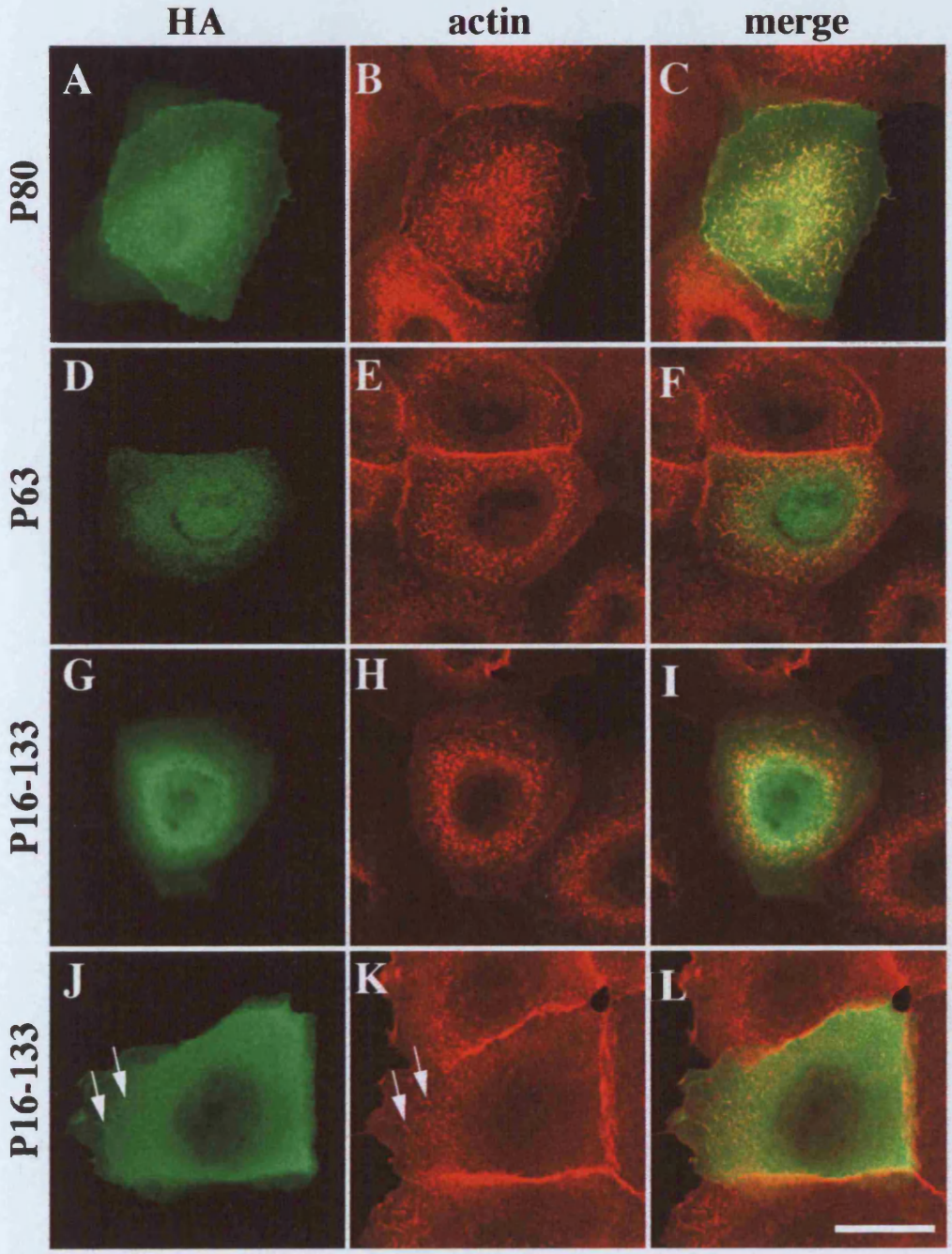

Fig 3.7 P80 colocalises with CD44 at microvilli. Single confocal slices of primary human keratinocytes transfected with periplakin deletion constructs stained for the HA tag and CD44. (A-C) P80, (D-F) P63, (G-L) P16-133. (G-I) show P16-133 not localising to microvilli, (J-L) shows some P16-133 colocalising with CD44. Arrows mark microvillar staining seen in some cells transfected with P16-133. Green fluorescence, HA; red fluoresence CD44. Scale bar: 20μm.

stained with HA antibody detecting P63. P63 staining was seen at the plasma membrane and the nucleus to some extent (Fig. 3.6 I-L and Fig. 3.7 D-F). The level of fluorescence detected in cells expressing P63, in contrast to the P133 protein signal, was very low, suggesting that the protein was not efficiently expressed or unstable.

The first 80 amino acids of periplakin, encoding the first one and a half α-helical domains, localised to the plasma membrane, including the microvilli where it colocalises with actin and CD44 (Fig. 3.6 E-H and Fig. 3.7 A-C). P80, in contrast to P133, was not at microvilli in 100% of cells, suggesting that the efficiency of the localisation is increased by the presence of an intact NN subdomain.

3.3 Discussion

In this chapter I have shown that the envoplakin N-terminus does not localise efficiently to desmosomes or microvilli (Bornslaeger et al., 1996; DiColandrea et al., 2000). It was thought that phosphorylation of E1/2N might prevent its localisation to the microvilli and desmosomes since phosphorylation of desmoplakin negatively regulates its ability to interact with intermediate filaments (Stappenbeck et al., 1994). However, phosphorylation of E1/2N by MAPK showed that phosphorylation by ERK1 and ERK2 is unlikely to be preventing E1/2N localisation to microvilli and desmosomes as treatment of transfected cells with UO126 did not alter its localisation. Treatment of cells with the PKC inhibitor BimI did not result in localisation of E1/2N to microvilli or the desmosomes. The role of the atypical PKCs, such as PKCs ζ and ι, was not analysed, and thus it remains a possibility that they regulate E1/2N localisation. However, removal of the N-terminal extension of envoplakin (amino acids 1-41) did not lead to recruitment to microvilli or desmosomes.

My experiments do not exclude the possibility that phosphorylation of envoplakin is required for it to localise to the desmosomes and microvilli. Envoplakin may only be efficiently phosphorylated in the context of the full length molecule and thus E1/2N may remain unphosphorylated in transfected cells. However, the localisation of endogenous envoplakin was unaltered in cells treated with inhibitors to MEK and PKC.

This suggests that envoplakin already at desmosomes remains localised there independently of treatment with kinase inhibitors (Fig. 3.3).

One reason that E1/2N does not, but P1/2N does, localise to desmosomes and microvilli may be that the envoplakin N-terminus is insoluble. Kalinin et al. (2004) showed that the envoplakin head domain (amino acids 1-917) is insoluble when expressed in *E. coli*, in contrast to the periplakin head domain (amino acids 1-948). The difference in the behaviour of the two head domains *in vitro* may explain our differing findings for E1/2N and P1/2N localisation *in vivo;* alternatively the differences may be a result of the sequence variation between the envoplakin and periplakin N termini (sequence identity <40%). DiColandrea et al. (2000) noted that only a proportion of full length envoplakin localised to the desmosomes of stably transfected mouse keratinocytes and that envoplakin may depend on periplakin in order to localise to the interdesmosomal plasma membrane.

Analysis of the periplakin N-terminus shows that the non-helical region preceding the NN-subdomain is important for stable localisation of periplakin to the microvilli. In addition, although the first 80 amino acids of periplakin N-terminus were able to localise to microvilli, this localisation was more efficient when the whole NN subdomain was used. Thus the minimal region of periplakin, that is capable of mediating the interaction of periplakin with the plasma membrane and the cortical actin cytoskeleton, is P133. I would predict that deletion of the first 133 amino acids of periplakin would prevent membrane localisation of periplakin, although this had not been tested.

A proportion of the periplakin deletion constructs showed nuclear staining, particularly those proteins that were not able to localise efficiently to the microvilli (P16-133, and P63). We have no evidence that endogenous periplakin localises to the nucleus despite the presence of a putative nuclear localisation signal (NLS) within the rod domain. Thus, P16-133 and P63 do not contain an NLS and thus the inability to bind factors to target the proteins correctly may result in aberrant localisation of the proteins to the nucleus.

Periplakin N-terminal deletion constructs localise not just to the microvilli but also to the plasma membrane (Fig. 3.6). Envoplakin/periplakin heterodimers and periplakin

homodimers bind phospholipids of synthetic lipid vesicles (SLV) *in vitro*. Individual domains of envoplakin and periplakin (head, rod, tail) did not bind to SLV significantly (Kalinin et al., 2004). My analysis suggests that the periplakin N-terminus may have some lipid-binding capacity or, alternatively the periplakin N-terminal deletion constructs bind proteins at the plasma membrane.

T. DiColandrea (Keratinocyte laboratory, CR-UK) found that periplakin does not bind actin directly. I therefore set out to discover what proteins bind P133 and potentially determine its localisation to the plasma membrane.

Chapter 4.

In this chapter I will present data on the isolation of kazrin, a novel periplakin interacting protein. I shall discuss the genomic organisation of the kazrin gene and the expression of its alternative splice forms. I shall describe further mapping of the interaction between kazrin and periplakin by the yeast two-hybrid system and verification of the interaction by GST pull-down assay.

4.1 Identification of periplakin-interacting proteins by yeast two-hybrid screening.

In Chapter 3 I presented data suggesting that P133, encoding the first 133 amino acids of periplakin, was the minimal unit of periplakin which localised efficiently to the plasma membrane and microvilli. In order to identify proteins involved in targeting periplakin to the plasma membrane a yeast two-hybrid screen was carried out by K. Nishi (Keratinocyte laboratory, CR-UK). Dr K. Nishi returned to Japan shortly after isolating a partial kazrin cDNA, the rest of the experiments described in the Chapter were performed by myself.

The yeast two-hybrid system allows the identification of novel protein-protein interactions *in vivo*. In the MATCHMAKER GAL4 two-hybrid 3 system (Clontech), a 'bait' gene, in this case the P133 coding sequence, is expressed as a fusion protein with the GAL4 DNA-binding domain (GAL4-BD) (Fig. 4.1 A). A human foreskin keratinocyte cDNA library (the 'prey') was cloned such that the cDNAs were expressed as GAL4 activation domain (GAL4-AD) fusion proteins (Fig. 4.1 A). Interactions occurring between P133 and proteins encoded by the keratinocyte cDNA library bring the GAL4 DNA-BD and GAL4-AD into close proximity, activating transcription of reporter genes.

The AH109 yeast strain used in the yeast two-hybrid screen has three selectable markers which are activated when proteins interact. The ADE2 gene encodes Ade2p which allows the yeast to grow in the absence of adenine in the growth medium. The ADE2

A

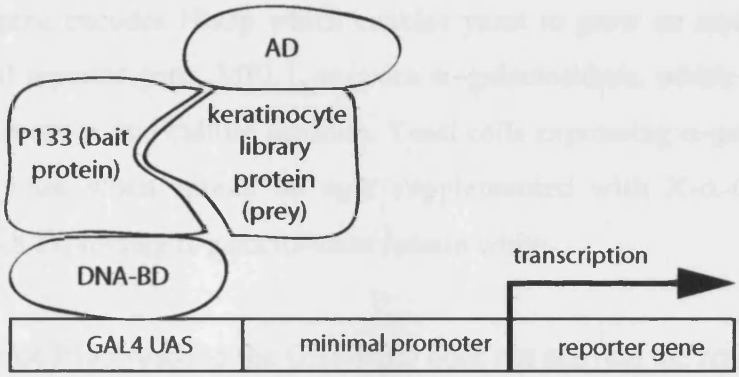

B

Transformation no.	DNA-BD (bait)	AD (prey)	Growth on selective agar ($A^-L^-T^-H^-$)
1	p53	Large T antigen	+
2	lamin	Large T antigen	-
3	P133	Empty vector	-

C

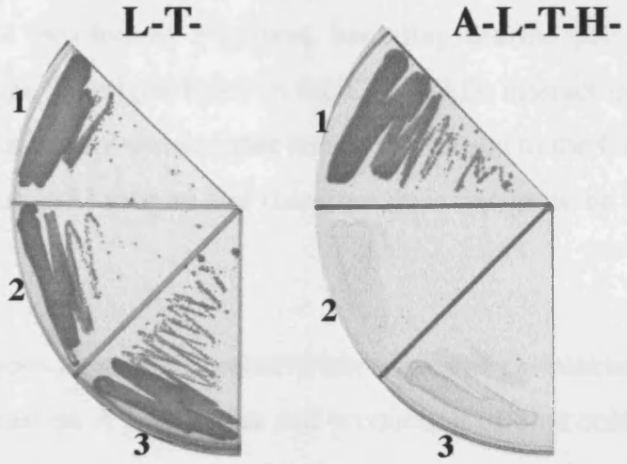

Fig 4.1 Yeast two hybrid screen set-up and controls. **(A)** Periplakin P133 was fused to the GAL4 DNA-binding domain (vector pGBKT7). A human keratinocyte cDNA library was fused to the activation domain of GAL4 (vector pGAD10). (B-C) Periplakin P133, fused to the GAL4 DNA-binding domain, does not have auto-activating activity. (B) Chart of vectors used in the transformations. (C) Selection for the the pGAD and pGBKT vectors, to confirm transformation efficiency, carried out on medium lacking Leucine/Tryptophan (L-T-). Selection for binding of the proteins encoded by the pGBKT7 and pGAD vectors, carried out on medium lacking Adenine/Leucine/Tryptophan/Histadine (A-L-T-H-).

reporter is a strong nutritional selection marker, but can be used in combination with HIS3. The HIS3 gene encodes His3p which enables yeast to grow on media lacking histidine. The final reporter gene, MEL1, encodes α–galactosidase, which is secreted into the periplasmic space and culture medium. Yeast cells expressing α-galactosidase produce blue colonies when spread on agar supplemented with X-α-Gal, while colonies of yeast not expressing α-galactosidase remain white.

In order to verify that P133 fused to the GAL4-BD does not activate the reporter genes in the absence of a GAL4-AD fusion protein, control yeast transformations were set up as shown Fig. 4.1 B,C. To verify that yeast have been transformed with both vectors, yeast are grown on agar lacking leucine and tryptophan (L^-T^- agar), while selection for an interaction between P133-GAL4-BD and GAL4-AD alone is analysed on agar lacking leucine, tryptophan, adenine and histidine ($A^-L^-T^-H^-$ agar). P133 alone grows well on L^-T^- agar; thus the transformation was successful. There is no growth on $A^-L^-T^-H^-$ agar, showing that P133 fused to the GAL4-BD does not have the ability to activate the reporter genes alone (Fig. 4.1 C). A positive control provided with the MATCHMAKER GAL4 two-hybrid 3 system, encoding murine p53 fused to the GAL4-BD and SV40 large T antigen fused to the GAL4-AD, interact in our analysis (Fig. 4.1 B-C). A negative control showed that lamin when fused to the GAL4-BD does not interact with SV40 large T antigen and therefore does not grow on $A^-L^-T^-H^-$ agar (Fig. 4.1.B-C).

The yeast two-hybrid screen identified 3 putative interactors of periplakin P133 at high stringency (growth of yeast on $A^-L^-T^-H^-$ agar and production of blue colonies on X-α-Gal agar). The putative interactors were isolated and retransformed into yeast in the presence of P133 to reconfirm their ability to interact with P133. Only one cDNA was found to bind strongly to P133 and be in frame to the GAL4-AD. Sequencing of the cDNA showed that it encoded a novel protein which we have named kazrin. The kazrin sequence, encoding 279 amino acids, was partial as it lacked the translation initiation codon.

4.2 Analysis of kazrin nucleotide and amino acid sequences.

4.2.1 Analysis of the kazrin gene

The partial kazrin nucleotide sequence obtained from the yeast two-hybrid screen was screened against the human and mouse genome using BLAT (BLAST-like alignment tool). BLAT is designed to find genomic regions of very high homology (95% over 40nt or more) to an input sequence, allowing identification of the chromosomal location of your sequence of interest. Using the partial kazrin sequence the gene was found on the forward strand of human chromosome 1 (band 1p36.21) and the reverse strand of mouse chromosome 4 (band 4E1).

The kazrin fragment we isolated was composed of several exons. In order to identify upstream exons, the nucleotide sequence was searched against the BLAST (basic local alignment search tool) human nucleotide sequence database. BLAST searches identified several spliced expressed sequence tags (ESTs) which contained the known sequence at the 3' end, and additional sequence at the 5' end. Spliced EST sequences, relating to human kazrin, were pieced together and compared to the human genome in order to establish the genomic layout of the kazrin gene (Fig. 4.2 A). The kazrin gene is composed of 7 exons (exons 2-8) that may be spliced together with one of four alternative first exons. The first exons are designated 1a, 1b, 1c and 1d, with respect to their distance from exon 2, with 1a being the furthest upstream from exon 2. The region of kazrin isolated in the yeast two-hybrid screen is present in all kazrin isoforms.

Exons 1a and 1b contain start codons generating proteins of 421 amino acids (kazrin A) and 414 amino acids (kazrin B) (Fig. 4.2 A-B). Exons 1c and 1d do not contain in-frame start codons. Translation from transcripts containing exons 1c or 1d begin at the start codon located in exon 2 (Fig 4.2 A-B). Protein synthesis from exon 1c and exon 1d-containing mRNAs generate identical 327 amino acid proteins which we refer to as kazrin C protein for simplicity. Consensus splice sites were found at the start and end of each intron (GU and AG respectively) (Alberts et al., 2002). In-frame stop codons are located upstream of the start sites, two within exon 1b and one within exon 1d (Fig. 4.2 B).

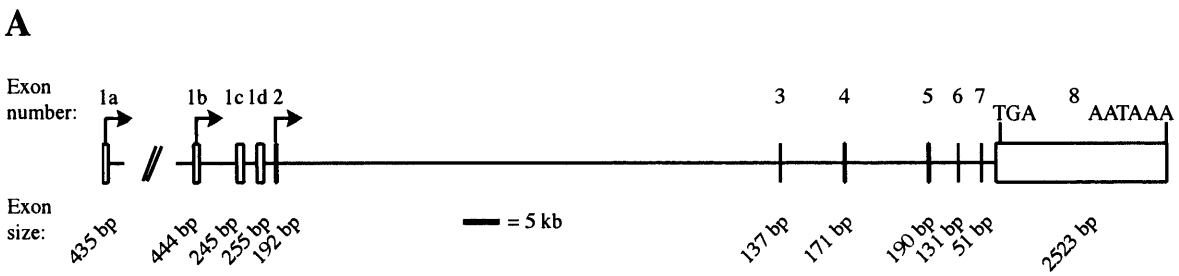

B

Exon 1a

```
   1  GGGGTCTCGGCGATCGCTGCTCCTCCTCCTTCTCCTCCTCTTTTTTCTCCTCCGCCTCCTCCCCCCGCCGCCTCGCCACCGCCGCGGCTAGGGCTGGAGGCGCCGCCTGTCATTCCTGTGCCGGAGGAACCGG  135
 136  CGCTGCCGGTGCCTGGGGGTCGGGGCGCGGGCGAAGCCGGGCCGCGGAGGACACAACAGGCCAAAATCCTGAGCATGATGGAAGACAATAAGCAGCTCGCGCTCCGCATCGATGGGGCGGTCCAGTCGGCCAGCC  270
   1                                                                                                  M  M  E  D  N  K  Q  L  A  L  R  I  D  G  A  V  Q  S  A  S  Q   22
 271  AGGAGGTGACCAACCTGCGAGCCGAACTCACGGCCACCAACCGGAGACTGGCGGAACTGAGCGGCGGCGGCCGGCCCCGGCCCGGGCCCGGGAGCCGCGGCCAGCGCCTCGGCGGCGGGGGACTCGGCGGCGACGA  405
  23    E  V  T  N  L  R  A  E  L  T  A  T  N  R  R  L  A  E  L  S  G  G  G  G  P  G  P  G  P  G  A  A  A  S  A  S  A  A  G  D  S  A  A  T  N   67

 406  ACATGGAGAACCCCCAGCTTGGAGCGCAAG                                                                                                                  435
  68    M  E  N  P  Q  L  G  A  Q  V                                                                                                                    77
```

Exon 1b

```
   1  GAGCCGTTCCCACCTGAGAGGCTCCGCGGCCGAATTCCTCGCGTGCAGCAGGCGCGGACCGCCCGGCGTCCGGCCGGACTGAGAGCCCTGGTCCGGCGCGCGCCGCCGGCCGGGCGGGAGGCGGGGGCGGGCTCG  135
 136  GCTGCGCCCCGATGCGGCGGCGACCTCCGGGTCTGTGAGCCCGGCGCGCGCCGTCGGAGCCCCTCGCGCAGCCGCTGGTAGCGTCCCCCGGGCACCCGGCATGCGGGCGGCCGACTCGGGCTCGTGGGAGCGCG  270
   1                                                                                                                                  M  R  A  A  D  S  G  S  W  E  R  V   12

 271  TCCGCCAGCTCGCGGCGCAGGGCGAGCCGGCGCCTTCCTGCGGGGCGGGGGCCGGGCCCGCGCGGCCCCCGGGACCCGCAGCCTGCGAGCAGTGCGTGGACGCGGCGGGGCCCGGCGATCGGCCCCGCGCCGGGG  405
  13    R  Q  L  A  A  Q  G  E  P  A  P  S  C  G  A  G  A  G  P  A  R  P  P  G  P  A  A  C  E  Q  C  V  D  A  A  G  P  G  D  R  P  R  A  G  V   57

 406  TTCCCCGGGTCCGAGCGGATGGCGACTGCAGCCAGCCCG                                                                                                        444
  58    P  R  V  R  A  D  G  D  C  S  Q  P  V                                                                                                          70
```

Exon 1c

```
   1  GGGAGAGGGAAGGTCAGGCTTGCCTCCTGTTCACAAGGACAACCTCTGTCTCCCTTGTGGCGGCTTCTATGAAGGTGGGGACTCCAGGCTTTCTCTCGTCTGCTTTTTGGATGCCTTCAAGAGAGGCCAGTTAGA  135
 136  GGATATCAATTGTGGCAATTCCCCAGAGCCCTCATCAGATGGCATTAGCCCGTCATGTGCTGCAGTGGCACCCAGTTTGGAGGAAATTCGGAACCAGAAGAGTGTGACAG                              245
```

Exon 1d

```
   1  GCATCAGCAGCTGTCTGCCAGTGTTGACGGAGGGCTCATGGGTGCCAGGCCGCTTGCTGGGGCTTTTTATCTGTCCTCAGGCATTGGCACAGCAGCCCTGGGAGATGAATACTATTGTGATCTTCATTCTCCACA  135
 136  CAAGGACAGGGAAGTGACGTGCCAGGGTCAAACAACTACCCAAGGACAGAGCCAGGATTTGAACCAGGCCATCCAGTTCCAGAACCACTGCTCTTCACTGTCATTGTGGCCATTTTACAG                          255
```

Exon 2-8

```
   1  TGCTCCTGCGGGAAGAAGTGTCGCGGCTCCAGGAGGAAGTTCACCTTCTCCGGCAGATGAAGGAGATGTTGGCGAAGGACCTGGAGGAGTCGCAGGGCGGCAAGTCCTCTGAGGTCCTCTCGGCCACCGAGCTCA  135
   1    (L) (L) (R) (E) (E) (V) (S) (R) (L) (Q) (E) (E) (V) (H) (L) (L) (R) (Q)  M  K  E  M  L  A  K  D  L  E  E  S  Q  G  G  K  S  S  E  V  L  S  A  T  E  L  R   45

 136  GGGTCCAGCTGGCCCAGAAGGAGCAGGAGCTAGCCAGAGCCAAAGAAGCCTTGCAGGCCATGAAAGCTGATCGGAAGCGCTTAAAGGGCGAGAAGACAGACCTGGTGAGCCAGATGCAGCAGCTGTATGCCACAC  270
  46    V  Q  L  A  Q  K  E  Q  E  L  A  R  A  K  E  A  L  Q  A  M  K  A  D  R  K  R  L  K  G  E  K  T  D  L  V  S  Q  M  Q  Q  L  Y  A  T  L   90

 271  TGGAGAGCCGCGAGGAGCAGCTCCGAGACTTCATCCGCAACTATGAGCAGCACCGCAAGGAGAGCGAGGATGCGGTCAAAGCGCTGGCCAAGGAGAAGGACCTGCTGGAGCGTGAGAAGTGGGAGCTGCGGCGCC  405
  91    E  S  R  E  E  Q  L  R  D  F  I  R  N  Y  E  Q  H  R  K  E  S  E  D  A  V  K  A  L  A  K  E  K  D  L  L  E  R  E  K  W  E  L  R  R  Q  135

 406  AAGCCAAGGAGGCCACAGACCACGCCACGGCACTGCGCTCCCAGCTGGACCTCAAGGACAACCGGATGAAGGAGCTGGAGGCCGAGCTGGCCATGGCCAAACAGTCCTTAGCTACGCTGACCAAGGACGTCCCCA  540
  136    A  K  E  A  T  D  H  A  T  A  L  R  S  Q  L  D  L  K  D  N  R  M  K  E  L  E  A  E  L  A  M  A  K  Q  S  L  A  T  L  T  K  D  V  P  K  180

 541  AGCGGCATTCCCTCGCCATGCCGGGCGAGACGGTGCTCAATGGCAACCAGGAGTGGGTGGTGCAGGCGGACCTCCCGCTGACCGCAGCCATCCGGCAGAGTCAACAGACTCTCTACCACTCACACCCCCTCACC  675
  181    R  H  S  L  A  M  P  G  E  T  V  L  N  G  N  Q  E  W  V  V  Q  A  D  L  P  L  T  A  A  I  R  Q  S  Q  Q  T  L  Y  H  S  H  P  P  H  P  225

 676  CTGCGGACCGGCAAGCGGTCAGGGTGAGCCCCTGCCACTCCCGGCAGCCCTCTGTCATCTCCGACGCATCTGCCGCCGAAGGCGACCGGTCGTCCACACCGAGCGACATCAACTCCCCTCGACACCGGACACACT  810
  226    A  D  R  Q  A  V  R  V  S  P  C  H  S  R  Q  P  S  V  I  S  D  A  S  A  A  E  G  D  R  S  S  T  P  S  D  I  N  S  P  R  H  R  T  H  S  270

 811  CCCTCTGCAACGGCGACAGTCCCGGCCCAGTTCAGAAGAACCTGCACAACCCTATTGTACAGTCACTAGAGGATCTTGAAGACCAAAAACGGAAAAAGAAGAAAGAGAAGATGGGATTCGGCTCCATCTCCCGCG  945
  271    L  C  N  G  D  S  P  G  P  V  Q  K  N  L  H  N  P  I  V  Q  S  L  E  D  L  E  D  Q  K  R  K  K  K  K  E  K  M  G  F  G  S  I  S  R  V  315

 946  TCTTCGCCAGAGGGAAGCAGCGGAAGTCCCTCGACCCCGGCCTCTTTGATGGTACCGCCCCTGATTATTACATAGAGGAGGACGCGGACTGGTGA                                            1040
  316    F  A  R  G  K  Q  R  K  S  L  D  P  G  L  F  D  G  T  A  P  D  Y  Y  I  E  E  D  A  D  W  *                                              345
```

Figure 4.2 Genomic organisation, nucleotide and amino acid sequences of kazrin. (A) Intron-exon organisation of the kazrin gene, drawn to scale. The gene consists of 7 exons (exons 2-8) that may be spliced to one of four alternative first exons (1a, 1b, 1c, 1d). Arrows; translation initiation sites of exons 1a, 1b and 2; two diagonal lines: 320 kb gap between exons 1a and 1b; TGA: translation termination codon; AATAAA: polyadenylation signal. (B) Nucleotide and corresponding amino acid sequences of the 5' UTR and coding regions of kazrin isoforms. ATG start sites are shown in bold, underlined; upstream termination codons are underlined; arrows indicate exon boundaries; asterisk marks translation termination site. Leucine zipper-like domain is marked by solid box and NLS by dashed line box. Amino acids are shown in single letter format; those in brackets are not translated from kazrin c and d mRNAs, as their translation initiation site is downstream in exon 2. Sequence data are available from GenBank/EMBL/DDBJ under accession numbers AY505119, AY505120, AY505121, and AY505122, corresponding to kazrin isoform a, b, c, and d, respectively.

4.2.2 Confirmation of the human kazrin nucleotide sequence

IMAGE (Integrated Molecular Analysis of Genomes and their Expression) clones are publicly available clones obtained from oligo(dT)–primed cDNA libraries that typically encode full length, spliced cDNAs. The IMAGE clones used to sequence kazrin are listed in Table 4.1. IMAGE clones were sequenced using primers specific to the vector into which the cDNA was cloned, as well as internal primers, as listed in Chapter 2.1.3. The sequence data of the 5'UTR and coding regions of kazrin a, b, c and d mRNAs were submitted to GenBank/EMBL/DDBJ under accession numbers AY505119, AY505120, AY505121, AY505122, respectively (Fig. 4.2 B). The GenBank entries can be found in the appendix.

Table 4.1 IMAGE clones containing kazrin cDNA sequences

Kazrin isoform	IMAGE clone number	Source of cDNA library	Vector
a	6180253	Dorsal root ganglion	pCMV-SPORT6
b	4556194	Uterine leiomyosarcoma cell line	pOTB7
c	4651187	Placental choriocarcinoma	pOTB7
d	4472821	Liver adenocarcinoma cell line	pCMV-SPORT6

4.2.3 *In vitro* transcription and translation of kazrin isoforms

The kazrin A, B, C proteins have predicted molecular weights (MW) of 46.8, 46.2 and 37.0 kDa respectively, as calculated by MacVector 6.3.5. In order to analyse the kazrin proteins encoded by the IMAGE clones, and compare the actual MWs with the predicted MWs, *in vitro* transcription and translation reactions were carried out (Fig. 4.3). Each of the kazrin isoforms was transcribed from an Sp6 polymerase binding site within the IMAGE clone vectors. Fig 4.3 A shows the ^{35}S -labelled kazrin proteins generated from the IMAGE clones. In the absence of DNA in the reaction mix no background ^{35}S -labelled proteins were generated (Fig. 4.3 A,B).

The upper protein bands generated from kazrin A cDNA are slightly larger than the predicted size of 46.8 kDa. The multiple high molecular weight protein bands seen for kazrin A suggest either that there are alternate start sites (though these were not found by sequencing of the 5'UTRs) or that there is post-translational modification, such as

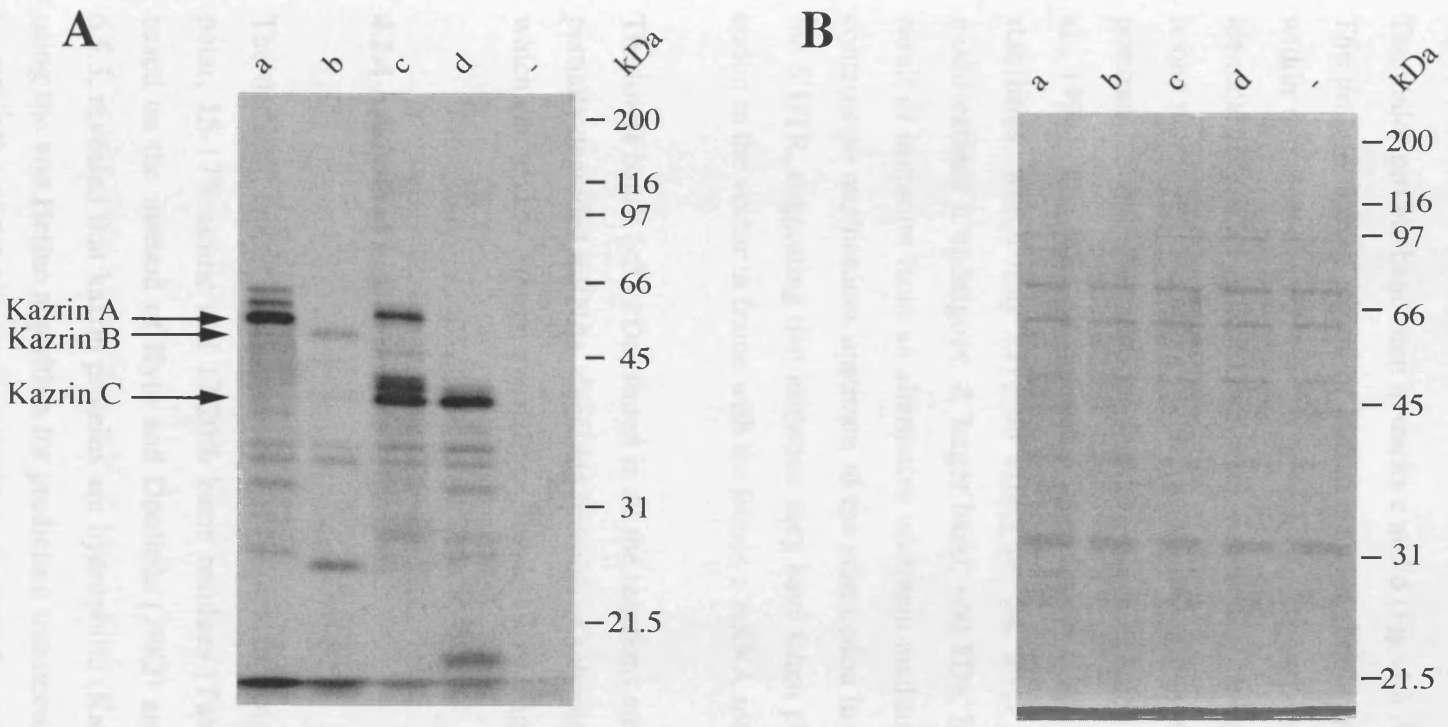

Fig 4.3 *In vitro* transcription and translation of IMAGE clones encoding kazrin cDNAs generate proteins of the expected size. (A) 0.5µg of each IMAGE clone, and a negative control lane with no DNA (-), was used in each reaction using the Sp6 polymerase and ^{35}S – methionine. IMAGE clones encoding kazrin a, b, c and d were used. IMAGE clone numbers are indicated in Table 4.1. 10% (1µl) of the reaction was run on an SDS-PAGE gel. The gel was dried and exposed on film at room temperature for 4 days. Arrows highlight the position of the putative full length kazrin protein isoforms. (B) Coomassie stained SDS-PAGE gel of reactions run in (A) to show equal loading of lanes. BioRad molecular weight markers shown in kDa.

phosphorylation of kazrin A protein (Joshi et al., 1995; Schubert et al., 1994). The major band from kazrin b is a little larger than the predicted size of 46.2 kDa, however no other proteins bands were detected in track b which could represent full length kazrin B protein (Fig. 4.3 A).

The major protein band seen in tracks c and d (Fig. 4.3 A) is at approximately 37.0 kDa. The protein coding region of kazrin c and d should be identical as translation starts within common exon 2, yet the protein bands generated in the TNT reactions are not identical (Fig. 4.3). At 37 kDa in track c there is a triplet of bands while in track d there is one major and one minor band. The additional bands around 37 kDa may be due to posttranslational modifications such as phosphorylation (Joshi et al., 1995; Schubert et al., 1994). The mRNAs generated from kazrin c and d cDNAs may have different stabilities, which may have an effect on the level of protein produced and any modifications it undergoes. A larger band, ~60 kDa, is seen in C, which may be the result of initiation from an alternative upstream methionine. The sequence of kazrin c contains no methionines upstream of the start codon in exon 2, nor stop codons within the 5'UTR, suggesting that initiation may have taken place from a spurious ATG start codon in the vector in frame with the kazrin c mRNA sequence (Fig. 4.3 A).

The lower bands (<35 kDa) found in all the reactions are attributable to translation from partially degraded mRNAs, degraded proteins or suboptimal magnesium concentrations, which can lead to internal translation (Kozak, 1996) (Fig. 4.3 A).

4.2.4 Analysis of kazrin protein sequences

The deduced amino acid sequences of the kazrin isoforms are composed of 28-30% polar, 15-17% acidic and 17-20% basic residues (Table 4.2). A hydrophilicity plot, based on the method of Kyte and Doolittle (1982) and implemented by MacVector 6.5.3, revealed that kazrin proteins are hydrophilic (Kazrin C in Fig. 4.4 A). Analysis using the von Heijne algorithm for predicting transmembrane regions, as implemented by MacVector 6.5.3, suggests that kazrin proteins are not transmembrane proteins (Sipos and von Heijne, 1993).

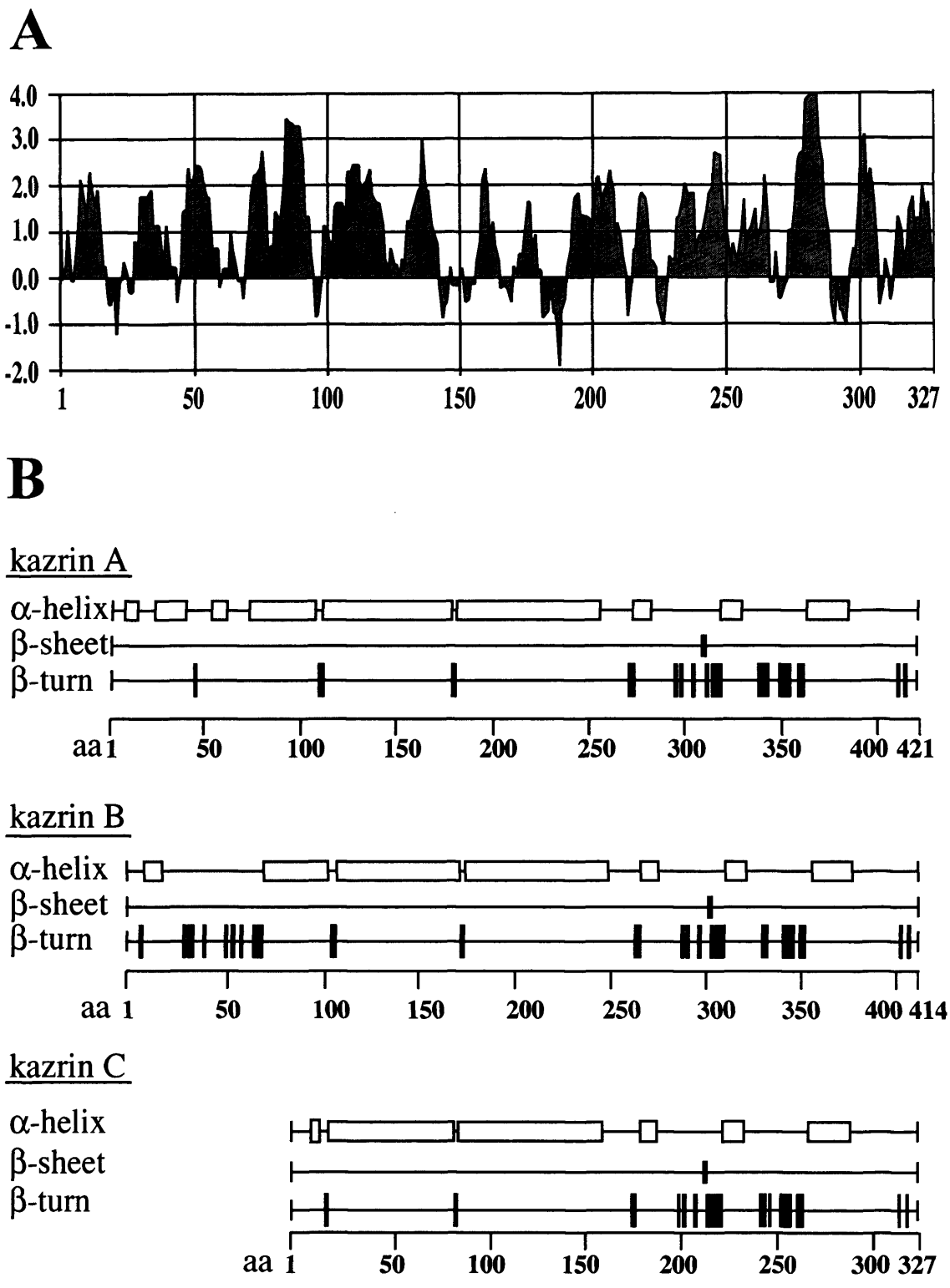

Fig 4.4 Kazrin is hydrophilic and contains predominantly α-helices and β-turns. (A) Hydrophilicity plot of kazrin C, based on the method of Kyte and Doolitle (1982), as implemented by MacVector 6.5.3. Positive values on the y-axis denote hydrophilic regions predicted to be on the outside of the protein; negative values on the y-axis are predicted to be on the inside of the protein or inside other hydrophobic environments. (B) Concensus secondary structure prediction of kazrin A, B and C, based on the algorithms of Chou and Fasman (1978) and Garnier and Robson (1978), as implemented by MacVector 6.5.3.

Secondary structure analysis based on the algorithms of Chou and Fasman (1978) and Robson and Garnier (1978), as implemented by MacVector 6.5.3, predicts kazrin C has a highly α-helical N-terminal region, while its C-terminus is predicted to form a small β-sheet, multiple β-turns and 3 α–helical stretches. The N-terminal region unique to kazrin A is predicted to form 4 α-helices and a β-turn, while the N-terminal region unique to kazrin B is predicted to form two short α-helical stretches and multiple β-turns (Fig 4.4 B).

Table 4.2 Amino acid composition of kazrin isoforms

Kazrin isoform	% polar aa	% non-polar aa	% basic aa	% acidic aa
A	29.7	37.3	17.3	15.7
B	28.1	37.5	18.3	15.9
C	28.0	35.7	19.5	16.5

Kazrin proteins are likely to form coiled coils, as calculated by COILS using the Lupas algorithm (1991) (Fig. 4.5). Parallel two-stranded coiled coils consist of two right-handed α-helixes wrapped around each other with a left-handed superhelical twist. Coiled-coil-forming proteins have heptad repeats, $(abcdefg)_n$, in which residues in positions a and d are generally hydrophobic and form the interface between the two proteins. Coiled-coils are found in many proteins which dimerise, or form higher order structures, such as the plakins and keratins (Ruhrberg and Watt, 1997; Strelkov et al., 2003). The analysis suggests that kazrin proteins may form hetero-or homo-dimers with themselves or form dimers with other heptad-repeat containing proteins. The ability of kazrin isoforms to form coiled-coil dimers may explain the formation of the >60 kDa band seen in Fig. 4.3 A, track c.

Leucine zippers are a specialised form of the coiled coil in which residue d in the heptad repeat is a leucine (Alber, 1992). Leucine zipper sequences are generally composed of 3 to 6 leucine-containing heptad repeats (Bornberg-Bauer et al., 1998). 2ZIP, a program used to predict the presence of leucine zipper sequences, suggests a region encoded by exon 2, prior to the translation start site of kazrin C, consists of a leucine repeat (three heptads) (Fig. 4.6). The leucine zipper-like repeats are predicted to form part of a coiled-coil region (asterisk, Fig. 4.5).

kazrin A

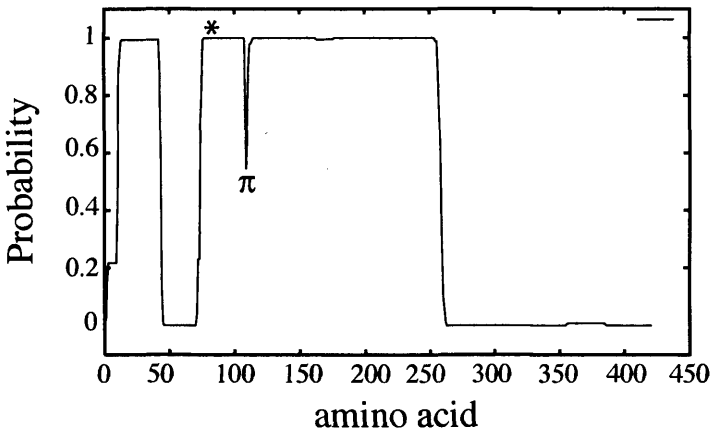

kazrin B

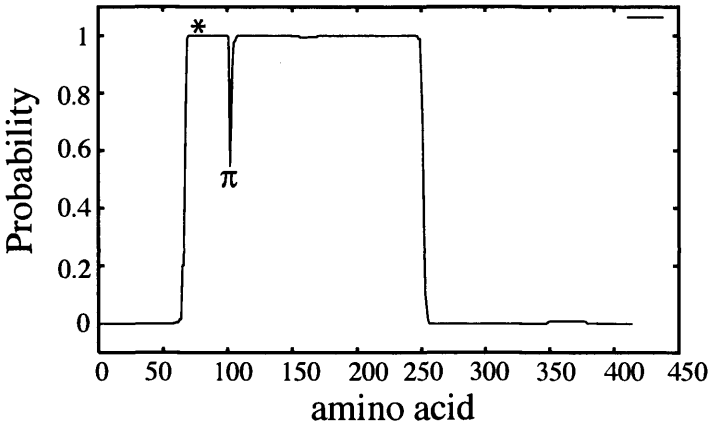

kazrin C

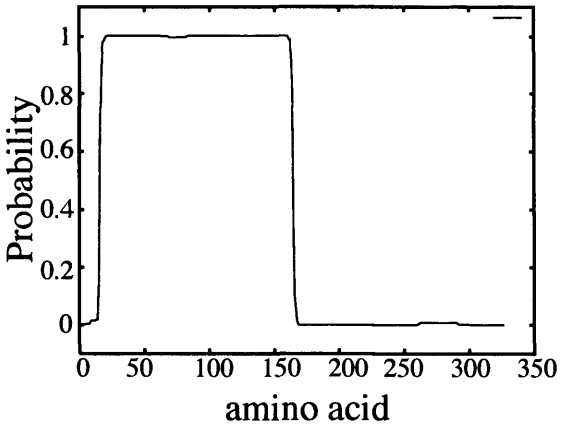

Fig 4.5 Kazrin isoforms are likely to form coiled coils. Probability graphs of the likelihood that a particular amino acid is part of a coiled coil, as calculated by the Lupas algorithm (Lupas et al. 1991). Kazrin sequences were analysed, with a 28 amino acid window, for regions with a high probability of forming coiled coils. Amino acids with a probability value > 0.9 for 35 consecutive amino acids or more, are likely to form coiled coil structures. Asterisks indicate the location of the leucine zipper-like repeats of kazrin A and B. π indicates the non-helical region between the predicted leucine zipper region and the large α-helical domain of kazrin.

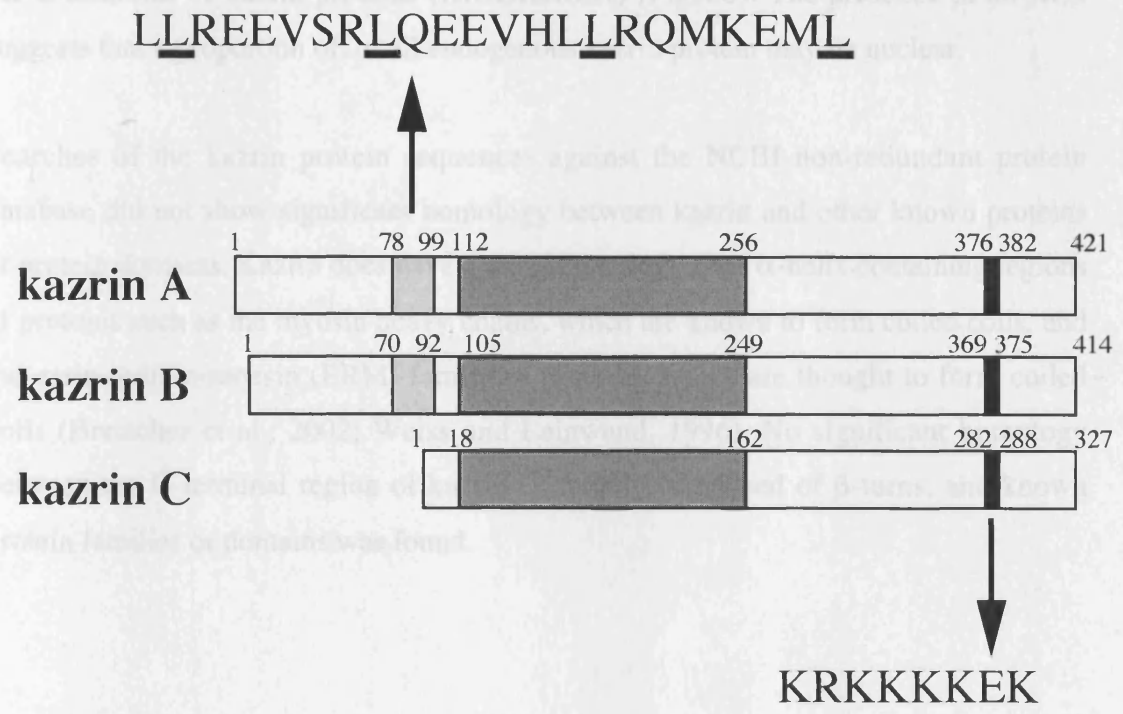

Fig 4.6 Kazrin proteins contain putative leucine zipper domains and nuclear localisation signals. Schematic diagram (to scale) of structural features of the kazrin protein isoforms based on analysis by MacVector 6.5.3, NLS prediction and 2ZIP. Light grey box: leucine zipper-like domain; dark grey box: α-helical domain; black box: nuclear localisation signal (NLS). Sequence of the leucine zipper-like domain is shown with leucines in position *d* of the heptad repeat underlined. Sequence of the NLS is indicated. Numbers indicate the amino acid positions at which domains are predicted to start and finish.

Proteins destined for the nucleus generally contain a nuclear localisation signal (NLS) composed of a cluster of basic amino acids (Makkerh et al., 1996). The NLS is bound by α-importin, which facilitates protein transport through the nuclear pore complex. The NLS prediction algorithm of Cokol et al. (2000) suggests the presence of an NLS in the C-terminus of kazrin proteins (KRKKKKEK) (Fig.4.6). The presence of an NLS suggests that a proportion of, or all endogenous kazrin protein may be nuclear.

Searches of the kazrin protein sequences against the NCBI non-redundant protein database did not show significant homology between kazrin and other known proteins or protein domains. Kazrin does have a weak homology with α-helix-containing regions of proteins such as the myosin heavy chains, which are known to form coiled-coils, and the ezrin-radixin-moesin (ERM) family of proteins, which are thought to form coiled-coils (Bretscher et al., 2002; Weiss and Leinwand, 1996). No significant homology between the C-terminal region of kazrin C, largely composed of β-turns, and known protein families or domains was found.

4.2.5 Sequence comparison of kazrin proteins

The mouse kazrin gene, as analysed by BLAT and BLAST, has a similar structure to the human gene (compare Fig. 4.2 A and 4.7 A). Kazrin a and b, but not kazrin c or d, mRNAs have been identified in mouse EST databases thus far. The predicted amino acid sequence of human and mouse kazrin, over the region encompassing kazrin C protein are 98% identical. The changes of amino acids between human and mouse sequences, over the region encompassing kazrin C, are 17 S to C, 31 A to V, 126 T to A, 212 A deleted, 265 N to S. Fig 4.7 B shows the alignment of human and mouse exons 1a and 1b up to the translation initiation site of kazrin C in exon 2. The N-terminal domains of mouse and human kazrin A show 84% identity and 88% similarity, while the kazrin B N-terminal sequences show 63% identity and 72% similarity.

BLAST searches of the human kazrin C sequence against the GenBank non-human and non-mouse EST translated database indicated the expression of kazrin-like proteins in other species. Kazrin homologues are found in many bony vertebrates (Table 4.3). No sequences with significant homology to kazrin were identified in the worm *C. elegans*

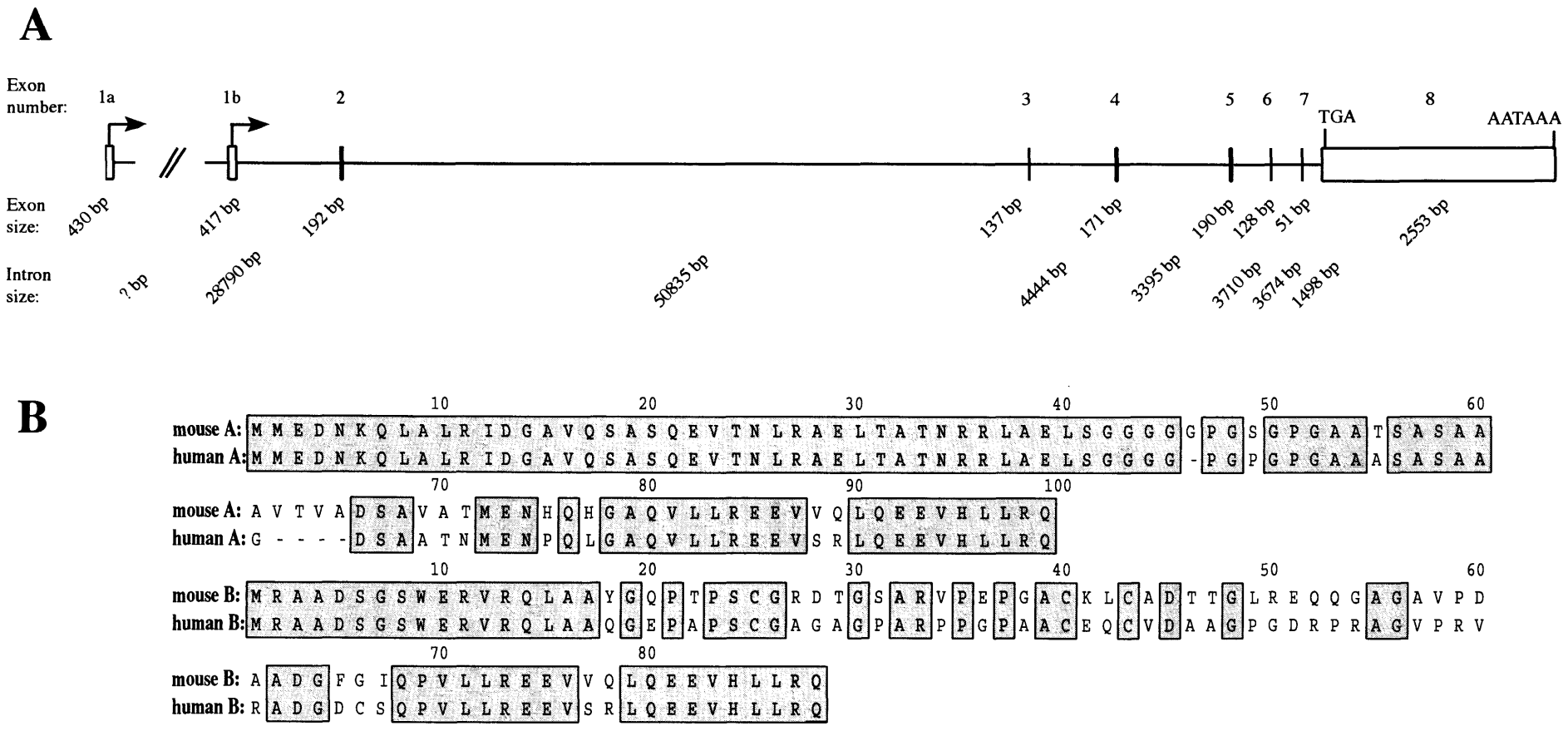

Fig 4.7 Human and mouse kazrin genes are highly conserved. (A) Schematic of the mouse kazrin gene. Mouse exon 1a has been identified in EST databases but its location on chromosome 4 relative the rest of the gene is unknown. TGA, termination codon; AATAAA, transcription termination signal. (B) Alignment of amino acid sequences encoded by human and mouse exons 1a and 1b, up to the translation initiation site of kazrin C in exon 2. Amino acid numbers are shown above the alignment. Identical amino acids are boxed. Amino acid sequences of mouse kazrin isoforms are predicted from publicly available databases.

or yeast. An EST (AI063603) with 36% identity, 76% similarity with the α-helical region of kazrin was identified in the fruit fly (*Drosophila melanogaster*). The kazrin C protein sequence was subsequently searched against a BLAST database of *Drosophila* translated ESTs. The search indicated that kazrin C showed homology to a region of two *Drosophila* proteins, from the same gene, known as CG11206-PA (1013 amino acids; accession no. AAF46835) and RE35867p (653 amino acids; accession no. AAQ22463).

Table 4.3 Kazrin is highly conserved amongst vertebrates

Percentage identity	Percentage similarity	Species name	GenBank accession no.
99	99	*Rattus norvegicus* (Rat)	BF548714
94	94	*Bos taurus* (Bull)	AW462068
92	94	*Gallus gallus* (Chicken)	AJ451182
83	92	*Danio rerio* (Zebrafish)	AI332211
89	94	*Xenopus laevis* (Frog)	BI314816
77	80	*Xenopus laevis* (Frog)	BJ032461
77	80	*Xenopus laevis* (Frog)	BG555153
77	80	*Xenopus laevis* (Frog)	BG554572
76	79	*Xenopus laevis* (Frog)	BG410176
73	78	*Silurane tropicalis* (Frog)	BG512962
70	71	*Silurane tropicalis* (Frog)	AL681984

NCBI-BLAST searches of the human kazrin C amino acid sequence against the GenBank non-mouse and non-human EST database indicated the expression of kazrin-like proteins in other species, all of which belong to the taxon Euteleostomi or bony vertebrates. Species included in the list have an EST represented in the database with greater than 70% identity at the amino acid level, over a length of greater than 100 amino acids, with human kazrin C. Percentage identity and similarity at the amino acid level and the relevant GenBank accession numbers are shown.

4.3 Further analysis of the interaction between kazrin and periplakin

The yeast two-hybrid screen demonstrated that kazrin C (amino acids 49-327) could bind periplakin P133. In order to map the regions of periplakin and kazrin necessary for this interaction, yeast two-hybrid analysis was carried out with periplakin and kazrin

deletion mutants. To demonstrate that kazrin could bind endogenous full length periplakin, GST pull-downs were carried out.

4.3.1 Mapping of the interaction between kazrin and periplakin by yeast-two hybrid screening

Deletion mutants of kazrin ('prey') were tested for their ability to interact with P133 ('bait') by yeast two-hybrid analysis. The binding was analysed by growth of transformed yeast on $A^-L^-T^-H^-$ agar.

Full length kazrin C and kazrin C aa 49-327 both bound P133 (Fig. 4.8). Further deletions showed that the minimal region necessary for P133 binding was amino acids 89-239 of kazrin C, encoding the latter half of the α-helical domain and a series of β-turns (Fig. 4.8).

Periplakin deletion constructs were tested for their ability to bind kazrin C and kazrin C amino acids 88-239. P80 and P63 did not detectably bind kazrin C. Kazrin C was able to bind P16-133, indicating that the non-helical region preceding the periplakin NN sub-domain is not essential for the interaction. Finally, P16-133 was found to bind kazrin C amino acids 89-239 (Fig. 4.9)

In conclusion, the minimal regions required for the interaction are amino acids 88-239 of kazrin C and amino acids 16 to 133 of periplakin.

4.3.2 Confirmation of the interaction between kazrin and periplakin by GST pull-down

To validate the association of kazrin with P133, kazrin-GST fusion proteins were used in pull-down assays with human keratinocyte lysates as a source of periplakin (Fig. 4.10). The partial clone obtained in the yeast two-hybrid screen (KCΔ), full-length kazrin A, B, and C all bound periplakin, while GST protein alone did not. Envoplakin was also pulled down by kazrin-GST fusion proteins but not by GST protein alone.

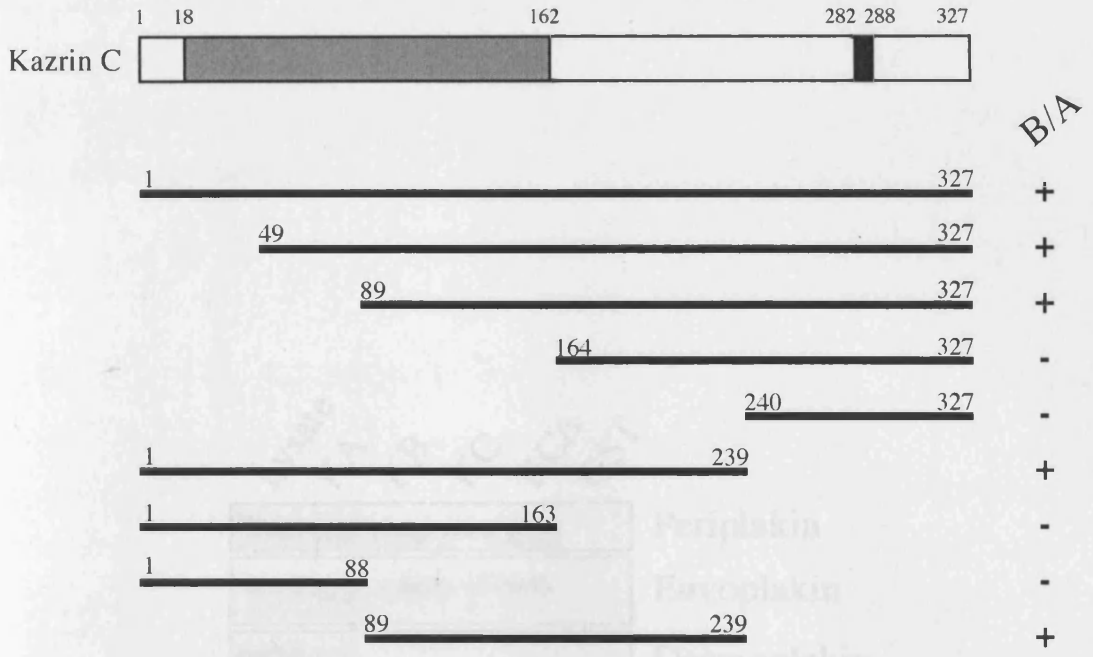

Fig 4.8 The minimal region of kazrin that binds P133 encompasses half the α–helical domain and a series of β-turns. Deletion analysis of kazrin C protein by yeast two-hybrid analysis. Yeast transformations were performed using P133 in combination with different portions of kazrin C protein, as shown above. B/A: binding activity, assessed by growth of yeast on selective media. A schematic picture of the kazrin C protein is shown at top. Dark grey box: α-helical domain; black box: nuclear localisation signal. Numbers indicate the amino acid positions at which domains start and finish.

Periplakin (bait)	Kazrin (prey)	Binding activity
Periplakin (P133)	Kazrin C (aa 1-327)	+
Periplakin (P80)	Kazrin C (aa 1-327)	-
Periplakin (P63)	Kazrin C (aa 1-327)	-
Periplakin (P16-133)	Kazrin C (aa 1-327)	+
Periplakin (P16-133)	Kazrin C (aa 88-239)	+

Fig 4.9 Periplakin P16-133 binds kazrin C efficiently. Deletion analysis of periplakin N-terminus. Yeast transformations were performed using a variety of periplakin bait vectors, in combination with different portions of kazrin C (prey) protein. Binding activity was assessed by growth of yeast on selective media.

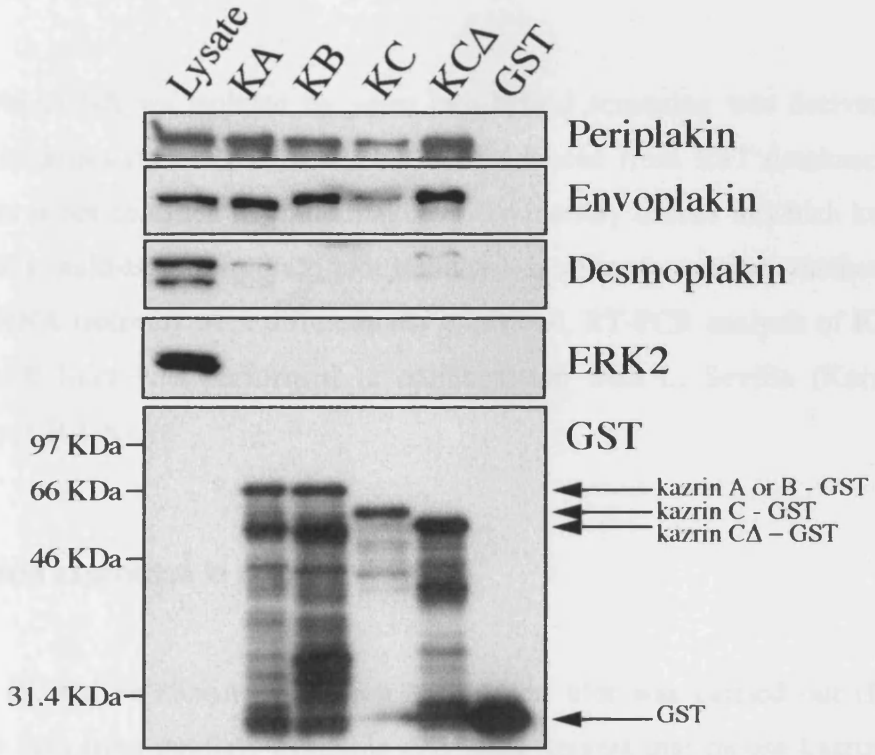

Fig 4.10 Kazrin binds periplakin and envoplakin in GST pull-down experiments. 10μg of kazrin-GST fusion proteins or GST alone were bound to GST beads and incubated with primary human keratinocyte lysate. As a positive control 4% of the cell lysate was run alongside the pull down reactions. Immunoblots were probed with antibodies to periplakin (TD2), envoplakin (CR5), desmoplakin (Dp115F), ERK2 (ERK2 anti-serum) and GST (GST anti-serum). KA: kazrin A-GST; KB: kazrin B-GST; KC: kazrin C-GST; KCΔ: Kazrin C aa 49-327-GST; GST: GST alone. Arrows highlight the position of full length kazrin - GST fusion proteins and GST protein alone bands.

Desmoplakin was readily detected in keratinocyte lysates, but was either undetectable or weakly detectable in the GST pull-downs (Fig. 4.10). An ERK2 control was carried out for non-specific interactions. ERK2 was readily detected in the lysate but undetectable in pull-down lanes.

4.4 Analysis of the expression pattern of kazrin

The kazrin cDNA we isolated by yeast two-hybrid screening was derived from a foreskin keratinocyte cDNA library but, as evidenced from EST databases, kazrin expression is not confined to epidermal cells. To identify tissues in which kazrin was expressed, a multi-tissue Northern blot was used. In order to analyse whether the four kazrin mRNA isoforms were differentially expressed, RT-PCR analysis of RNA from various cell lines was performed in collaboration with L. Sevilla (Keratinocyte laboratory, CR-UK).

4.4.1 Kazrin expression in mouse tissues

In order to analyse kazrin expression a Northern blot was carried out (Fig 4.11) Sequence data from publicly available databases suggest that mouse kazrin a and b mRNAs are roughly 3.85kb in length. A 585bp DNA probe, able to recognise both kazrin a and b mRNAs, identified a band below the 4.4kb marker, presumably kazrin a and b transcripts (Fig. 4.11 A). The data suggest that kazrin mRNAs are highly expressed in the brain and kidney. Lower levels of kazrin expression were detected in lung, testis and spleen. Kazrin is not expressed or expressed at undetectable levels in heart, liver and skeletal muscle (Fig. 4.11 A).

Fig. 4.11 B shows that in addition to the predicted 3.85kb kazrin a and b transcripts other transcripts are recognised by the kazrin probe. Transcripts of ~2.3kb and ~5.1kb were readily identified using the kazrin cDNA probe in mouse spleen and testis samples. The transcripts identified may be other kazrin splice variants or sequences with some homology to the kazrin sequence.

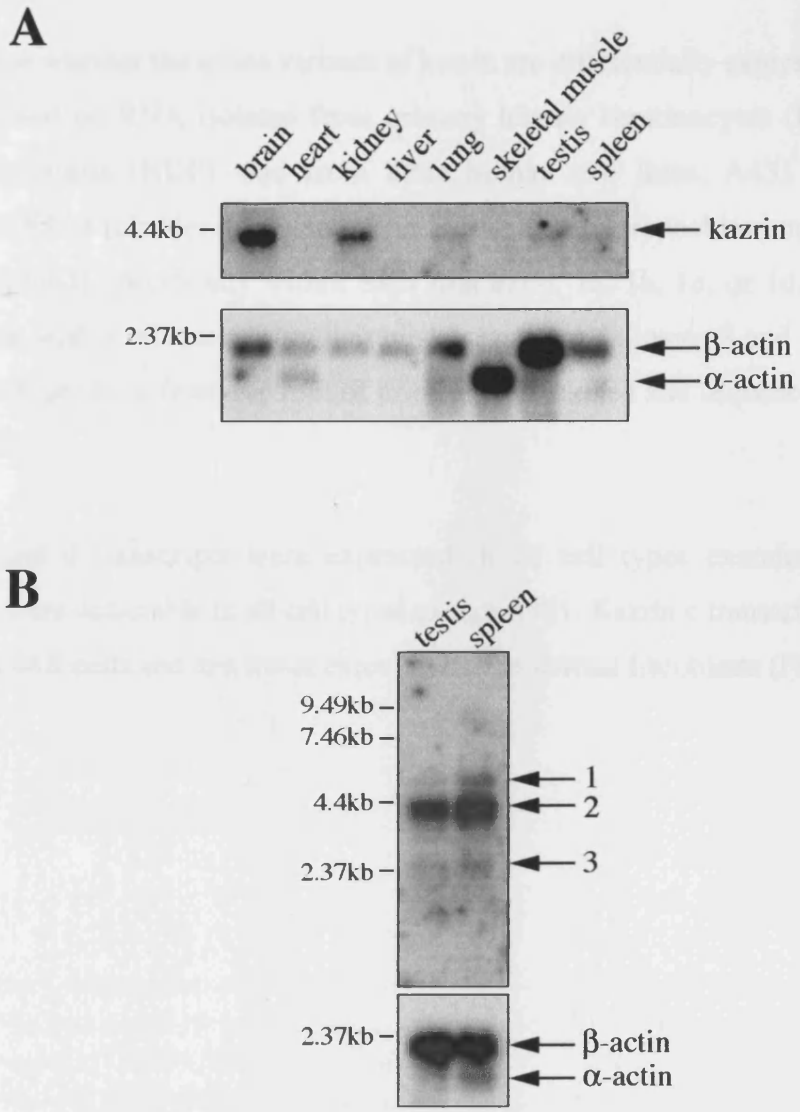

Fig 4.11 Kazrin mRNA is expressed in a range of mouse organs. Message-Map northern blots of mRNA from a panel of mouse organs (Stratagene). Northern blots were probed with a 585bp probe recognising both kazrin a and kazrin b mRNAs. (A) Northern blot showing kazrin mRNA expression in brain, kidney, lung, testis and spleen. (B) Northern blot showing RNA from mouse testis and spleen. Arrows mark putative kazrin transcripts. Arrow 2 marks a kazrin transcript of the predicted size, based on analysis of publicly available sequence data; arrows 1 and 3 may represent other kazrin mRNA splice variants. An actin loading control is shown in each case. The β-actin probe binds α-actin, resulting in the appearance of an additional band.

4.4.2 Analysis of the expression of the different kazrin isoforms

To determine whether the splice variants of kazrin are differentially expressed, RT-PCR was performed on RNA isolated from primary human keratinocytes (HK), primary dermal fibroblasts (HDF), and from three human cell lines, A431 (epidermoid carcinoma), EJ/28 (bladder carcinoma), and JAR (placental trophoblastoma). A forward primer that binds specifically within each first exon, 1a, 1b, 1c, or 1d, was used in combination with a reverse primer that binds sequences in exons 3 and 4 (Fig. 4.12). The RT-PCR products from each set of primers were cloned and sequenced to confirm their identity.

Kazrin b and d transcripts were expressed in all cell types examined. Kazrin a transcripts were detectable in all cell types except A431. Kazrin c transcripts were only detected in JAR cells and to a lesser extent in human dermal fibroblasts (Fig. 4.12).

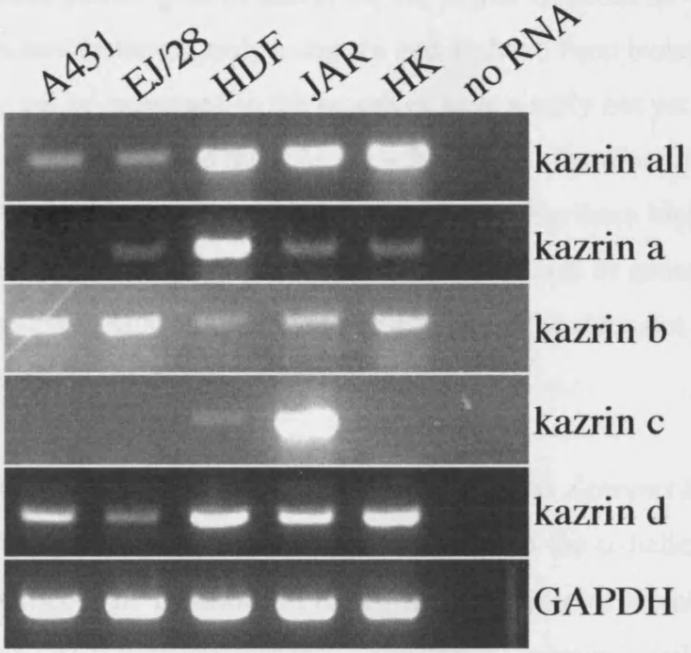

Fig 4.12 Expression of kazrin isoforms. RT-PCR analysis of kazrin mRNA in a panel of primary cells and cell lines: A431 (epidermoid carcinoma), EJ/28 (bladder carcinoma), HDF (human dermal fibroblasts), JAR (placental trophoblastoma), HK (human primary keratinocytes). Forward primers specific for each of the four alternatively spliced first exons (1a, 1b, 1c, 1d) were used in combination with a reverse primer that binds within the third and fourth exons common to all splice forms. As control for the total level of kazrin transcripts, a forward primer was used that binds within exon 2 (kazrin all) in combination with the reverse primer. Primers specfic for GAPDH were used to control for the input level of mRNA.

4.5 Discussion

In this chapter I have shown that kazrin is a novel interactor of periplakin. Analysis of the nucleotide and amino acid sequences of kazrin isoforms suggests it is highly conserved. Mouse homologues of kazrin 1a, 1b, 1c and 1d exons have been identified in the mouse genome; however, only exons 1a and 1b have been isolated as ESTs. Exons 1c and 1d may not be expressed in the mouse or have simply not yet been reported. The predicted size of kazrin c and d mRNAs are ~ 3.67kb and therefore it may not be easy to differentiate kazrin a, b, c and d mRNA isoforms on a Northern blot. Northern blotting of mouse tissues suggests that further kazrin splice variants or genes with homology to the kazrin gene exist. Analysis of the mouse EST database does not reveal the presence of other kazrin splice variants at present.

Kazrin homologs were found in many vertebrates, such as *Xenopus laevis* and chickens. Two *Drosophila* proteins which showed homology to the α-helical region of kazrin were also identified. The functions of the ***Drosophila*** proteins are not known, although analysis using COILS suggests that they, like kazrin, contain a coiled-coil region. The similarity seen with the vertebrate kazrin sequences may be suggestive of the existence of a kazrin homolog in *Drosophila.*

Kazrin was isolated in a yeast two-hybrid screen to find interactors of periplakin (P133) which may be involved in targeting periplakin to the microvilli. Yeast two-hybrid analysis showed that P16-133 could, but P80 could not, interact with kazrin C. Analysis of periplakin localisation by transient transfection suggested that P80 could localise to the microvilli, while P16-133 could do so much less efficiently. The disparity between the yeast two-hybrid analysis and the transient transfections suggests that kazrin is not the protein that targets periplakin to the microvilli. Alternatively the yeast system may not be a complete predictor of kazrin/periplakin interactions in primary keratinocytes.

The interaction between P133 and kazrin was mapped to the latter half of the kazrin α–helical domain and a series of β-turns. How the interaction is achieved in three-dimensions is not known and would require analysis of the crystal structure of kazrin/periplakin complexes. It is tempting to speculate that some or all of the short α-

helical regions of periplakin P133 form a coiled coil-like structure with the kazrin α-helical region. The non-helical section and β-turns of kazrin may act to stabilise and strengthen the interaction with P133.

Kazrin and P133 can associate in intact cells, as shown by immunoprecipitation experiments (L Sevilla, Keratinocyte laboratory, CR-UK). Immunoprecipitations using COS cells co-transfected with C-terminal FLAG-tagged kazrin C and C-terminal HA tagged P133 in COS cells (Groot el al., 2004).

A lack of suitable antibodies capable of immunoprecipitating kazrin or periplakin prevented us from showing the interaction of endogenous kazrin and periplakin in keratinocytes. LS4, our rabbit polyclonal antibody to kazrin, does not immunoprecipitate. We have antibodies capable of immunoprecipitating periplakin, but these are all rabbit polyclonals.

Endogenous periplakin binds kazrin in GST pull-down experiments. Envoplakin was pulled down by kazrin-GST but not by GST protein alone, suggesting that kazrin and envoplakin can interact, presumably indirectly through heterodimerisation of envoplakin and periplakin. The pull-down of envoplakin suggests that the binding of periplakin and kazrin and the binding of envoplakin and periplakin are not mutually exclusive.

Northern blotting data from mouse tissues (Fig. 4.12) suggested that kazrin was expressed in several mouse tissues. Real-time PCR analysis of kazrin expression, using cDNA preparations of multiple human tissues, indicated that it is expressed widely (K. Nishi, Keratinocyte laboratory, CR-UK). Kazrin was expressed highly in brain, kidney, lung, placenta and spleen. Expression of kazrin was low in skeletal muscle (Groot et al., 2004).

Kazrin was detected in many tissues that have previously been shown to express periplakin, including bladder, brain, colon, heart, kidney, liver, lung, pancreas, placenta, and small intestine (Aho and Kazerounian, 2003; Aho et al., 1998; Ma and Sun, 1986; Ruhrberg et al., 1997). Periplakin expression is not confined to epidermal epithelial cells, the function of periplakin in transitional, pseudo-stratified and simple epithelia, as

well as non-epithelial tissues such as the brain, is not well understood (Ruhrberg et al., 1997). The presence of kazrin in many of the cell types that express periplakin suggests the interaction between kazrin and periplakin is not restricted to epidermal cells.

RT-PCR analysis of the kazrin mRNA isoforms suggests that kazrin mRNA splicing differs between cell types. Keratinocytes express mRNA isoforms a, b and d and thus are predicted to express all three kazrin proteins. All three of these proteins are able to interact with periplakin. EJ/28, HDF and JAR cells are also predicted to express all three kazrin protein isoforms, while A431 cells, which do not express kazrin a mRNA, are expected to express only kazrin B and C proteins. As there is differential expression of the different kazrin mRNA isoforms and there are likely to be differences in the relative levels of kazrin A, B and C proteins expressed in different tissues, it will be of interest to know the function of the unique N-termini of kazrin A and B.

Chapter 5.

In this chapter I will present data on the localisation of endogenous kazrin in epithelial tissues and cultured primary keratinocytes. The localisation and effect of expression of individual kazrin isoforms was analysed by means of transient transfection of kazrin cDNA constructs into cultured primary keratinocytes and cell lines.

5.1 Kazrin localisation in epithelial cells and tissues

In order to analyse the localisation of endogenous kazrin proteins, a rabbit antiserum (LS4) was raised against a peptide corresponding to the C-terminal 20 amino acids of kazrin. The sequence used is found in all three kazrin isoforms and is entirely conserved between mice and humans. The affinity purified antiserum recognized bands of approximately 47 kDa and 37 kDa on Western blots of lysates from A431, EJ/28 and primary keratinocytes (Groot et al., 2004). The bands corresponded to the predicted molecular weights of kazrin A (46.8 kDa), kazrin B (46.2 kDa) and kazrin C (37.0 kDa).

5.1.1 Kazrin localises to cell-cell borders

To detect endogenous kazrin in frozen tissue sections the LS4 antiserum was used for immunostaining. Kazrin was detected in all layers of the epidermis (Fig. 5.1 A) and in the hair follicle (Groot et al., 2004). Periplakin is upregulated in suprabasal cells of the epidermis (Fig. 5.1 B). In suprabasal layers, where periplakin is expressed, kazrin localised to cell-cell borders. In the basal layer, which lacks periplakin expression, kazrin was more diffusely localised (Fig. 5.1 A). Some kazrin signal was detected in the dermis, consistent with the expression of kazrin mRNAs in human dermal fibroblasts (Fig. 5.1 A and Fig. 4.12).

In oesophageal mucosa and cervical mucosa, kazrin was expressed in all the epithelial cell layers. Kazrin partially colocalised with desmoplakin at cell-cell borders; this was

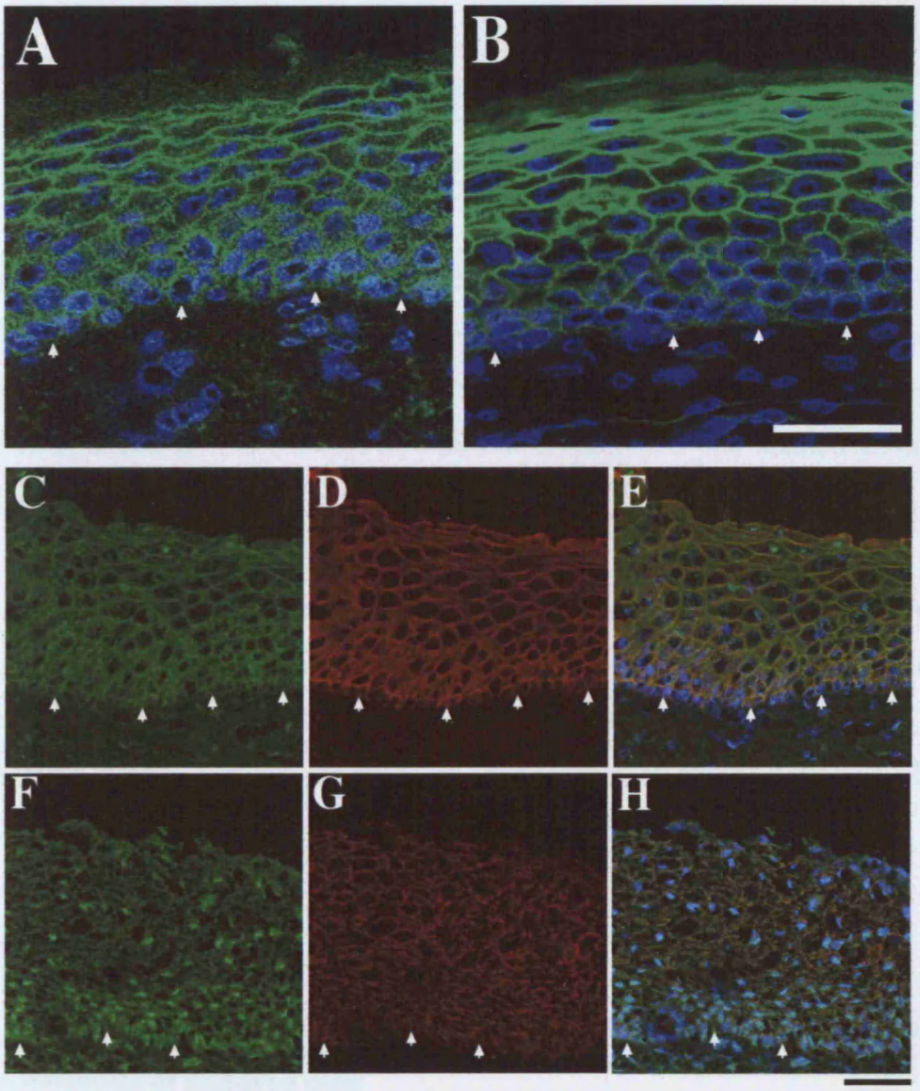

Fig 5.1 Kazrin localises to cell-cell borders, partially colocalising with desmoplakin. Immunofluorescence staining of sections of frozen human epidermis (A,B), oesophageal mucosa (C-E) and cervical mucosa (F-H). Green fluorescence: kazrin (A, C-H); periplakin (B). Blue fluorescence: (A-B) TOPRO3 nuclear counterstain; (C-E) DAPI nuclear counterstain. Red Fluorescence: desmoplakin (C-H). Arrows mark the position of the basement membrane. Scale bars: (A-B) 50μm; (C-H) 42μm. (A-B) Immunofluorescence staining by Lisa Sevilla (Keratinocyte laboratory, CR-UK)

observed most prominently in suprabasal layers (Fig. 5.1 C-H). Some kazrin signal was detected in the sub-mucosal tissue of the oesophagus and cervix (Fig. 5. C-H). Kazrin was detected in the nucleus of some epithelial and non-epithelial cells (Fig. 5.1 C-H). However, this was not a consistent finding (Fig. 5.1 A).

5.1.2 Kazrin localises to the desmosomes of epidermis

The immunofluorescence staining of epidermis suggested that kazrin might, like desmoplakin and periplakin, be a component of desmosomes. In collaboration with the Electron Microscopy Department (CR-UK) we set out to analyse kazrin localisation by immuno-electron microscopy. Samples were prepared and stained as detailed in the Materials and Methods.

Desmoplakin was found at the desmosomes of adult breast epidermis (Fig. 5.2 A,B). Kazrin was found at desmosomes (Fig. 5.2 C-D) and in the nucleus (Fig. 5.2 E), as detected using LS4 antiserum. There was little staining of adult breast epidermis in negative control samples stained with secondary antibody or protein A alone (Fig. 5.2 F,G).

5.1.3 Kazrin partially colocalises with desmoplakin and periplakin at the desmosomes of cultured cells

Primary human keratinocytes stratify and differentiate in culture. In stratified cultures kazrin was observed at cell-cell borders and in the nucleus (Fig. 5.3). At the interface between the apical surfaces of basal layer cells and the basal surfaces of suprabasal cells large numbers of desmosomes assemble. Kazrin partially colocalised with periplakin, which localises to the desmosomes and the interdesmosomal plasma membrane (Fig. 5.3 A-D). Kazrin partially colocalised with desmoplakin at the desmosomes (Fig. 5.3 E-H). Periplakin and kazrin were localised to puncta, corresponding to desmosomes, where intermediate filaments in neighbouring cells aligned (Fig. 5.3 I-L).

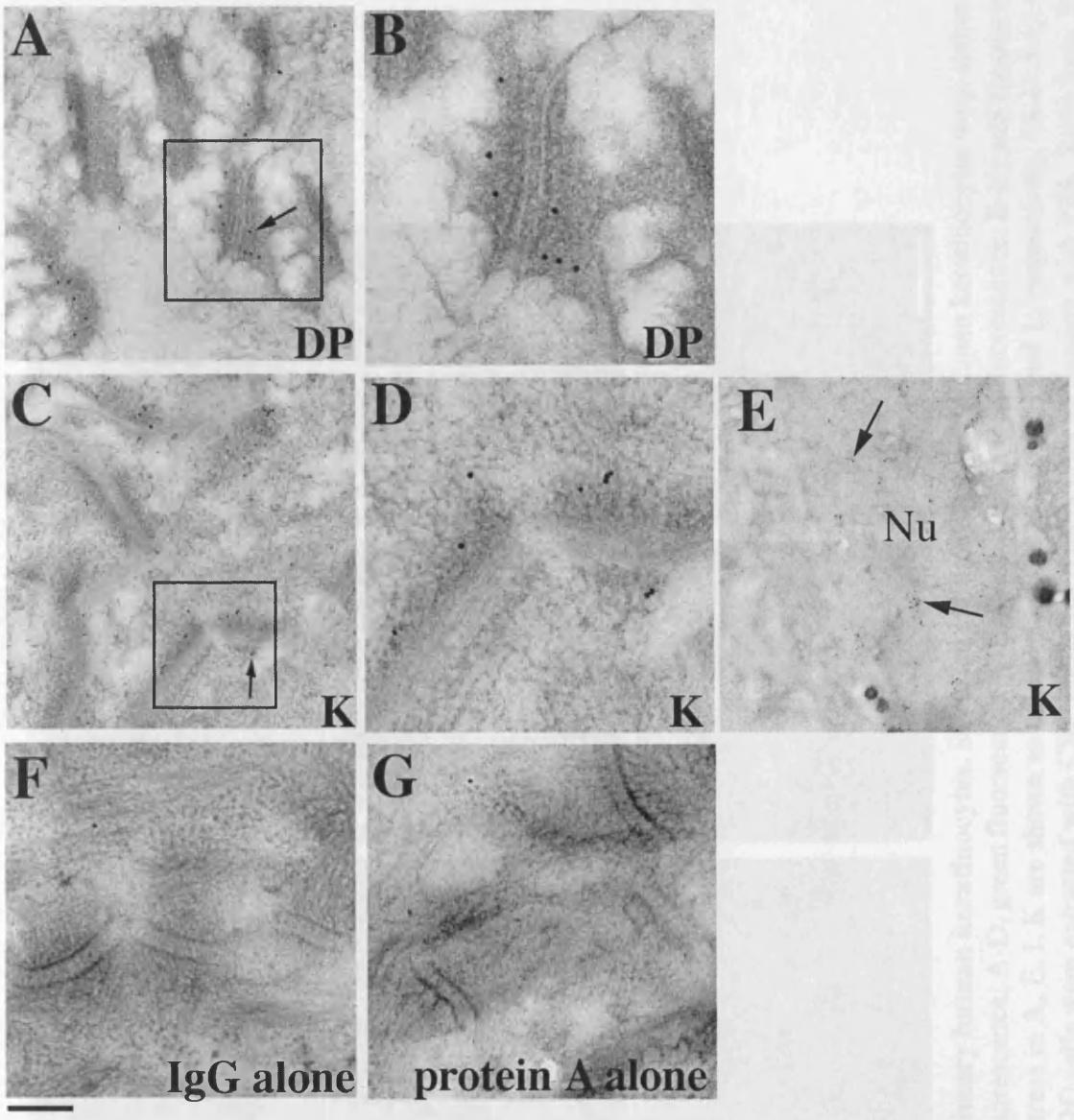

Fig 5.2 Kazrin localises to desmosomes and the nucleus of interfollicular epidermal cells. Adult breast epidermis was subjected to high pressure freezing/freeze substitution and sections labelled with antibodies to desmoplakin and kazrin. (A,B) desmoplakin (DP, Dp115F antibody); (C-E) kazrin (K, LS4 antibody); (F) Secondary antibody alone (goat anti-mouse IgG conjugated to 10nm gold); (G) protein A conjugated to 10nm gold. Boxed areas in A and C are shown as zooms in B and D, respectively. Arrows indicate gold particles localised at the desmosomes (A, C) or in the nucleus (Nu) (E). Scale bar: 200nm (A, F), 90 nm (B), 330nm (C, G), 120 nm (D), 487nm (E).

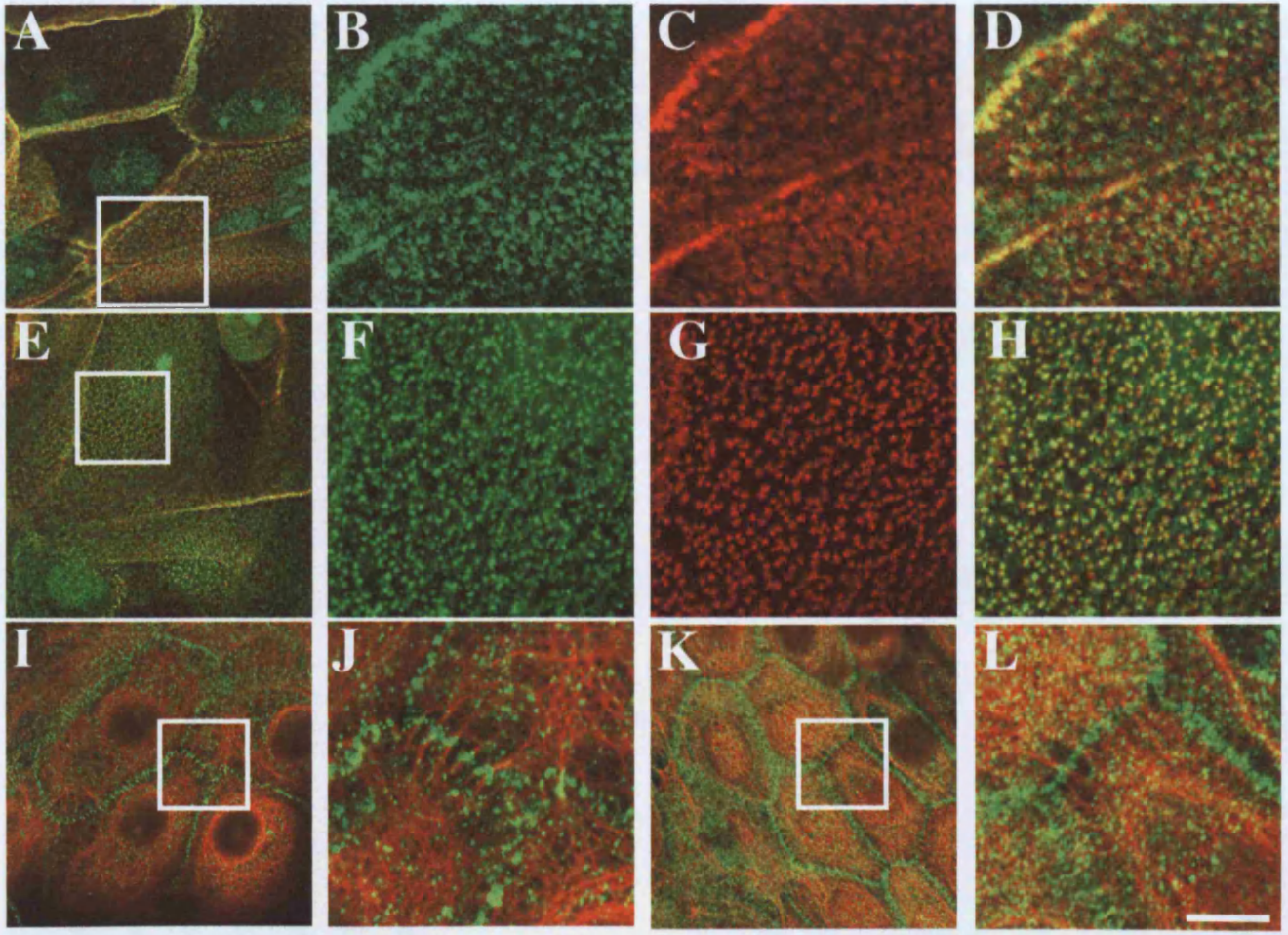

Fig 5.3 Kazrin localises to the desmosomes of primary human keratinocytes. Stratified cultures of primary human keratinocytes were stained for kazrin (green fluorescence;A-J), periplakin (red fluorescence; A-D, green fluorscence; K-L), desmoplakin (red fluorescence; E-H) and keratin intermediate filaments (red fluorescence; I-L). Boxed areas in A, E, I, K are shown as enlargements in B-D,F-H, J and L, respectively. (A-D, I-L) cells were fixed in ice-cold methanol for 2 - 5 mins. (E-H) cells were extracted with CSK buffer for 5 mins prior to fixation with PFA. Scale bars: 20µm (A, E, I, K), 7µm (B-D), 8.2µm (F-H), 5.4µm (J,L). (A-D) Immunofluorescence by Lisa Sevilla (Keratinocyte Laboratory, CR-UK).

5.1.4 Kazrin depends on actin but not periplakin for its localisation

Primary keratinocytes were cultured and treated with latrunculin B to disassemble the actin cytoskeleton (Fig. 5.4). Treatment with latrunculin B caused the redistribution of kazrin into actin-rich patches. Latrunculin B treatment also results in the redistribution of periplakin into actin-rich patches, in contrast to desmoplakin, which remains at the desmosomes (DiColandrea et al., 2000).

Immortalised keratinocyte lines were generated from wild type mice (Romero et al., 1999) and periplakin knock-out mice ($MKP^{-/-}$). The cell lines were grown to confluence in high calcium medium to induce differentiation and stratification (see Materials and Methods for more details). Kazrin partially colocalised with desmoplakin at the cell-cell borders of differentiated wild type and $MKP^{-/-}$ mouse keratinocytes (Fig. 5.5). The results suggest that kazrin is not dependent upon periplakin to localise to cell-cell borders. The nuclei of wild type and $MKP^{-/-}$ mouse keratinocytes stained strongly with LS4 antiserum (Fig. 5.5).

5.1.5 Kazrin can be incorporated into the cornified envelope

To determine whether kazrin, like periplakin, can be incorporated into the cornified envelope, confluent keratinocyte cultures were treated with 0.04% Triton X-100 for 5 hours to induce envelope assembly (Fig. 5.6). Perforations in the plasma membrane, formed by Triton X-100 treatment, allow entry of extracellular Ca^{2+} ions into the cell. The extracellular Ca^{2+} activates the crosslinking of cornified envelope precursors by Ca^{2+}-dependent tranglutaminases. Proteins that become cross-linked into the cornified envelope are no longer extractable in buffers containing SDS and reducing agents (Rice and Green, 1979). Transglutaminase-mediated crosslinking is inhibited by cystamine (Ruhrberg et al., 1997; Siefring et al., 1978).

Periplakin was readily detected in control lysates in the presence (Cy) or absence of cystamine (-). Periplakin became non-extractable following Triton X-100 treatment (T)

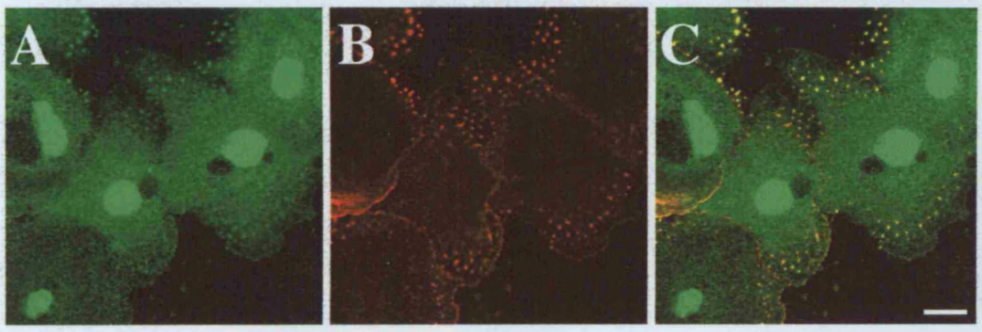

Fig 5.4 Kazrin partially localises to actin-rich patches formed upon latrunculin B treatment. Primary human keratinocytes were treated with latrunculin B (200ng/ml, 3hr) prior to fixation with 3% PFA and permeabilisation with 0.2% Triton X-100. Green fluorescence: kazrin (LS4). Red fluorescence: actin (phalloidin). Scale bar: 20μm.

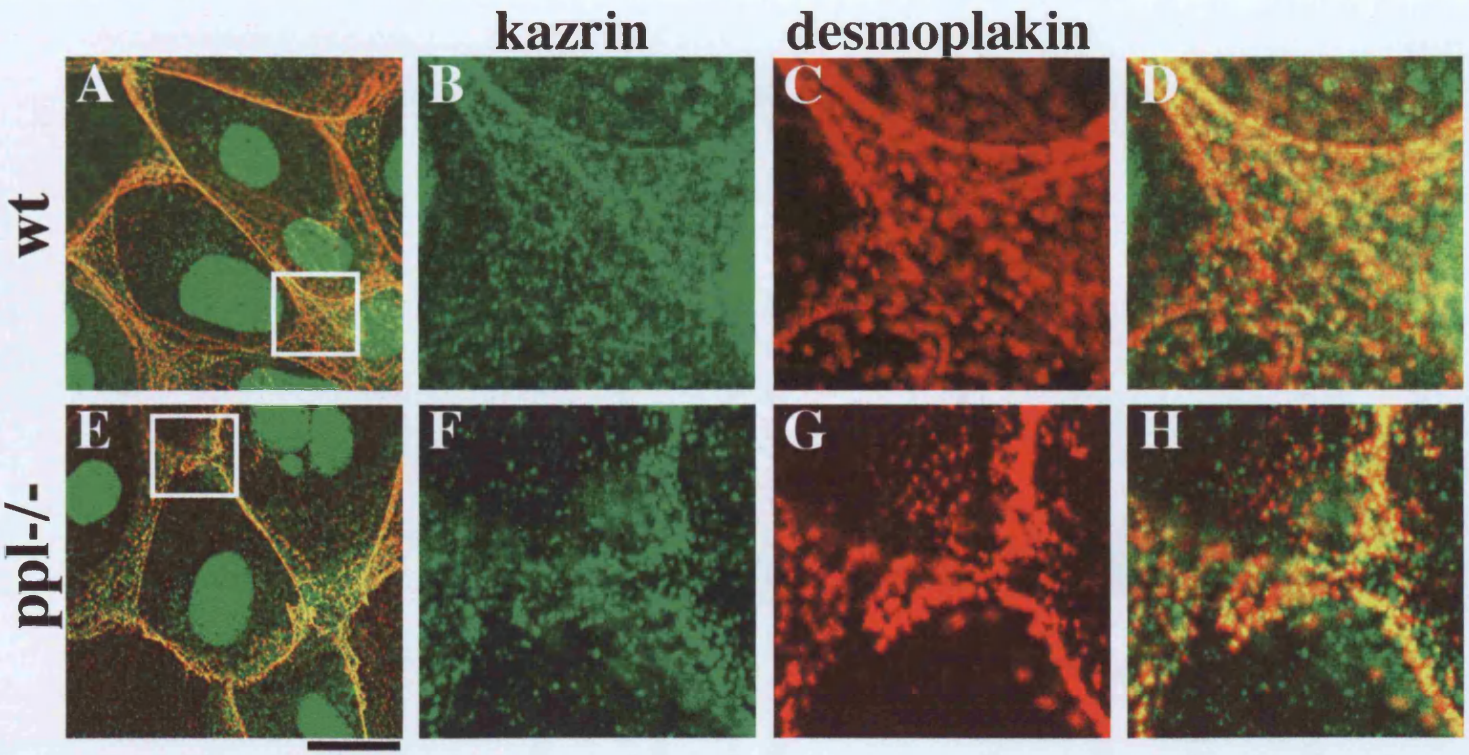

Fig 5.5 Kazrin localises to cell-cell borders independently of periplakin. Wild type (wt) and periplakin knockout (ppl-/-) mouse keratinocyte cell lines stained for kazrin (green fluorescence) and desmoplakin (red fluorescence). Boxed areas in A and E are shown as zooms in B-D and F-H respectively. Scale bar: (A,E) 20μm; (B-D,F-H), 5μm. Cells were extracted with CSK buffer for 5 mins prior to fixation with PFA. (A-H) Immunofluorescence staining by Lisa Sevilla (Keratinocyte Laboratory, CR-UK).

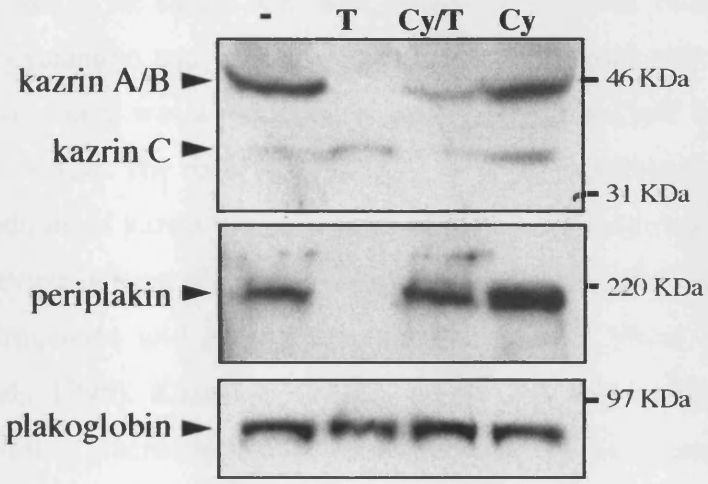

Fig 5.6 Kazrin can be incorporated into the cornified envelope upon activation of transglutaminases. Primary human keratinocytes were treated for 5hrs in serum-free FAD in the absence (-) or presence of Triton X-100 (T), or in serum-free medium containing 20mM cystamine in the absence (Cy) or presence of Triton X-100 (Cy/T). Immunoblots of the protein extracts were probed with antibodies to kazrin (LS4), periplakin (AE11) or plakoglobin (VB3).

and this was inhibited by cystamine (Cy/T), as previously shown (Ruhrberg et al., 1997; Simon and Green, 1984) (Fig. 5.6).

A 47 kDa band, corresponding to kazrin A and/or B proteins, was readily detected in the control lanes (- and Cy) probed with LS4. Treatment of the cells with Triton X-100 resulted in the loss of the kazrin A/B band on the Western blot. Following treatment of the cells with cystamine and Triton X-100, kazrin A/B could still be detected in the lysates; however, there was a reduction in the signal in the Cy/T lane, relative to the control lanes (- or Cy). The reduction in the signal is presumably the result of loss, into the culture medium, of kazrin proteins. Loss of cellular proteins upon permeabilisation of cells has previously been seen for involucrin (a known cornified envelope precursor), lactate dehydrogenase and even transglutaminase itself (Rice and Green, 1979; Ruhrberg et al., 1996). Kazrin C (37kDa band) was less readily detected in the keratinocyte lysates, precluding conclusions on whether kazrin C can be incorporated into the CE.

Plakoglobin, a component of desmosomes that can be incorporated into cornified envelopes (Robinson et al., 1997), was found to be only slightly reduced in cells treated with Triton X-100 alone (Fig. 5.6), as previously described by Christiana Ruhrberg (Keratinocyte Laboratory, Cancer Research UK).

5.2 Analysis of the localisation of transfected kazrin isoforms

To determine the subcellular localisation of kazrin proteins, constructs encoding tagged kazrin proteins were made. The constructs encoded N-terminally HA-tagged kazrin A, B and C or C-terminally FLAG-tagged kazrin C.

5.2.1 Kazrin localises to the plasma membrane

HA-tagged constructs encoding kazrin A, B or C were transiently transfected into primary human keratinocytes (Fig. 5.7). All three kazrin isoforms had similar

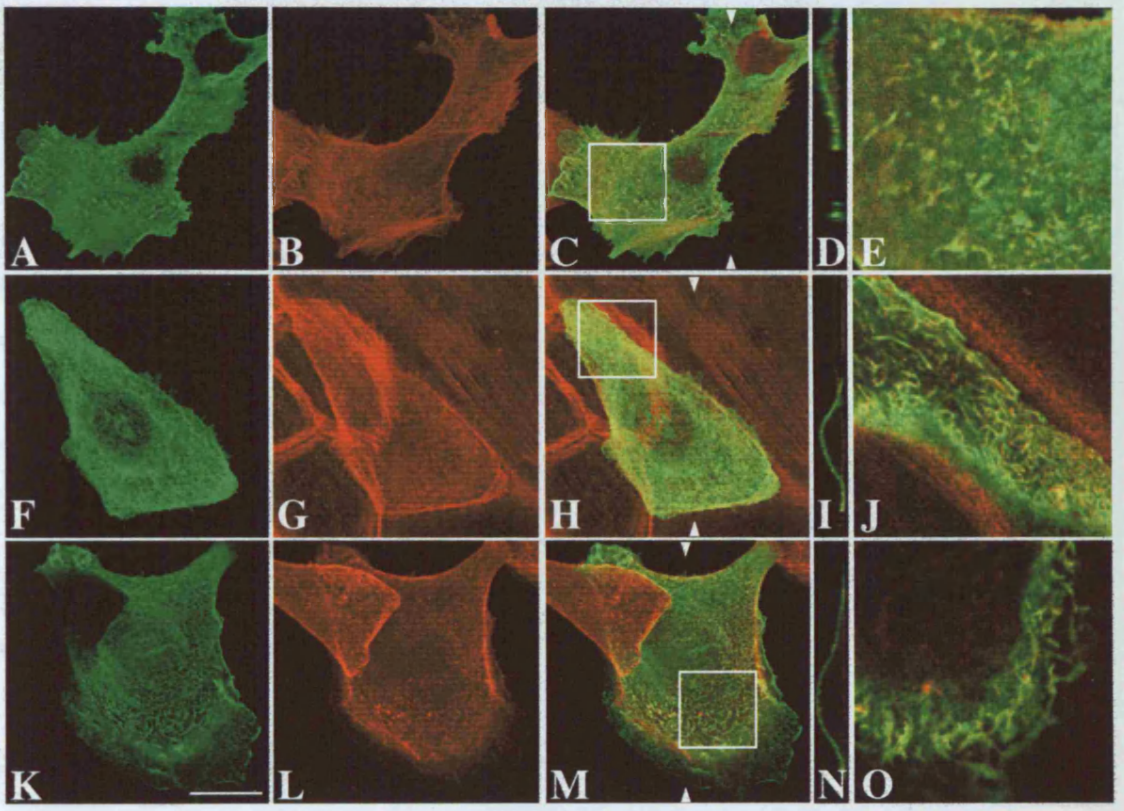

Fig. 5.7 Kazrin isoforms localise to the plasma membrane. Kazrin isoforms with N-terminal HA tags were transiently transfected into primary human keratinocytes. (A-O): anti-HA (green), phalloidin-TRITC (red). (A-E) kazrin A; (F-J) kazrin B; (K-O) kazrin C. A-C, F-H, K-M are composite images of z-stacks. Arrowheads indicate position of orthogonal views shown in D, I, N. Areas boxed in C, H, and M are shown as single confocal slice in E, J, and O, respectively. Z-stack size: (D) 8.2 µm, (I) 11.1 µm, (N) 11.6 µm. Scale bars: 20 µm (A-D, F-I, K-N); 6 µm (E, J, O).

distributions. Kazrin isoforms were found predominantly at the plasma membrane of primary keratinocytes (Fig. 5.7 D, I, N) with some signal in the cytoplasm and variable amounts in the nucleus (see below). All three kazrin isoforms partially colocalised with actin structures at the apical plasma membrane of keratinocytes (Fig. 5.7). Kazrin isoforms partially colocalised with CD44, a marker of microvilli (Fig. 5.8).

N-terminally HA-tagged forms of kazrin C were localised to actin structures at the plasma membrane in ~23% of cells (n=82). C-terminally FLAG-tagged forms of kazrin C were seen at apical plasma membrane structures, colocalising with actin, in ~26% of cells (n=42). The kazrin proteins were not seen at apical plasma membrane structures in every cell, as many of the cells had very small, and/or few, microvilli or ruffle structures at their surface (see below).

5.2.2 Kazrin colocalises with P133 at microvilli

Kazrin was identified as a binding partner of periplakin P133. Primary keratinocytes were co-transfected with N-terminally HA-tagged P133 and C-terminally FLAG-tagged kazrin C (Fig. 5.9). Keratinocytes generally have short microvilli over their apical surface (DiColandrea et al., 2000). In keratinocytes transfected with P133, P133 was seen prominently at the microvilli. The microvilli of cells co-expressing P133 and kazrin-C did not always cover the whole apical surface of the cells; however, kazrin C and P133 could colocalise at apical plasma membrane structures (Fig. 5. 9). Quantitation of the colocalisation suggested that P133 and kazrin C colocalised at apical plasma membrane structures in ~42% of transfected primary keratinocytes (n=119). The orthogonal views indicated that kazrin is found at plasma membrane projections colocalising with P133 (Fig. 5.9 D). Kazrin, and some P133, can also be seen in the cytoplasm of the transfected keratinocytes (Fig. 5.9 D).

Cells transfected with P133 often have large prominent microvilli, while cells transfected with kazrin often have very small or no microvilli on their surface. There were a greater number of kazrin-positive apical plasma membrane structures in the presence of P133.

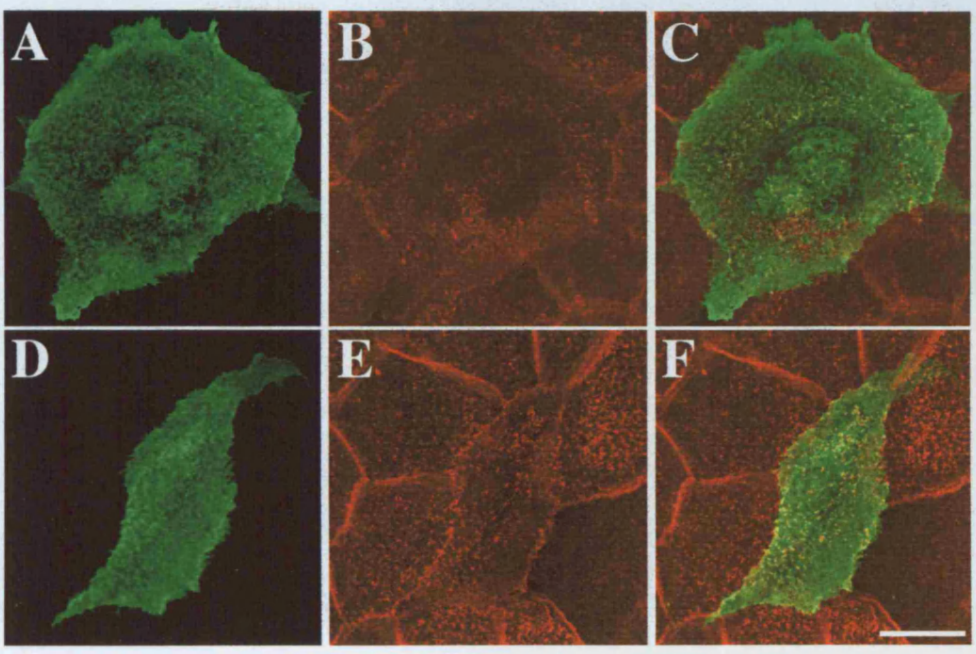

Fig 5.8 Kazrin partially colocalises with CD44. Composite images of z-stacks of primary keratinocytes transfected with N-terminally HA-tagged kazrin isoforms. Green fluorescence: kazrin A (A-C), kazrin C (D-F). Red fluorescence: CD44 (IM7 antiserum). Scale bar: (A-C) 26μm; (D-F) 20μm.

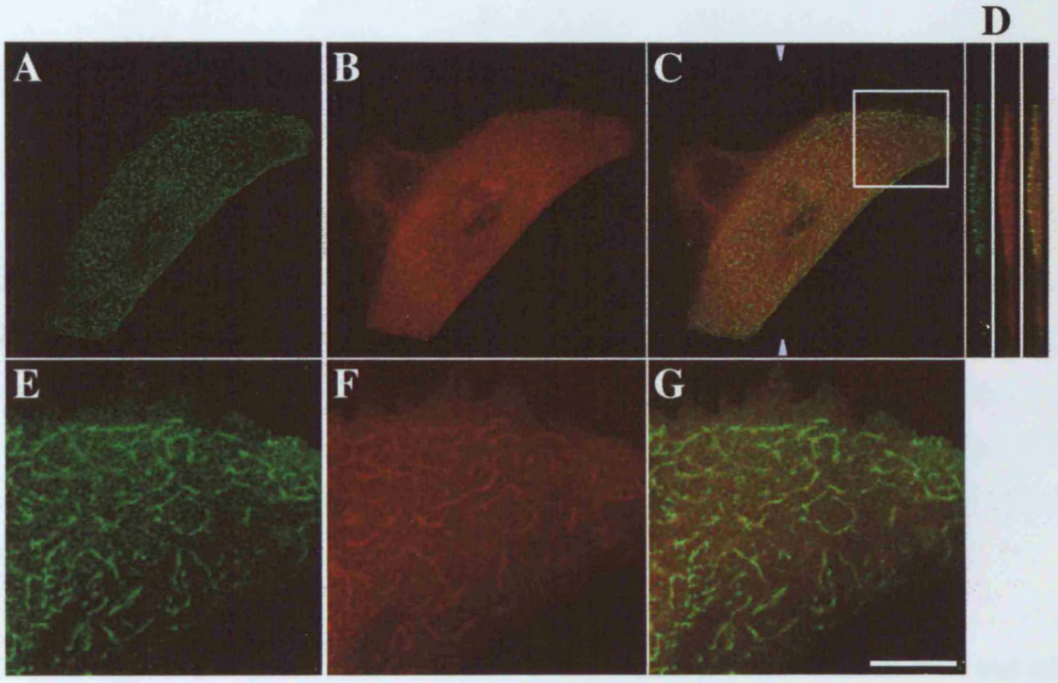

Fig 5.9. Kazrin colocalises with P133. Primary keratinocytes were transfected with P133-HA-tagged (green fluorescence) and Kazrin-C-FLAG (red fluorescence). Arrows in (C) mark the position of the orthogonal views shown in (D). Boxed area is shown as a single confocal slice at higher magnification in (E-G). Z-stack size: 5.2 µm. Scale bars: (A-D) 20µm; (E-G) 6.5µm. C+G

A greater proportion of FLAG-tagged kazrin C localised to the cytoplasm than HA-tagged kazrin C. A proportion of P133 was cytoplasmic in cells cotransfected with kazrin C; in contrast when P133 was transfected alone it did not accumulate in the cytoplasm significantly (Fig. 3.4). It is possible that the reason for the differences in the subcellular localisation of kazrin tagged at the C-or N-terminus is that the tags interfere with additional kazrin binding proteins.

5.2.3 Kazrin localises to the nucleus

N-terminally HA-tagged kazrin A, B and C and C-terminally FLAG-tagged kazrin C could be detected in the nuclei of transfected cells, although to different extents. Many primary keratinocytes showed weak nuclear kazrin staining (Fig. 5.10 A-B and data not shown). Nuclear kazrin proteins were also detected in many A431 cells (epidermoid carcinoma cell line; Fig. 5.10 C-D) and most Cos7 cells (African green monkey kidney cells, Fig. 5.10 E-H).

At present the variability in the extent of nuclear localisation seen between cells and cell types is not well understood. It should be noted that periplakin does have a putative NLS and it has been found in the nucleus of some cell types (van den Heuvel et al., 2002); thus the interaction of periplakin and kazrin may occur both in the nucleus and at the plasma membrane.

5.3 Analysis of the effect of kazrin overexpression on primary keratinocytes

Many keratinocytes expressing HA-tagged kazrin proteins underwent changes in cell shape. The cells spread out in multiple directions, producing thin and/or thick membrane projections (Fig. 5.11). The actin cytoskeleton of these cells was altered, with the induction of stress fiber-like structures that are not normally observed in keratinocytes (Fig. 5.11). The actin cytoskeletons of adjacent untransfected cells were

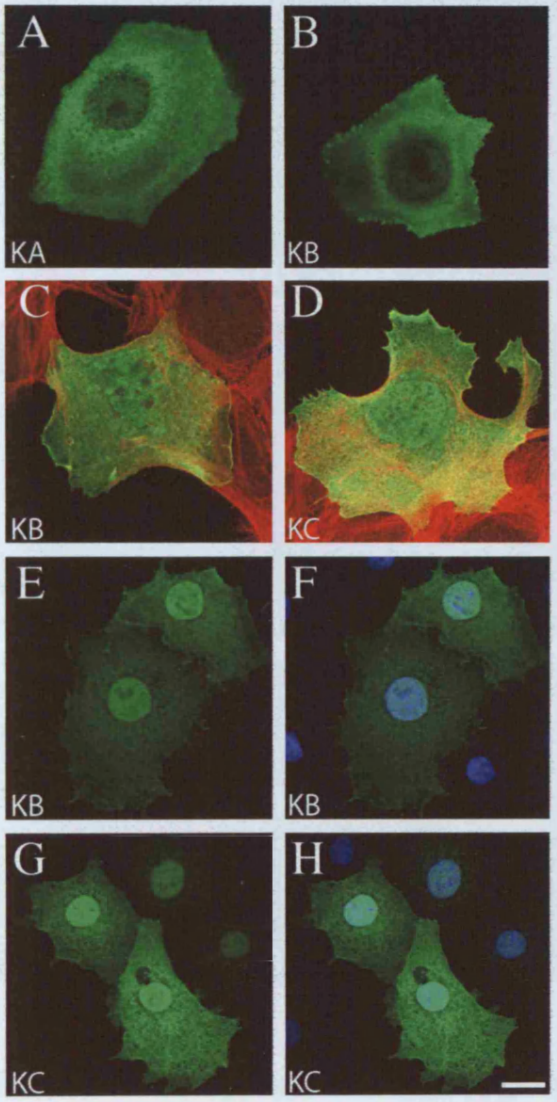

Fig 5.10 Kazrin localises to the nucleus of some cells. Primary keratinocytes (A-B), A431 (C-D) and Cos7 (E-H) cells were transfected with N-terminally HA-tagged kazrin isoforms: kazrin A (KA); kazrin B (KB); kazrin C (KC). Green fluorescence: kazrin. Red fluorescence: actin. Blue fluorescence: nuclear counter stain (DAPI). Scale bars: (A–B) 10μm; (C-D) 9μm; (E-F) 20.5μm; (G-H) 29.4μm.

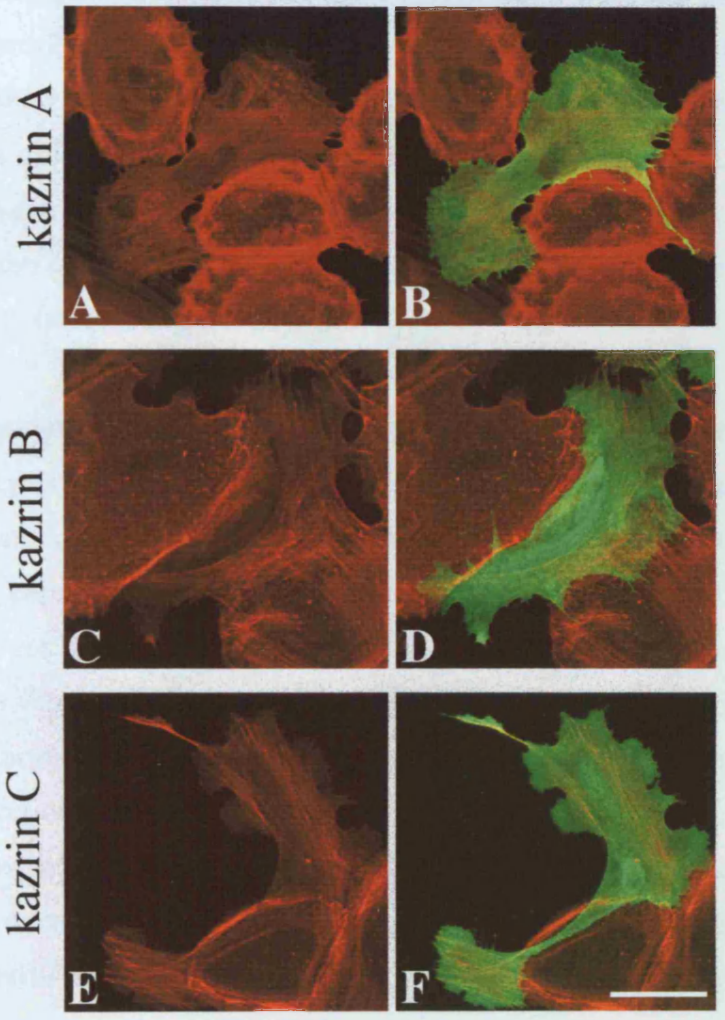

Fig 5.11 Overexpression of kazrin proteins causes changes in cell shape and the actin cytoskeleton. (A-F) primary keratinocytes transfected with HA-tagged kazrin constructs. Red fluorescence: actin (phalloidin); green fluorescence: kazrin. Kazrin A (A-B), kazrin B (C-D), kazrin C (E-F). Scale bar: 40μm (A-B), 27.6μm (C-D), 33.6μm (E-F).

unaffected, displaying bands of cortical actin around the edges of the cells, apical microvilli and few membrane projections (Fig. 5.11).

The profound changes observed in the actin cytoskeleton were not paralleled in the microtubule network (Fig. 5.12 A-I). The microtubule network of cells with altered cell shapes did not show gross changes in organisation relative to untransfected cells. The keratin filaments of kazrin-expressing cells were also largely unchanged. The cells with altered cell shapes were generally much flatter than cells unaffected by kazrin expression. At the cell edges where cells were flattest, keratin filaments were often reduced in density (arrows, Fig. 5.12 J-M).

In order to quantitate the changes in cell shape and the actin cytoskeleton, primary human keratinocytes were transfected in parallel with the HA-tagged kazrin A, B, C and as a negative control, GFP. The cells were analysed 16-18hrs post-transfection, at which stage the cells expressed low to medium levels of the transfected proteins. The keratinocytes were stained with phalloidin and an antibody to the HA tag. The transfected cells were scored blindly for changes in their actin cytoskeleton and cell shape. A keratinocyte was deemed *normal* if it was round or cuboidal in shape, with few membrane projections. Normal keratinocytes generally had a cortical band of actin, numerous microvilli and few stress fibers. A keratinocyte was deemed *altered* if it was no longer round or cuboidal in shape, had loss of the cortical actin belt, reduction or loss of apical microvilli and displayed multiple small membrane projections or longer membrane projections, as shown Fig. 5.11.

The results of quantitation of cell changes from three different transfection experiments were pooled (Fig. 5.13). As not all cells could be assigned to either the normal or altered category these cells were removed from the analysis. Over 60% of cells transfected with kazrin isoforms were scored as altered, relative to only 14% of cells transfected with GFP. The difference was statistically significant: two-tailed p value < 0.0001, by the Fisher's exact test for each kazrin isoform when compared to GFP.

The results of one of the transfection experiments was corroborated by Lisa Sevilla (Keratinocyte laboratory, CR-UK), who independently and blindly scored the transfected keratinocytes for changes and found a similar trend (data not shown).

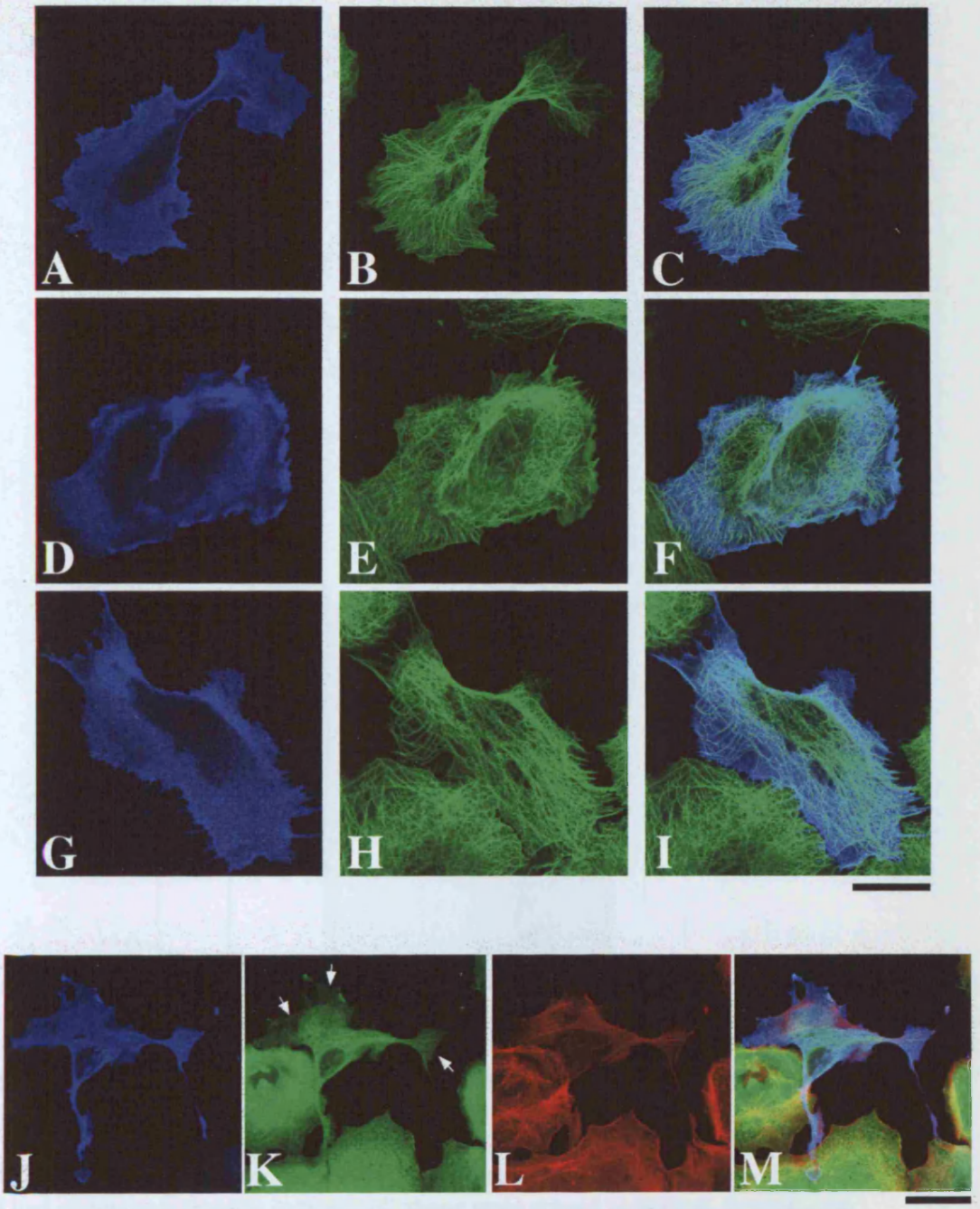

Fig 5.12 Analysis of the microtubule and keratin intermediate filament cytoskeletons of primary keratinocytes expressing transfected kazrin proteins. Primary keratinocytes transfected with kazrin A (A-C, J-M), kazrin B (D-F) or kazrin C (G-I). Green fluorescence: microtubule cytoskeleton (TUB1A2, A-I); red fluorescence: keratin intermediate filament cytoskeleton (LP34, J-M), actin cytoskeleton (phalloidin, J-M). Blue fluorescence: HA tag to kazrin proteins (HA Y11) (A-M). Arrows highlight cell areas with a reduced density of keratin filaments. (A-I) single confocal slices. (J-M) composite images of z-stacks. Scale bar: 26.6µm (A-C), 20µm (D-F), 22.1µm (G-I), 40µm (G-I).

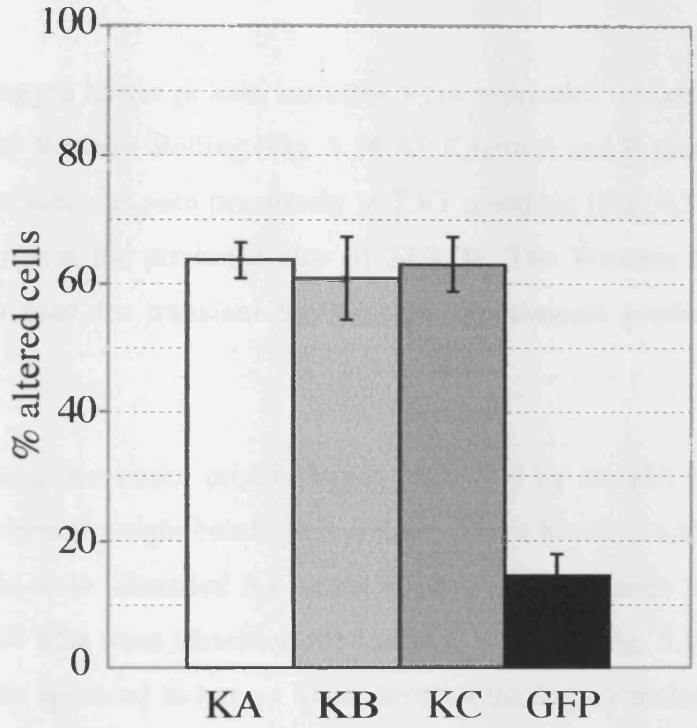

Fig 5.13 Quantitation of the changes in cell shape and the actin cytoskeleton seen in kazrin-expressing cells. Primary keratinocytes were transfected in parrallel with kazrin isoforms (KA, KB, KC) or GFP. 16-18 hrs post-transfection, cells were fixed, stained and scored blindly. Cells that had lost the cortical actin band and had undergone changes in their cell shape were scored as altered. In each case there were cells that could not be assigned to either the normal or altered category; these cells were removed from the analysis. The number of removed cells and the total cells counted were as follows; kazrin A, 134 of 437; kazrin B, 93 of 380; kazrin C, 80 of 421; GFP, 92 of 464. The graph shows the mean percentage of altered cells, with error bars indicating the standard error of the mean.

5.4 Analysis of kazrin proteins *in vitro* and *in vivo*

In this section I will discuss the findings that kazrin proteins are phosphorylated and may form higher-order structures.

5.4.1 Kazrin proteins are phosphorylated

The HA-tagged kazrin protein isoforms were expressed in Cos7 cells and the proteins analysed by Western blotting (Fig. 5.14 A). Kazrin A and B proteins ran at ~ 52 and 50 kDa respectively, as seen previously in TNT reactions (Fig. 4.3); kazrin C protein was found to run at the predicted size of 37 kDa. The Western blot suggested that the constructs used for transient transfection experiments produced full length kazrin proteins.

In addition to the major protein bands identified by the HA Y11 antibody, multiple higher molecular weight bands were visible. Three bands in addition to the major band at ~50 kDa were identified for kazrin B protein. Two bands in addition to the major band at ~37 kDa were identified for kazrin C protein. (Fig. 5.14 A). Kazrin A protein consistently appeared to have a lower level of the higher molecular weight bands, but three additional bands could be identified at longer exposures (Fig. 5.14 A). The presence of multiple higher molecular weight bands, which are not lost upon boiling of lysates in β-mercaptoethanol/SDS, suggests that kazrin proteins are covalently modified.

Many proteins are modified by phosphorylation. Protein phosphorylation can change the function, activity, stability and many other characteristics of a protein. Phosphate groups may be attached, through the activity of specific protein kinases, to serine, threonine, tyrosine or histidine residues. Phosphoserine and phosphothreonine residues are thought to account for >97% of protein-bound phosphate in eukaryotic cells (Shenolikar, 2004).

Calf intestinal alkaline phosphatases (CIPs) can be used to dephosphorylate proteins containing phosphoserine or phosphothreonine residues *in vitro*. In order to analyse

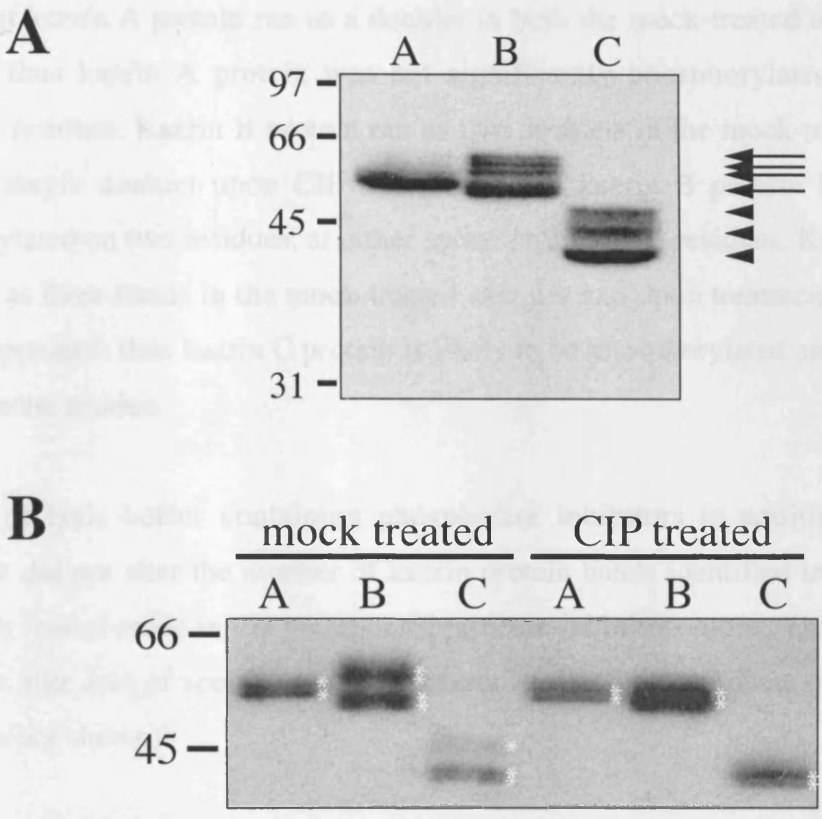

Fig 5.14 Kazrin proteins are phosphorylated (A) Cos7 cells were transfected with HA-tagged kazrin constructs. Protein extracts were made in SDS Laemmli buffer and immunoblotted with an antibody to the HA tag (HA-Y11). Multiple bands can be seen for kazrin B and C isoforms, marked by arrows and arrowheads respectively. At longer exposures faint higher molecular weight bands can be seen for kazrin A. (B) Cos7 cells were transfected with HA-tagged kazrin constructs. Cells were lysed in Western lysis buffer. Lysates were either treated or mock treated with calf intestinal phosphatase (CIP) for 10 mins at 30°C, as explained in the Materials and Methods. Asterisks mark the positions of all kazrin isoforms identified by Western blotting with an antibody to the HA tag (HA Y11). A, B, C are kazrin A, B, C respectively.

whether kazrin proteins were phosphorylated, Cos7 cells were transfected with the HA-tagged kazrin isoforms. The cell lysates were either treated or mock-treated with CIP, after which the reaction was quenched by the addition of Laemmli sample buffer. In mock-treated samples CIP was replaced with an equal volume of water. Fig. 5.14 B shows that kazrin A protein ran as a doublet in both the mock-treated and CIP-treated samples; thus kazrin A protein was not significantly phosphorylated on serine or threonine residues. Kazrin B protein ran as two doublets in the mock-treated samples, but as a single doublet upon CIP treatment; thus kazrin B protein is likely to be phosphorylated on two residues, at either serine or threonine residues. Kazrin C protein appeared as three bands in the mock-treated samples and upon treatment with CIP one band disappeared; thus kazrin C protein is likely to be phosphorylated on either a serine or a threonine residue.

The use of lysis buffer containing phosphatase inhibitors in addition to protease inhibitors did not alter the number of kazrin protein bands identified in Western blots relative to lysates made in the presence of protease inhibitors alone. This suggests that there was little loss of specific phospho-kazrin species in the process of lysis of Cos7 cells (data not shown).

5.4.2 Identification of putative kazrin phosphorylation sites

The kazrin protein sequences were analysed by PROSITE motif search to identify putative phosphorylation sites (Table 5.1). The most commonly predicted phosphorylation site was that of casein kinase 2 (CK2). CK2 is a ubiquitous, constitutively active serine/threonine kinase with a large number of target proteins (Meggio and Pinna, 2003). Many of the proteins it phosphorylates are involved in gene expression, protein synthesis or cell signalling. Other CK2 targets include junctional proteins, such as occludin and E-cadherin, and cytoskeletal elements, such as β-tubulin and filaggrin (Meggio and Pinna, 2003).

Table 5.1 Consensus phosphorylation sites of kazrin proteins as identified by PROSITE motif search

Kazrin isoform	PKA/PKG	PKC	CK2
A	RKES (184) KRHS (256)	* TNR (33) SPR (339)	* TNME (65) SATE (116) SREE (168) SQLD (224) SAAE (324) TPSD (333) SLED (367) TAPD (409)
B	RKES (177) KRHS (249)	SPR (332)	SATE (109) SREE (161) SQLD (217) SAAE (317) TPSD (326) SLED (360) TAPD (402)
C	RKES (90) KRHS (162)	SPR (245)	SATE (22) SREE (74) SQLD (130) SAAE (230) TPSD (239) SLED (273) TAPD (315)

Amino acids written in single letter code. Numbers in brackets indicate the amino acid number at which the protein is phosphorylated; the amino acid is also underlined. Kazrin isoform unique protein phosphorylation sites are marked with an asterisk. PKA/PKG: protein kinase A and G; PKC: protein kinase C; CK2: casein kinase 2.

There is a putative PKC phosphorylation site in the C-terminal region of kazrin proteins, in addition to a unique site in the N-terminus of kazrin A (Table 5.1). Keratinocytes typically express 5 PKC isoforms (classical α, novel δ, ε, η and atypical ζ). PKC isoforms have diverse functions in proliferation, differentiation and apoptosis in keratinocytes (Denning, 2004). PKCα associates with the plasma membrane and desmosomes in suprabasal cells (Wallis et al., 2000) and thus would be suitably localised to phosphorylate kazrin there. Alternatively, the predominantly cytoplasmic novel or atypical PKCs may phosphorylate kazrin (Denning, 2004).

There are two putative protein kinase A (PKA)/protein kinase G (PKG) phosphorylation sites located within the α-helical domain of kazrin. PKA and PKG are activated by cyclic AMP and cyclic GMP, respectively. PKA and PKG have similar phosphorylation consensus sequences (Francis and Corbin, 1997). The subcellular localisation of PKA is determined by A-kinase anchoring proteins (AKAPs), which can target the kinase to e.g. the plasma membrane, nuclear membrane, cytoskeleton and mitochondria (Colledge and Scott, 1999).

The PROSITE motif search did not identify any putative tyrosine phosphorylation sites. NetPhos 2.0 calculates the probability that serine, threonine or tyrosine residues within a protein sequence are phosphorylated based upon experimentally verified phosphorylation sites. NetPhos2 does not predict which kinases may act on the sites found. NetPhos2 analysis predicted 3 tyrosine phosphorylation and three threonine sites in the C-terminus of kazrin, in addition numerous serine phosphorylation sites in the C terminus of kazrin and unique serine sites in the N-termini of kazrin A and B proteins were identified.

5.4.3 Kazrin forms higher-order structures

In Cos7 cells transfected with HA-tagged versions of kazrin B or C and FLAG-tagged kazrin C, I frequently observed multiple large protein bands, which were not present in empty vector control lanes. Fig. 5.15 A shows lysates from Cos7 cells transfected with kazrin B. A large band of monomeric kazrin B (arrowhead) is seen in addition to 4 large protein bands (asterisks). The larger proteins bands are ~ 120 kDa, ~190 kDa, ~210 kDa and >220 kDa. Each of these protein bands most likely represents a protein complex which was not disrupted by boiling in Laemmli sample buffer. Each of the protein complexes identified contains one or more HA-tagged kazrin B proteins. The existence and/or identity of other proteins within these complexes is not known. At present it is not possible to conclude whether or not transfected forms of kazrin A are able to form higher order structures, as fewer Western blots have been performed with HA-tagged kazrin A protein.

Multiple bands were identified in primary keratinocyte lysates using LS4 anti-kazrin antiserum. Kazrin A, B and C bands can be clearly seen at the expected sizes, in addition to 5 larger protein bands. The larger proteins bands ran at ~62 kDa, ~96 kDa, ~120 kDa, ~180 kDa and ~190 kDa (Fig. 5.15 B). The kazrin antiserum LS4 identifies only protein bands of the predicted sizes of kazrin or higher, and the larger protein bands are similar to those identified in kazrin B-transfected Cos7 cells; thus the higher molecular weight bands are unlikely to be non-specific bands. The protein complexes are likely to contain one or more kazrin proteins. The existence and/or identity of other proteins within these complexes are not known.

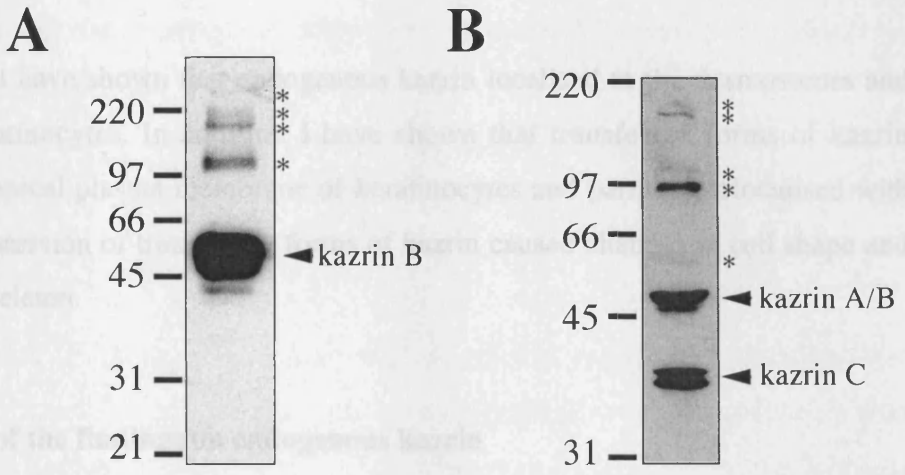

Fig. 5.15 Kazrin forms higher order structures. (A) Cos7 cells were transfected with kazrin B. Lysates were made in CSK buffer, spun and the supernatant boiled in the presence of 2%SDS, 10% β-mercaptoethanol. Immunoblots were probed with an antibody to the HA tag (HA Y11). (B) Immunoblots of primary human keratinocyte lysates probed with LS4 antibody to detect endogenous kazrin. Arrowheads mark the expected size of kazrin proteins; asterisks mark protein complexes containing kazrin B protein (A) or containing endogenous kazrin proteins (B).

The complexes seen in Western blots remain following boiling of protein lysates in ~10% β-mercaptoethanol and ~2% SDS suggesting that the proteins within the complexes are tightly bound to each other.

5.5 Discussion

In this chapter I have shown that endogenous kazrin localised to the desmosomes and nucleus of keratinocytes. In addition I have shown that transfected forms of kazrin localise to the apical plasma membrane of keratinocytes and partially colocalised with actin there. Expression of transfected forms of kazrin caused changes in cell shape and the actin cytoskeleton.

5.5.1 Analysis of the findings on endogenous kazrin

Kazrin was detected at the desmosomes in a variety of tissues and cultured cells. Kazrin was able to localise to cell-cell borders, even in the absence of periplakin (Fig. 5.15). The periplakin-negative mouse cells contain the envoplakin gene. Due to the lack of an antibody to mouse envoplakin it is not known if in the absence of periplakin, envoplakin proteins are produced or localise properly within the cell. Envoplakin may be the factor targeting kazrin to the cell-cell borders in the absence of periplakin, as full length human envoplakin stably expressed in mouse cell lines can localise to the desmosomes to some extent (DiColandrea et al., 2000). It remains to be analysed whether envoplakin and kazrin can interact directly. However, it has been found that kazrin localises to cell-cell borders in all suprabasal layers of the oesophageal epithelium. While periplakin is expressed in all suprabasal layers of the oesophageal epithelium, envoplakin is expressed only in the very outer layers of the epithelium (Ma and Sun, 1986; Ruhrberg et al., 1997).

Desmosomes increase in number and size as keratinocytes differentiate. Desmosomes are multiprotein complexes, the protein composition of which changes as cells differentiate (Getsios et al., 2004). Kazrin localises to cell-cell borders most prominently in the suprabasal layers of epithelia (Fig. 5.1). Desmoglein 1, desmoglein 4

and desmocollin 1 and plakophilin 1 are upregulated as keratinocytes differentiate and it is possible that kazrin associates with these proteins in suprabasal desmosomes (Arnemann et al., 1993; King et al., 1996; Kljuic et al., 2003; Moll et al., 1997).

Disassembly of the actin cytoskeleton, by latrunculin B, causes kazrin and periplakin to accumulate in actin-rich patches; in contrast, desmoplakin is not affected by the treatment (Fig. 5.4 and DiColandrea et al., 2000). Transfection experiments and endogenous staining suggest that both periplakin and kazrin have some dependence on an intact actin cytoskeleton for proper localisation. The importance of actin in the plasma membrane localisation of kazrin and periplakin *in vivo* is not fully understood and will require further analysis, for example, by real time imaging of fluorescently-tagged proteins.

The colocalisation of endogenous kazrin with periplakin and desmoplakin was not complete (Fig. 5.3 and Fig. 5.5). As the cells are stratified and very thin, combined with a rather speckled staining obtained with the LS4 antiserum it is not possible to conclude whether the non-desmosomal staining is at or merely close to the plasma membrane.

Endogenous and transfected forms of kazrin were detected in the nucleus. In the case of endogenous kazrin the extent of nuclear staining was variable in cultured mouse and human keratinocytes. The extent of nuclear signal detected was dependent upon the fixation method used: the signal was highest in cells fixed in PFA alone; weaker in cells extracted with CSK buffer prior to fixation; and weakest in cells fixed in cold methanol. Nuclear staining was more prominent in mouse cells than in human cells.

The variability in the extent of nuclear staining seen in tissue sections is more complex and as yet not fully understood. All tissue sections were treated with 0.1% Triton X-100 prior to staining, yet the extent of nuclear staining differed, even when analysing the same tissue type from different patients.

Kazrin staining is detected in the dermis of the skin, and the submucosal tissue of the oesophagus and cervix (Fig. 5.1). In addition, kazrin transcripts were detected in tissues that do not have desmosomes, such as skeletal muscle (Groot et al., 2004). The function and subcellular localisation of kazrin in these cells will require further analysis.

All tissue section and cell stainings with LS4 antibody involved an extraction step in order to obtain a clear signal. Thus we may not be analysing the full extent of kazrin localisation in cultured cells or tissue sections.

Kazrin appears to be a component of the cornified envelope, as it becomes insoluble upon treating cells with Triton X-100, and in the presence of cystamine and Triton X-100 it remains soluble. Kazrin is found at the cell periphery of suprabasal keratinocytes and thus would be well placed to be a transglutaminase substrate *in vivo*. The cornified layer of the epidermal sections was not stained with LS4 antiserum; however not all CE components can be detected in the CE by immunofluorescence staining due to loss or masking of the epitopes involved; for example periplakin as detected by TD2 anti-periplakin antiserum (Fig. 5.1 B). It will be of interest to see whether there are kazrin-derived peptides in enzymatically digested CE preparations (Steinert and Marekov, 1999).

5.5.2 Analysis of the localisation and effect on cell shape of transfected forms of kazrin

Changes in cell shape and the actin cytoskeleton were observed in primary keratinocytes transiently transfected with HA-tagged kazrin proteins and with FLAG-tagged kazrin proteins (though in the latter case the effect was not quantified). To further corroborate the findings on the effect of kazrin on keratinocyte cell shape and the actin cytoskeleton transiently transfected cell lines and stable cell lines which efficiently express kazrin proteins should be analysed. For this reason, I made retroviral constructs (pBabePuro vector) expressing N-terminally HA-tagged kazrin isoforms. The use of a retroviral system allows sustained expression and 100% transduction efficiency in keratinocytes (Levy et al., 1998). However, the expression level of HA-tagged kazrin isoforms was very low and unstable in the infected keratinocytes. The retrovirally-expressing keratinocytes were therefore unsuitable for analysis of the localisation of HA-tagged kazrin proteins and for analysis of the effect of their expression on cell shape and the actin cytoskeleton. The results suggest that kazrin expression is deleterious to keratinocytes, even at relatively low levels.

Members of the Rho GTPase family of proteins are important regulators of the actin cytoskeleton and cell shape and thus may be directly or indirectly involved in the cell shape changes induced by kazrin overexpression (Burridge and Wennerberg, 2004). The family includes Rho-like GTPases, which are largely responsible for the formation of stress fibers and associated focal adhesion complexes, Rac-like GTPases which are responsible for the formation of lamellipodia and membrane ruffles, and Cdc42-like GTPases which are responsible for the formation of filopodia (Burridge and Wennerberg, 2004). There is a lot of interplay between factors that activate and inhibit different members of the Rho GTPase family, thereby finely regulating cell shape, the actin cytoskeleton and cell migration (Burridge and Wennerberg, 2004). The formation of stress fibre-like structures maybe due to the activity of Rho GTPases and cell shape changes may be the result of Rac and Cdc42 GTPase activity induced directly or indirectly by the expression of kazrin in keratinocytes.

GFP-tagged kazrin proteins were made for live cell imaging in order to analyse the time course and mechanism by which the cell shape and actin cytoskeleton changes occur. N-terminally GFP-tagged kazrin C was largely excluded from the nucleus, while C-terminally GFP-tagged kazrin C localised strongly to the nucleus. Both GFP-tagged kazrin proteins formed aggregates, predominantly in the cytoplasm, in a proportion of the transfected cells. This suggested that the kazrin fusion proteins were unstable and/or misfolding and so no further analysis was performed with GFP-tagged kazrin proteins. Thus,further analysis of the effect of kazrin on cells in real time will require the fusion of kazrin with other fluorescent tags, such as DsRed, or it will require the parallel expression or transfection of kazrin with, for example fluorescent actin. Live cell imaging of kazrin-expressing cells together with fluorescent cytoskeletal components or in the presence of actin/microtubule depolymerisation or stabilisation factors or in the presence of constitutively active and dominant negative forms of Rho GTPases, may help us to understand the how keratinocyte shape and actin cytoskeleton changes are induced.

5.5.3 Analysis of kazrin isoforms *in vitro*

My experiments suggest that kazrin proteins are covalently modified in Cos7 cells and that phosphorylation at serine/threonine residues occurs. To further analyse the serine/threonine phosphorylation of kazrin, lysates should be treated with more specific protein phosphatases such as protein phosphatases 1 and 2A (PP1 and PP2A). The addition of okadaic acid or calyculin A, PP1 and PP2A inhibitors, to the reaction, can be used to exclude non-specific effects of PP1 and PP2A.

Following CIP treatment all three kazrin proteins appeared as a doublet in Western blots (Fig. 5.15 B), suggesting serine/threonine phosphorylation is not the only covalent modification that kazrin proteins undergo *in vivo*. Kazrin proteins may be phosphorylated on tyrosine residues; in order to analyse this, transfected Cos7 lysates could be treated with protein tyrosine phosphatase 1B, which specifically dephosphorylates tyrosine residues (Shenolikar, 2004). Alternatively, transfected forms of kazrin could be immunoprecipitated and subsequently probed on a Western blot with a phospho-tyrosine specific antibody.

The NetPhos2 and PROSITE analysis raises the possibility that there are multiple phosphorylation sites within kazrin proteins. The signalling pathways involved in the phosphorylation pathways remain to be resolved. Once resolved, kazrin may be phosphorylated *in vitro* by the relevant kinases and the phosphorylated residues identified by mass spectrometry.

Both endogenous and transfected forms of kazrin proteins were detected in higher order complexes. Higher order complexes were formed by N-terminally HA-tagged and C-terminally FLAG-tagged kazrin C proteins, suggesting that the tags do not interfere with the protein-protein interactions involved in forming the complexes. All three kazrin proteins are strongly predicted to form a coiled coil. Coiled coils are found in many proteins that dimerise. Many of the HA-tagged kazrin B containing complexes could be formed from kazrin B dimers (~ 100 kDa) or tetramers (~ 200 kDa). At present it is not known whether there is endogenous kazrin in Cos7 cells, which could be involved, nor is it known whether there are non-kazrin proteins in these complexes. It will be of

interest to isolate the kazrin complexes in order to elucidate which proteins associate with kazrin.

The localisation patterns and effects of kazrin upon cells have not been shown to be significantly different between the three kazrin isoforms despite their unique N-termini. The kazrin A protein was consistently less modified than kazrin B and C proteins. Kazrin A protein contains all of the kazrin C protein sequence, yet only kazrin C is consistently significantly modified. The structure of the proteins is not known in three dimensions, and it could be that the kazrin A N-terminus somehow interferes with the modification reactions on the rest of the protein.

It will be of interest in the future to analyse the effect of kazrin phosphorylation and oligomerisation on the subcellular localisation and function of kazrin proteins.

Chapter 6.

The epidermis functions as a chemical, physical and water barrier, which prevents desiccation and protects against infections. The epidermal barrier is largely dependent on the cornified envelope (CE), the corneocyte lipid envelope (CLE) and the lipid lamellae lying in the stratum corneum intercellular spaces. The importance of these components of the stratum corneum are highlighted by transglutaminase I (TGase I) knock-out mice (Kuramoto et al., 2002; Matsuki et al., 1998).

TGase I is responsible for the crosslinking of CE precursors. TGase I also catalyses the covalent attachment of longchain ω-hydroxyceramide lipids to CE precursors, to form the extracellular CLE. In the absence of TGase I, mice die 4-5hrs after birth due to dehydration (Matsuki et al., 1998). TGase I knock-out mice have an almost complete lack of CEs and CLEs, and they have disorganised lipid lamellae (Kuramoto et al., 2002). The rate of trans-epidermal water loss (TEWL) is 1000-fold greater for TGase I knock-out mouse skin compared to wild type and heterozygous mouse skin. Similarly, the epidermis is an ineffective barrier to the entry of Lucifer yellow, a fluorescent dye. The dye is retained in the upper stratum corneum of control mice while in TGase I knock out mice the dye is detected in all layers of the epidermis and even in the dermis (Matsuki et al., 1998).

Mutations in human TGase I have been identified in patients with an autosomal recessive form of lamellar ichthyosis (LI). LI is characterised by the formation of large, thick, dark-brown hyperkeratotic scales (Kuramoto et al., 2002; Matsuki et al., 1998). These scales are similar to those formed when TGase $I^{-/-}$ skin is grafted onto wild type mice. The hyperkeratotic scales are formed, in the absence of an efficient epidermal barrier, to reduce evaporation from the skin surface (Kuramoto et al., 2002).

The current model of CE assembly, as described in Chapter 1, suggests that the process is highly ordered. Early CE components, involucrin, periplakin and envoplakin, are crosslinked at the membrane by TGase I and thought to form a scaffold (Fig. 1.3). Later CE components, such as loricrin and the SPR proteins, are subsequently added to the CE scaffold to form the final mature CE structure (Fig. 1.4). The ω-hydroxyceramide

lipids, which form the CLE, are crosslinked predominantly to the early CE components, periplakin, envoplakin and involucrin (Marekov and Steinert, 1998).

To understand the role of individual CE components in the formation of the CE and epidermal barrier function, several knock-out mice have been generated (Aho et al., 2004; Djian et al., 2000; Koch et al., 2000; Määttä et al., 2001). Loricrin-deficient mice have a slight delay in epidermal barrier formation, as indicated by the permeability of the skin to toluidine blue dye. At embryonic day 16.5 (E16.5) loricrin null skin is almost completely permeable to the dye whereas the skin of wild type controls is almost completely impermeable (Koch et al., 2000). The skin of newborn loricrin$^{-/-}$ mice is shiny, erythematous and more sensitive to tape stripping than wild type control skin. Newborn loricrin knock-out keratinocytes form CEs, but the CEs are less resistant to sonication than those of wild type keratinocytes (Koch et al., 2000). The phenotype of loricrin knock-out mice is normalised 4-5 days after birth through upregulation of SPR-2D, SPR-2H and other proteins. The SPR proteins are incorporated into the CE together with other protein(s) which, like loricrin, are rich in glycine and serine residues (Jarnik et al., 2002; Koch et al., 2000).

In the absence of involucrin mice develop normally with no gross defects in epidermal morphology (Djian et al., 2000). The CEs of involucrin single knock-out mice develop normally and are as sensitive to sonication, detergent treatment and proteases as wild type control CEs. The absence of involucrin is not compensated for by the upregulation of loricrin or SPR-1 at the mRNA level. The upregulation of other CE components has not been examined (Djian et al., 2000).

Envoplakin single knock-out mice were generated in our lab (Määttä et al., 2001). Envoplakin knock-out mice develop normally and show no gross defects in epidermal morphology. CEs isolated from wild type epidermis are of two types: rigid, mature CEs which are highly refractile when viewed by phase contrast microscopy; and fragile, immature CEs which are less refractile and come from lower layers of the stratum corneum (Michel et al., 1988). The mature CEs isolated from envoplakin knock-out mice are ~24% larger than those from wild type mice. The envoplakin knock-out mice have a slight delay (~1 day) in the formation of a mature epidermal barrier, as measured by the penetration of toluidine blue dye into the epidermis (Määttä et al., 2001).

Periplakin knock out mice do not show a gross phenotype up to one year of age (Aho et al., 2004). In the absence of periplakin epithelial morphology is largely normal. Envoplakin, involucrin, desmoplakin and plectin protein levels are similar between periplakin knock out and heterozygous mice. CEs prepared from periplakin knock-out mice show no discernible difference from wild type CEs when examined by phase contrast or transmission electron microscopy (TEM). The epidermal barrier forms normally, and is complete at around E17.5 in heterozygous and knock-out mice (Aho et al., 2004).

The mild phenotypes of loricrin, involucrin, envoplakin and periplakin single knock-out mice suggest there are compensatory mechanisms to ensure the formation of a functional CE and epidermal barrier in the absence of individual CE components (Aho et al., 2004; Djian et al., 2000; Koch et al., 2000; Määttä et al., 2001). In order to analyse the consequence of the simultaneous deletion of involucrin, periplakin and envoplakin, triple knock-out mice were generated. The envoplakin/periplakin/involucrin triple knock out mice were generated by successive crossing of single knock out mice. Periplakin single knock-out mice were kindly provided by J. Uitto (Aho et al., 2004). Involucrin single knock-out mice were kindly provided by P. Djian (Djian et al., 2000). Envoplakin single knock-out mice were generated in our lab (Määttä et al., 2001). Mouse breeding was coordinated by Arto Määttä, Lisa Sevilla and Clare Hall transgenic services (Cancer Research UK).

Envoplakin/periplakin/involucrin triple knock out mice are viable and do not show any gross phenotype up to one year of age. The epidermis of triple knock-out mice appears largely normal compared to control mice as analysed using histological stains and by TEM. There is no defect in skin wound healing when triple knock out mice are compared with wild type and triple heterozygous controls.

In this chapter I shall discuss my analysis of the CEs from triple knock-out mice in addition to the assessment of their water barrier function.

6.1 Analysis of the CEs obtained from envoplakin/periplakin/involucrin triple knock out mice

CE samples were prepared from ear tips of adult triple knock-out and triple heterozygous mice. In each sample fragile and rigid CEs could be identified (Fig. 6.1 A, B). The fragile CEs are immature envelopes from lower layers of the stratum corneum and are thought to be rich in involucrin. The rigid, mature CEs are from the upper layers of the stratum corneum; they are thought to be associated with extracellular lipids and rich in loricrin (Lazo et al., 1995; Michel et al., 1988; Steinert and Marekov, 1997; Steinert and Marekov, 1999).

There was no obvious reduction in the number of CEs generated in triple knock-out mouse epidermis compared to the number generated in triple heterozygous mouse epidermis. There was no obvious difference in the ratio of fragile versus rigid envelopes present between triple knock-out and triple heterozygous mouse epidermis.

The surface area of individual CEs from three triple knock out and two triple heterozygous mice was analysed using NIH Image v 1.58, as described in the Materials and Methods. The analysis indicated that the CEs from triple knock-out mice were on average 17% larger than those from triple heterozygous mice (Fig. 6.1 C). The difference in the mean size of the CEs isolated from triple knock-out mice versus triple heterozygous mice (1862.19 pixels versus 1591.52 pixels) is statistically significant, as analysed by the paired Student's t test (two tailed P value < 0.0001).

6.2 Barrier function analysis of envoplakin/periplakin/involucrin triple knock-out mice

The epidermal barrier begins to form late in embryonic development as keratinocytes differentiate. As the epidermal barrier forms at around E16.5 there is a drastic reduction in TEWL and the reduction continues until birth or slightly after birth (Hardman et al., 1998). Hardman and colleagues have developed a whole mount *in situ* assay to monitor the first stages of barrier formation. Analysis of the permeability of the skin to toluidine

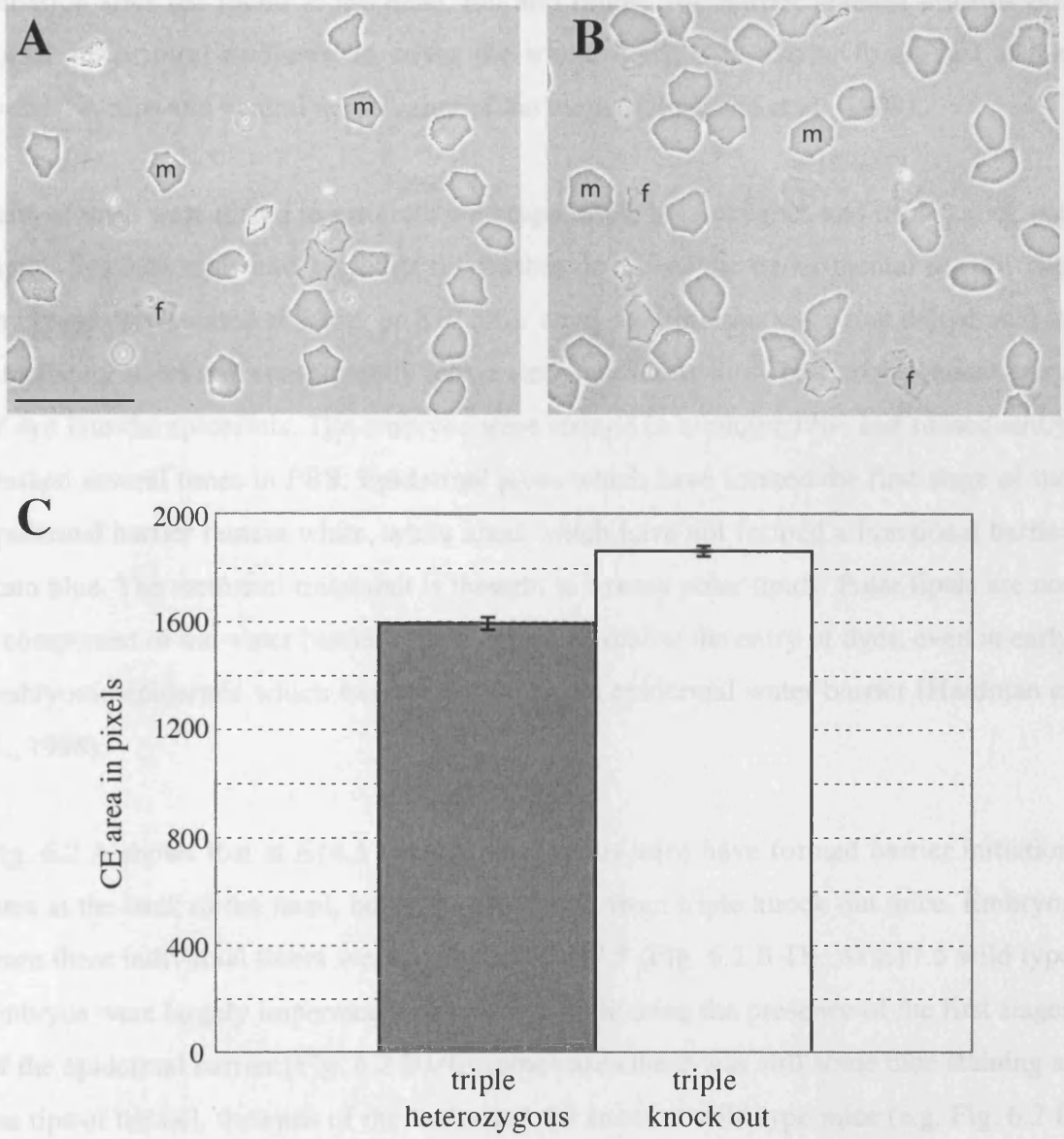

Fig 6.1 Cornified envelopes (CEs) isolated from triple knock-out mice are larger than those isolated from triple heterozygous mice. The surface areas of the mature CEs, isolated from triple heterozygous and triple knockout mice, were measured in pixels using NIH Image v 1.58. Representative micrographs of the CEs isolated from triple heterozygous (A) and triple knock-out (B) mice. m: mature CE; f: fragile CE. (C) Graph shows average surface areas +/- the standard error of the mean. The total numbers of CEs counted were 433 from triple knockout mice and 215 from triple heterozygous mice. Two-tailed P value < 0.0001, by paired Student's t test. Scale bar: 100μm.

blue suggests that the epidermal barrier forms in a patterned way (Hardman et al., 1998). Epidermal barrier formation starts at distinct initiation sites, which form in a defined sequence. The first initiation sites are at dorsal regions of the mouse. Later initiation sites are found at the head, tail and limbs. The barrier spreads towards the dorsal and ventral midlines, to cover the whole body. The barrier forms last at the eyelids, eartips and ventral neck region of the mouse (Hardman et al., 1998).

Pairs of mice were mated to generate wild type, triple heterozygous and triple knock out litters. See Materials and Methods for further details of the experimental set up. The embryos were isolated at E16.5 or E17.5 for analysis. Embryos were first dehydrated in a methanol series and subsequently rehydrated in order to allow barrier-dependent entry of dye into the epidermis. The embryos were stained in toluidine blue and subsequently washed several times in PBS. Epidermal areas which have formed the first stage of the epidermal barrier remain white, while areas which have not formed a functional barrier stain blue. The methanol treatment is thought to extract polar lipids. Polar lipids are not a component of the water barrier but do appear to inhibit the entry of dyes, even in early embryonic epidermis which has not yet formed a epidermal water barrier (Hardman et al., 1998).

Fig. 6.2 A shows that at E16.5 triple heterozygous mice have formed barrier initiation sites at the back of the head, but these are absent from triple knock out mice. Embryos from three individual litters were analysed at E17.5 (Fig. 6.2 B-D). At E17.5 wild type embryos were largely impermeable to the dye, indicating the presence of the first stages of the epidermal barrier (Fig. 6.2 B). In some cases there was still some blue staining at the tips of the tail, the ends of the limbs and the snout of wild type mice (e.g. Fig. 6.2 B i). The epidermal barrier of triple heterozygous mice was present over most of the body (Fig. 6.2 C), although there was an absence of epidermal barrier on the snout and ends of the limbs of some mice (Fig. 6.2 C ii-iii). There is variability in the extent of staining within litters irrespective of their genotype and the difference between triple heterozygous and wild type mice is probably due to this variation.

Triple knock out mice had delayed barrier formation compared to control wild type and triple heterozygous mice (Fig. 6.2 B-D). Some triple knock out mice were almost completely stained, indicating a lack of the first stages of epidermal barrier formation

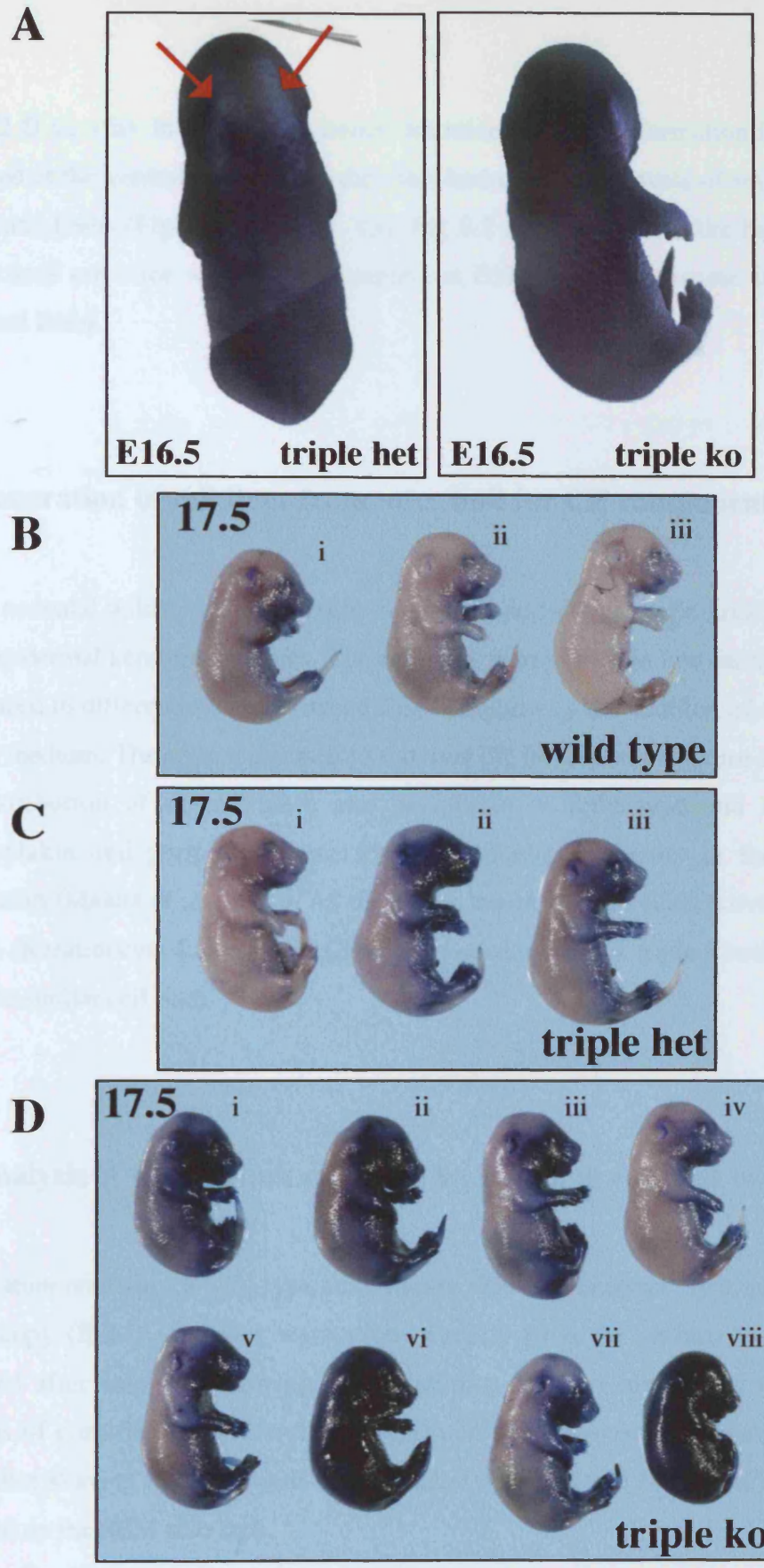

Fig 6.2 Mice lacking envoplakin, periplakin and involucrin (triple ko) have a delay in epidermal barrier formation relative to triple heterozygous (triple het) and wild type mice. Toluidine blue staining of embryos at E16.5 (A) and E17.5 (B-D). Blue skin indicates dye penetration and thus an immature epidermal barrier; unstained skin indicates a functional epidermal barrier. Arrows in (A) highlight epidermal barrier initiation sites. Epidermal barrier formation experiments were performed in collaboration with Lisa Sevilla (CR-UK).

(Fig 6.2 D vi, viii). In other triple knock out mice the barrier formation fronts had not yet fused at the ventral midline and they still had significant levels of staining on their snouts and limbs (Fig. 6.2 D i-iii, v, vii). Fig 6.2 D iv shows that the barrier of some triple knock out mice was almost complete at E17.5, with only some staining of the snout and limbs.

6.3 Generation of cell lines from mice null for CE components

I used neonatal wild type, envoplakin single and periplakin single knock out mice to make epidermal keratinocyte lines. The cell lines were grown in low calcium, but could be induced to differentiate and produce CEs in culture by the addition of calcium to the culture medium. The cells were used to monitor CE formation in culture and to analyse the distribution of desmoplakin and periplakin in wild type and mutant cells. Desmoplakin and periplakin were found to localise normally in the absence of envoplakin (Määttä et al., 2001). As the single knock out cell lines proved useful Lisa Sevilla (Keratinocyte Laboratory, CR-UK) used double and triple knock out mice to generate similar cell lines.

6.4 Analysis of the stratum corneum by scanning electron microscopy

The stratum corneum of wild type adult mouse skin was analysed by scanning electron microscopy (SEM). Samples were taken directly from the surface of the skin and analysed after rotary shadowing with platinum. Initial experiments indicated that analysis of cornified cells from hairy skin such as the mouse back was not feasible. Even after shaving samples were contaminated with hair and few cornified cells were obtained on the SEM stub tape.

Fig. 6.3 A shows the sheet-like structure of the stratum corneum plantar skin from an adult wild type mouse. At higher magnifications (Fig. 6.3 B-C) individual cornified cells are apparent. The cornified cells have ridges, grooves and villi over their surface. The overlap between cornified cells and cells in the cornified layer below can be seen (Fig. 6.3. B-C).

Cornified cells of triple knock out and wild type control mice can now be compared by SEM in order analyse if there are any differences in the surface structures of these cells.

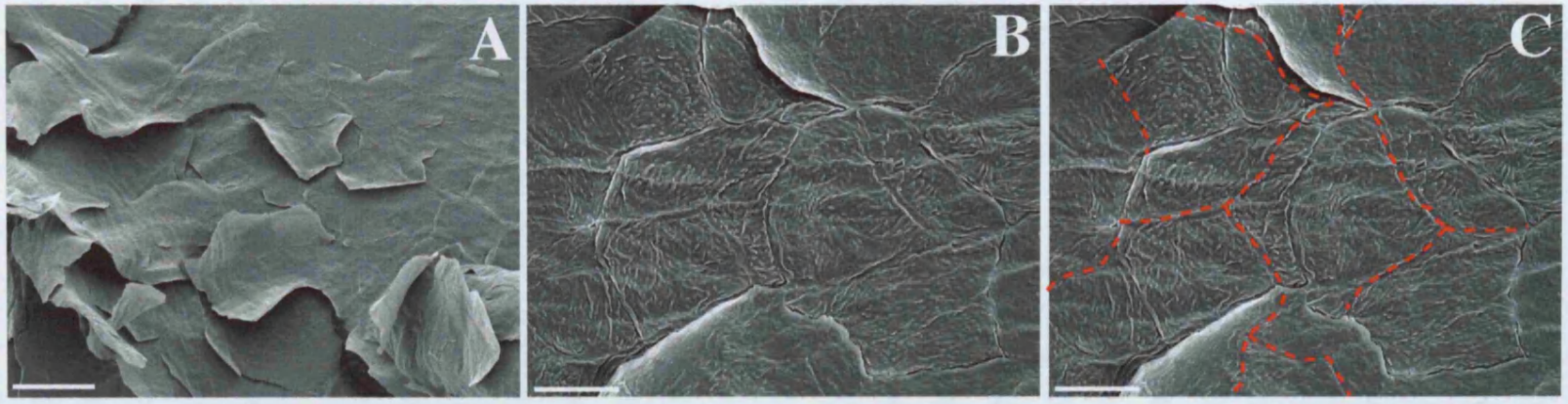

Fig. 6.3 Analysis of cornified envelopes from wild type mouse plantar skin. (A) Samples were taken directly from the foot of a mouse using an SEM stub with tape and analysed without critical point drying. Low magnification image showing the sheet-like structure of the stratum corneum. (B-C) High magnification image of cornified cells from the upper layers of the stratum corneum. The outlines of the cornified cells from the layer below can be seen on the surface of the CEs. The outlines of the cornified cells below are highlighted in (C) by dotted lines. Scale bars: 30μm (A), 10μm (B-C) .

6.5 Discussion

The analysis of envoplakin/periplakin/involucrin triple knock out mice has shown that the mice are viable. The mice are able to produce rigid, mature CEs in the absence of envoplakin, periplakin and involucrin. In this chapter I describe a small effect of envoplakin/periplakin/involucrin gene deletion on CE surface area and on skin barrier development.

Previously a 24% increase in the surface area of mature envelopes from envoplakin single knock out mice relative to wild type mice was reported (Määttä et al., 2001). In this study I found a 17% increase in the size of triple knock out mouse CEs compared to triple heterozygous mouse CEs. There are several possible reasons for the less dramatic difference in surface area between triple knock out and triple heterozygous envelopes. I compared triple knock out CEs with triple heterozygous, not wild type, controls. I compared CEs derived from adult mouse ears, not newborn back skin. I analysed the CEs in this study, while the analysis of CEs from envoplakin single knock out mice was performed by A. Määttä (Määttä et al., 2001).

It is, however, possible that the difference in size is biologically significant. In this case in the absence of envoplakin, periplakin and involucrin the phenotype may be less dramatic due to a more effective protein compensation mechanism compared to that of envoplakin single knock out mice. To distinguish between the different possibilities it will be important to analyse envoplakin single knock out mouse CEs in parallel with those from triple knock out, triple heterozygous and wild type mice from the same body site.

There are several possible reasons for the increased size of the CEs of triple knock out mice compared with triple heterozygous mice. In the absence of envoplakin, periplakin and involucrin, which form the bulk of the early CE components there may be a slight delay in the formation of an early CE structure. The delay in expression or crosslinking of CE components may allow the cells to flatten, and thus increase surface area, for longer during the last stages of terminal differentiation. Alternatively the CEs may be less strong and thus become slightly more flattened with increased surface area as the cells differentiate.

To investigate the basis of the difference in size, cells from wild type and triple knock out mice could be used. The cells could be placed in suspension to generate CEs (Romero et al., 1999). The kinetics of CE formation and CE size could then be examined.

The CEs of loricrin deficient mice are more sensitive to sonication than those from control mice (Koch et al., 2000). It will be of interest in the future to analyse the sensitivity of CEs from triple knock out mice to sonication or other mechanical or chemical stresses.

SEM revealed that the cornified cells of wild type plantar skin have many ridges, grooves and villi over their surface. These structures are thought to be important for interdigitation of cornified cells. The interdigitation and overlapping of the cells increases the mechanical stability of the stratum corneum and are particularly prominent features of plantar skin (Holbrook, 1994). Analysis of the surface of cornified cells by SEM may prove useful in future analyses of the skin of triple knock out mice.

Patterned barrier formation is not restricted to the epidermis. Initiation sites and moving fronts of barrier formation can be detected in oral epithelia such as the tongue and hard palate (Marshall et al., 2000). Patterned barrier formation is also detected in rats, rabbits and humans, although the exact pattern differs somewhat between species because of their different body shapes (Hardman et al., 1999; Hardman et al., 1998).

The first stages of epidermal barrier formation, as measured by staining with toluidine blue are coincident with the relocalisation of loricrin from keratohyalin L-granules to the plasma membrane and with the formation of mature, rigid CEs, which are thought to have covalently associated lipids (Hardman et al., 1998; Lazo et al., 1995). After the formation of the first stages of the barrier, filaggrin becomes fully processed, LEP proteins are expressed and the lamellar lipids become organised into long flat sheets (Hardman et al., 1998; Marshall et al., 2001).

The toluidine blue experiments indicated that, though there is variation within a litter, the extent of barrier formation was reduced at E17.5 in all triple knock out mice relative

to the wild type and triple heterozygous control mice. The delay suggests that the deposition of loricrin may occur later than in wild type embryos. Loricrin forms the bulk of the CE and it is often found crosslinked to early CE components such as involucrin (Steinert and Marekov, 1997; Steinert and Marekov, 1999). In the absence of envoplakin, periplakin and involucrin there may be a delay in the expression of alternative early CE components or a delay in the deposition of loricrin due to the reduced availability of crosslinking sites at the plasma membrane. Alternatively there may be a slight delay in the formation of rigid CEs and CLEs. TEM analysis of epidermis from triple knock out and wild type mice suggested that there are no gross differences between them (Lisa Sevilla, Keratinocyte laboratory). More detailed analysis by TEM may reveal subtle changes in the timing of the deposition of loricrin or CLE formation which could explain the slight delay in barrier formation.

A fraction of the lipo-peptides present in human CLEs were isolated in experiments by Marekov and Steinert (Marekov and Steinert, 1998). Their analysis indicated that >50% of the ω-hydroxy ceramides of the CLE were attached to envoplakin, periplakin and involucrin. Rigid, mature CEs, which can be seen in triple knock out and triple heterozygous mice, are thought to have covalently attached lipids (Hirao et al., 2001; Lazo et al., 1995). This suggests that a CLE can form in the absence of envoplakin, periplakin and involucrin. At present it is not known to which proteins ceramides are added in the absence of envoplakin, periplakin and involucrin. Since the CLE is thought to be important for the organisation of the lamellar lipids (Behne et al., 2000; Downing, 1992; Kuramoto et al., 2002), it will be of interest to analyse triple knock out epidermis to analyse to which proteins the ceramide lipids are attached.

The analysis of the triple knock out mice demonstrates that envoplakin, periplakin and involucrin are not required for CE formation. It is now of interest to determine the protein composition of CEs from triple knock out mice. Three strategies have been considered. One is to determine the composition of the CEs directly. Second is to study CE formation in culture. A third possibility is to analyse gene expression profiles of the epidermis of triple knock out and wild type mice by mRNA microarray.

A collaboration with Andrey Kalinin (Laboratory of Skin Biology, NIAMS, NIH) was set up in order to analyse the protein composition of the CEs from triple knock out

mice. Our initial experiments focussed on analysis of CEs from triple heterozygous mice. He analysed the protein composition of the CEs in two ways: by mass spectroscopic analysis of the peptides released from proteolytically digested CEs and by analysis of the relative amino acid levels after complete hydrolysis of the component proteins by 6 M HCl/0.5% phenol (Jarnik et al., 1996; Steinert and Marekov, 1999). The mathematical analysis of the amino acid composition of the CEs suggested that they were composed of 82.4% loricrin, 6.3% SPR proteins, 5.2% filaggrin and 6.9% envoplakin/periplakin, by weight. However, he couldn't detect envoplakin or periplakin by mass spectroscopic analysis of peptides released from proteolytically digested CEs from triple heterozygous mice. The mass spectroscopy sequencing data indicated that the predominance of loricrin and the large size of envoplakin and periplakin make it difficult to detect envoplakin and periplakin in CE peptide preparations. In the absence of envoplakin, periplakin and involucrin the changes in the protein composition of the CEs are likely to be too subtle to detect by the sequencing of CE-derived peptides and by analysis of the amino acid composition of CEs.

CEs can be generated in stratified cultures of keratinocytes or by growing cells in suspension (Romero et al., 1999; Steinert and Marekov, 1999). The CEs generated in culture are more immature and have a significantly lower loricrin content than CEs generated *in vivo* (Steinert and Marekov, 1999). The triple knock out and control cell lines may therefore be useful to analyse the effects of loss of envoplakin, periplakin and involucrin on CE protein composition.

The third approach that can be taken is to obtain gene expression profiles of the epidermis of triple knock out, triple heterozygous mice and wild type mice by mRNA microarray, for example (Frye et al., 2003). The analysis may yield some answers about the nature of the compensatory mechanisms which allow the formation of a functional stratum corneum in the absence of three early CE proteins and may reveal perturbations in other aspects of the epidermis that have not yet been considered.

Envoplakin, periplakin and involucrin are considered to be important components of the CE scaffold on to which the CLE and later components of the CE are added. It is remarkable that loss of expression of these three proteins causes only a mild phenotype in the mice.

In any case it seems that loss of envoplakin, periplakin and involucrin expression are not essential for the formation of CEs or the formation of the first stages of the epidermal barrier.

Chapter 7.

In this general discussion chapter I will summarise the main findings of my thesis and suggest directions for future research.

7.1 Envoplakin and periplakin N-termini

I have extended the findings of DiColandrea et al. (2000) to establish that the N-terminus of envoplakin does not efficiently localise to desmosomes or microvilli when transfected into primary human keratinocytes. In contrast, a similar region of perpiplakin localises efficiently to the microvilli and partially colocalises with desmoplakin at the desmosomes (DiColandrea et al., 2000). The KGSP repeats found in the very N-terminus of mouse and human envoplakin are potential phosphorylation sites. I found that removal of the KGSP repeat regions and treatment of transfected cells with protein kinase inhibitors did not affect the localisation of envoplakin constructs in transfected primary human keratinocytes. Data from stably transfected mouse keratinocytes expressing full length human envoplakin indicate that envoplakin can localise to the desmosomes and suggest that it may depend upon heterodimerisation with periplakin in order to efficiently localise to the interdesmosomal plasma membrane (DiColandrea et al., 2000).

The first 495 amino acids of periplakin were found to be sufficient to target periplakin to the microvilli and to the desmosomes (DiColandrea et al., 2000). By generating further deletions of periplakin, I found that the first 133 amino acids, up to the end of the NN subdomain, target periplakin to the apical plasma membrane, where it colocalises with the actin cytoskeleton in microvilli. The N-terminal 584 amino acids of desmoplakin, which includes the NN, Z, Y and most of the X subdomain, targets the protein to the desmosomes where it interacts with plakoglobin and plakophilin (Bornslaeger et al., 1996; Kowalczyk et al., 1997). Sequence comparisons between the first 133 aa of periplakin and a similar region of desmoplakin indicates that they have low sequence identity (<17%). However, the first 63 aa of desmoplakin may be sufficient to target desmoplakin to plasma membrane attachments sites, the desmosome

in the case of desmoplakin, as they are sufficient to interact with plakophilin 3 in yeast two-hybrid assays, but analysis of the localisation of this desmoplakin fragment in cells had as yet not been carried out (Bonné et al., 2003). It will interesting to understand how the very N-terminal regions and the NN subdomains of plakin proteins are involved in their targetting.

7.2 Identification of kazrin

In order to identify proteins which might mediate the interaction of periplakin with the actin cytoskeleton or the plasma membrane a yeast two-hybrid screen was performed. Using the first 133 amino acids of periplakin as 'bait' and a human keratinocyte cDNA library as 'prey' we identified a novel protein, which we have named kazrin.

The kazrin gene consists of four alternative first exons, 1a, 1b, 1c and 1d, which may be spliced to exons 2 to 8. The four alternative kazrin transcripts encode three different proteins with unique N-termini. Kazrin proteins are highly conserved between mice and humans.

Immunofluorescence staining of epidermal tissue sections suggested that kazrin localised to the cell periphery of differentiated cells, but it was more diffusely localised in basal layers of the epidermis. In stratified cultures kazrin partially colocalised with desmoplakin and periplakin at the desmosomes and with periplakin at the interdesmosomal plasma membrane. The localisation of kazrin to desmosomes was found to be independent of periplakin, as kazrin was detected at cell-cell borders in mouse cell lines lacking periplakin expression. Additional staining of kazrin was detected in the nuclei of cultured cells and in tissue sections, but the significance of this is currently unknown.

All transfected forms of kazrin localised to the apical plasma membrane of primary keratinocytes and caused changes in cell shape and the actin cytoskeleton. Transfected forms of kazrin proteins are phosphorylated as CIP treatment resulted in the specific loss of certain kazrin protein bands, as detected by Western blotting. Future experiments

will investigate how kazrin affects the cytoskeleton and whether phosphorylation affects kazrin localisation and/or function.

7.3 An additional kazrin isoform belongs to the liprin family of proteins

7.3.1 Identification of novel kazrin isoforms

Initial analysis of the human genome using BLAT suggested that there were 4 alternative human kazrin mRNA isoforms (a to d) and two mouse mRNA isoforms (a and b). Analysis of *Drosophila*-derived cDNA sequences indicated a 36% identity and 76% similarity between an EST clone (AI063603) and the human kazrin C protein. In collaboration with Nick Brown (Wellcome trust/CR-UK, Cambridge) we analysed this sequence further. The analysis suggests that AI063603 encodes a novel 1023 amino acid protein with sequence similarity to the liprin family of LAR transmembrane protein tyrosine phosphatase (PTPase) interacting proteins.

The novel *Drosophila* liprin sequence was used to search for kazrin-like liprin sequences in human EST databases. A human EST with homology to the liprin family of proteins and kazrin was identified (BC036877), and mapped to the human *kazrin* locus. Analysis of the EST sequence suggests it is formed from the splicing together of exons 1a to exons 2 to 8. A splicing event within exon 8, prior to the translation termination codon, results in splicing of exon 8 to novel exons 9 to 15. I shall refer to this novel splice variant as kazrin a1 to indicate it is a long kazrin isoform. Kazrin al is predicted to encode a 775 aa protein which I shall refer to as kazrin AL (Fig. 7.1 A). A mouse liprin-like kazrin isoform has recently been isolated (AK173090). The mouse kazrin long isoform includes exon 1a and thus I shall refer to this splice variant as mouse kazrin al and the protein as mouse kazrin AL. Mouse kazrin AL is predicted to be 779 aa in length.

Northern blotting of mouse tissue mRNA identified ~2.3kb, ~3.85kb and ~5.1kb bands using a probe against murine kazrin (Fig. 4.11). The ~3.85kb band is thought to relate to mouse kazrin a and b mRNAs. The mouse kazrin al mRNA is predicted to be ~4.9kb and therefore could represent the 5.1kb band identified by Northern blotting. Currently

A

```
  1 MMEDNKQLAL RIDGAVQSAS QEVTNLRAEL TATNRRLAEL SGGGGPGPGP GAAASASAAG 60
 61 DSAATNMENP QLGAQVLLRE EVSRLQEEVH LLRQMKEMLA KDLEESQGGK SSEVLSATEL 120
121 RVQLAQKEQE LARAKEALQA MKADRKRLKG EKTDLVSQMQ QLYATLESRE EQLRDFIRNY 180
181 EQHRKESEDA VKALAKEKDL LEREKWELRR QAKEATDHAT ALRSQLDLKD NRMKELEAEL 240
241 AMAKQSLATL TKDVPKRHSL AMPGETVLNG NQEWVVQADL PLTAAIRQSQ QTLYHSHPPH 300
301 PADRQAVRVS PCHSRQPSVI SDASAAEGDR SSTPSDINSP RHRTHSLCNG DSPGPVQKNL 360
361 HNPIVQSLED LEDQKRKKKK EKMGFGSISR VFARGKQRKS LDPGLFDDSD SQCSPTRQSL 420
421 SLSEGEEQMD RLQQVELVRT TPMSHWKAGT VQAWLEVVMA MPMYVKACTE NVKSGKVLLS 480
481 LSDEDLQLGL GVCSSLHRRK LRLAIEDYRD AEAGRSLSKA AELDHHWVAK AWLNDIGLSQ 540
541 YSQAFQNHLV DGRMLNSLMK RDLEKHLNVS KKFHQVSILL GIELLYQVNF SREALQERRA 600
601 RCETQNIDPV VWTNQRVLKW VRDIDLKEYA DNLTNSGVHG AVLVLEPTFN AEAMATALGI 660
661 PSGKHILRRH LAEEMSAVFH PANSTGIREA ERFGTPPGRA SSVTRAGKEE NSSGLKYKAG 720
721 RLPLGKIGRG FSSKDPDFHD DYGSLQNEDC GDDDPQSRLE QCRLEGYNSL EVTNV*     775
```

B

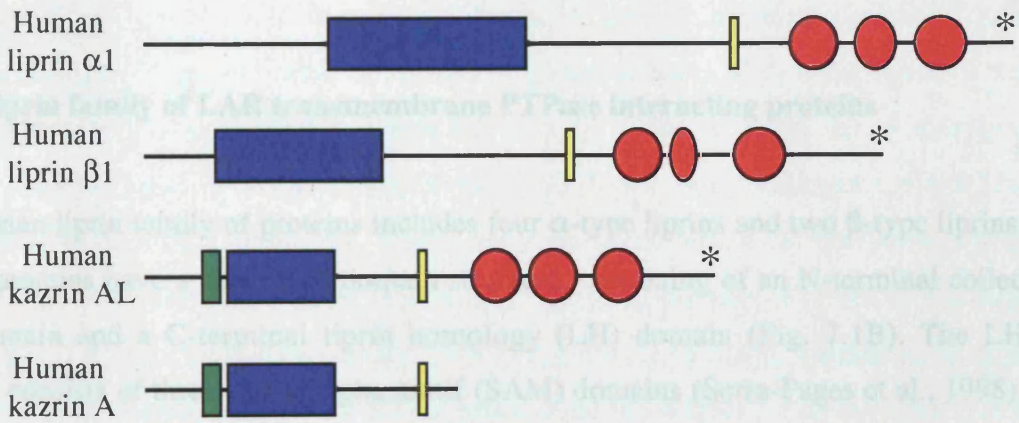

Fig. 7.1 Kazrin AL protein, a member of the liprin family of proteins. (A) Amino acid sequence of human kazrin AL protein. Arrow indicates the start of the protein region unique to kazrin AL. The putative NLS is single underlined, the leucine zipper-like domain is double underlined. Kazrin AL contains three SAM domains, 1, 2 and 3, boxed in green, red and blue, respectively. The putative PDZ domain is boxed in black. Amino acids are shown in single letter format. Asterisk: translation termination codon. (B) Schematic (to scale) of human liprin α1, human liprin β1, human kazrin AL and human kazrin A. Green box: putative leucine zipper-like domain. Blue box: coiled coil domains. Yellow box: putative NLS. Red circles: SAM domains. The liprin homology (LH) domain encompasses the three SAM domains. Asterisks at the very C-termini of human liprin α1, human liprin β1 and kazrin AL represent putative PDZ-binding motifs.

only long kazrin mRNA isoforms containing sequences from kazrin exon 1a have been isolated. It remains to be seen whether exons 1b, 1c and 1d may also be components of kazrin long type mRNAs. The expression of long forms of kazrin mRNA in primary human keratinocytes and human dermal fibroblasts, in addition to A431, EJ/28 and JAR cells, has been confirmed by RT-PCR (Lisa Sevilla, Keratinocyte Laboratory).

The protein sequences of human, mouse and *Drosophila* kazrin AL can be found in the appendices. The kazrin proteins initially identified, kazrin A, B and C, I shall collectively refer to as kazrin short isoforms. It should be noted that the antibody we generated to kazrin (LS4) was made against the last 20 aa of the short kazrin isoforms. Only the 6 most N-terminal of these amino acids are found in kazrin AL proteins. Thus it seems probable that LS4 antiserum does not crossreact with kazrin AL proteins; indeed we did not detect any bands ~85 KDa, the predicted molecular weight of kazrin AL, in Western blots carried out with the LS4 antiserum. Generation of an antibody to the long kazrin isoform will allow us to determine whether the subcellular localisation of kazrin short and long forms is similar.

7.3.2 Liprin family of LAR transmembrane PTPase interacting proteins

The human liprin family of proteins includes four α-type liprins and two β-type liprins. Liprin proteins have a conserved domain structure, consisting of an N-terminal coiled-coil domain and a C-terminal liprin homology (LH) domain (Fig. 7.1B). The LH domain consists of three sterile alpha motif (SAM) domains (Serra-Pages et al., 1998). SAM domains generally function as protein:protein interaction domains (Kim and Bowie, 2003).

Like liprin α and β proteins, all kazrin isoforms have an N-terminal coiled-coil domain. The C-terminal region of kazrin AL contains three predicted SAM domains, which together constitute the LH domain (Fig. 7.1 B). We identified a putative NLS in all kazrin proteins. NLS sequences can be identified in similar regions of liprin α and β proteins (Fig. 7.1 B). However, there have been no reports of nuclear α or β liprins. Kazrin AL, liprin α1 splice form B, liprin β1, and some other members of the liprin

family of proteins, have PDZ motifs that may be bound by PDZ binding domain-containing proteins (Harris and Lim, 2001).

The sequence identity between the four human α liprins is 69-76% and between human liprin β1 and 2 is 51% (Serra-Pages et al., 1998). ClustalW amino acid sequence alignments show that human kazrin AL and human liprin α1 have 33% identity and 46% similarity. When compared to human liprin β1, human kazrin AL has 31% identity and 45% similarity. The sequence comparisons suggest that kazrin AL is neither an α nor a β liprin family member. Future analysis of the liprin and long kazrin isoform amino acid sequences from different species will allow us to further define the subgroups within the liprin family and may shed light on how this protein family evolved.

7.3.3 Liprin protein binding partners and their functions

The N-terminal coiled-coil domain of liprin α and β proteins mediates their homodimerisation. Liprins within the α and β subfamilies can also heterodimerise via the N-terminal coiled-coil domain (Serra-Pages et al., 1998). α liprin family members interact with the LAR family of transmembrane PTPases, which includes LAR, PTPσ and PTPδ, through the LH domain. The β liprin family members do not interact with LAR PTPases directly but do interact with the C-terminal domain of α liprins via their C-terminal domains (Serra-Pages et al., 1998). The ability of liprin proteins to interact with each other through their N-and C-terminal domains suggests that they may form higher order structures.

The kazrin A, B, C and kazrin AL proteins all contain an N-terminal coiled-coil domain, but only kazrin AL contains the LH domain. Analysis of transfected and endogenous forms of short kazrin proteins suggests that they are able to form oligomers (Fig. 5.15). Generation of differently tagged kazrin short and long isoforms in addition to α and β liprins, will allow us to analyse the types of interactions that can occur between these proteins by immunoprecipitation and colocalisation studies.

Transfected forms of liprin α1 and β1 localise to the plasma membrane of Cos7 cells (Serra-Pages et al., 1998). Indeed transfected forms of liprin α2 localise to plaques at the plasma membrane, in contrast to LAR, which localises to the plasma membrane and Golgi of transfected Cos7 cells. Cotransfection of LAR and liprin α2 causes LAR to relocalise, with liprin α2, to plasma membrane plaques and membrane ruffles (Serra-Pages et al., 1998). The domains necessary for the localisation of α1, α2 and β1 liprins to plasma membrane structures has not been mapped, but since I have found short kazrin isoforms localise predominantly to the plasma membrane the sequences necessary may be located in the N-terminal regions of liprin proteins. Alternatively the short kazrin isoforms may be directed to the plasma membrane by endogenous long kazrin isoforms.

Liprin proteins contain domains and motifs important for protein-protein interactions and are thought to play important roles as protein scaffolds in cellular processes. For example, at the presynaptic plasma liprin-containing complexes are important for the regulated release of neurotransmitter (Ko et al., 2003b; Schoch et al., 2002). At the post-synaptic membrane liprin α interacts with a variety of proteins, including neurotransmitter receptors and LAR transmembrane PTPases, to form a complex. The complex is important for the targeting of neurotransmitter receptors (AMPA-type glutamate receptors) to the postsynaptic membrane and their clustering there, processes which are important for efficient neurotransmission (Baran and Jin, 2002; Ko et al., 2003a; Shin et al., 2003; Wyszynski et al., 2002).

Liprin α1 localises to focal adhesions, sites of cell-extracellular matrix adhesion and important sites for cell signalling (Serra-Pages et al., 1995). The colocalisation of liprin α1 and LAR PTPase at the ends of focal adhesions closest to the nucleus, suggested LAR and liprin α1 may regulate focal adhesion disassembly (Serra-Pages et al., 1995).

The overexpression of short kazrin isoforms caused changes in cell shape and the actin cytoskeleton. Based on analysis of the roles of liprin proteins kazrin AL may play a scaffolding role. It is possible that kazrin short isoforms, which lack the LH domain and PDZ motif, may interfere with normal scaffold formation, thereby altering normal cellular functions. Such disruptive functions have been shown for human liprin α1A. The α1A splice form, which lacks the C-terminal 17 amino acids, including the PDZ

motif, does not interact with the scaffold protein GRIP (Wyszynski et al., 2002). Overexpression of liprin α1A interferes with normal AMPA receptor targeting and clustering at the postsynaptic membrane as the liprin containing-complexes necessary for clustering are disrupted (Wyszynski et al., 2002).

7.4 Future directions and questions

The exogenous expression of kazrin caused changes in the actin cytoskeleton and keratinocyte cell shape. Attempts to make retrovirally-infected kazrin-expressing keratinocyte lines failed, suggesting that expression of kazrin at low levels is detrimental to the cells. In the future, it will be of interest to design RNAi expression vectors to specifically knock down the expression of kazrin proteins and analyse the effects on keratinocytes or other cell types. I have shown periplakin is not necessary for kazrin localisation to cell-cell borders. Knocking down expression of kazrin by RNAi may allow us to test whether kazrin is necessary for targeting periplakin to the plasma membrane and/or desmosomes.

Previously, periplakin has been found to interact with and affect a variety of signalling molecules (Beekman et al., 2004; Feng et al., 2003; van den Heuvel et al., 2002). Periplakin and kazrin are expressed widely and thus the interaction between periplakin and kazrin may be important in a wide variety of cell types (Aho et al., 1998; Groot et al., 2004; Ma and Sun, 1986; Ruhrberg et al., 1997). It will be of interest to understand the effect of the interaction of kazrin with periplakin on kazrin protein:protein interactions and on cellular functions.

I carried out *in vivo* analysis of the function of periplakin and envoplakin using mice lacking periplakin, envoplakin and involucrin expression. Triple knock-out mice had a slight delay in epidermal barrier formation, as measured by Toluidine blue dye penetration, relative to triple heterozygous and wild type mice. The CEs isolated from triple knock out mice were ~17% larger than those from triple heterozygous mice. In the future it will be of great interest to establish the consequences of deleting the kazrin gene in mice.

[see additional pages inside back cover]

References

Aho, S. and Kazerounian, S. (2003) Molecular interactions of periplakin in epithelial cells. *Recent Res. Devel. Cell. Biochem.*, **1**, 131-141.

Aho, S., Li, K., Ryoo, Y., McGee, C., Ishida-Yamamoto, A., Uitto, J. and Klement, J.F. (2004) Periplakin gene targeting reveals a constituent of the cornified cell envelope dispensable for normal mouse development. *Mol Cell Biol*, **24**, 6410-6418.

Aho, S., McLean, W.H., Li, K. and Uitto, J. (1998) cDNA cloning, mRNA expression, and chromosomal mapping of human and mouse periplakin genes. *Genomics*, **48**, 242-247.

Alber, T. (1992) Structure of the leucine zipper. *Curr Opin Genet Dev*, **2**, 205-210.

Alberts, B., Johnson, A., Lewis, J., Raff, M., Roberts, K. and Walter, P. (2002) *Molecular Biology of the Cell.* Garland Science, Taylor and Francis Group, New York.

Amagai, M., Hashimoto, T., Green, K.J., Shimizu, N. and Nishikawa, T. (1995) Antigen-specific immunoadsorption of pathogenic autoantibodies in pemphigus foliaceus. *J Invest Dermatol*, **104**, 895-901.

Amagai, M., Hashimoto, T., Shimizu, N. and Nishikawa, T. (1994) Absorption of pathogenic autoantibodies by the extracellular domain of pemphigus vulgaris antigen (Dsg3) produced by baculovirus. *J Clin Invest*, **94**, 59-67.

Amagai, M., Koch, P.J., Nishikawa, T. and Stanley, J.R. (1996) Pemphigus vulgaris antigen (desmoglein 3) is localized in the lower epidermis, the site of blister formation in patients. *J Invest Dermatol*, **106**, 351-355.

Ändra, K., Lassmann, H., Bittner, R., Shorny, S., Fässler, R., Propst, F. and Wiche, G. (1997) Targeted inactivation of plectin reveals essential function in maintaining the integrity of skin, muscle, and heart cytoarchitecture. *Genes & Development*, **11**, 3143-3156.

Andra, K., Nikolic, B., Stocher, M., Drenckhahn, D. and Wiche, G. (1998) Not just scaffolding: plectin regulates actin dynamics in cultured cells. *Genes Dev*, **12**, 3442-3451.

Armstrong, D.K., McKenna, K.E., Purkis, P.E., Green, K.J., Eady, R.A., Leigh, I.M. and Hughes, A.E. (1999) Haploinsufficiency of desmoplakin causes a striate subtype of palmoplantar keratoderma. *Human Molecular Genetics*, **8**, 143-148.

Arnemann, J., Sullivan, K.H., Magee, A.I., King, I.A. and Buxton, R.S. (1993) Stratification-related expression of isoforms of the desmosomal cadherins in human epidermis. *J Cell Sci*, **104 (Pt 3)**, 741-750.

Baran, R. and Jin, Y. (2002) Getting a GRIP on liprins. *Neuron*, **34**, 1-2.

Beekman, J.M., Bakema, J.E., van de Winkel, J.G. and Leusen, J.H. (2004) Direct interaction between FcgammaRI (CD64) and periplakin controls receptor endocytosis and ligand binding capacity. *Proc Natl Acad Sci U S A*, **101**, 10392-10397.

Behne, M., Uchida, Y., Seki, T., de Montellano, P.O., Elias, P.M. and Holleran, W.M. (2000) Omega-hydroxyceramides are required for corneocyte lipid envelope (CLE) formation and normal epidermal permeability barrier function. *J Invest Dermatol*, **114**, 185-192.

Bierkamp, C., McLaughlin, K.J., Schwarz, H., Huber, O. and Kemler, R. (1996) Embryonic heart and skin defects in mice lacking plakoglobin. *Dev Biol*, **180**, 780-785.

Bierkamp, C., Schwarz, H., Huber, O. and Kemler, R. (1999) Desmosomal localization of beta-catenin in the skin of plakoglobin null-mutant mice. *Development*, **126**, 371-381.

Boggon, T.J., Murray, J., Chappuis-Flament, S., Wong, E., Gumbiner, B.M. and Shapiro, L. (2002) C-cadherin ectodomain structure and implications for cell adhesion mechanisms. *Science*, **296**, 1308-1313.

Bonné, S., Gilbert, B., Hatzfeld, M., Chen, X., Green, K.J. and van Roy, F. (2003) Defining desmosomal plakophilin-3 interactions. *J Cell Biol*, **161**, 403-416.

Bonné, S., van Hengel, J., Nollet, F., Kools, P. and van Roy, F. (1999) Plakophilin-3, a novel armadillo-like protein present in nuclei and desmosomes of epithelial cells. *J Cell Sci*, **112 (Pt 14)**, 2265-2276.

Bornberg-Bauer, E., Rivals, E. and Vingron, M. (1998) Computational approaches to identify leucine zippers. *Nucleic Acids Res*, **26**, 2740-2746.

Bornslaeger, E.A., Corcoran, C.M., Stappenbeck, T.S. and Green, K.J. (1996) Breaking the connection: displacement of the desmosomal plaque protein desmoplakin from cell-cell interfaces disrupts anchorage of intermediate filament bundles and alters intercellular junction assembly. *J Cell Biol*, **134**, 985-1001.

Bornslaeger, E.A., Godsel, L.M., Corcoran, C.M., Park, J.K., Hatzfeld, M., Kowalczyk, A.P. and Green, K.J. (2001) Plakophilin 1 interferes with plakoglobin binding to desmoplakin, yet together with plakoglobin promotes clustering of desmosomal plaque complexes at cell-cell borders. *J Cell Sci*, **114**, 727-738.

Braga, V.M., Hodivala, K.J. and Watt, F.M. (1995) Calcium-induced changes in distribution and solubility of cadherins, integrins and their associated cytoplasmic proteins in human keratinocytes. *Cell Adhes Commun*, **3**, 201-215.

Bretscher, A., Edwards, K. and Fehon, R.G. (2002) ERM proteins and merlin: integrators at the cell cortex. *Nat Rev Mol Cell Biol*, **3**, 586-599.

Broome, A.M. and Eckert, R.L. (2004) Microtubule-dependent redistribution of a cytoplasmic cornified envelope precursor. *J Invest Dermatol*, **122**, 29-38.

Burridge, K. and Wennerberg, K. (2004) Rho and Rac take center stage. *Cell*, **116**, 167-179.

Cabral, A., Voskamp, P., Cleton-Jansen, A.M., South, A., Nizetic, D. and Backendorf, C. (2001) Structural organization and regulation of the small proline-rich family of cornified envelope precursors suggest a role in adaptive barrier function. *J Biol Chem*, **276**, 19231-19237.

Candi, E., Melino, G., Mei, G., Tarcsa, E., Chung, S.I., Marekov, L.N. and Steinert, P.M. (1995) Biochemical, structural, and transglutaminase substrate properties of human loricrin, the major epidermal cornified cell envelope protein. *J Biol Chem*, **270**, 26382-26390.

Candi, E., Tarcsa, E., Digiovanna, J.J., Compton, J.G., Elias, P.M., Marekov, L.N. and Steinert, P.M. (1998) A highly conserved lysine residue on the head domain of type II keratins is essential for the attachment of keratin intermediate filaments to the cornified cell envelope through isopeptide crosslinking by transglutaminases. *Proc Natl Acad Sci U S A*, **95**, 2067-2072.

Candi, E., Tarcsa, E., Idler, W.W., Kartasova, T., Marekov, L.N. and Steinert, P.M. (1999) Transglutaminase cross-linking properties of the small proline-rich 1 family of cornified cell envelope proteins. Integration with loricrin. *Journal of Biological Chemistry*, **274**, 7226-7237.

Chakravarty, R. and Rice, R.H. (1989) Acylation of keratinocyte transglutaminase by palmitic and myristic acids in the membrane Anchorage region. *J Biol Chem*, **264**, 625-629.

Chen, X., Bonné, S., Hatzfeld, M., van Roy, F. and Green, K.J. (2002) Protein binding and functional characterization of plakophilin 2. Evidence for its diverse roles in desmosomes and beta -catenin signaling. *J Biol Chem*, **277**, 10512-10522.

Chitaev, N.A. and Troyanovsky, S.M. (1997) Direct Ca2+-dependent heterophilic interaction between desmosomal cadherins, desmoglein and desmocollin, contributes to cell-cell adhesion. *J Cell Biol*, **138**, 193-201.

Choi, H.J., Park-Snyder, S., Pascoe, L.T., Green, K.J. and Weis, W.I. (2002) Structures of two intermediate filament-binding fragments of desmoplakin reveal a unique repeat motif structure. *Nat Struct Biol*, **9**, 612-620.

Cokol, M., Nair, R. and Rost, B. (2000) Finding nuclear localization signals. *EMBO Rep*, **1**, 411-415.

Colledge, M. and Scott, J.D. (1999) AKAPs: from structure to function. *Trends Cell Biol*, **9**, 216-221.

Davis, R.J. (1993) The mitogen-activated protein kinase signal transduction pathway. *J Biol Chem*, **268**, 14553-14556.

Denning, M.F. (2004) Epidermal keratinocytes: regulation of multiple cell phenotypes by multiple protein kinase C isoforms. *Int J Biochem Cell Biol*, **36**, 1141-1146.

Denning, M.F., Dlugosz, A.A., Williams, E.K., Szallasi, Z., Blumberg, P.M. and Yuspa, S.H. (1995) Specific protein kinase C isozymes mediate the induction of keratinocyte differentiation markers by calcium. *Cell Growth Differ*, **6**, 149-157.

DiColandrea, T., Karashima, T., Maatta, A. and Watt, F.M. (2000) Subcellular distribution of envoplakin and periplakin: insights into their role as precursors of the epidermal cornified envelope. *J Cell Biol*, **151**, 573-586.

Djian, P., Easley, K. and Green, H. (2000) Targeted ablation of the murine involucrin gene. *J Cell Biol*, **151**, 381-388.

Downing, D.T. (1992) Lipid and protein structures in the permeability barrier of mammalian epidermis. *J Lipid Res*, **33**, 301-313.

Eckert, R.L. and Green, H. (1986) Structure and evolution of the human involucrin gene. *Cell*, **46**, 583-589.

Elias, P.M., Matsuyoshi, N., Wu, H., Lin, C., Wang, Z.H., Brown, B.E. and Stanley, J.R. (2001) Desmoglein isoform distribution affects stratum corneum structure and function. *J Cell Biol*, **153**, 243-249.

Elias, P.M., Schmuth, M., Uchida, Y., Rice, R.H., Behne, M., Crumrine, D., Feingold, K.R., Holleran, W.M. and Pharm, D. (2002) Basis for the permeability barrier abnormality in lamellar ichthyosis. *Exp Dermatol*, **11**, 248-256.

Elliott, C.E., Becker, B., Oehler, S., Castanon, M.J., Hauptmann, R. and Wiche, G. (1997) Plectin transcript diversity: identification and tissue distribution of variants with distinct first coding exons and rodless isoforms. *Genomics*, **42**, 115-125.

Favata, M.F., Horiuchi, K.Y., Manos, E.J., Daulerio, A.J., Stradley, D.A., Feeser, W.S., Van Dyk, D.E., Pitts, W.J., Earl, R.A., Hobbs, F., Copeland, R.A., Magolda, R.L., Scherle, P.A. and Trzaskos, J.M. (1998) Identification of a novel inhibitor of mitogen-activated protein kinase kinase. *J Biol Chem*, **273**, 18623-18632.

Feinberg, A.P. and Vogelstein, B. (1983) A technique for radiolabeling DNA restriction endonuclease fragments to high specific activity. *Anal Biochem*, **132**, 6-13.

Feng, G.J., Kellett, E., Scorer, C.A., Wilde, J., White, J.H. and Milligan, G. (2003) Selective interactions between helix VIII of the human mu-opioid receptors and the C terminus of periplakin disrupt G protein activation. *J Biol Chem*, **278**, 33400-33407.

Foisner, R., Malecz, N., Dressel, N., Stadler, C. and Wiche, G. (1996) M-phase-specific phosphorylation and structural rearrangement of the cytoplasmic cross-linking protein plectin involve p34cdc2 kinase. *Mol Biol Cell*, **7**, 273-288.

Foisner, R., Traub, P. and Wiche, G. (1991) Protein kinase A- and protein kinase C-regulated interaction of plectin with lamin B and vimentin. *Proc Natl Acad Sci U S A*, **88**, 3812-3816.

Foisner, R. and Wiche, G. (1987) Structure and hydrodynamic properties of plectin molecules. *J Mol Biol*, **198**, 515-531.

Fontao, L., Favre, B., Riou, S., Geerts, D., Jaunin, F., Saurat, J.H., Green, K.J., Sonnenberg, A. and Borradori, L. (2003) Interaction of the Bullous Pemphigoid Antigen 1 (BP230) and Desmoplakin with Intermediate Filaments Is Mediated by Distinct Sequences within Their COOH Terminus. *Mol Biol Cell*, **14**, 1978-1992.

Fontao, L., Geerts, D., Kuikman, I., Koster, J., Kramer, D. and Sonnenberg, A. (2001) The interaction of plectin with actin: evidence for cross-linking of actin filaments by dimerization of the actin-binding domain of plectin. *J Cell Sci*, **114**, 2065-2076.

Francis, S.H. and Corbin, J.D. (1997) Cyclic AMP and cyclic GMP in cell signalling. In Heldin, C. and Purton, M. (eds.), *Signal transduction*. Chapman Hill Ltd. part of Thomson Science, London, pp. 223-240.

Frye, M., Gardner, C., Li, E.R., Arnold, I. and Watt, F.M. (2003) Evidence that Myc activation depletes the epidermal stem cell compartment by modulating adhesive interactions with the local microenvironment. *Development*, **130**, 2793-2808.

Fuchs, P., Zorer, M., Rezniczek, G.A., Spazierer, D., Oehler, S., Castanon, M.J., Hauptmann, R. and Wiche, G. (1999) Unusual 5' transcript complexity of plectin isoforms: novel tissue- specific exons modulate actin binding activity. *Hum Mol Genet*, **8**, 2461-2472.

Gallicano, G.I., Bauer, C. and Fuchs, E. (2001) Rescuing desmoplakin function in extra-embryonic ectoderm reveals the importance of this protein in embryonic heart, neuroepithelium, skin and vasculature. *Development*, **128**, 929-941.

Gallicano, G.I., Kouklis, P., Bauer, C., Yin, M., Vasioukhin, V., Degenstein, L. and Fuchs, E. (1998) Desmoplakin is required early in development for assembly of desmosomes and cytoskeletal linkage. *Journal of Cell Biology*, **143**, 2009-2022.

Garrod, D.R., Merritt, A.J. and Nie, Z. (2002) Desmosomal cadherins. *Curr Opin Cell Biol*, **14**, 537-545.

Gaudry, C.A., Palka, H.L., Dusek, R.L., Huen, A.C., Khandekar, M.J., Hudson, L.G. and Green, K.J. (2001) Tyrosine-phosphorylated plakoglobin is associated with desmogleins but not desmoplakin after epidermal growth factor receptor activation. *J Biol Chem*, **276**, 24871-24880.

Geerts, D., Fontao, L., Nievers, M.G., Schaapveld, R.Q., Purkis, P.E., Wheeler, G.N., Lane, E.B., Leigh, I.M. and Sonnenberg, A. (1999) Binding of integrin alpha6beta4 to plectin prevents plectin association with F-actin but does not interfere with intermediate filament binding. *J Cell Biol*, **147**, 417-434.

Getsios, S., Huen, A.C. and Green, K.J. (2004) Working out the strength and flexibility of desmosomes. *Nat Rev Mol Cell Biol*, **5**, 271-281.

Green, K.J., Virata, M.L., Elgart, G.W., Stanley, J.R. and Parry, D.A. (1992) Comparative structural analysis of desmoplakin, bullous pemphigoid antigen and plectin: members of a new gene family involved in organization of intermediate filaments. *Int J Biol Macromol*, **14**, 145-153.

Gregory, S.L. and Brown, N.H. (1998) kakapo, a gene required for adhesion between and within cell layers in Drosophila, encodes a large cytoskeletal linker protein related to plectin and dystrophin. *J Cell Biol*, **143**, 1271-1282.

Groot, K.R., Sevilla, L.M., Nishi, K., DiColandrea, T. and Watt, F.M. (2004) Kazrin, a novel periplakin-interacting protein associated with desmosomes and the keratinocyte plasma membrane. *J Cell Biol*, **166**, 653-659.

Hanakawa, Y., Matsuyoshi, N. and Stanley, J.R. (2002) Expression of desmoglein 1 compensates for genetic loss of desmoglein 3 in keratinocyte adhesion. *J Invest Dermatol*, **119**, 27-31.

Hardman, M.J., Moore, L., Ferguson, M.W. and Byrne, C. (1999) Barrier formation in the human fetus is patterned. *J Invest Dermatol*, **113**, 1106-1113.

Hardman, M.J., Sisi, P., Banbury, D.N. and Byrne, C. (1998) Patterned acquisition of skin barrier function during development. *Development*, **125**, 1541-1552.

Harlow, E. and Lane, D. (1998) *Antibodies. A laboratory Manual.* Cold Spring Harbor Laboratory, New York.

Harris, B.Z. and Lim, W.A. (2001) Mechanism and role of PDZ domains in signaling complex assembly. *J Cell Sci*, **114**, 3219-3231.

Hatzfeld, M., Haffner, C., Schulze, K. and Vinzens, U. (2000) The function of plakophilin 1 in desmosome assembly and actin filament organization. *Journal of Cell Biology*, **149**, 209-222.

He, W., Cowin, P. and Stokes, D.L. (2003) Untangling desmosomal knots with electron tomography. *Science*, **302**, 109-113.

Herman, I.M. (1993) Actin isoforms. *Curr Opin Cell Biol*, **5**, 48-55.

Hirao, T., Denda, M. and Takahashi, M. (2001) Identification of immature cornified envelopes in the barrier-impaired epidermis by characterization of their hydrophobicity and antigenicities of the components. *Exp Dermatol*, **10**, 35-44.

Hofmann, I., Mertens, C., Brettel, M., Nimmrich, V., Schnolzer, M. and Herrmann, H. (2000) Interaction of plakophilins with desmoplakin and intermediate filament proteins: an in vitro analysis. *J Cell Sci*, **113 (Pt 13)**, 2471-2483.

Hohl, D., Mehrel, T., Lichti, U., Turner, M.L., Roop, D.R. and Steinert, P.M. (1991) Characterization of human loricrin. Structure and function of a new class of epidermal cell envelope proteins. *J Biol Chem*, **266**, 6626-6636.

Holbrook, K. (1994) *The keratinocyte handbook.* Cambridge University Press, Great Britain.

Huber, M., Rettler, I., Bernasconi, K., Frenk, E., Lavrijsen, S.P., Ponec, M., Bon, A., Lautenschlager, S., Schorderet, D.F. and Hohl, D. (1995) Mutations of keratinocyte transglutaminase in lamellar ichthyosis. *Science*, **267**, 525-528.

Hudson, D.L., Weiland, K.L., Dooley, T.P., Simon, M. and Watt, F.M. (1992) Characterisation of eight monoclonal antibodies to involucrin. *Hybridoma*, **11**, 367-379.

Huen, A.C., Park, J.K., Godsel, L.M., Chen, X., Bannon, L.J., Amargo, E.V., Hudson, T.Y., Mongiu, A.K., Leigh, I.M., Kelsell, D.P., Gumbiner, B.M. and Green, K.J. (2002) Intermediate filament-membrane attachments function synergistically with actin-dependent contacts to regulate intercellular adhesive strength. *J Cell Biol*, **159**, 1005-1017.

Jarnik, M., de Viragh, P.A., Scharer, E., Bundman, D., Simon, M.N., Roop, D.R. and Steven, A.C. (2002) Quasi-normal cornified cell envelopes in loricrin knockout mice imply the existence of a loricrin backup system. *J Invest Dermatol*, **118**, 102-109.

Jarnik, M., Kartasova, T., Steinert, P.M., Lichti, U. and Steven, A.C. (1996) Differential expression and cell envelope incorporation of small proline-rich protein 1 in different cornified epithelia. *J Cell Sci*, **109 (Pt 6)**, 1381-1391.

Jefferson, J.J., Leung, C.L. and Liem, R.K. (2004) Plakins: goliaths that link cell junctions and the cytoskeleton. *Nat Rev Mol Cell Biol*, **5**, 542-553.

Johnson, G.L. and Lapadat, R. (2002) Mitogen-activated protein kinase pathways mediated by ERK, JNK, and p38 protein kinases. *Science*, **298**, 1911-1912.

Joshi, B., Cai, A.L., Keiper, B.D., Minich, W.B., Mendez, R., Beach, C.M., Stepinski, J., Stolarski, R., Darzynkiewicz, E. and Rhoads, R.E. (1995) Phosphorylation of eukaryotic protein synthesis initiation factor 4E at Ser-209. *J Biol Chem*, **270**, 14597-14603.

Kalinin, A., Marekov, L.N. and Steinert, P.M. (2001) Assembly of the epidermal cornified cell envelope. *J Cell Sci*, **114**, 3069-3070.

Kalinin, A.E., Idler, W.W., Marekov, L.N., McPhie, P., Bowers, B., Steinert, P.M. and Steven, A.C. (2004) Co-assembly of Envoplakin and Periplakin into Oligomers and Ca2+-dependent Vesicle Binding: IMPLICATIONS FOR CORNIFIED CELL ENVELOPE FORMATION IN STRATIFIED SQUAMOUS EPITHELIA. *J Biol Chem*, **279**, 22773-22780.

Kalinin, A.E., Kajava, A.V. and Steinert, P.M. (2002) Epithelial barrier function: assembly and structural features of the cornified cell envelope. *Bioessays*, **24**, 789-800.

Karakesisoglou, I., Yang, Y. and Fuchs, E. (2000) An epidermal plakin that integrates actin and microtubule networks at cellular junctions. *J Cell Biol*, **149**, 195-208.

Karashima, T. and Watt, F.M. (2002) Interaction of periplakin and envoplakin with intermediate filaments. *J Cell Sci*, **115**, 5027-5037.

Kartasova, T., Parry, D.A.D. and Steinert, P.M. (1995) Modeling of small proline rich protein evolution and structure. *Journal of Investigative Dermatology*, **104**, 611 abstract.

Kazerounian, S. and Aho, S. (2003) Characterization of periphilin, a widespread, highly insoluble nuclear protein and potential constituent of the keratinocyte cornified envelope. *J Biol Chem*, **278**, 36707-36717.

Kazerounian, S., Uitto, J. and Aho, S. (2002) Unique role for the periplakin tail in intermediate filament association: specific binding to keratin 8 and vimentin. *Exp Dermatol*, **11**, 428-438.

Kim, C.A. and Bowie, J.U. (2003) SAM domains: uniform structure, diversity of function. *Trends Biochem Sci*, **28**, 625-628.

Kim, H.C., Lewis, M.S., Gorman, J.J., Park, S.C., Girard, J.E., Folk, J.E. and Chung, S.I. (1990) Protransglutaminase E from guinea pig skin. Isolation and partial characterization. *J Biol Chem*, **265**, 21971-21978.

King, I.A., O'Brien, T.J. and Buxton, R.S. (1996) Expression of the "skin-type" desmosomal cadherin DSC1 is closely linked to the keratinization of epithelial tissues during mouse development. *J Invest Dermatol*, **107**, 531-538.

Kljuic, A., Bazzi, H., Sundberg, J.P., Martinez-Mir, A., O'Shaughnessy, R., Mahoney, M.G., Levy, M., Montagutelli, X., Ahmad, W., Aita, V.M., Gordon, D., Uitto, J., Whiting, D., Ott, J., Fischer, S., Gilliam, T.C., Jahoda, C.A., Morris, R.J., Panteleyev, A.A., Nguyen, V.T. and Christiano, A.M. (2003) Desmoglein 4 in hair follicle differentiation and epidermal adhesion: evidence from inherited hypotrichosis and acquired pemphigus vulgaris. *Cell*, **113**, 249-260.

Ko, J., Kim, S., Valtschanoff, J.G., Shin, H., Lee, J.R., Sheng, M., Premont, R.T., Weinberg, R.J. and Kim, E. (2003a) Interaction between liprin-alpha and GIT1 is required for AMPA receptor targeting. *J Neurosci*, **23**, 1667-1677.

Ko, J., Na, M., Kim, S., Lee, J.R. and Kim, E. (2003b) Interaction of the ERC family of RIM-binding proteins with the liprin-alpha family of multidomain proteins. *J Biol Chem*, **278**, 42377-42385.

Koch, P.J., Viragh, P.A.d., Scharer, E., Bundman, D., Longley, M.A., Bickenbach, J., Kawachi, Y., Suga, Y., Zhou, Z., Huber, M., Hohl, D., Kartasova, T., Jarnik, M., Steven, A.C. and Roop, D.R. (2000) Lessons from loricrin-deficient mice: compensatory mechanisms maintaining skin barrier function in the absence of a major cornified envelope protein. *Journal of Cell Biology*, **151**, 389-400.

Koster, J., Geerts, D., Favre, B., Borradori, L. and Sonnenberg, A. (2003) Analysis of the interactions between BP180, BP230, plectin and the integrin alpha6beta4 important for hemidesmosome assembly. *J Cell Sci*, **116**, 387-399.

Kowalczyk, A.P., Bornslaeger, E.A., Borgwardt, J.E., Palka, H.L., Dhaliwal, A.S., Corcoran, C.M., Denning, M.F. and Green, K.J. (1997) The amino-terminal domain of desmoplakin binds to plakoglobin and clusters desmosomal cadherin-plakoglobin complexes. *J Cell Biol*, **139**, 773-784.

Kowalczyk, A.P., Bornslaeger, E.A., Norvell, S.M., Palka, H.L. and Green, K.J. (1999a) Desmosomes: intercellular adhesive junctions specialized for attachment of intermediate filaments. *Int Rev Cytol*, **185**, 237-302.

Kowalczyk, A.P., Hatzfeld, M., Bornslaeger, E.A., Kopp, D.S., Borgwardt, J.E., Corcoran, C.M., Settler, A. and Green, K.J. (1999b) The head domain of plakophilin-1 binds to desmoplakin and enhances its recruitment to desmosomes. Implications for cutaneous disease. *Journal of Biological Chemistry*, **274**, 18145-18148.

Kozak, M. (1996) Interpreting cDNA sequences: some insights from studies on translation. *Mamm Genome*, **7**, 563-574.

Kuramoto, N., Takizawa, T., Matsuki, M., Morioka, H., Robinson, J.M. and Yamanishi, K. (2002) Development of ichthyosiform skin compensates for defective permeability barrier function in mice lacking transglutaminase 1. *J Clin Invest*, **109**, 243-250.

Laemmli, U.K. (1970) Cleavage of structural proteins during the assembly of the head of bacteriophage T4. *Nature*, **227**, 680-685.

Lane, E.B., Bartek, J., Purkis, P.E. and Leigh, I.M. (1985) Keratin antigens in differentiating skin. *Ann N Y Acad Sci*, **455**, 241-258.

Lazo, N.D., Meine, J.G. and Downing, D.T. (1995) Lipids are covalently attached to rigid corneocyte protein envelopes existing predominantly as beta-sheets: a solid-state nuclear magnetic resonance study. *J Invest Dermatol*, **105**, 296-300.

Lee, S. and Kolodziej, P.A. (2002) Short Stop provides an essential link between F-actin and microtubules during axon extension. *Development*, **129**, 1195-1204.

Leung, C.L., Green, K.J. and Liem, R.K. (2002) Plakins: a family of versatile cytolinker proteins. *Trends Cell Biol*, **12**, 37-45.

Leung, C.L., Liem, R.K., Parry, D.A. and Green, K.J. (2001) The plakin family. *J Cell Sci*, **114**, 3409-3410.

Levy, L., Broad, S., Zhu, A.J., Carrol, J.M., Khazaal, I., Péault, B. and Watt, F.M. (1998) Optimised retroviral infection of human epidermal keratinocytes: long-term expression of transduced integrin gene following grafting onto SCID mice. *Gene Therapy*, **5**, 913-922.

Li, E.R., Owens, D.M., Djian, P. and Watt, F.M. (2000) Expression of involucrin in normal, hyperproliferative and neoplastic mouse keratinocytes. *Exp Dermatol*, **9**, 431-438.

Lorand, L. and Graham, R.M. (2003) Transglutaminases: crosslinking enzymes with pleiotropic functions. *Nat Rev Mol Cell Biol*, **4**, 140-156.

Lupas, A., Van Dyke, M. and Stock, J. (1991) Predicting coiled coils from protein sequences. *Science*, **252**, 1162-1164.
Ma, A.S. and Sun, T.T. (1986) Differentiation-dependent changes in the solubility of a 195-kD protein in human epidermal keratinocytes. *J Cell Biol*, **103**, 41-48.
Määttä, A., DiColandrea, T., Groot, K. and Watt, F.M. (2001) Gene targeting of envoplakin, a cytoskeletal linker protein and precursor of the epidermal cornified envelope. *Mol Cell Biol*, **21**, 7047-7053.
Määttä, A., Ruhrberg, C. and Watt, F.M. (2000) Structure and regulation of the envoplakin gene. *Journal of Biological Chemistry*, **275**, 19857-19865.
Makkerh, J.P., Dingwall, C. and Laskey, R.A. (1996) Comparative mutagenesis of nuclear localization signals reveals the importance of neutral and acidic amino acids. *Curr Biol*, **6**, 1025-1027.
Marcozzi, C., Burdett, I.D., Buxton, R.S. and Magee, A.I. (1998) Coexpression of both types of desmosomal cadherin and plakoglobin confers strong intercellular adhesion. *J Cell Sci*, **111 (Pt 4)**, 495-509.
Marekov, L.N. and Steinert, P.M. (1998) Ceramides are bound to structural proteins of the human foreskin epidermal cornified cell envelope. *J Biol Chem*, **273**, 17763-17770.
Marshall, D., Hardman, M.J. and Byrne, C. (2000) SPRR1 gene induction and barrier formation occur as coordinated moving fronts in terminally differentiating epithelia. *J Invest Dermatol*, **114**, 967-975.
Marshall, D., Hardman, M.J., Nield, K.M. and Byrne, C. (2001) Differentially expressed late constituents of the epidermal cornified envelope. *Proc Natl Acad Sci U S A*, **98**, 13031-13036.
Martiny-Baron, G., Kazanietz, M.G., Mischak, H., Blumberg, P.M., Kochs, G., Hug, H., Marme, D. and Schachtele, C. (1993) Selective inhibition of protein kinase C isozymes by the indolocarbazole Go 6976. *J Biol Chem*, **268**, 9194-9197.
Matsuki, M., Yamashita, F., Ishida-Yamamoto, A., Yamada, K., Kinoshita, C., Fushiki, S., Ueda, E., Morishima, Y., Tabata, K., Yasuno, H., Hashida, M., Iizuka, H., Ikawa, M., Okabe, M., Kondoh, G., Kinoshita, T., Takeda, J. and Yamanishi, K. (1998) Defective stratum corneum and early neonatal death in mice lacking the gene for transglutaminase 1 (keratinocyte transglutaminase). *Proc Natl Acad Sci U S A*, **95**, 1044-1049.
McGrath, J.A., McMillan, J.R., Shemanko, C.S., Runswick, S.K., Leigh, I.M., Lane, E.B., Garrod, D.R. and Eady, R.A. (1997) Mutations in the plakophilin 1 gene result in ectodermal dysplasia/skin fragility syndrome. *Nat Genet*, **17**, 240-244.
McLean, W.H., Pulkkinen, L., Smith, F.J., Rugg, E.L., Lane, E.B., Bullrich, F., Burgeson, R.E., Amano, S., Hudson, D.L., Owaribe, K., McGrath, J.A., McMillan, J.R., Eady, R.A., Leigh, I.M., Christiano, A.M. and Uitto, J. (1996) Loss of plectin causes epidermolysis bullosa with muscular dystrophy: cDNA cloning and genomic organization. *Genes & Development*, **10**, 1724-1735.
Meggio, F. and Pinna, L.A. (2003) One-thousand-and-one substrates of protein kinase CK2? *Faseb J*, **17**, 349-368.
Mehrel, T., Hohl, D., Rothnagel, J.A., Longley, M.A., Bundman, D., Cheng, C., Lichti, U., Bisher, M.E., Steven, A.C., Steinert, P.M. and et al. (1990) Identification of a major keratinocyte cell envelope protein, loricrin. *Cell*, **61**, 1103-1112.
Meng, J.J., Bornslaeger, E.A., Green, K.J., Steinert, P.M. and Ip, W. (1997) Two-hybrid analysis reveals fundamental differences in direct interactions between desmoplakin and cell type-specific intermediate filaments. *J Biol Chem*, **272**, 21495-21503.

Mertens, C., Kuhn, C. and Franke, W.W. (1996) Plakophilins 2a and 2b: constitutive proteins of dual location in the karyoplasm and the desmosomal plaque. *J Cell Biol*, **135**, 1009-1025.

Michel, S., Schmidt, R., Shroot, B. and Reichert, U. (1988) Morphological and biochemical characterization of the cornified envelopes from human epidermal keratinocytes of different origin. *J Invest Dermatol*, **91**, 11-15.

Mischke, D., Korge, B.P., Marenholz, I., Volz, A. and Ziegler, A. (1996) Genes encoding structural proteins of epidermal cornification and S100 calcium-binding proteins form a gene complex ("epidermal differentiation complex") on human chromosome 1q21. *J Invest Dermatol*, **106**, 989-992.

Mitev, V. and Miteva, L. (1999) Signal transduction in keratinocytes. *Exp Dermatol*, **8**, 96-108.

Moll, I., Kurzen, H., Langbein, L. and Franke, W.W. (1997) The distribution of the desmosomal protein, plakophilin 1, in human skin and skin tumors. *J Invest Dermatol*, **108**, 139-146.

Nakane, H., Ishida-Yamamoto, A., Takahashi, H. and Iizuka, H. (2002) Elafin, a secretory protein, is cross-linked into the cornified cell envelopes from the inside of psoriatic keratinocytes. *J Invest Dermatol*, **119**, 50-55.

Nemes, Z., Marekov, L.N., Fesus, L. and Steinert, P.M. (1999a) A novel function for transglutaminase 1: attachment of long-chain omega- hydroxyceramides to involucrin by ester bond formation. *Proc Natl Acad Sci U S A*, **96**, 8402-8407.

Nemes, Z., Marekov, L.N. and Steinert, P.M. (1999b) Involucrin cross-linking by transglutaminase 1. Binding to membranes directs residue specificity. *J Biol Chem*, **274**, 11013-11021.

Nikolic, B., Mac Nulty, E., Mir, B. and Wiche, G. (1996) Basic amino acid residue cluster within nuclear targeting sequence motif is essential for cytoplasmic plectin-vimentin network junctions. *J Cell Biol*, **134**, 1455-1467.

North, A.J., Bardsley, W.G., Hyam, J., Bornslaeger, E.A., Cordingley, H.C., Trinnaman, B., Hatzfeld, M., Green, K.J., Magee, A.I. and Garrod, D.R. (1999) Molecular map of the desmosomal plaque. *Journal of Cell Science*, **112**, 4325-4336.

O'Keefe, E.J., Erickson, H.P. and Bennett, V. (1989) Desmoplakin I and desmoplakin II. Purification and characterization. *J Biol Chem*, **264**, 8310-8318.

Odland, G. (1991) *Structure of the skin.* Oxford University Press.

Okumura, M., Yamakawa, H., Ohara, O. and Owaribe, K. (2002) Novel Alternative Splicings of BPAG1 (Bullous Pemphigoid Antigen 1) Including the Domain Structure Closely Related to MACF (Microtubule Actin Cross-linking Factor). *J Biol Chem*, **277**, 6682-6687.

Palka, H.L. and Green, K.J. (1997) Roles of plakoglobin end domains in desmosome assembly. *J Cell Sci*, **110 (Pt 19)**, 2359-2371.

Papp, H., Czifra, G., Lazar, J., Gonczi, M., Csernoch, L., Kovacs, L. and Biro, T. (2003) Protein kinase C isozymes regulate proliferation and high cell density-mediated differentiation in HaCaT keratinocytes. *Exp Dermatol*, **12**, 811-824.

Parrish, E.P., Steart, P.V., Garrod, D.R. and Weller, R.O. (1987) Antidesmosomal monoclonal antibody in the diagnosis of intracranial tumours. *J Pathol*, **153**, 265-273.

Pearson, R.B. and Kemp, B.E. (1991) Protein kinase phosphorylation site sequences and consensus specificity motifs: tabulations. *Methods Enzymol*, **200**, 62-81.

Porter, R.M. and Lane, E.B. (2003) Phenotypes, genotypes and their contribution to understanding keratin function. *Trends Genet*, **19**, 278-285.

Prokop, A., Uhler, J., Roote, J. and Bate, M. (1998) The kakapo mutation affects terminal arborization and central dendritic sprouting of Drosophila motorneurons. *J Cell Biol*, **143**, 1283-1294.

Rezniczek, G.A., de Pereda, J.M., Reipert, S. and Wiche, G. (1998) Linking integrin alpha6beta4-based cell adhesion to the intermediate filament cytoskeleton: direct interaction between the beta4 subunit and plectin at multiple molecular sites. *J Cell Biol*, **141**, 209-225.

Rheinwald, J.G. and Green, H. (1975) Serial cultivation of strains of human epidermal keratinocytes: the formation of keratinizing colonies from single cells. *Cell*, **6**, 331-343.

Rice, R.H. and Green, H. (1979) Presence in human epidermal cells of a soluble protein precursor of the cross-linked envelope: activation of the cross-linking by calcium ions. *Cell*, **18**, 681-694.

Rice, R.H., Pinkus, G.S., Warhol, M.J. and Antonioli, D.A. (1984) *Involucrin: Biochemistry and immunohistochemistry*. Masson Press, U.S.A.

Robinson, N.A., Lapic, S., Welter, J.F. and Eckert, R.L. (1997) S100A11, S100A10, annexin I, desmosomal proteins, small proline-rich proteins, plasminogen activator inhibitor-2, and involucrin are components of the cornified envelope of cultured human epidermal keratinocytes. *J Biol Chem*, **272**, 12035-12046.

Romero, M.R., Carrol, J.M. and Watt, F.M. (1999) Analysis of cultured keratinocytes from a transgenic mouse model of psoriasis: effects of suprabasal integrin expression on keratinocyte adhesion, proliferation, and terminal differentiation. *Experimental Dermatology*, **8**, 53-67.

Roper, E., Weinberg, W., Watt, F.M. and Land, H. (2001) p19ARF-independent induction of p53 and cell cycle arrest by Raf in murine keratinocytes. *EMBO Rep*, **2**, 145-150.

Roper, K. and Brown, N.H. (2003) Maintaining epithelial integrity: a function for gigantic spectraplakin isoforms in adherens junctions. *J Cell Biol*, **162**, 1305-1315.

Ruhrberg, C., Hajibagheri, M.A., Parry, D.A. and Watt, F.M. (1997) Periplakin, a novel component of cornified envelopes and desmosomes that belongs to the plakin family and forms complexes with envoplakin. *J Cell Biol*, **139**, 1835-1849.

Ruhrberg, C., Hajibagheri, M.A., Simon, M., Dooley, T.P. and Watt, F.M. (1996) Envoplakin, a novel precursor of the cornified envelope that has homology to desmoplakin. *J Cell Biol*, **134**, 715-729.

Ruhrberg, C. and Watt, F.M. (1997) The plakin family: versatile organizers of cytoskeletal architecture. *Curr Opin Genet Dev*, **7**, 392-397.

Ruiz, P., Brinkmann, V., Ledermann, B., Behrend, M., Grund, C., Thalhammer, C., Vogel, F., Birchmeier, C., Gunthert, U., Franke, W.W. and Birchmeier, W. (1996) Targeted mutation of plakoglobin in mice reveals essential functions of desmosomes in the embryonic heart. *J Cell Biol*, **135**, 215-225.

Russell, L.J., DiGiovanna, J.J., Rogers, G.R., Steinert, P.M., Hashem, N., Compton, J.G. and Bale, S.J. (1995) Mutations in the gene for transglutaminase 1 in autosomal recessive lamellar ichthyosis. *Nat Genet*, **9**, 279-283.

Schafer, S., Koch, P.J. and Franke, W.W. (1994) Identification of the ubiquitous human desmoglein, Dsg2, and the expression catalogue of the desmoglein subfamily of desmosomal cadherins. *Exp Cell Res*, **211**, 391-399.

Schmidt, A., Langbein, L., Rode, M., Pratzel, S., Zimbelmann, R. and Franke, W.W. (1997) Plakophilins 1a and 1b: widespread nuclear proteins recruited in specific epithelial cells as desmosomal plaque components. *Cell Tissue Res*, **290**, 481-499.

Schoch, S., Castillo, P.E., Jo, T., Mukherjee, K., Geppert, M., Wang, Y., Schmitz, F., Malenka, R.C. and Sudhof, T.C. (2002) RIM1alpha forms a protein scaffold for regulating neurotransmitter release at the active zone. *Nature*, **415**, 321-326.

Schubert, U., Henklein, P., Boldyreff, B., Wingender, E., Strebel, K. and Porstmann, T. (1994) The human immunodeficiency virus type 1 encoded Vpu protein is phosphorylated by casein kinase-2 (CK-2) at positions Ser52 and Ser56 within a predicted alpha-helix-turn-alpha-helix-motif. *J Mol Biol*, **236**, 16-25.

Serra-Pages, C., Kedersha, N.L., Fazikas, L., Medley, Q., Debant, A. and Streuli, M. (1995) The LAR transmembrane protein tyrosine phosphatase and a coiled-coil LAR-interacting protein co-localize at focal adhesions. *Embo J*, **14**, 2827-2838.

Serra-Pages, C., Medley, Q.G., Tang, M., Hart, A. and Streuli, M. (1998) Liprins, a family of LAR transmembrane protein-tyrosine phosphatase-interacting proteins. *J Biol Chem*, **273**, 15611-15620.

Sevcik, J., Urbanikova, L., Kost'an, J., Janda, L. and Wiche, G. (2004) Actin-binding domain of mouse plectin. Crystal structure and binding to vimentin. *Eur J Biochem*, **271**, 1873-1884.

Shenolikar, S. (2004) Detection of phosphorylation by enzymatic techniques. In Ausubel, F.M., Brent, R., Kingston, R.E., Moore, D.D., Seidman, J.G., Smith, J.A. and Struhl, K. (eds.), *Current protocols in molecular biology*. John Wiley and Sons. Inc., Vol. 18.5.

Shin, H., Wyszynski, M., Huh, K.H., Valtschanoff, J.G., Lee, J.R., Ko, J., Streuli, M., Weinberg, R.J., Sheng, M. and Kim, E. (2003) Association of the kinesin motor KIF1A with the multimodular protein liprin-alpha. *J Biol Chem*, **278**, 11393-11401.

Siefring, G.E., Jr., Apostol, A.B., Velasco, P.T. and Lorand, L. (1978) Enzymatic basis for the Ca2+-induced cross-linking of membrane proteins in intact human erythrocytes. *Biochemistry*, **17**, 2598-2604.

Simon, M. and Green, H. (1984) Participation of membrane-associated proteins in the formation of the cross-linked envelope of the keratinocyte. *Cell*, **36**, 827-834.

Simon, M. and Green, H. (1985) Enzymatic cross-linking of involucrin and other proteins by keratinocyte particulates in vitro. *Cell*, **40**, 677-683.

Sipos, L. and von Heijne, G. (1993) Predicting the topology of eukaryotic membrane proteins. *Eur J Biochem*, **213**, 1333-1340.

Smith, E.A. and Fuchs, E. (1998) Defining the interactions between intermediate filaments and desmosomes. *Journal of Cell Biology*, **141**, 1229-1241.

Song, H.J., Poy, G., Darwiche, N., Lichti, U., Kuroki, T., Steinert, P.M. and Kartasova, T. (1999) Mouse Sprr2 genes: a clustered family of genes showing differential expression in epithelial tissues. *Genomics*, **55**, 28-42.

Spazierer, D., Fuchs, P., Proll, V., Janda, L., Oehler, S., Fischer, I., Hauptmann, R. and Wiche, G. (2003) Epiplakin gene analysis in mouse reveals a single exon encoding a 725-kDa protein with expression restricted to epithelial tissues. *J Biol Chem*, **278**, 31657-31666.

Stappenbeck, T.S., Bornslaeger, E.A., Corcoran, C.M., Luu, H.H., Virata, M.L. and Green, K.J. (1993) Functional analysis of desmoplakin domains: specification of the interaction with keratin versus vimentin intermediate filament networks. *J Cell Biol*, **123**, 691-705.

Stappenbeck, T.S., Lamb, J.A., Corcoran, C.M. and Green, K.J. (1994) Phosphorylation of the desmoplakin COOH terminus negatively regulates its interaction with keratin intermediate filament networks. *J Biol Chem*, **269**, 29351-29354.

Steinbock, F.A., Nikolic, B., Coulombe, P.A., Fuchs, E., Traub, P. and Wiche, G. (2000) Dose-dependent linkage, assembly inhibition and disassembly of

vimentin and cytokeratin 5/14 filaments through plectin's intermediate filament-binding domain. *Journal of Cell Science*, **113**, 483-491.
Steinert, P.M. (1995) A model for the hierarchical structure of the human epidermal cornified envelope. *Cell Death Differ*, **2**, 33-40.
Steinert, P.M., Kartasova, T. and Marekov, L.N. (1998) Biochemical evidence that small proline-rich proteins and trichohyalin function in epithelia by modulation of the biomechanical properties of their cornified cell envelopes. *J Biol Chem*, **273**, 11758-11769.
Steinert, P.M. and Marekov, L.N. (1995) The proteins elafin, filaggrin, keratin intermediate filaments, loricrin, and small proline-rich proteins 1 and 2 are isodipeptide cross-linked components of the human epidermal cornified cell envelope. *J Biol Chem*, **270**, 17702-17711.
Steinert, P.M. and Marekov, L.N. (1997) Direct evidence that involucrin is a major early isopeptide cross-linked component of the keratinocyte cornified cell envelope. *Journal of Biological Chemistry*, **272**, 2021-2030.
Steinert, P.M. and Marekov, L.N. (1999) Initiation of assembly of the cell envelope barrier structure of stratified squamous epithelia. *Mol Biol Cell*, **10**, 4247-4261.
Steven, A.C., Bisher, M.E., Roop, D.R. and Steinert, P.M. (1990) Biosynthetic pathways of filaggrin and loricrin--two major proteins expressed by terminally differentiated epidermal keratinocytes. *J Struct Biol*, **104**, 150-162.
Straub, B.K., Boda, J., Kuhn, C., Schnoelzer, M., Korf, U., Kempf, T., Spring, H., Hatzfeld, M. and Franke, W.W. (2003) A novel cell-cell junction system: the cortex adhaerens mosaic of lens fiber cells. *J Cell Sci*, **116**, 4985-4995.
Strelkov, S.V., Herrmann, H. and Aebi, U. (2003) Molecular architecture of intermediate filaments. *Bioessays*, **25**, 243-251.
Studer, D., Michel, M. and Muller, M. (1989) High pressure freezing comes of age. *Scanning Microsc Suppl*, **3**, 253-268; discussion 268-259.
Sun, D., Leung, C.L. and Liem, R.K. (2001) Characterization of the microtubule binding domain of microtubule actin crosslinking factor (MACF): identification of a novel group of microtubule associated proteins. *J Cell Sci*, **114**, 161-172.
Syed, S.E., Trinnaman, B., Martin, S., Major, S., Hutchinson, J. and Magee, A.I. (2002) Molecular interactions between desmosomal cadherins. *Biochem J*, **362**, 317-327.
Takahashi, M., Tezuka, T. and Katunuma, N. (1992) Phosphorylated cystatin alpha is a natural substrate of epidermal transglutaminase for formation of skin cornified envelope. *FEBS Lett*, **308**, 79-82.
Tang, H.Y., Chaffotte, A.F. and Thacher, S.M. (1996) Structural analysis of the predicted coiled-coil rod domain of the cytoplasmic bullous pemphigoid antigen (BPAG1). Empirical localization of the N-terminal globular domain-rod boundary. *J Biol Chem*, **271**, 9716-9722.
Teumer, J. and Green, H. (1989) Divergent evolution of part of the involucrin gene in the hominoids: unique intragenic duplications in the gorilla and human. *Proc Natl Acad Sci U S A*, **86**, 1283-1286.
Theis, D.G., Koch, P.J. and Franke, W.W. (1993) Differential synthesis of type 1 and type 2 desmocollin mRNAs in human stratified epithelia. *Int J Dev Biol*, **37**, 101-110.
Tomasz, M., Lipman, R., Lee, M.S., Verdine, G.L. and Nakanishi, K. (1987) Reaction of acid-activated mitomycin C with calf thymus DNA and model guanines: elucidation of the base-catalyzed degradation of N7-alkylguanine nucleosides. *Biochemistry*, **26**, 2010-2027.

Angst, B. D., Nilles, L. A., and Green, K. J. (1990): Desmoplakin II expression is not restricted to stratified epithelia. *J Cell Sci* **97**, 247-57.

Green, K. J., Parry, D. A., Steinert, P. M., Virata, M. L., Wagner, R. M., Angst, B. D., and Nilles, L. A. (1990): Structure of the human desmoplakins. Implications for function in the desmosomal plaque. *J Biol Chem* **265**, 2603-2612.

Hatsell, S., and Cowin, P. (2001): Deconstructing desmoplakin. *Nat Cell Biol* **3**, E270-2.

Perez-Moreno, M., Jamora, C., and Fuchs, E. (2003): Sticky business: orchestrating cellular signals at adherens junctions. *Cell* **112**, 535-48.

Sipos, L., and von Heijne, G. (1993): Predicting the topology of eukaryotic membrane proteins. *Eur J Biochem* **213**, 1333-40.

Skerrow, C. J., Clelland, D. G., and Skerrow, D. (1989): Changes to desmosomal antigens and lectin-binding sites during differentiation in normal human epidermis: a quantitative ultrastructural study. *J Cell Sci* **92 (Pt 4)**, 667-77.

Trowbridge, I.S., Lesley, J., Schulte, R., Hyman, R. and Trotter, J. (1982) Biochemical characterization and cellular distribution of a polymorphic, murine cell-surface glycoprotein expressed on lymphoid tissues. *Immunogenetics*, **15**, 299-312.

Troyanovsky, S.M., Troyanovsky, R.B., Eshkind, L.G., Leube, R.E. and Franke, W.W. (1994) Identification of amino acid sequence motifs in desmocollin, a desmosomal glycoprotein, that are required for plakoglobin binding and plaque formation. *Proc Natl Acad Sci U S A*, **91**, 10790-10794.

Tseng, H. and Green, H. (1988) Remodeling of the involucrin gene during primate evolution. *Cell*, **54**, 491-496.

van den Heuvel, A.P., de Vries-Smits, A.M., van Weeren, P.C., Dijkers, P.F., de Bruyn, K.M., Riedl, J.A. and Burgering, B.M. (2002) Binding of protein kinase B to the plakin family member periplakin. *J Cell Sci*, **115**, 3957-3966.

Vasioukhin, V., Bowers, E., Bauer, C., Degenstein, L. and Fuchs, E. (2001) Desmoplakin is essential in epidermal sheet formation. *Nat Cell Biol*, **3**, 1076-1085.

Wallis, S., Lloyd, S., Wise, I., Ireland, G., Fleming, T.P. and Garrod, D. (2000) The alpha isoform of protein kinase C is involved in signaling the response of desmosomes to wounding in cultured epithelial cells. *Mol Biol Cell*, **11**, 1077-1092.

Watt, F.M. (1984) Selective migration of terminally differentiating cells from the basal layer of cultured human epidermis. *J Cell Biol*, **98**, 16-21.

Watt, F.M. (1998) Cultivation of human epidermal keratinocytes with a 3T3 feeder layer. In J.E., C. (ed.), *Cell Biology: A Laboratory Handbook.* Academic Press Inc., London, Vol. 1, pp. 113-118.

Weiss, A. and Leinwand, L.A. (1996) The mammalian myosin heavy chain gene family. *Annu Rev Cell Dev Biol*, **12**, 417-439.

Wiche, G., Becker, B., Luber, K., Weitzer, G., Castanon, M.J., Hauptmann, R., Stratowa, C. and Stewart, M. (1991) Cloning and sequencing of rat plectin indicates a 466-kD polypeptide chain with a three-domain structure based on a central alpha-helical coiled coil. *Journal of Cell Biology*, **114**, 83-99.

Witcher, L.L., Collins, R., Puttagunta, S., Mechanic, S.E., Munson, M., Gumbiner, B. and Cowin, P. (1996) Desmosomal cadherin binding domains of plakoglobin. *J Biol Chem*, **271**, 10904-10909.

Wyszynski, M., Kim, E., Dunah, A.W., Passafaro, M., Valtschanoff, J.G., Serra-Pages, C., Streuli, M., Weinberg, R.J. and Sheng, M. (2002) Interaction between GRIP and liprin-alpha/SYD2 is required for AMPA receptor targeting. *Neuron*, **34**, 39-52.

Xia, Y., Gil, S.G. and Carter, W.G. (1996) Anchorage mediated by integrin alpha6beta4 to laminin 5 (epiligrin) regulates tyrosine phosphorylation of a membrane-associated 80-kD protein. *J Cell Biol*, **132**, 727-740.

Yang, Y., Bauer, C., Strasser, G., Wollman, R., Julien, J.P. and Fuchs, E. (1999) Integrators of the cytoskeleton that stabilize microtubules. *Cell*, **98**, 229-238.

Yang, Y., Dowling, J., Yu, Q.C., Kouklis, P., Cleveland, D.W. and Fuchs, E. (1996) An essential cytoskeletal linker protein connecting actin microfilaments to intermediate filaments. *Cell*, **86**, 655-665.

Yonemura, S. and Tsukita, S. (1999) Direct involvement of ezrin/radixin/moesin (ERM)-binding membrane proteins in the organization of microvilli in collaboration with activated ERM proteins. *J Cell Biol*, **145**, 1497-1509.

Young, K.G., Pool, M. and Kothary, R. (2003) Bpag1 localization to actin filaments and to the nucleus is regulated by its N-terminus. *J Cell Sci*, **116**, 4543-4555.

Abbreviations

aa	amino acid
ABD	actin binding domain
AD	activation domain
BCA	bicinchoninic acid
BLAST	basic local alignment search tool
BLAT	BLAST-like alignment tool
bp	base pair
BPAG	bullous pemphigoid antigen 1
cDNA	complementary DNA
CE	cornified cell envelope
CIP	calf intestinal phosphatase
CLE	corneocyte lipid envelope
CR-UK	Cancer Research UK
DCS	donor calf serum
DMEM	Dulbecco's modified Eagles medium
DMSO	dimethyl sulfoxide
DNA	deoxyribonucleic acid
DNA-BD	DNA binding domain
dNTP	deoxynucleotide
Dsc	desmocollin
Dsg	desmoglein
EDTA	ethylldiaminotetraacetic acid, disodium salt
ERM	ezrin, radixin, moesin family of proteins
EST	expressed sequence tags
FAD	F12 powder, adenine, DMEM
FBS	fetal bovine serum
FCS	fetal calf serum
FSG	fish skin gelatin
GAPDH	glyceraldehyde phosphate dehydrogenase
GFP	green fluorescent protein
GS	goat serum
GST	glutathione S-transferase
HA	hemagglutinin
HDF	human dermal fibroblast
HICE	hydrocortisone, Insulin, Cholera toxin, Epidermal growth factor
HK	human keratinocyte
hr	hours
HRP	horse radish peroxidase
IF	intermediate filament
IgG	immunoglobulin
IPTG	isopropyl b – D - thiogalactoside
KA	kazrin A protein
KB	kazrin B protein
KC	kazrin C protein
Kazrin AL	kazrin A long protein
Kb	kilobase
kDa	kilodalton
KSFM	keratinocytes serum free medium
LAR	leukocyte common antigen-related

LSB	Laemmli sample buffer
L-T- agar	yeast agar lacking:leucine, tryptophan
L-T-A-H- agar	yeast agar lacking:leucine, tryptophan, adenine, histidine
MACF	microtubule associated crosslinking factor
MAPK	mitogen-activated protein kinase
MEK1/2	mitogen-activated protein kinase-kinase
mRNA	messenger RNA
MT	microtubule
NLS	nuclear localisation signal
° C	degrees Celcius
ORF	open reading frame
PBS	phosphate buffered saline
PBS-ABC	PBS with Mg2+ and Ca2+
PCR	polymerase chain reaction
PFA	paraformaldehyde
PKA	protein kinase A
PKB	protein kinase B
PKC	protein kinase C
PTPase	protein tyrosine phosphatase
RNA	ribonucleic acid
rpm	rotations per minute
RT	room temperature
RT-PCR	reverse transcription polymerase chain reaction
SDS-PAGE	sodium-dodecyl sulphate polyacrylimide gel electrophoresis
SEM	standard error of the mean
SPR	small proline rich (protein)
TAE	Tris/Acetic acid/EDTA
TGase	transglutaminase
Tris	tris(hydroxymethyl) aminomethane
UTR	untranslated region
v/v	volume:volume ratio
w/v	weight:volume ratio

Appendix

```
LOCUS       AY505119              1475 bp    mRNA    linear   PRI 02-SEP-2004
DEFINITION  Homo sapiens kazrin isoform A mRNA, complete cds.
ACCESSION   AY505119
VERSION     AY505119.1  GI:46276353
KEYWORDS    .
SOURCE      Homo sapiens (human)
  ORGANISM  Homo sapiens
            Eukaryota; Metazoa; Chordata; Craniata; Vertebrata; Euteleostomi;
            Mammalia; Eutheria; Primates; Catarrhini; Hominidae; Homo.
REFERENCE   1  (bases 1 to 1475)
  AUTHORS   Groot,K.R., Sevilla,L.M., Nishi,K., DiColandrea,T. and Watt,F.M.
  TITLE     Kazrin, a novel periplakin-interacting protein associated with
            desmosomes and the keratinocyte plasma membrane
  JOURNAL   J. Cell Biol. 166 (5), 653-659 (2004)
   PUBMED   15337775
REFERENCE   2  (bases 1 to 1475)
  AUTHORS   Groot,K.R., Sevilla,L.M., Nishi,K., DiColandrea,T. and Watt,F.M.
  TITLE     Direct Submission
  JOURNAL   Submitted (15-DEC-2003) Keratinocyte Laboratory, Cancer Research
            UK, 44 Lincoln's Inn Fields, London WC2A 3PX, UK
FEATURES             Location/Qualifiers
     source          1..1475
                     /organism="Homo sapiens"
                     /mol_type="mRNA"
                     /db_xref="taxon:9606"
                     /chromosome="1"
                     /map="1p36.21"
                     /clone="IMAGE:6180253"
                     /tissue_type="dorsal root ganglia"
     5'UTR           1..209
     CDS             210..1475
                     /codon_start=1
                     /product="kazrin isoform A"
                     /protein_id="AAS86434.1"
                     /db_xref="GI:46276354"

/translation="MMEDNKQLALRIDGAVQSASQEVTNLRAELTATNRRLAELSGGG
              GPGPGPGAAASASAAGDSAATNMENPQLGAQVLLREEVSRLQEEVHLLRQMKEMLAKD
              LEESQGGKSSEVLSATELRVQLAQKEQELARAKEALQAMKADRKRLKGEKTDLVSQMQ
              QLYATLESREEQLRDFIRNYEQHRKESEDAVKALAKEKDLLEREKWELRRQAKEATDH
              ATALRSQLDLKDNRMKELEAELAMAKQSLATLTKDVPKRHSLAMPGETVLNGNQEWVV
              QADLPLTAAIRQSQQTLYHSHPPHPADRQAVRVSPCHSRQPSVISDASAAEGDRSSTP
              SDINSPRHRTHSLCNGDSPGPVQKNLHNPIVQSLEDLEDQKRKKKKEKMGFGSISRVF
              ARGKQRKSLDPGLFDGTAPDYYIEEDADW"

ORIGIN
        1 ggggtctcgg cgatcgctgc tcctcctcct ccttctcctc ctctttttc tcctccgcct
       61 cctcccccg ccgcctcgcc accgccgcgg ctagggctgg aggcgccgct gtcattcctg
      121 tgccggagga accggcgctg ccggtgcctg ggggtcgggg cgcgggcgaa gccgggccgc
      181 ggaggacaca acaggccaaa atcctgagca tgatggaaga caataagcag ctcgcgctcc
      241 gcatcgatgg ggcggtccag tcggccagcc aggaggtgac caacctgcga gccgaactca
      301 cggccaccaa ccggagactg gcggaactga gcggcggcgg cggccccggc ccgggcccgg
      361 gagccgcggc cagcgcctcg gcggcggggg actcggcggc gacgaacatg gagaaccccc
      421 agcttggagc gcaagtgctc ctgcgggaag aagtgtcgcg gctccaggag gaagttcacc
      481 ttctccggca gatgaaggag atgttggcga aggacctgga ggagtcgcag ggcggcaagt
      541 cctctgaggt cctctcggcc accgagctca gggtccagct ggcccagaag gagcaggagc
      601 tagccagagc caaagaagcc ttgcaggcca tgaaagctga tcggaagcgc ttaaagggcg
      661 agaagacaga cctggtgagc cagatgcagc agctgtatgc cacactggag agccgcgagg
      721 agcagctccg agacttcatc cgcaactatg agcagcaccg caaggagagc gaggatgcgg
      781 tcaaagcgct ggccaaggag aaggacctgc tggagcgtga gaagtgggag ctgcggcgcc
      841 aagccaagga ggccacagac cacgccacgg cactgcgctc ccagctggac ctcaaggaca
      901 accggatgaa ggagctggag gccgagctgg ccatggccaa acagtcctta gctacgctga
      961 ccaaggacgt ccccaagcgg cattccctcg ccatgccggg cgagacggtg ctcaatggca
     1021 accaggagtg ggtggtgcag gcggacctcc cgctgaccgc agccatccgg cagagtcaac
     1081 agactctcta ccactcacac ccccctcacc ctgcggaccg gcaagcggtc agggtgagcc
     1141 cctgccactc ccggcagccc tctgtcatct ccgacgcatc tgccgccgaa ggcgaccggt
     1201 cgtccacacc gagcgacatc aactcccctc gacaccggac acactccctc tgcaacggcg
     1261 acagtcccgg cccagttcag aagaacctgc acaaccctat tgtacagtca ctagaggatc
```

```
     1321 ttgaagacca aaaacggaaa aagaagaaag agaagatggg attcggctcc atctcccgcg
     1381 tcttcgccag agggaagcag cggaagtccc tcgaccccgg cctctttgat ggtaccgccc
     1441 ctgattatta catagaggag gacgcggact ggtga
//
```

```
LOCUS       AY505120             1484 bp    mRNA    linear   PRI 02-SEP-2004
DEFINITION  Homo sapiens kazrin isoform B mRNA, complete cds.
ACCESSION   AY505120
VERSION     AY505120.1  GI:46276355
KEYWORDS    .
SOURCE      Homo sapiens (human)
  ORGANISM  Homo sapiens
            Eukaryota; Metazoa; Chordata; Craniata; Vertebrata; Euteleostomi;
            Mammalia; Eutheria; Primates; Catarrhini; Hominidae; Homo.
REFERENCE   1  (bases 1 to 1484)
  AUTHORS   Groot,K.R., Sevilla,L.M., Nishi,K., DiColandrea,T. and Watt,F.M.
  TITLE     Kazrin, a novel periplakin-interacting protein associated with
            desmosomes and the keratinocyte plasma membrane
  JOURNAL   J. Cell Biol. 166 (5), 653-659 (2004)
   PUBMED   15337775
REFERENCE   2  (bases 1 to 1484)
  AUTHORS   Groot,K.R., Sevilla,L.M., Nishi,K., DiColandrea,T. and Watt,F.M.
  TITLE     Direct Submission
  JOURNAL   Submitted (15-DEC-2003) Keratinocyte Laboratory, Cancer Research
            UK, 44 Lincoln's Inn Fields, London WC2A 3PX, UK
FEATURES             Location/Qualifiers
     source          1..1484
                     /organism="Homo sapiens"
                     /mol_type="mRNA"
                     /db_xref="taxon:9606"
                     /chromosome="1"
                     /map="1p36.21"
                     /clone="IMAGE:4556194"
                     /tissue_type="leiomyosarcoma"
     5'UTR           1..236
     CDS             237..1484
                     /codon_start=1
                     /product="kazrin isoform B"
                     /protein_id="AAS86435.1"
                     /db_xref="GI:46276356"

/translation="MRAADSGSWERVRQLAAQGEPAPSCGAGAGPARPPGPAACEQCV
              DAAGPGDRPRAGVPRVRADGDCSQPVLLREEVSRLQEEVHLLRQMKEMLAKDLEESQG
              GKSSEVLSATELRVQLAQKEQELARAKEALQAMKADRKRLKGEKTDLVSQMQQLYATL
              ESREEQLRDFIRNYEQHRKESEDAVKALAKEKDLLEREKWELRRQAKEATDHATALRS
              QLDLKDNRMKELEAELAMAKQSLATLTKDVPKRHSLAMPGETVLNGNQEWVVQADLPL
              TAAIRQSQQTLYHSHPPHPADRQAVRVSPCHSRQPSVISDASAAEGDRSSTPSDINSP
              RHRTHSLCNGDSPGPVQKNLHNPIVQSLEDLEDQKRKKKKEKMGFGSISRVFARGKQR
              KSLDPGLFDGTAPDYYIEEDADW"

ORIGIN
        1 gagccgttcc cacgtgagag gctccgcggc cgaattcctc gcgtgcagca ggcgcggacc
       61 gcccggcgtc cggccggact gagagccctg gtccggcgcg cgccgccggc cgggcgggag
      121 gcgggggcgg gctcggctgc gccccgatgc ggcggcgacc tccgggtctg tgagcccggc
      181 gcgcgccgtc ggagcccctc gcgcagccgc tggtagcgtc cccccgggca cccggcatgc
      241 gggcggccga ctcgggctcg tgggagcgcg tccgccagct cgcggcgcag ggcgagccgg
      301 cgccttcctg cggggcgggg gccgggcccg cgcggccccc gggacccgca gcctgcgagc
      361 agtgcgtgga cgcggcgggg cccggcgatc ggccccgcgc cggggttccc cgggtccgag
      421 cggatggcga ctgcagccag cccgtgctcc tgcgggaaga agtgtcgcgg ctccaggagg
      481 aagttcacct tctccggcag atgaaggaga tgttggcgaa ggacctggag gagtcgcagg
      541 gcggcaagtc ctctgaggtc ctctcggcca ccgagctcag ggtccagctg gcccagaagg
      601 agcaggagct agccagagcc aaagaagcct tgcaggccat gaaagctgat cggaagcgct
      661 taaagggcga gaagacagac ctggtgagcc agatgcagca gctgtatgcc acactggaga
      721 gccgcgagga gcagctccga gacttcatcc gcaactatga gcagcaccgc aaggagagcg
      781 aggatgcggt caaagcgctg gccaaggaga aggacctgct ggagcgtgag aagtgggagc
      841 tgcggcgcca agccaaggag gccacagacc acgccacggc actgcgctcc cagctggacc
      901 tcaaggacaa ccggatgaag gagctggagg ccgagctggc catggccaaa cagtccttag
      961 ctacgctgac caaggacgtc cccaagcggc attccctcgc catgccgggc gagacggtgc
     1021 tcaatggcaa ccaggagtgg gtggtgcagg cggacctccc gctgaccgca gccatccggc
     1081 agagtcaaca gactctctac cactcacacc cccctcaccc tgcggaccgg caagcggtca
     1141 gggtgagccc ctgccactcc cggcagccct ctgtcatctc cgacgcatct gccgccgaag
     1201 gcgaccggtc gtccacaccg agcgacatca actcccctcg acaccggaca cactccctct
     1261 gcaacggcga cagtcccggc ccagttcaga agaacctgca caaccctatt gtacagtcac
     1321 tagaggatct tgaagaccaa aaacggaaaa agaagaaaga gaagatggga ttcggctcca
     1381 tctcccgcgt cttcgccaga gggaagcagc ggaagtccct cgaccccggc ctctttgatg
     1441 gtaccgcccc tgattattac atagaggagg acgcggactg gtga
//
```

```
LOCUS       AY505121            1285 bp    mRNA    linear   PRI 02-SEP-2004
DEFINITION  Homo sapiens kazrin isoform C mRNA, complete cds.
ACCESSION   AY505121
VERSION     AY505121.1  GI:46276357
KEYWORDS    .
SOURCE      Homo sapiens (human)
  ORGANISM  Homo sapiens
            Eukaryota; Metazoa; Chordata; Craniata; Vertebrata; Euteleostomi;
            Mammalia; Eutheria; Primates; Catarrhini; Hominidae; Homo.
REFERENCE   1  (bases 1 to 1285)
  AUTHORS   Groot,K.R., Sevilla,L.M., Nishi,K., DiColandrea,T. and Watt,F.M.
  TITLE     Kazrin, a novel periplakin-interacting protein associated with
            desmosomes and the keratinocyte plasma membrane
  JOURNAL   J. Cell Biol. 166 (5), 653-659 (2004)
   PUBMED   15337775
REFERENCE   2  (bases 1 to 1285)
  AUTHORS   Groot,K.R., Sevilla,L.M., Nishi,K., DiColandrea,T. and Watt,F.M.
  TITLE     Direct Submission
  JOURNAL   Submitted (15-DEC-2003) Keratinocyte Laboratory, Cancer Research
            UK, 44 Lincoln's Inn Fields, London WC2A 3PX, UK
FEATURES             Location/Qualifiers
     source          1..1285
                     /organism="Homo sapiens"
                     /mol_type="mRNA"
                     /db_xref="taxon:9606"
                     /chromosome="1"
                     /map="1p36.21"
                     /clone="IMAGE:4651187"
                     /tissue_type="placenta"
     CDS             302..1285
                     /codon_start=1
                     /product="kazrin isoform C"
                     /protein_id="AAS86436.1"
                     /db_xref="GI:46276358"

/translation="MKEMLAKDLEESQGGKSSEVLSATELRVQLAQKEQELARAKEAL
              QAMKADRKRLKGEKTDLVSQMQQLYATLESREEQLRDFIRNYEQHRKESEDAVKALAK
              EKDLLEREKWELRRQAKEATDHATALRSQLDLKDNRMKELEAELAMAKQSLATLTKDV
              PKRHSLAMPGETVLNGNQEWVVQADLPLTAAIRQSQQTLYHSHPPHPADRQAVRVSPC
              HSRQPSVISDASAAEGDRSSTPSDINSPRHRTHSLCNGDSPGPVQKNLHNPIVQSLED
              LEDQKRKKKKEKMGFGSISRVFARGKQRKSLDPGLFDGTAPDYYIEEDADW"

ORIGIN
        1 gggagaggga aggtcaggct tgcctcctgt tcacaaggac aacctctgtc tcccttgtgg
       61 cggcttctat gaaggtgggg actccaggct ttctctcgtc tgctttttgg atgccttcaa
      121 gagaggccag ttagaggata tcaattgtgg caattcccca gagccctcat cagatggcat
      181 tagcccgtca tgtgctgcag tggcacccag tttggaggaa attcggaacc agaagagtgt
      241 gacagtgctc ctgcgggaag aagtgtcgcg gctccaggag gaagttcacc ttctccggca
      301 gatgaaggag atgttggcga aggacctgga ggagtcgcag ggcggcaagt cctctgaggt
      361 cctctcggcc accgagctca gggtccagct ggcccagaag gagcaggagc tagccagagc
      421 caaagaagcc ttgcaggcca tgaaagctga tcggaagcgc ttaaagggcg agaagacaga
      481 cctggtgagc cagatgcagc agctgtatgc cacactggag agccgcgagg agcagctccg
      541 agacttcatc cgcaactatg agcagcaccg caaggagagc gaggatgcgg tcaaagcgct
      601 ggccaaggag aaggacctgc tggagcgtga gaagtgggag ctgcggcgcc aagccaagga
      661 ggccacagac cacgccacgg cactgcgctc ccagctggac ctcaaggaca accggatgaa
      721 ggagctggag gccgagctgg ccatggccaa acagtcctta gctacgctga ccaaggacgt
      781 ccccaagcgg cattccctcg ccatgccggg cgagacggtg ctcaatggca accaggagtg
      841 ggtggtgcag gcggacctcc cgctgaccgc agccatccgg cagagtcaac agactctcta
      901 ccactcacac ccccctcacc ctgcggaccg gcaagcggtc agggtgagcc cctgccactc
      961 ccggcagccc tctgtcatct ccgacgcatc tgccgccgaa ggcgaccggt cgtccacacc
     1021 gagcgacatc aactcccctc gacaccggac acactccctc tgcaacggcg acagtcccgg
     1081 cccagttcag aagaacctgc acaaccctat tgtacagtca ctagaggatc ttgaagacca
     1141 aaaacggaaa aagaagaaag agaagatggg attcggctcc atctcccgcg tcttcgccag
     1201 agggaagcag cggaagtccc tcgaccccgg cctctttgat ggtaccgccc ctgattatta
     1261 catagaggag gacgcggact ggtga
//
```

```
LOCUS       AY505122            1295 bp    mRNA    linear   PRI 02-SEP-2004
DEFINITION  Homo sapiens kazrin isoform D mRNA, complete cds.
ACCESSION   AY505122
VERSION     AY505122.1  GI:46276359
KEYWORDS    .
SOURCE      Homo sapiens (human)
  ORGANISM  Homo sapiens
            Eukaryota; Metazoa; Chordata; Craniata; Vertebrata; Euteleostomi;
            Mammalia; Eutheria; Primates; Catarrhini; Hominidae; Homo.
REFERENCE   1  (bases 1 to 1295)
  AUTHORS   Groot,K.R., Sevilla,L.M., Nishi,K., DiColandrea,T. and Watt,F.M.
  TITLE     Kazrin, a novel periplakin-interacting protein associated with
            desmosomes and the keratinocyte plasma membrane
  JOURNAL   J. Cell Biol. 166 (5), 653-659 (2004)
   PUBMED   15337775
REFERENCE   2  (bases 1 to 1295)
  AUTHORS   Groot,K.R., Sevilla,L.M., Nishi,K., DiColandrea,T. and Watt,F.M.
  TITLE     Direct Submission
  JOURNAL   Submitted (15-DEC-2003) Keratinocyte Laboratory, Cancer Research
            UK, 44 Lincoln's Inn Fields, London WC2A 3PX, UK
FEATURES             Location/Qualifiers
     source          1..1295
                     /organism="Homo sapiens"
                     /mol_type="mRNA"
                     /db_xref="taxon:9606"
                     /chromosome="1"
                     /map="1p36.21"
                     /clone="IMAGE:4472821"
                     /tissue_type="liver adenocarcinoma"
     5'UTR           1..311
     CDS             312..1295
                     /codon_start=1
                     /product="kazrin isoform D"
                     /protein_id="AAS86437.1"
                     /db_xref="GI:46276360"

/translation="MKEMLAKDLEESQGGKSSEVLSATELRVQLAQKEQELARAKEAL
              QAMKADRKRLKGEKTDLVSQMQQLYATLESREEQLRDFIRNYEQHRKESEDAVKALAK
              EKDLLEREKWELRRQAKEATDHATALRSQLDLKDNRMKELEAELAMAKQSLATLTKDV
              PKRHSLAMPGETVLNGNQEWVVQADLPLTAAIRQSQQTLYHSHPPHPADRQAVRVSPC
              HSRQPSVISDASAAEGDRSSTPSDINSPRHRTHSLCNGDSPGPVQKNLHNPIVQSLED
              LEDQKRKKKKEKMGFGSISRVFARGKQRKSLDPGLFDGTAPDYYIEEDADW"

ORIGIN
        1 gcatcagcag ctgtctgcca gtgttgacgg agggctcatg ggtgccaggc cgcttgctgg
       61 ggctttttat ctgtcctcag gcattggcac agcagccctg ggagatgaat actattgtga
      121 tcttcattct ccacacaagg acagggaagt gacgtgccag ggtcaaacaa ctacccaagg
      181 acagagccag gatttgaacc aggccatcca gttccagaac cactgctctt cactgtcatt
      241 gtggccattt tacagtgctc ctgcgggaag aagtgtcgcg gctccaggag gaagttcacc
      301 ttctccggca gatgaaggag atgttggcga aggacctgga ggagtcgcag ggcggcaagt
      361 cctctgaggt cctctcggcc accgagctca gggtccagct ggcccagaag gagcaggagc
      421 tagccagagc caaagaagcc ttgcaggcca tgaaagctga tcggaagcgc ttaaagggcg
      481 agaagacaga cctggtgagc cagatgcagc agctgtatgc cacactggag agccgcgagg
      541 agcagctccg agacttcatc cgcaactatg agcagcaccg caaggagagc gaggatgcgg
      601 tcaaagcgct ggccaaggag aaggacctgc tggagcgtga gaagtgggag ctgcggcgcc
      661 aagccaagga ggccacagac cacgccacgg cactgcgctc ccagctggac ctcaaggaca
      721 accggatgaa ggagctggag gccgagctgg ccatggccaa acagtcctta gctacgctga
      781 ccaaggacgt ccccaagcgg cattccctcg ccatgccggg cgagacggtg ctcaatggca
      841 accaggagtg ggtggtgcag gcggacctcc cgctgaccgc agccatccgg cagagtcaac
      901 agactctcta ccactcacac ccccctcacc ctgcggaccg gcaagcggtc agggtgagcc
      961 cctgccactc ccggcagccc tctgtcatct ccgacgcatc tgccgccgaa ggcgaccggt
     1021 cgtccacacc gagcgacatc aactcccctc gacaccggac acactccctc tgcaacggcg
     1081 acagtcccgg cccagttcag aagaacctgc acaaccctat tgtacagtca ctagaggatc
     1141 ttgaagacca aaaacggaaa aagaagaaag agaagatggg attcggctcc atctcccgcg
     1201 tcttcgccag agggaagcag cggaagtccc tcgaccccgg cctctttgat ggtaccgccc
     1261 ctgattatta catagaggag gacgcggact ggtga
//
```

Human kazrin A long protein sequence as derived from BC036877

Sequence compiled by Nick Brown (Wellcome/CR-UK, Cambridge)

```
LOCUS       Human kazrin A long    775 AA PROT          SYN       20-AUG-2004
DEFINITION  Pearson file capture
ACCESSION   -
KEYWORDS    -
SOURCE      -
COMMENT     Non-sequence data from original file:
            >kazrin [org=Homo sapiens] kazrin isoform a protein

ORIGIN      -
        1 MMEDNKQLAL RIDGAVQSAS QEVTNLRAEL TATNRRLAEL SGGGGPGPGP GAAASASAAG
       61 DSAATNMENP QLGAQVLLRE EVSRLQEEVH LLRQMKEMLA KDLEESQGGK SSEVLSATEL
      121 RVQLAQKEQE LARAKEALQA MKADRKRLKG EKTDLVSQMQ QLYATLESRE EQLRDFIRNY
      181 EQHRKESEDA VKALAKEKDL LEREKWELRR QAKEATDHAT ALRSQLDLKD NRMKELEAEL
      241 AMAKQSLATL TKDVPKRHSL AMPGETVLNG NQEWVVQADL PLTAAIRQSQ QTLYHSHPPH
      301 PADRQAVRVS PCHSRQPSVI SDASAAEGDR SSTPSDINSP RHRTHSLCNG DSPGPVQKNL
      361 HNPIVQSLED LEDQKRKKKK EKMGFGSISR VFARGKQRKS LDPGLFDDSD SQCSPTRQSL
      421 SLSEGEEQMD RLQQVELVRT TPMSHWKAGT VQAWLEVVMA MPMYVKACTE NVKSGKVLLS
      481 LSDEDLQLGL GVCSSLHRRK LRLAIEDYRD AEAGRSLSKA AELDHHWVAK AWLNDIGLSQ
      541 YSQAFQNHLV DGRMLNSLMK RDLEKHLNVS KKFHQVSILL GIELLYQVNF SREALQERRA
      601 RCETQNIDPV VWTNQRVLKW VRDIDLKEYA DNLTNSGVHG AVLVLEPTFN AEAMATALGI
      661 PSGKHILRRH LAEEMSAVFH PANSTGIREA ERFGTPPGRA SSVTRAGKEE NSSGLKYKAG
      721 RLPLGKIGRG FSSKDPDFHD DYGSLQNEDC GDDDPQSRLE QCRLEGYNSL EVTNV*
```

Drosophila melanogaster kazrin-like liprin protein sequence as derived from BT009994 and NM206200.

Protein sequence compiled by Nick Brown (Wellcome/CR-UK, Cambridge).

```
LOCUS       DMKAZRIN1.   1023 AA    PROT            SYN       27-AUG-2004
DEFINITION  -
ACCESSION   -
KEYWORDS    -
SOURCE      -
FEATURES             Location/Qualifiers
     DOMAIN          589..657
                     /note="SAM"
     DOMAIN          669..733
                     /note="SAM"
     DOMAIN          754..826
                     /note="SAM"
ORIGIN      -
        1 MTADNQPLQQ QLQHHQHRSP AYPGKPAEAA GGVPQQQQQQ QQLPNGIGSS HCNSNSNGIS
       61 STCNSGTAMI HANNSNLIAA GHLAQAAGPA HNAPSSGSAL NAVDKRNANL SEPDQDLPPN
      121 LNVNLSPNPS LALGAPHSPT SAASAALLLL ESCDGNRNDE SRFHHLHSAP RPEATMKLRE
      181 ENDRLNAELL RLRRLLELST DGAVGGVDTA PEMEAVASGE GSAAKERIER LESELRSVKN
      241 QLLTMRLERK KLRTDKSDLL GQVKQLCASL QEKEQELRDF IRNYQERVRE TETTNAKISG
      301 DRDRERFQLL KQARDEAERS LALAQQLSAR DLQLQRLQEQ LQEARRQLTG CLSDQESLHS
      361 FAPLTPPSAA SGMLSQMAAA SGMGGGLAGM RGTTEDSGRG NSLSAFSGSL SGGSGATAGD
      421 RNSCSNDSGL RNSSDRESTG GELNFSDGTC DNGPCITVDP DSISLVSSQN MYQFGTPKER
      481 SPTLSPLNSA AYSRSVEQLG SPVDPEGPGN GAISRKFANA SKSGPLGARN GRGGTWGSIS
      541 RVFARSRNKN KALSADGVTE YADYSWNPLT EEGYAEKLRL LREASQLPID RWRATQVLAW
      601 LEVALGMPQY SARCAENVKS GKVLLELNDV ELEAGLGLAH PMHRKKLRLA IEEQRRPEMV
      661 RYPLITQLGH TWVATEWLPD IGLPQYAEPF VQSLVDARML DTLSKKELEK FLGVTRKFHQ
      721 ASIVHGIHVL RIVKYDRQTL AMRRVQSETV DTDPIVWTNQ RFIRWVRSID LGEYADNLKD
      781 SGVHGGLVVL EPSFSGDTMA TALGIPPSKN IIRRHLNTEF DALILPARAT LGQGIRSGCG
      841 VVPLTGPGGL QHYATTDRRS SGNLRISAWK GSQSSLSKAF RFNSKPHRTG DRSSFGNSTS
      901 PTPSYSSSEG GGGIYATIGH QYPNPHTNLQ QQHYHHFLPP PTTAPPPIPS AGGIYSHGPP
      961 PGHRVSAPPV GGALDAVSTD PQMLYEQSRR RVKSISDIGA STSAGSVGAC SLGGISASSE
     1021 SPE*
//
```

Future experiments and directions.

Analysis of the kazrin protein and its function.

Immunofluorescence studies indicated that a proportion of kazrin protein localises to the nucleus. Analysis of endogenous kazrin levels in nuclear, cell membrane and cytoplasmic cell extracts will determine what proportion of kazrin localises to the nucleus.

Transfected forms of kazrin were found to localise to the nucleus though the proportion of cells having nuclear kazrin varied between cell types (Fig. 5.10). A putative NLS was identified in the kazrin protein sequence. Mutation of the NLS will determine if it is required for nuclear localisation.

My analysis indicated that kazrin proteins may be phosphorylated on either serine or threonine residues. Following CIP treatment, which specifically removes serine and threonine phosphorylation, a doublet remained in each case suggesting further covalent modification of the kazrin protein e.g. tyrosine phosphorylation. Activators and inhibitors of signalling pathways will be used to identify the kinases involved in kazrin phosphorylation.

To identify the phosphorylated residues recombinant kazrin will be phosphorylated *in vitro* by the relevant kinase and the phosphorylated residues identified by mass spectrometry. Kazrin constructs in which the serine, threonine or tyrosine residues which are phosphorylated are mutated to alanine, a non-phosphorylatable residue, or aspartic acid/glutamic acid, phospho-mimicking residues, should be generated. The kazrin mutants will allow us to identify factors which bind kazrin in a phosphorylation-dependent manner.

My analysis has demonstrated that kazrin is widely expressed. At present the function of kazrin is not well understood. Kazrin-related sequences have been identified in *Xenopus tropicalis* EST databases. Using the *X. tropicalis* kazrin sequence morpholino-modified antisense oligonucleotides have been designed to specifically knock-down expression of kazrin in the developing embryo. Analysis of the development of the embryo in the presence of a kazrin-targeted morpholino and a control morpholino will help to establish a functional role for kazrin. An alternative approach is to ablate the kazrin gene in mice. The targeting of the kazrin gene with the incorporation of lox P sites will allow the generation of both complete kazrin knockout mice and tissue-specific kazrin knockout mice by crossing kazrin-targeted mice with mice expressing Cre recombinase in a tissue-specific fashion.

In vitro analysis of transfected and endogenous forms of kazrin suggested that kazrin proteins could be part of a higher-order protein complex. The identity of the other proteins within the complexes are not known. The N-terminal α-helical domain of kazrin is predicted to form a coiled-coil thus the complexes may be formed by the association of the kazrin coiled-coil domains with each other or other coiled-coil domain-containing proteins. The generation of differently tagged kazrin proteins will allow us to identify whether kazrin proteins can homodimerise and/or heterodimerise. Immunoprecipitation of transfected forms of kazrin proteins will allow us to isolate kazrin-interacting proteins. The kazrin-interacting bands can subsequently be identified by mass spectrometry.

Bioinformatic analysis suggested the existence of a long isoform of kazrin which had homology to the liprin family of LAR PTPase interacting proteins. Further analysis suggests that the long form of kazrin is expressed in a number of epithelial cell lines. The liprin family of proteins are known to hetero- and homo-dimerise via their N-terminal coiled-coil domains and their C-terminal liprin domain. It will be of interest to understand if kazrin proteins are able to interact

with other members of the liprin family of proteins or with the LAR PTPases. The ability of kazrin to interact with these proteins will be determined by immunoprecipitation experiments.

The activation of TGase I activity in keratinocytes by treatment of the cells with 0.1% Triton-X100 suggested that kazrin is a CE component. Analysis of peptides from proteolytically digested CEs would confirm if kazrin is a CE component. In addition using our LS4 anti-kazrin antibody could be used to stain CEs isolated from human or mouse keratinocyte cultures.

Analysis of mice triple knockout for involucrin, periplakin and envoplakin.

The general ultrastructure of the epidermis from triple knockout mice appears largely normal. To analyse the lipid component of the epidermis the samples should be post-fixed in osmium tetraoxide to allow more detailed analysis of the lamellar lipids and CLE. This fixation method will allow us to identify if the lack of periplakin, envoplakin and involucrin causes a mild defect in the manner or timing of deposition of lamellar lipids and their attachment to CE proteins. Such a mild defect would not be visible by analysis of the epidermis by conventional EM.

Marekov and Steinert (1998) previously isolated lipo-peptides from proteolytically digested CEs. Their analysis suggested that the majority of the hydroxyceramides which form the CLE are covalently linked to the proteins envoplakin, periplakin and involucrin. Isolation of lipopeptides from CEs from triple knockout mice may allow us to identify to which proteins the hydroxyceramides are attached in the absence of envoplakin, periplakin and involucrin.

Epithelial barrier formation is patterned not only in the epidermis but also in oral epithelia (Marshall et al., 2000). I found that the formation of a functional epidermal barrier is slightly delayed in triple knockout mice compared to control mice. It would be interesting to analyse the formation of epithelial barrier function in the tongue and hard palate to see if the formation of an epithelial barrier oral epithelia is also delayed in the absence of envoplakin, periplakin and involucrin expression.

The SEM proved a useful technique with which to analyse the surface of cornified cells. This technique may in future be used to compare the structure of cornified cells from triple knockout and control mice.

The CEs isolated from newborn loricrin–deficient mice were more sensitive to sonication that the CEs isolated from control mice (Koch et al., 2000). It would be of interest to analyse the sensitivity of CEs from triple knockout mice compared to CEs from control mice.

My results indicated that the CEs from triple knockout mice were larger than those from triple heterozygous mice. The epidermal cells of triple knockout mice may be larger than the epidermal cells of triple heterozygote mice thereby leading to the formation of larger CEs. Cell size could be measured by analysis of the number of cells in a given area of epidermis. Alternatively the cell lines generated from the triple knockout, triple heterozygote and wild type mice may be used to analyse cell size *in vitro.*

In order to further investigate the delay in formation of the epidermal barrier by triple knockout mice versus triple heterozygote and wild type mice mRNA will be isolated from the mouse epidermis. The mRNA will be applied to mRNA microarray analysis in order to identify factors that are up-regulated in the absence of envoplakin, periplakin and involcurin expression. The analysis of the whole epidermis by microarray could allow us to identify factors not previously considered important for the formation of a functional epidermal barrier.